

FILTRATION PROPERTIES OF WATER BASED DRILLING FLUIDS

BY

SHUANG JIU PENG

**SUBMITTED FOR THE DEGREE OF
DOCTOR OF PHILOSOPHY
AT HERIOT-WATT UNIVERSITY
ON COMPLETION OF RESEARCH IN THE
DEPARTMENT OF PETROLEUM ENGINEERING
OCTOBER 1990**

This copy of the thesis has been supplied on the condition that anyone who consults it is understood to recognise that the copyright rests with its author and that no quotation from the thesis and no information derived from it may be published without the prior written consent of the author or the university (as may be appropriate).

I hereby declare that the work presented in this thesis was carried out by myself at Heriot-Watt University, Edinburgh, except where due acknowledgement is made, and has not been submitted for any other degree.

S J Peng (Candidate)

Professor J M Peden (Supervisor)

Date: December 1990

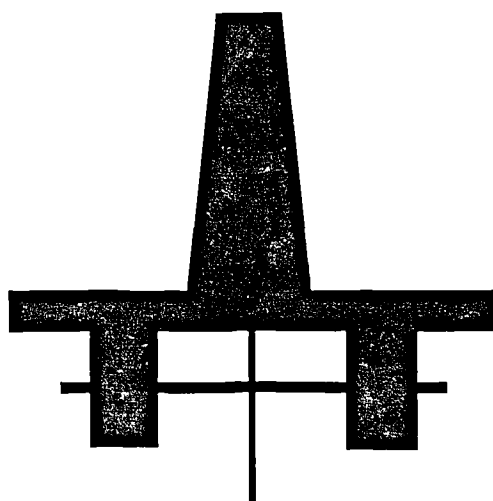


TABLE OF CONTENTS

TABLE OF CONTENTS	i
LIST OF TABLES	vii
LIST OF FIGURES	viii
ACKNOWLEDGEMENTS	xvi
ABSTRACT	xvii
NOMENCLATURE	xviii
INTRODUCTION	1
CHAPTER ONE	
FILTRATION PROPERTIES OF DRILLING FLUIDS AND ASSOCIATED DRILLING AND PRODUCTION PROBLEMS	
1.1 FILTRATION BEHAVIOUR OF DRILLING FLUIDS	3
1.1.1 Definition of Liquid Filtration	3
1.1.2 Borehole Filtration of Drilling and Completion Fluids	4
1.1.3 Invasion of Filtrate into Formation	5
1.2 THE PROBLEMS CAUSED BY FILTRATION OF DRILLING FLUIDS	6
1.2.1 Formation Damage	6
1.2.1.1 Clay Swelling	6
1.2.1.2 Dispersion and Migration of Formation Clay Particles	7
1.2.1.3 Particle Plugging	7
1.2.1.4 Wettability	7
1.2.1.5 Water Blocking	8
1.2.1.6 Emulsions	8
1.2.1.7 Scales and Precipitates	8
1.2.2 Other Problems	9

1.2.2.1	Differential Sticking	9
1.2.2.2	Hole Instability	9

CHAPTER TWO

LITERATURE SURVEY ON FILTRATION PROPERTIES OF DRILLING FLUIDS

2.1	AN OVERVIEW OF LITERATURE ON BOREHOLE FILTRATION OF DRILLING MUDS	11
2.2	THE EFFECTS OF INDIVIDUAL WELLBORE VARIABLES UPON STATIC AND DYNAMIC FILTRATION PERFORMANCE	43
2.2.1	The Effect of Absolute Pressure and Differential Pressure	43
	Absolute Pressure	43
	Pressure Differential	44
2.2.2	The Effect of Temperature	45
2.2.3	The Effect of the Properties of Filter Medium	47
2.2.4	The Effect of the Mechanical Erosion of Dynamically Deposited Cakes	49
2.2.5	The Effect of Annular Hydraulics on Dynamic Fluid Loss	50
2.2.6	The Effect of Mud Properties and Constituents	52
2.2.7	The Sequential Filtration	54

CHAPTER THREE

NUMERICAL MODELLING OF THE FILTRATION OF DRILLING FLUIDS

3.1	LITERATURE SURVEY ON CAKE FILTRATION THEORY	56
3.1.1	The Behaviour of Fluid Flowing Through Porous Medium	56
3.1.2	The Flow Through Filter Cake	57
	3.1.2.1 Direct Filtration Measurement	57
	3.1.2.2 Simulation of Filter Cake Compressibility	65
3.1.3	Summary of Cake Filtration Theory	72
3.2	LITERATURE REVIEW OF FILTRATION EQUATIONS OF DRILLING FLUIDS	73
3.3	DEVELOPMENT OF GENERAL FILTRATION	

EQUATION OF DRILLING FLUIDS	87
3.3.1 External Mass Balance	87
3.3.2 Solution of Differential Equation of Filtration	90
3.3.3 Applications of General Filtration Equation	92
3.3.3.1 Erodability of Dynamically Deposited Cake	92
3.3.3.2 Static Filtration Equation	93
3.4 THE DIMENSIONAL ANALYSIS OF DYNAMIC FILTRATION OF DRILLING FLUIDS	94
3.4.1 The Buckingham Π Theorem	94
3.4.2 The Application of Π Theorem to the Dynamic Filtration	95
CHAPTER FOUR	
THE EXPERIMENTAL EQUIPMENT AND PROCEDURES	
4.1 STATIC FILTRATION	101
4.1.1 Description of the Modified Static Filtration Cell	101
4.1.2 Muds Tested for Static Filtration	102
4.1.3 Mud Preparation	102
4.1.4 Core Preparation	106
4.1.5 Experimental Procedure	106
4.2 DYNAMIC FILTRATION	109
4.2.1 Experimental Rig and Procedure	109
4.2.2 The Determination of Shear Rate and Rotational Speed From Equivalent Annular Velocity	110
4.3 THE ADVANTAGES OF THE MODIFIED FILTRATION CELL	111
CHAPTER FIVE	
PRESENTATION OF STATIC FILTRATION EXPERIMENTAL RESULTS	
5.1 MUDS TESTED AND THEIR PROPERTIES	112
5.2 EXPERIMENTAL RESULTS OF STATIC FILTRATION	115
5.2.1 Spurt Loss	115

5.2.2	Effect of Pressure and Barite Concentration upon Cumulative Filtrate Volume	115
5.2.3	Effect of Pressure and Barite Concentration upon Filter Cake Thickness	116
5.2.4	Effect of Pressure and Barite Concentration upon Ratio of Wet to Dry Cake Mass	116
5.3	THEORETICAL MODELLING OF STATIC FILTRATION EXPERIMENT	117
5.3.1	Derivation of Static Filtration Equation	117
5.3.2	Application of Static Filtration Equation to Experimental Data	121
5.3.2.1	Average Specific Cake Resistance and Effective Filter Medium Resistance	121
5.3.2.2	Average Cake Porosity and Permeability	124
CHAPTER SIX		
PRESENTATION OF DYNAMIC FILTRATION EXPERIMENTAL RESULTS		
6.1	MUD SYSTEMS TESTED AND THEIR PROPERTIES	127
6.2	EXPERIMENTAL RESULTS	128
6.2.1	Spurt Loss and Cumulative Filtrate Volume	128
6.2.2	Derivation of Dynamic Filtration Equation	130
6.2.3	Applications of Dynamic Filtration Equation	131
6.3	RESULTS OF SEQUENTIAL FILTRATION EXPERIMENTS	140
CHAPTER SEVEN		
DISCUSSION OF EXPERIMENTAL RESULTS		
7.1	DEVIATIONS FROM THE MODIFIED EQUATIONS	143
7.1.1	Static Filtration Modelling	143
7.1.2	Dynamic Filtration Modelling	146
7.2	PRESSURE DIFFERENTIAL ACROSS THE FILTER CAKE	147
7.2.1	Pressure Differential Across Static Filter Cake	147
7.2.2	Pressure Differential Across Dynamic Filter Cake	149
7.3	SUMMARY	151

7.3.1	Cake Erodability	151
7.3.2	Average Specific Cake Resistance	152
CHAPTER EIGHT		
COMPARISON OF PREDICTED AND EXPERIMENTAL OBTAINED DATA		
		153
8.1	PREDICTIVE TECHNIQUE	153
8.1.1	Estimation of Average Specific Cake Resistance	154
8.1.2	Prediction of Effective Filter Medium Resistance	154
8.1.3	Determination of Erodability of Dynamically Deposited Cake	155
8.1.4	Ratio of Wet to Dry Cake Mass or Cake Porosity	155
8.1.5	Assumption on Spurt Time and Spurt Loss	156
8.2	PREDICTION OF DYNAMIC FILTRATION DATA FROM STATIC FILTRATION RESULTS	156
8.3	PREDICTION OF FILTRATION DATA IN A SEQUENTIAL PROCESS	157
CHAPTER NINE		
CONCLUSIONS		
9.1	EXPERIMENTAL CONCLUSIONS	159
9.1.1	Conclusions for Static Filtration Tests	159
9.1.2	Conclusions for Dynamic Filtration Tests	160
9.2	GENERAL CONCLUSIONS	161
CHAPTER TEN		
RECOMMENDATIONS FOR FUTURE WORK		
10.1	FILTRATION MODELLING	163
10.1.1	Further Verification of Dynamic Filtration Equation Under Downhole Conditions	163
10.1.2	Determination of Dynamic Filter Cake Characteristics	164
10.1.3	The Study of the Effect of Effective Filter Medium Resistance	165
10.1.4	Fluid Loss Study and Associated Formation Damage	165

10.2 FILTRATION EQUIPMENT	166
10.3 THEORETICAL STUDY OF DYNAMIC FILTRATION — MULTIPHASE THEORY OF CAKE FILTRATION	167
REFERENCES	170
APPENDIX I	

LIST OF TABLES

Table 2.1	Equilibrium Cake Thickness under Dynamic Filtration ¹⁰
Table 2.2	Drilling Schedule and Filtration Invasion ¹³
Table 2.3	Comparison Between Calculated and Experimental Bottom Hole Filtration Rates ¹⁴
Table 2.4	The Viscosity of Water and 6% Sodium Chloride Brine at Various Temperature ⁹⁵
Table 4.1	Composition of the Two Basic Muds Used
Table 4.2	Brief Description of Mud Components
Table 4.3	Composition of Simulated North Sea Water
Table 5.1	Composition of the Tested Seawater/KCL/Polymer Mud
Table 5.2	Composition of the Tested Freshwater/Gypsum/Lignosulphonate Mud
Table 5.3	The Properties of Seawater/KCL/Polymer Mud
Table 5.4	The Properties of Freshwater/Gypsum/Lignosulphonate Mud
Table 5.5	Regression Coefficients of Static Filtration Experiments (Seawater/KCL/Polymer Mud)
Table 5.6	Regression Coefficients of Static Filtration Experiments (Freshwater/Gypsum/Lignosulphonate Mud)
Table 6.1	Regression Coefficients of Dynamic Filtration Experiments (Seawater/KCL/Polymer Mud)
Table 6.2	Regression Coefficients of Dynamic Filtration Experiments (Freshwater/Gypsum/Lignosulphonate Mud)
Table 6.3	Regression Coefficients of Dynamic Filtration Experiments (Freshwater/Gypsum/Lignosulphonate Mud)
Table 6.4	Shear Stresses Acted on Filter Cake Surface for Different Mud Systems

LIST OF FIGURES

- Figure(1-1.1) Invasion of a Permeable Formation by Mud Solids⁹⁵
- Figure(1-2.1) Types of Formation Damage
- Figure(2-1.1) Transition Layer Between Drilling Mud Filter Cake and Mud Fluid¹³
- Figure(2-1.2) Dynamic Filtration From Bentonite Mud¹³
- Figure(2-1.3) Dynamic Filtration From Lime-Starch Mud¹³
- Figure(2-1.4) Dynamic Filtration From Oil Base Mud¹³
- Figure(2-1.5) Dynamic Filtration From Emulsion Mud¹³
- Figure(2-1.6) A Typical Plot of Cumulative Filtrate Volume Collected as a Function of Time for Sequential Filtration²⁰
- Figure(2-1.7) The Examples of Three Types of Filtration Curves²⁸
- Figure(2-1.8) Dynamic Filtration Cell and Filtrate Collection System³⁹
- Figure(2-1.9) Filtration and Sticking Simulator⁴⁰
- Figure(2-1.10) Filtration vs. Flow Changes⁴⁰
- Figure(2-1.11) Automatic Shearometer Unit⁴³
- Figure(2-1.12) HPHT Dynamic Filtration Tester⁴³
- Figure(2-1.13) Manual Filter Cake Penetrometer⁴³
- Figure(2-1.14) Motorized Filter Cake Penetrometer⁴³
- Figure(2-1.15) The Annular Flow Dynamic Filtration Cell (Section)⁴⁵
- Figure(2-1.16) (a) Basic ideas of Convection-Diffusion Models⁴⁵ and
(b) Basic Ideas of Particle Adhesion Models⁴⁵
- Figure(3-1.1) Schematic Diagram of Important Parameters in Cake Formation
- Figure(3-1.2) Compressive Force due to Frictional Drag
- Figure(3-1.3) Simulation of Filtration by Using Compression Permeability Cell⁶⁵
- Figure(3-3.1) Relationship between Filter Cake and Cumulative Deposited Cake

- Figure(4-1.1) Schematic of Room Temperature Filtration cell and Associated Equipments
- Figure(4-1.2) A Schematic Drawing of Cross-Section of Static Filtration Cell
- Figure(4-1.3) A Schematic of Liquid Permeability Measurement
- Figure(4-1.4) A Schematic of Micrometer Arrangement for Measuring Filter Cake Thickness
- Figure(4-2.1) A Schematic Diagram of the Cone-and-Plate Viscometer.
- Figure(4-2.2) A Schematic of Assembled Dynamic Filtration Rig
- Figure(4-2.3) A Schematic Drawing of Cross-Section of Dynamic Filtration Cell
- Figure(5-2.1) Spurt Loss as Function of Pressures and Barite Concentrations for Seawater/KCL/Polymer Mud in Static Filtration Tests
- Figure(5-2.2) Cumulative Filtrate Volume Per Unit Area as Function of Time Under Various Differential Pressures for 50 lbs/bbl Barite Concentration of Seawater/KCL/Polymer Mud in Static Filtration Tests
- Figure(5-2.3) Cumulative Filtrate Volume Per Unit Area as Function of Time Under Various Differential Pressures for 70 lbs/bbl Barite Concentration of Seawater/KCL/Polymer Mud in Static Filtration Tests
- Figure(5-2.4) Cumulative Filtrate Volume Per Unit Area as Function of Time Under Various Differential Pressures for 140 lbs/bbl Barite Concentration of Seawater/KCL/Polymer Mud in Static Filtration Tests
- Figure(5-2.5) Cumulative Filtrate Volume Per Unit Area as Function of Time Under Various Differential Pressures for 210 lbs/bbl Barite Concentration of Seawater/KCL/Polymer Mud in Static Filtration Tests
- Figure(5-2.6) Measured Filter Cake Thickness as Function of Pressures and Barite Concentrations for Seawater/KCL/Polymer Mud in Static Filtration Tests
- Figure(5-2.7) Measured Ratio of Wet to Dry Filter Cake Mass as Function of Pressures and Barite Concentrations for Seawater/KCL/Polymer Mud in Static Filtration Tests
- Figure(5-3.1) $(t - t_{sp} - t_0) / (V - V_{sp})$ versus $(V - V_{sp})$ Plottings Under Various Differential Pressures for 50 lbs/bbl Barite Concentration of Seawater/KCL/Polymer Mud in Static Filtration Tests
- Figure(5-3.2) $(t - t_{sp} - t_0) / (V - V_{sp})$ versus $(V - V_{sp})$ Plottings Under Various Differential Pressures for 70 lbs/bbl Barite Concentration of Seawater/KCL/Polymer Mud in Static Filtration Tests
- Figure(5-3.3) $(t - t_{sp} - t_0) / (V - V_{sp})$ versus $(V - V_{sp})$ Plottings Under Various Differential Pressures for 140 lbs/bbl Barite Concentration of Seawater/KCL/Polymer Mud in Static Filtration Tests

- Figure(5-3.4) $(t - t_{sp} - t_0) / (V - V_{sp})$ versus $(V - V_{sp})$ Plottings Under Various Differential Pressures for 210 lbs/bbl Barite Concentration of Seawater/KCL/Polymer Mud in Static Filtration Tests
- Figure(5-3.5) Average Filter Cake Specific Resistance as Function of Barite Concentrations and Pressures for Seawater/KCL/Polymer in Static Filtration Tests
- Figure(5-3.6) Effective Filter Medium Resistance as Function of Pressures and Barite Concentrations for Seawater/KCL/Polymer in Static Filtration Tests
- Figure(5-3.7) Average Filter Cake Porosity as Function of Pressures and Barite Concentrations for Seawater/KCL/Polymer Mud in Static Filtration Tests
- Figure(5-3.8) Average Filter Cake Permeability as Function of Barite Concentrations and Pressures for Seawater/KCL/Polymer Mud in Static Filtration Tests
- Figure(6-2.1) Spurt Loss as Function of Pressures and Shear Rates for Seawater/KCL/Polymer Mud in Dynamic Filtration Tests
- Figure(6-2.2) Spurt Loss as Function of Pressures and Shear Rates for Freshwater/Gypsum/Lignosulphonate Mud in Dynamic Filtration Tests
- Figure(6-2.3) Cumulative Filtrate Volume at 8 hours as Function of Shear Rate and Differential Pressure for Seawater/KCL/Polymer Mud in Dynamic Filtration Tests
- Figure(6-2.4) Cumulative Filtrate Volume at 8 hours as Function of Shear Rate and Differential Pressure for Freshwater/Gypsum/Lignosulphonate Mud in Dynamic Filtration Tests
- Figure(6-2.5) Cumulative Filtrate Volume Per Unit Area as Function of Time Under Various Differential Pressures at Shear Rate of 107 1/s for Seawater/KCL/Polymer Mud in Dynamic Filtration Tests
- Figure(6-2.6) Cumulative Filtrate Volume Per Unit Area as Function of Time Under Various Differential Pressures at Shear Rate of 125 1/s for Seawater/KCL/Polymer Mud in Dynamic Filtration Tests
- Figure(6-2.7) Cumulative Filtrate Volume Per Unit Area as Function of Time Under Various Differential Pressures at Shear Rate of 71 1/s for Freshwater/Gypsum/Lignosulphonate Mud in Dynamic Filtration Tests
- Figure(6-2.8) Cumulative Filtrate Volume Per Unit Area as Function of Time Under Various Differential Pressures at Shear Rate of 89 1/s for Freshwater/Gypsum/Lignosulphonate Mud in Dynamic Filtration Tests
- Figure(6-2.9) Cumulative Filtrate Volume Per Unit Area as Function of Time Under Various Differential Pressures at Shear Rate of 107 1/s for Freshwater/Gypsum/Lignosulphonate Mud in Dynamic Filtration Tests

- Figure(6-2.10) Cumulative Filtrate Volume Per Unit Area as Function of Time Under Various Differential Pressures at Shear Rate of 125 1/s for Freshwater/Gypsum/Lignosulphonate Mud in Dynamic Filtration Tests
- Figure(6-2.11) Cumulative Filtrate Volume Per Unit Area as Function of Time Under Various Shear Rates at the Differential Pressure of 50 psi for Seawater/KCL/Polymer Mud in Dynamic Filtration Tests
- Figure(6-2.12) Average Filter Cake Specific Resistance as Function of Pressures and Shear Rates for Seawater/KCL/Polymer Mud in Dynamic Filtration Tests
- Figure(6-2.13) Average Filter Cake Specific Resistance as Function of Pressures and Shear Rates for Freshwater/Gypsum/Lignosulphonate Mud in Dynamic Filtration Tests
- Figure(6-2.14) Effective Filter Medium Resistance as Function of Pressures and Shear Rates for Seawater/KCL/Polymer Mud in Dynamic Filtration Tests
- Figure(6-2.15) Effective Filter Medium Resistance as Function of Pressures and Shear Rates for Freshwater/Gypsum/Lignosulphonate Mud in Dynamic Filtration Tests
- Figure(6-2.16) Filter Cake Erodability as Function of Pressures and Shear Rates for Seawater/KCL/Polymer Mud in Dynamic Filtration Tests
- Figure(6-2.17) Filter Cake Erodability as Function of Pressures and Shear Rates for Freshwater/Gypsum/Lignosulphonate Mud in Dynamic Filtration Tests
- Figure(6-2.18) Equilibrium Filtrate Flow Rate as Function of Pressures and Shear Rates for Seawater/KCL/Polymer Mud in Dynamic Filtration Tests
- Figure(6-2.19) Equilibrium Filtrate Flow Rate as Function of Pressures and Shear Rates for Freshwater/Gypsum/Lignosulphonate Mud in Dynamic Filtration Tests
- Figure(6-2.20) Average Filter Cake Permeability as Function of Pressures and Shear Rates for Seawater/KCL/Polymer Mud in Dynamic Filtration Tests
- Figure(6-2.21) Average Filter Cake Permeability as Function of Pressures and Shear Rates for Freshwater/Gypsum/Lignosulphonate Mud in Dynamic Filtration Tests
- Figure(6-3.1) Cumulative Filtrate Volume Per Unit Area as Function of Time at Pressure of 50 psi for Seawater/KCL/Polymer Mud in Sequential Filtration Tests
- Figure(6-3.2) Filtrate Flow Rate as Function of Time at Pressure of 50 psi for Seawater/KCL/Polymer Mud in Sequential Filtration Tests
- Figure(6-3.3) Cumulative Filtrate Volume Per Unit Area as Function of Time at Pressure of 50 psi for Freshwater/Gypsum/Lignosulphonate Mud in Sequential Filtration Tests

- Figure(6-3.4) Filtrate Flow Rate as Function of Time at Pressure of 50 psi for Freshwater/Gypsum/ Lignosulphonate Mud in Sequential Filtration Tests
- Figure(6-3.5) Cumulative Filtrate Volume Per Unit Area as Function of Time at Pressure of 200 psi for Seawater/KCL/Polymer Mud in Sequential Filtration Tests(Experimentally and Theoretically)
- Figure(6-3.6) Filtrate Flow Rate as Function of Time at Pressure of 200 psi for Seawater/KCL/Polymer Mud in Sequential Filtration Tests (Experimentally and Theoretically)
- Figure(6-3.7) Cumulative Filtrate Volume Per Unit Area as Function of Time at Pressure of 200 psi for Seawater/KCL/Polymer Mud in Sequential Filtration Tests (Experimentally and Theoretically)
- Figure(6-3.8) Filtrate Flow Rate as Function of Time at Pressure of 200 psi for Seawater/KCL/Polymer Mud in Sequential Filtration Tests (Experimentally and Theoretically)
- Figure(6-3.9) Cumulative Filtrate Volume Per Unit Area as Function of Time at Pressure of 50 psi for Seawater/KCL/Polymer Mud in Sequential Filtration Tests (Experimentally and Theoretically)
- Figure(6-3.10) Filtrate Flow Rate as Function of Time at Pressure of 50 psi for Seawater/KCL/Polymer Mud in Sequential Filtration Tests (Experimentally and Theoretically)
- Figure(6-3.11) Cumulative Filtrate Volume Per Unit Area as Function of Time at Pressure of 50 psi for Freshwater/Gypsum/Lignosulphonate Mud in Sequential Filtration Tests (Experimentally and Theoretically)
- Figure(6-3.12) Filtrate Flow Rate as Function of Time at Pressure of 50 psi for Freshwater/Gypsum/ Lignosulphonate Mud in Sequential Filtration Tests (Experimentally and Theoretically)
- Figure(7-1.1) Cumulative Filtrate Volume Per Unit Area as Function of Time at Pressure of 500 psi for 140 lbs/bbl Barite Concentration of Seawater/KCL/Polymer Mud in Long Time Static Filtration Test
- Figure(7-1.2) Filtrate Flow Rate as Function of Time at Pressure of 500 psi for 140 lbs/bbl Barite Concentration of Seawater/KCL/Polymer Mud in Long Time Static Filtration Test
- Figure(7-1.3) t/V versus V Plotting at Pressure of 500 psi for 140 lbs/bbl Barite Concentration of Seawater/KCL/Polymer Mud in Long Time Static Filtration Test
- Figure(7-1.4) $(t - t_{sp}) / (V - V_{sp})$ versus $V - V_{sp}$ Plotting at Pressure of 500 psi for 140 lbs/bbl Barite Concentration of Seawater/KCL/Polymer Mud in Long Time Static Filtration Test
- Figure(7-1.5) $(t - t_{sp} - t_0) / (V - V_{sp})$ versus $V - V_{sp}$ Plotting at Pressure of 500 psi for 140 lbs/bbl Barite Concentration of Seawater/KCL/Polymer Mud in Long Time Static Filtration Test

- Figure(7-1.6) Filter Cake Build-Up as Function of Time in Theoretically Dynamic and Static Filtration Simulation
- Figure(7-1.7) Comparison of Filtrate Flow Rate Calculated From Dynamic Filtration Equation(Correlated Results) and Experimental Data as Function of Time and Mud Types at Pressure of 100 psi and Shear Rate of 71 1/s
- Figure(7-1.8) Comparison of Filtrate Flow Rate Calculated From Dynamic Filtration Equation(Correlated Results) and Experimental Data as Function of Time and Mud Types at Pressure of 100 psi and Shear Rate of 89 1/s
- Figure(7-1.9) Comparison of Filtrate Flow Rate Calculated From Dynamic Filtration Equation(Correlated Results) and Experimental Data as Function of Time and Mud Types at Pressure of 100 psi and Shear Rate of 107 1/s
- Figure(7-1.10) Comparison of Filtrate Flow Rate Calculated From Dynamic Filtration Equation(Correlated Results) and Experimental Data as Function of Time and Mud Types at Pressure of 100 psi and Shear Rate of 125 1/s
- Figure(7-1.11) Comparison of Filtrate Flow Rate Calculated From Dynamic Filtration Equation(Correlated Results) and Experimental Data as Function of Time and Mud Types at Pressure of 200 psi and Shear Rate of 71 1/s
- Figure(7-1.12) Comparison of Filtrate Flow Rate Calculated From Dynamic Filtration Equation(Correlated Results) and Experimental Data as Function of Time and Mud Types at Pressure of 200 psi and Shear Rate of 89 1/s
- Figure(7-1.13) Comparison of Filtrate Flow Rate Calculated From Dynamic Filtration Equation(Correlated Results) and Experimental Data as Function of Time and Mud Types at Pressure of 200 psi and Shear Rate of 107 1/s
- Figure(7-1.14) Comparison of Filtrate Flow Rate Calculated From Dynamic Filtration Equation(Correlated Results) and Experimental Data as Function of Time and Mud Types at Pressure of 200 psi and Shear Rate of 125 1/s
- Figure(7-1.15) Comparison of Filtrate Flow Rate Calculated From Dynamic Filtration Equation(Correlated Results) and Experimental Data as Function of Time and Mud Types at Pressure of 300 psi and Shear Rate of 71 1/s
- Figure(7-1.16) Comparison of Filtrate Flow Rate Calculated From Dynamic Filtration Equation(Correlated Results) and Experimental Data as Function of Time and Mud Types at Pressure of 300 psi and Shear Rate of 89 1/s
- Figure(7-1.17) Comparison of Filtrate Flow Rate Calculated From Dynamic Filtration Equation(Correlated Results) and Experimental Data as Function of Time and Mud Types at Pressure of 300 psi and Shear Rate of 107 1/s
- Figure(7-1.18) Comparison of Filtrate Flow Rate Calculated From Dynamic Filtration Equation(Correlated Results) and Experimental Data as Function of Time and Mud Types at Pressure of 300 psi and Shear Rate of 125 1/s
- Figure(7-1.19) Comparison of Filtrate Flow Rate Calculated From Dynamic Filtration Equation(Correlated Results) and Experimental Data as Function of Time and Mud Types at Pressure of 400 psi and Shear Rate of 71 1/s
- Figure(7-1.20) Comparison of Filtrate Flow Rate Calculated From Dynamic Filtration Equation(Correlated Results) and Experimental Data as Function of Time and Mud Types at Pressure of 400 psi and Shear Rate of 89 1/s

- Figure(7-1.21) Comparison of Filtrate Flow Rate Calculated From Dynamic Filtration Equation(Correlated Results) and Experimental Data as Function of Time and Mud Types at Pressure of 400 psi and Shear Rate of 107 1/s
- Figure(7-1.22) Comparison of Filtrate Flow Rate Calculated From Dynamic Filtration Equation(Correlated Results) and Experimental Data as Function of Time and Mud Types at Pressure of 400 psi and Shear Rate of 125 1/s
- Figure(7-2.1) Pressure Differential Across Filter Cake and Filter Medium Over the Total Applied Pressure as Function of Time at Pressure of 200 psi for Seawater/KCL/Polymer Mud in Static Filtration Test
- Figure(7-2.2) Pressure Differential Across Filter Cake and Filter Medium Over the Total Applied Pressure as Function of Time at Pressure of 200 psi for Freshwater/Gypsum/Lignosulphonate Mud in Static Filtration Test
- Figure(7-2.3) Pressure Differential Across Filter Cake and Filter Medium Over the Total Applied Pressure as Function of Time at Pressure of 200 psi and Shear Rate of 125 1/s for Seawater/KCL/Polymer Mud in Dynamic Filtration Test
- Figure(7-2.4) Pressure Differential Across Filter Cake and Filter Medium Over the Total Applied Pressure as Function of Time at Pressure of 200 psi and Shear Rate of 125 1/s for Freshwater/Gypsum/Lignosulphonate Mud in Dynamic Filtration Test
- Figure(7-2.5) Pressure Differential Across Filter Cake and Filter Medium Over the Total Applied Pressure as Function of Time at Pressure of 200 psi and Shear Rate of 125 1/s for Seawater/KCL/Polymer Mud in Dynamic Filtration Test
- Figure(7-2.6) Pressure Differential Across Filter Cake and Filter Medium Over the Total Applied Pressure as Function of Time at Pressure of 200 psi and Shear Rate of 125 1/s for Freshwater/Gypsum-Lignosulphonate Mud in Dynamic Filtration Test
- Figure(8-2.1) Comparison of Dynamic Filtration Predicted From Static Filtration Data with Experimental Results at Pressure of 200 psi and Shear Rate of 71 1/s for Seawater/KCL/Polymer Mud — Filtrate Flow Rate as a Function of Time
- Figure(8-2.2) Comparison of Dynamic Filtration Predicted From Static Filtration Data with Experimental Results at Pressure of 200 psi and Shear Rate of 71 1/s for Seawater/KCL/Polymer Mud — Cumulative Filtrate Volume as a Function of Time
- Figure(8-3.1) Filtrate Flow Rate as Function of Time at Pressure of 200 psi for Seawater/KCL/Polymer Mud in a Sequence of Dynamic-Static-Dynamic Process (Experimentally and Theoretically)
- Figure(8-3.2) Cumulative Filtrate Volume as Function of Time at Pressure of 200 psi for Seawater/KCL/Polymer Mud in a Sequence of Dynamic-Static-Dynamic Process (Experimentally and Theoretically)
- Figure(8-3.3) Filtrate Flow Rate as Function of Time at Pressure of 50 psi for Seawater/KCL/Polymer Mud in a Sequence of Dynamic-Static-Dynamic Process (Experimentally and Theoretically)

- Figure(8-3.4) Cumulative Filtrate Volume as Function of Time at Pressure of 50 psi for Seawater/KCL/Polymer Mud in a Sequence of Dynamic-Static-Dynamic Process (Experimentally and Theoretically)
- Figure(8-3.5) Filtrate Flow Rate as Function of Time at Pressure of 50 psi for Freshwater/Gypsum/Lignosulphonate Mud in a Sequence of Dynamic-Static-Dynamic Process (Experimentally and Theoretically)
- Figure(8-3.6) Cumulative Filtrate Volume as Function of Time at Pressure of 50 psi for Freshwater/Gypsum/Lignosulphonate Mud in a Sequence of Dynamic-Static-Dynamic Process (Experimentally and Theoretically)
- Figure(9-1.1) Cumulative Filtrate Volume as a Function of Time at Pressure of 50 psi and Shear Rate of 71 1/s for Seawater/KCL/Polymer Mud in Dynamic Filtration Tests.
- Figure(9-1.2) Filtrate Flow Rate as a Function of Time at Pressure of 50 psi and Shear Rate of 71 1/s for Seawater/KCL/Polymer Mud in Dynamic Filtration Tests
- Figure(10-1.1) A Schematic of the Computer Programme to Predict Wellbore Fluid Loss of Drilling Muds
- Figure(10-1.2) A Schematic of Study on Relationship Between Fluid Loss and Wellbore Parameters and Associated Formation Damage
- Figure(10-2.1) Schematic Diagram of Concentric Cylinder Dynamic Filter Tester
- Figure(10-2.2) Multifunctional Circulating System

ACKNOWLEDGEMENTS

The author would like to take this opportunity to acknowledge the contributions to this work provided by the following:

Professor J M Peden who has provided guidance, advice, ideas and encouragement since the initiation of the project.

Mr Alan Brown, Mr George Pratt, Mr Walter Crawford and Mr Stevie Kelly, who machined and built the equipment and keep it operational.

The laboratory technicians Mrs Angela Nelson and Miss Elaine Blackie who provided their help with the experimental work.

Finally, my parents who provided their constant encouragement and unlimited support, and my wife, Saizhi Sun who provided patience and understanding.

ABSTRACT

This thesis reports an experimental and theoretical study on filtration properties of water based drilling fluids under dynamic and static conditions. The tested muds cover Freshwater/Gypsum/Lignosulphonate mud and Seawater/KCL/Polymer mud, barite-weighted and unweighted. The effects of the solid concentration, pressure and shear rate on the filter cake characteristics and the erodability were investigated. For static filtration experiments, all tests were conducted for two hours and the spurt loss, the filter cake thickness, the ratio of wet to dry cake mass and the cumulative filtrate volume against time were measured. For dynamic filtration experiments, however, only the spurt loss and the cumulative filtrate volume against time were measured and all tests were conducted for at least 8 hours. A general filtration equation was developed based on the cake filtration theory prevailing in the chemical engineering industry and it was utilised to obtain the modified classic static filtration equation and the dynamic filtration equation. The modified classic static filtration equation was then employed to fit the static filtration experimental data and the average specific static cake resistance and the effective filter medium resistance were calculated. The dynamic filtration equation showed a substantial agreement with the dynamic filtration experimental data. Using the static filter cake properties such as the ratio of wet to dry cake mass (m), the average specific dynamic cake resistance, the effective filter medium resistance and the dynamic filter cake erodability were calculated. In the study of the relationship between the static filtration data and the dynamic filtration data, an attempt of predicting the dynamic filtration data from the static filtration experimental data was conducted. Also, an attempt was carried out to predict the static filtration data and the dynamic filtration data in a sequential process.

The experimental data suggests that a substantial difference exists between the specific resistances of static and dynamic filter cakes. No apparent distinction was found, however, between spurt loss and effective filter medium resistance. The erodability of dynamically deposited mud cake for Seawater/KCL/Polymer mud was found to be three fold that for Freshwater/Gypsum/Lignosulphonate.

NOMENCLATURE

A	=	Cross-sectional area of filter cake	[m ²]
a	=	Constant defined in equation(3-1.33)	[N ⁿ m ¹⁻²ⁿ /Kg]
		Also constant defined in equation(3-1.41)	[m/Kg]
a ₁	=	Constant defined in equation(3-2.44)	[s/m ³]
a ₂	=	Constant defined in equation(3-2.45)	[s/m ⁶]
B	=	Dynamic filtration coefficient	[Kg/m ² s]
		Also constant defined in equation(3-1.31)	[m ^{2β} /N ^β]
		Also viscosity constant for newtonian fluid defined in equation(3-2.33)	[°C]
b	=	Constant defined in equation(3-1.41)	[m ⁴ /Kg · s]
C	=	Constant defined in equation(3-1.12)	[Kg/m ³]
C'	=	Proportional constant defined in equation(3-1.7)	[m ^{2m+3n-3} /N ^m s]
C ₁	=	Constant defined in equation(3-3.21)	[s/m ³]
		Also static filtration rate constant defined in equation(3-2.31)	[m/s ^{0.5}]
C ₂	=	Constant defined in equation(3-3.22)	[s]
		Also static filtration volume constant defined in equation(3-2.32)	[m/s ^{0.5}]
C ₃	=	Constant defined in equation(3-3.23)	[m ³]
		Also spurt loss volume defined in equation(3-2.32)	[m ³]
C ₄	=	Non-equilibrium shear rate multiplier defined in equation(3-2.35)	[m/s ^{0.5}]
C ₅	=	Dynamic non-equilibrium constant defined in equation(3-2.35)	[m]
C ₆	=	Dynamic equilibrium constant defined in equation(3-2.36)	[m/s ^{0.5}]
C ₇	=	Equilibrium shear rate multiplier defined in equation(3-2.36)	[m]
C _B	=	Constant defined in equation(3-2.20)	[m ³ /s ^{0.5}]

C'_B	=	Constant defined in equation(3-2.21)	[m]
C_F	=	Constant defined in equation(3-2.10)	[m ⁶ /s]
C_w	=	Constant defined in equation(3-2.2)	[m]
C'_w	=	Empirical constant defined in equation(3-2.4)	[1/m ^{0.5}]
D	=	The rate of deposition defined in equation(3-1.5)	[m ²]
D_1	=	Annular inner diameter defined in equation(3-2.38)	[m]
d_1	=	The diameter of drilling pipe defined in equation(4-2.1)	[m]
d_2	=	The diameter of wellbore defined in equation(4-2.1)	[m]
E	=	Fluid displacement efficiency of filtrate defined in equation(3-2.37)	[-]
e	=	Deviations defined in equation(3-2.7)	[m ³]
f	=	The coefficient of internal friction of the cake's surface layer defined in equation(3-2.19)	[-]
h_{∞}	=	Filter cake thickness after equilibrium attained	[m]
J_T	=	Correction out factor for filtration resistance defined in equation(3-1.38)	[-]
J_s	=	Correction out factor for filtration resistance defined in equation(3-1.40)	[-]
K	=	Permeability	[m ²]
		Also constant defined in equation(3-1.3)	[m ^{2m+3n+1} /N ^m s]
		Also constant defined in equation(3-1.16)	[m ⁶ /s]
K_1	=	the cake permeability at 1 psi pressure	[m ²]
K_{avg}	=	the average cake permeability	[m ²]
K_c	=	the cake permeability	[m ²]
K_f	=	the filter medium permeability	[m ²]
K_L	=	Constant for specific mud defined in equation(3-2.6)	[m ³]
K'_L	=	Constant for specific mud defined in equation(3-2.7)	[m ³ /s ^{0.5}]
K_e	=	Dynamic filtration erodability coefficient	[Kg/N·s]
k	=	Kozeny's constant defined in equation(3-1.24)	[-]
L	=	The length of filter bed defined in equation(3-1.2)	[m]
		Also filter cake thickness	[m]

l	=	The length of tube defined in equation(3-1.1)	[m]
L_c	=	The length of filter cake	[m]
L_f	=	The length of filter medium	[m]
M_w	=	Constant defined in equation(3-2.2)	[m ² /s]
M_G	=	Constant defined in equation(3-2.15)	[s/m ⁶]
M'_G	=	A number defining the filtration characteristics of the mud filter cake defined in equation(3-2.16)	[s/m ⁶]
m	=	Ratio of wet to dry cake mass	[-]
		Also constant defined in equation(3-1.3)	[-]
N_{max}	=	Maximum rotary speed	[rpm]
N_{min}	=	Minimum rotary speed	[rpm]
N_G	=	Constant defined in equation(3-2.15)	[s/m ³]
n	=	Constant defined in equation(3-1.3)	[-]
		Also constant defined in equation(3-1.33)	[-]
		Also behaviour index of mud	[-]
P	=	Filtration pressure	[N/m ²]
P_a	=	Applied filtration pressure	[N/m ²]
P_{ab}	=	Absolute pressure	[N/m ²]
P_{arb}	=	An arbitrary parameter used to make the equation dimensionless defined in equation(3-1.42)	[N/m ²]
P_i	=	Low pressure defined in equation(3-1.32)	[N/m ²]
P_s	=	Pressure on solids defined in equation(3-1.29)	[N/m ²]
P_x	=	Hydraulic pressure at distance x from the medium defined in equation(3-1.29)	[N/m ²]
ΔP	=	Pressure differential	[N/m ²]
ΔP_c	=	Pressure differential across cake	[N/m ²]
ΔP_{meff}	=	Pressure differential across effective filter medium	[N/m ²]
Q_∞	=	Pre-factor in dynamic fluid loss correlation defined in equation(3-2.41)	[m/s]
q	=	Filtrate flow rate per unit area	[m/s]
		$\frac{m^3}{m^2} = m/s$	

q_1	=	Filtrate flow rate per unit area at interface of medium and cake defined in equation(3-1.38)	[m/s]
q_{avg}	=	Average value of filtrate flow rate per unit area defined in equation(3-1.38)	[m/s]
q_{eq}	=	Dynamic equilibrium filtrate flow rate	[m/s]
q_{de}	=	Dynamic equilibrium filtrate flow rate	[m/s]
q_x	=	Local filtrate flow rate per unit area	[m/s]
q_{∞}	=	Dynamic filtrate flow rate per unit area	[m/s]
R	=	Resistance	[1/m]
R'	=	A function of resistivity of the cake defined in equation(3-2.2)	[1/m]
R_c	=	Resistance of filter cake	[1/m]
R_L	=	Ratio of filtrate volume / volume of deposited solids defined in equation(3-2.6)	[-]
R_m	=	Resistance of filter medium	[1/m]
R_{meff}	=	Effective resistance of filter medium	[1/m]
r	=	The internal radius of the tube defined in equation(3-1.1)	[m]
		Also resistance of material defined in equation(3-1.4)	[1/m ²]
		Also the well radius defined in equation(3-2.14)	[m]
		Also the constant resistance of filter medium defined in equation(3-2.22)	[1/m]
S	=	Sorptivity defined in equation(3-2.38)	[m/s ^{0.5}]
S_0	=	Specific surface of solids	[1/m]
s	=	Solid percentage concentration in slurry	[-]
		Also a compaction function of the cake defined in equation(3-2.2)	[-]
s_c	=	Solid percentage concentration in cake	[-]
T	=	Temperature	[°C]
t	=	Time	[s]
t'	=	Time	[s]
t_c	=	Some timescale for the transition to the dynamic phase defined in equation(3-2.39)	[s]

t_{eq}	=	Time at which dynamic equilibrium is attained	[s]
t_0	=	Time defined in equation(3-1.17)	[s]
		Also time defined in equation(3-2.11)	[s]
		Also time defined in equation(3-2.43)	[s]
t_{sp}	=	Spurt loss time	[s]
U	=	Drilling penetration rate defined in equation(3-2.37)	[m/s]
V	=	Cumulative filtrate volume	[m ³]
V'	=	Cumulative filtrate volume	[m ³]
V_{ANN}	=	Annular mud flow velocity	[m/s]
V_c	=	Volume of filtrate collected on cylindrical filter defined in equation(3-2.14)	[m ³]
V_o	=	Filtrate volume defined in equation(3-1.17)	[m ³]
		Also volume defined in equation(3-2.11)	[m ³]
V_p	=	Volume of filtrate collected on plane filter defined in equation(3-2.14)	[m ³]
V_s	=	Volume of filtrate that flows through the scraped portion of well wall defined in equation(3-2.12)	[m ³]
V_{sp}	=	Spurt loss volume	[m ³]
V_u	=	Volume of filtrate that flows through the unscraped portion of well wall defined in equation(3-2.12)	[m ³]
W	=	Cumulative deposited solids weight per unit area	[Kg/m ²]
W_c	=	Filter cake weight per unit area	[Kg/m ²]
W_e	=	Eroded solids weight per unit area	[Kg/m ²]
W_s	=	Solids weight as laid on the filter medium	[Kg]
X	=	Fraction of filtrate through hole bottom removed by drill bit defined in equation(3-2.37)	[-]
Z	=	Ratio of filtrate volume to cake volume defined in equation(3-2.14)	[-]

GREEK SYMBOLS

$-1+v$	=	A function of cake compressibility	
α	=	Specific cake resistance	[m/Kg]
α_0	=	Specific cake resistance constant defined in equation(3-2.46)	[m/Kg]
α_{avg}	=	Average specific cake resistance	[m/Kg]
α_i	=	Specific cake resistance defined in equation(3-1.34)	[m/Kg]
α_{mean}	=	Average specific cake resistance defined in equation(3-1.36)	[m/Kg]
β	=	Pressure constant defined in equation(3-1.31)	[-]
δ	=	The thickness of the cake subjected to erosion	[m]
ϵ	=	Porosity	[-]
ϵ_{avg}	=	Average cake porosity	[-]
ϵ_{avgx}	=	Average cake porosity for the portion of cake between medium and distance x as defined in equation(3-1.40)	[-]
ϵ_i	=	Cake porosity defined in equation(3-1.32)	[-]
ϵ_x	=	Local value of porosity at distance x from the medium	[-]
Γ_d	=	Scaling shear rate defined in equation(3-2.41)	[1/s]
ϕ	=	Formation porosity defined in equation(3-2.37)	[-]
φ	=	Pre-factor in transition time correlation defined in equation(3-2.42)	[s]
κ_1	=	Constant defined in equation(3-3.13)	[s/m ⁶]
κ_2	=	Constant defined in equation(3-3.14)	[1/m ³]
κ_3	=	Constant defined in equation(3-3.15)	[s/m ³]
γ	=	Shear rate	[1/s]
γ_{max}	=	Maximum shear rate	[1/s]
γ_{min}	=	Minimum shear rate	[1/s]
γ_w	=	Shear rate at channel wall	[1/s]
μ	=	Viscosity	[N · s/m ²]
μ_p	=	Plastic viscosity of Bingham Plastic mud	[N · s/m ²]

μ_f	=	Filtrate viscosity	$[\text{N} \cdot \text{s}/\text{m}^2]$
μ_m	=	Mud viscosity	$[\text{N} \cdot \text{s}/\text{m}^2]$
ρ	=	Density	$[\text{Kg}/\text{m}^3]$
ρ'	=	Resistance coefficient of filtering medium and sludge contained therein defined in equation(3-2.3)	$[-]$
$\rho'f(P)$	=	A function of the resistance of the filtering medium defined in equation(3-2.3)	$[-]$
ρ_f	=	Density of filtrate	$[\text{Kg}/\text{m}^3]$
ρ_m	=	Density of mud	$[\text{Kg}/\text{m}^3]$
ρ_s	=	Density of solids	$[\text{Kg}/\text{m}^3]$
τ	=	The shear stress on the cake surface exerted by the mud stream	$[\text{N}/\text{m}^2]$
τ_0	=	The yield point of the Bingham Plastic mud	$[\text{N}/\text{m}^2]$
v	=	Ratio of volume of filter cake to volume of filtration defined in equation(3-2.2)	$[-]$
ψ	=	The fraction of the well wall that is scraped clean defined in equation(3-2.12)	$[-]$

INTRODUCTION

In order to prevent formation fluids from entering the borehole, the hydraulic pressure of the mud column must exceed the pressure of the fluids in the pores of the formation. This differential pressure provides the driving force for mud movement through the borehole wall into the permeable formations. Massive loss of mud into the formation usually does not occur except in fractured formations, because the mud solids are filtered out onto the wall of the hole, forming a cake of relatively low permeability, through which only filtrate can mainly pass. The deposit of solids in the form of a cake contributes to borehole stability and limits the invasion of the permeable zone by the liquid phase and thus reduces the formation damage. Therefore, both borehole stability and formation damage are functions of the above process which is called the filtration behaviour of drilling fluids.

The petroleum industry has long been concerned that filtration of drilling fluids is a major cause of permeability damage to sensitive formations. Everyone concerned realizes that minimizing filtrate volume will be beneficial to production. The aim of this thesis is to report the results of an experimental and theoretical study on the static and dynamic filtration characteristics of drilling fluids under borehole conditions.

In chapter one, the objectives of the filtration study, e.g., for solving the problems caused by filtration occurrence under borehole conditions, are discussed. To attack these problems intelligently, it appears necessary to obtain a better understanding of the filtration mechanisms, hence, an extensive survey of literature spanning more than 5 decades of research on the filtration behaviour of drilling fluids with particular reference to the experimental investigation has been undertaken and is presented in chapter two.

The theoretical-empirical analysis on cake filtration performances carried out by

former investigators in both the chemical and petroleum engineering industries are reviewed in chapter three, which results in the development of a numerical filtration equation of drilling fluids. A dimensional analysis on dynamic equilibrium filtrate flow is also included in this chapter.

The experimental apparatus descriptions and procedure are shown in chapter four and the static and dynamic experimental tests results are presented in chapter five and chapter six, respectively.

In chapter seven, the analysis of the experimental results is presented.

A comparison of numerical modelling predictions and experimental results is presented in chapter eight.

Finally, the conclusions drawn from this study are presented in chapter 9 and the recommendations for future work is listed in chapter ten.

Chapter One

FILTRATION PROPERTIES OF DRILLING FLUIDS AND ASSOCIATED DRILLING AND PRODUCTION PROBLEMS

The estimation of filtration properties under borehole conditions is particularly important during well drilling as it ensures fewer drilling problems and improved productivity. The fundamental concepts of drilling fluids filtration and associated problems such as formation damage are discussed in this chapter.

1.1 FILTRATION BEHAVIOUR OF DRILLING FLUIDS

1.1.1 Definition of Liquid Filtration

There are many definitions of filtration both in the chemical engineering industry and in the petroleum engineering industry. The author prefers to use the following description¹⁰⁰:

Filtration is a fundamental unit operation aimed at the separation of suspended solid particles from a process fluid stream by passing the suspension through a porous substance referred to as a *filter medium*. In forcing the fluid through the voids of the filter medium, the liquid phase flows, but solid particles are retained on the surface and in the medium's pores. The fluid discharging from the medium is called *filtrate*.

1.1.2 Borehole Filtration of Drilling and Completion Fluids

There are usually three types of filtration¹⁰⁴ involved in drilling and completion operations:

BENEATH-THE-BIT FILTRATION:

Prior to being actually penetrated by the bit, the formation will be invaded by filtrate from the mud which is being discharged through the nozzles on the drilling bit. The hydraulic forces providing the driving force for filtration in such cases would be very large. In addition since the formation is being drilled, the tendency to create a filter cake would be counteracted by its removal and the consequent fluid loss could be substantial.

DYNAMIC FILTRATION:

After the bit has drilled out the formation, mud circulation between the drill string and borehole wall continues. This filtration process which can account for up to 80 percent of the fluid loss¹³ in a well is so called because the flow of mud across the borehole wall will cause erosion of the depositional force for cake build-up. With extended circulation time the depositional and erosional forces reach equilibrium and constant cake thickness and an equilibrium or quasi-steady state fluid loss rate is achieved. Dynamic fluid loss depends not only on the physical conditions in the circulating borehole but also on the properties of the components in the fluid system.

STATIC FILTRATION:

Static filtration takes place when the mud is not being circulated, and the filter cake grows undisturbed. In most cases, static filtration occurs through the cakes already formed during dynamic filtration.

1.1.3 Invasion of Filtrate into Formation

The invasion of filtrate occurs once filtration starts. It is well known that there is a mud spurt at the start of a filtration process before filtration proper begins. In the drilling well, mud spurt may be much larger when filtration takes place against the more permeable rocks⁹⁵: In fact they can be infinite (i.e. circulation is lost) unless the mud contains particles of the size required to bridge the pores of the rock, and thus establish a base on which the filter cake can form. However, the spurt loss may also be higher for low permeability formation⁹ if the internal filter cake forms inside the core. Only particles of a certain size relative to the pore size can bridge. Particles larger than the pore openings can not enter the pore, and are swept away by the mud stream, particles considerably smaller than the opening invade the formation unhindered, but particles of a certain critical size stick at bottle-necks in the flow channels, and form a bridge just inside the surface pores. Once a primary bridge is established, successively smaller particles, down to the fine colloids, are trapped, and thereafter only filtrate invades the formation. The mud spurt period is very brief, a matter of a second or two at the most²².

As a result of the process just described, three zones of mud particles are established on or in a permeable formation which are shown in Figure(1-1.1)⁹⁵.

- (i) An external filter cake on the walls of the borehole;
- (ii) An internal filter cake, extending a couple of grain diameters into the formation;
- (iii) A zone invaded by the fine particles during the mud spurt period, which normally extends about an inch into the formation^{15,25,89}.

Experimental results reported by Krueger and Vogel⁸⁵ suggest that these fine particles do not initially cause much permeability impairment, but may do so after filtration has proceeded for some hours, presumably because of migration and consequent pore

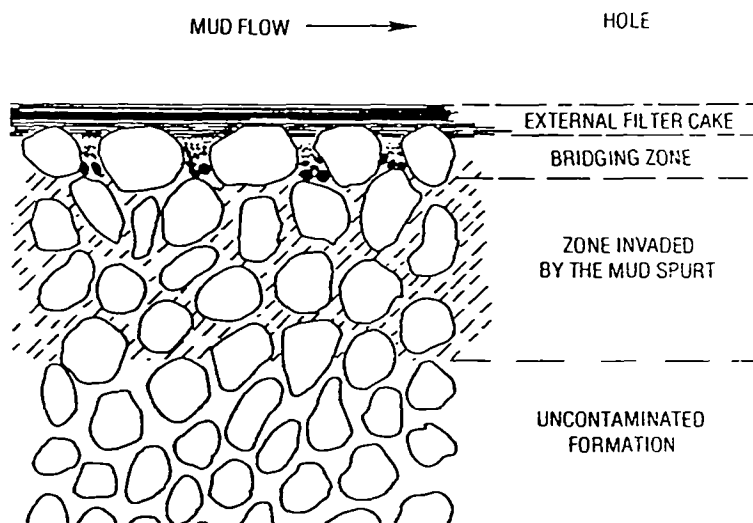


Figure (1 - 1.1) Invasion of a permeable formation by mud solids.

blocking.

1.2 THE PROBLEMS CAUSED BY FILTRATION OF DRILLING FLUIDS

1.2.1 Formation Damage

The formation damage is generally a reduction in permeability near the wellbore with perhaps a slight porosity reduction. Almost every field operation is a potential source of damage to well productivity. Diagnosis of formation damage problems has led to the conclusion that formation damage is usually associated with either the movement and bridging of fine solids or chemical reactions and thermodynamic considerations^{105,106}. The fine solids may be introduced from wellbore fluids or generated in situ by the interaction of invading fluids with rock minerals or formation fluids.

There are a number of ways that drilling fluid filtrate might interact with the formation to cause permeability damage. Some of these have been investigated in laboratories and described in published papers. Others are suggested by various observations and studies, but are not documented by actual damage tests. Some of the important formation damage mechanisms¹⁰⁴ which are related to the borehole filtration are shown in Figure(1-2.1) and briefly discussed below:

1.2.1.1 Clay Swelling

One of things to be aware of is that bentonite added to a mud system continues to hydrate for at least 24 hours. If this material is lost to potential producing zones, it can continue to swell in the reservoir and block permeability. Many producing formations also contain clay minerals such as illite, montmorillonite, and mixed layers clays. The

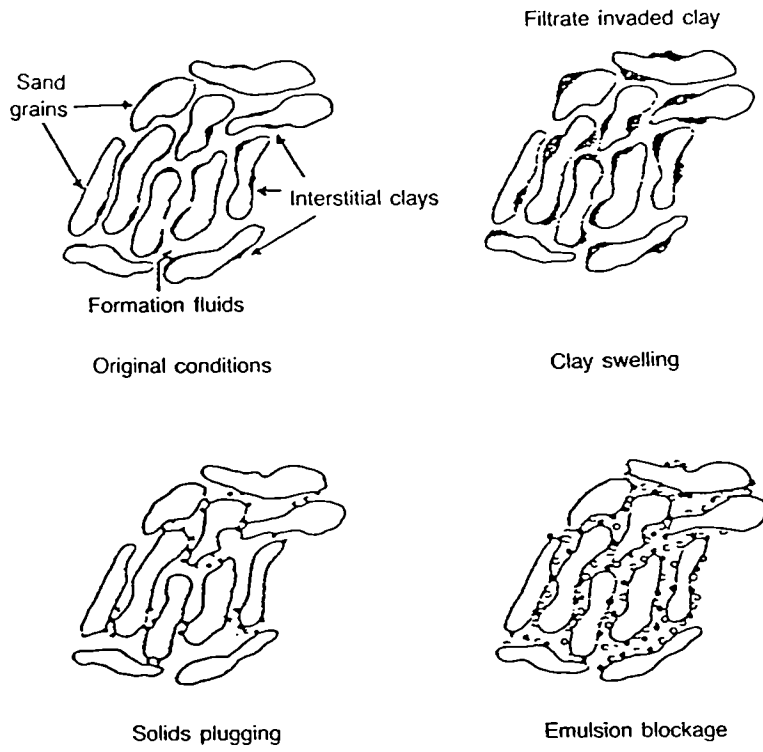


Figure (1 - 2.1) Types of formation damage

hydrated volume of the clay is dependent not only upon its composition and crystalline structure, but also upon the ionic environment. Certain clays such as the montmorillonite will upon contact with fresh water absorb hydrogen ions into the structure causing an increase in volume or swelling of the clay resulting in a reduction in pore volume and possibly plugging pore throats. In such cores the absolute permeability has been reduced. The hydration of clays can be prevented by using a mud system that offers ions which will be preferentially absorbed by the clay, e.g., Na^+ , Ca^{++} , K^+ by using an inhibited mud. Remedial treatments for swollen clays are available commercially but it is far easier to prevent clay swelling than it is to reverse it.

1.2.1.2 Dispersion and Migration of Formation Clay Particles

To control of flow properties, drilling fluid systems are usually maintained with high concentrations of strong dispersants. The filtrate from such a drilling fluid will tend to cause dispersion and migration of formation clay particles. Once dislodged, the clay particles will move back into the formation, plugging pores and reducing permeability.

1.2.1.3 Particle Plugging

In addition to formation damage from migrating fines generated in the formation, wellbore plugging may occur from fine solids carried by wellbore fluids during treatment. As distinct from particle migration, this term refers to the entry, movement and subsequent deposition in the pore space or pore throat of the porous media. The size of the particles which can invade the formation will depend on the porosity, permeability and stability of the filter cake on the wall of the borehole. Numerous investigators^{9,15,22,85,89} have considered the subject of mud particle invasion/plugging characteristics and others^{108,109,110} have considered the mechanics of particle deposition and plugging. Very few of the reported studies have adequately discussed particle entry and deposition with dynamic filtration as occurs in circulating boreholes.

1.2.1.4 Wettability

The use of complex organic chemicals often as finely divided particles (e.g., asphalts)

and surfactants in muds could have adverse effects on the wettability of cores. If reservoirs can be converted from being water wet to oil wet, the relative permeability to oil K_{rO} and thus the productivity will be reduced. Changes in physical conditions such as temperature, pressure and the pH environment could also cause changes in the wettability.

1.2.1.5 Water Blocking

The loss of large amounts of filtrate from water base muds could provide piston like displacement of in-situ oil. The water would then act as a barrier to oil production on a temporary basis. The impairment to productivity will reduce as cumulative production increases. However, if the filtrate has a very high viscosity, e.g., it contains polymer which is not completely solubilised, then the impairment might be more difficult to remove.

1.2.1.6 Emulsions

The formation of an emulsion of water and oil is promoted by a high degree of turbulence and mixing of two phases and by the presence of chemical emulsifier as used in oil emulsion mud systems. In the borehole filtration situation, it is unlikely that the filtration flow rate will be high enough to give rise to turbulence except in the spurt loss period. Chemicals which act as emulsifiers could be present, e.g., asphalt, bentonite, etc. Emulsions so formed can possess exceptionally high viscosity and if they are stable the productivity impairment is almost permanent. The use of surfactants to clear such emulsions has been tried but is only successful if intimate contact can be achieved which is very difficult.

1.2.1.7 Scales and Precipitates

The formation and subsequent deposition of precipitates or scales can occur when an insitu reservoir fluid is contacted with an incompatible filtrate. The salts so formed can be insoluble such as $BaSO_4$ or $CaSO_4$ and once present in the pore space they are difficult to remove. This mechanism can occur with both mud filtrates and also cement filtrates.

All the above formation damage mechanisms depend upon the invasion of filtrates from the wellbore filtration process and consequently the occurrence and severity of formation damage is very closely related to the filtration properties of the wellbore fluid and formation characteristics, i.e., controlled fluid loss will minimise near wellbore impairment.

1.2.2 Other Problems

1.2.2.1 Differential Sticking

Thick filter cakes may cause the drill pipe to become stuck by a mechanism known as differential sticking⁹⁵. This phenomenon occurs when part of the drill string bears against the side of the hole while drilling, and erodes away part of the filter cake. When rotation of the pipe is stopped, the part of the pipe in contact with the cake is isolated from the pressure of the mud column, and subject only to the pore pressure of the filter cake. The differential pressure thus created may be great enough to prevent the pipe from being moved.

The risk of stuck drill pipe may be reduced by using a mud that lays down a thin, tough filter cake.

1.2.2.2 Hole Instability

The filtration properties required for the successful completion of a well depend largely on the nature of the formations to be drilled. Stable formations⁹⁵ with low permeabilities, such as dense carbonates, sandstones, and lithified shales, can usually be drilled with little or no control of filtration properties. But many shales are water-sensitive, i.e., on contact with water, they develop swelling pressures which cause caving and hole enlargement. Sealing of incipient fractures by mud filter cake will help

control the caving, but the type of mud used and the chemical composition of its filtrate are more important factors.

Good filtration properties are also necessary when drilling in unconsolidated sands, which will slump into the hole unless protected by the rapid formation of a filter cake.

Chapter Two

LITERATURE SURVEY ON FILTRATION PROPERTIES OF DRILLING FLUIDS

The objectives of the study of the filtration of drilling fluids have been discussed in the preceding chapter. This chapter reviews the previous experimental studies of filtration properties of drilling muds with particular reference to those which are directly relevant to the subject under investigation and attempts are made to summarize from the literature, the effects of the individual parameters under downhole conditions upon the filtration performances.

2.1 AN OVERVIEW OF LITERATURE ON BOREHOLE FILTRATION OF DRILLING MUDS

The published investigations into the borehole filtration properties of drilling muds were first given by Jones and Babson¹ in 1935. Their tests were conducted upon the artificial formation prepared from the unconsolidated sand at pressures up to 4000 psi and temperatures up to 275 °F under dynamic conditions. The following results were reported:

- (1) Filtration flow rate attained a substantially-constant value at the end of about two hours;
- (2) There was no apparent penetration of mud into the formations, and in no case

was a penetration more than about 1/16 inch.

- (3) Regardless of the nature of the mud used or the temperature of the tests, variations in pressure above 500 psi had very little effect on the filtrate flow rate or on the thickness of the mud cake deposited.
- (4) Regardless of the pressure applied or the nature of the mud involved, both the fluid loss and mud cake thickness increased materially with an increase in temperature.
- (5) The fluid loss increased rapidly with reduced apparent viscosity for weakly thixotropic muds but it was not influenced for strong or moderately-strong thixotropic muds.
- (6) In all cases, very thin mud cakes were deposited by mud having low funnel viscosities, and with the thixotropic mud an increase in viscosity appeared to have no pronounced effect on the thickness of the mud cake. However, the mud cakes deposited by the muds having only moderately-strong or weak thixotropic properties, increased in thickness with an increase in funnel viscosity.

In 1937, Jones² presented a paper in which he described a static filter loss tester to be used for routine filter loss tests. This instrument subsequently was adopted by the API as the standard API filter loss tester.

Williams and Cannon³ performed a number of experimental tests to evaluate the properties of filter cakes deposited by static filtration at pressures ranging from 30-1500 psi for a wide range of drilling muds, The results concluded that:

- (a) The measured permeability values of filter cakes were between 0.2×10^{-3} and 0.6×10^{-3} md at 8 atmospheres pressure for Gulf Coast field muds, and more than 100 times higher for a West Texas mud;
- (b) At each temperature, the cake permeability increased with increased addition of weighting material;
- (c) Cake resistance was increased by the addition of Bentonite;
- (d) The rate of filtration could be varied considerably by adding weighting materials

having a particular particle-size distributions.

In 1938, Larsen⁴ reported a study of both static and dynamic filtration experiments of drilling muds conducted at pressures ranging from 25-8000 psi and temperatures in the range of 60-250 °F. The filter medium included filter paper, sintered aluminum disc, sand packs and cores. He also developed a relationship between filtrate volume and filtrate time which will be discussed in chapter three and tried to predict the effect of temperature on filter loss by relating temperature effects through the temperature dependence of filtrate viscosity. This was undoubtedly an over simplification of the temperature dependence of drilling fluid filter loss. The conclusions reported by Larsen highlighted the following:

- (1) Apart from a small zero error, fluid loss was proportional to the one-half power of time, and was best plotted against this power of time to give the best straight line.
- (2) Fluid loss was inversely proportional to the one half power of the filtrate viscosity, which might be calculated from the temperature if other conditions remained unaltered.
- (3) Fluid loss was generally an exponential power of the pressure, and thus might be plotted against pressure on log-log paper to give a straight line.
- (4) Cake thickness was proportional to fluid loss.
- (5) Cake composition was largely independent of time and did not vary for a given mud in various dilutions with water, that is, at different percent solids content of the mud.
- (6) Fluid loss was largely independent of the nature of the filter bed material.
- (7) Fluid loss was independent of circulation past the face of the core, as long as this circulation was slow enough not to hydraulic-erode-off the cake.
- (8) Fluid loss was increased by calcium ion flocculation of the mud.

Byck⁵ studied the plastering properties of six representative drilling muds over a temperature range of 70 °F to 175 °F at several mud weights, using a high-pressure circulating filter press similar to the one used by Jones and Babson¹, with full size

consolidated cores.

The following results were concluded:

- (1) In all tests, with untreated as well as with chemically treated muds, the filtration rates at elevated temperature were higher than at low temperatures and in nearly every case the increased filtration rate was notably larger than could be attributed alone to the decreased viscosity of fluid at elevated temperatures, e.g., it was found that the six muds tested, three had 8% to 58% greater filter loss at 175 °F (70 °C) than had been predicted from the filter loss at 70 °F (21 °C) by substituting the changes in filtrate viscosity. The permeability of the cake increased correspondingly, with the maximum change being from 2.2×10^{-3} to 4.5×10^{-3} md—an increase of over 100% . Filtration rates of the other three muds deviated from the predicted values by only $\pm 5\%$, and the permeabilities of the cakes remained essentially constant.
- (2) No existing method would permit even an approximate determination of the filtration rate at high temperature from data obtained at room temperature.
- (3) No relationship was observed between mud viscosity and filter cake characteristics.
- (4) It was found that chemical treatment of the muds for viscosity reduction shifted the temperature of minimum viscosity to appreciably higher values than for untreated muds.

Williams⁶ in a series of experiments conducted dynamic filtration and observed that the equilibrium filtrate flow rate was reached after only a short time. The value of the equilibrium filtration rate was related to a constant thickness filter cake which was produced by an equilibrium between the deposition and the erosion of solids. This value was to be a function of the pressure, mud circulation rate and the mud properties.

Byck⁷ investigated the effect of formation permeability on the filtration characteristics of drilling muds. The filter cake permeabilities measured by him were between 0.46×10^{-3} and 7.42×10^{-3} md at 34 atmospheres pressure with California muds. By

making some determinations on cores of permeabilities from 10 to 14,000 md, it was shown that the filtration rate was dependent only on the permeability of the cake—at least as long as it was several orders of magnitude lower than that permeability of the formation.

Gates and Bowie⁸ reported the relationship between particle size distribution and wall building or filtration properties, the viscosity, PH, and density of mud fluids samples from drilling wells and laboratory.

The conclusions indicated from the results of the tests described in their report were as follows:

- (a) Most of the mud fluids that had the best filtration or wall building properties (lowest filtration rates) were composed of particles having a relatively uniform particle size distribution.
- (b) The mud fluids that had the best filtration control properties were composed of approximately 65% (by weight) colloids (range of 42-88%), 30% silt (range of 7-46%), and 5% sand (range of 0-13%).
- (c) The samples of muds tested that had the poorest filtration properties (higher filtration rates) were composed of approximately 1% colloids (range of 0-6%), 94% silt (range of 87-100%), and 5% sand (range of 0-13).
- (d) Apparently no simple relationship exists between the viscosity as measured in the Stormer (600 rpm) and Funnel viscometers and the particle size distribution of the mud fluids tested.
- (e) Apparently no simple relationship exists between PH and particle size distribution or the filtration properties of the drilling mud fluids tested.
- (f) A small quantity of sand (less than 10% by weight) had no apparent effect upon the filtration properties of the samples of muds tested.
- (g) Without exception, increasing the temperature increased the filtration rates of the mud fluids tested.

Nowak and Krueger⁹ presented some results on studies of the effect of mud filtrates

and mud particles upon the permeabilities of the cores. Their filtration tests were conducted in a mudding-off cell in which mud and bit action could be simulated under temperature and pressure conditions approximating those in the wellbore. From the tests data, they concluded:

- (i) Particles were observed to penetrate into and through a test core of alundum, and plugging caused by mud particle invasion was indicated in deplastering tests.
- (ii) Filtrate loss curves for each of three field drilling fluids (Clay water base, Oil base, and Emulsion base) indicated from tests on 4 synthetic cores whose permeabilities ranged from 14 to 248 md that there was a dependence of filtrate loss upon the permeability of the formation. This result could apparently be explained by particle invasion into the core. In these particular tests, low permeability core showed filtrate losses higher than those for high permeability cores.

Prokop¹⁰ performed radial filtration of drilling mud in a laboratory tester, in which mud flowed through a concentric hole in a cylindrical artificial core. He measured the dynamic filtration rates and the filter cake thickness. In addition, he extensively investigated the mechanisms which govern the build-up of filter cakes and reported that the major factors controlling filter cake formation in a circulating system should be:

- (a) The rate of deposition of solids from the mud;
- (b) The erosive force that the flowing mud exerts upon the filter cake;
- (c) The erodability of the filter cake;
- (d) Any change in filter cake characteristics attributable to the scouring action of the mud.

He also thought that the rate at which solids were deposited from the mud would be controlled to a large degree by the filtration characteristics of the mud, the pressure differential, the temperature under which filtration was taking place, and the thickness of the filter cake already in place. The erosive action of the circulating fluid should be

dependent upon the circulation velocity, the fluid properties, and the type of flow existing in the fluid column, i.e., whether turbulent or viscous.

From the results, the following conclusions were suggested:

- (1) A filter cake deposited in a quiescent filter cell showed little change in permeability during a long filtration period. Filter cakes deposited during continuous circulation would gradually decrease in permeability as long as the experiment continued. This was evidenced by a continual decrease in filtration rate after the filter cake had reached a constant thickness.
- (2) A thick filter cake formed during a period of non-circulation was very hard to erode away by mud circulation.
- (3) Much thicker filter cakes were deposited with the mud flowing in viscous rather than in turbulent flow.
- (4) It was found that a fluid flowing in turbulent flow would erode a filter cake at a rate proportional to the square of the circulation velocity.
- (5) Experiments conducted by depositing a filter cake during continuous mud circulation showed that, in general, the higher the filtration rate of a mud, the thicker was the equilibrium filter cake and the higher was the eroding velocity necessary to stop further formation of filter cake. Table 2.1 illustrated the typical results.
- (6) Mud viscosity appeared to affect erosion only in as so far as it controlled the type of flow existing in the circulating fluid, i.e., whether it was turbulent or viscous.

Schremp and Johnson¹¹ divided the filtration process into two steps:

- (i) Bridging of opening in the filter medium;
- (ii) Filtration of fluid through the filter cake that developed on the filter medium as filtration takes place.

Table 2.1 Equilibrium Cake Thickness under Dynamic Filtration¹⁰

Mud Base (all muds treated with lime, caustic soda and quebracho)	API filter loss (cc in 30 min)	Equilibrium Cake Thickness		Mud Velocity Equilibrium	
		(inch)	(mm)	(ft/min)	(m/min)
Bentonite	19	1/32	0.8	125	38
Calcium Bentonite and Barite	8	3/32	2.4	48	15
Calcium Bentonite	10	6/32	4.7	72	22
Attapulgate and Bentonite	85	19/32	15.1	220	67
Attapulgate and Bentonite	148	21/32	16.6	530	161

Mud circulated through a 2 inch (5.08 cm) diameter hole in consolidated sand. Turbulent flow. Filtration pressure 350 psi (24.6 kg/cm²)

and reported the results obtained from high temperature, high pressure filter loss studies in which field samples of clay-water, emulsion and oil base fluids were used. The filter loss tests were conducted at temperatures of 150, 200, and 250 °F and at differential pressures of 100, 1000, and 2000 psi. They showed that there was no way that filter losses at high temperature could be predicted from measurements made at a lower temperature. It was therefore concluded by Schremp and Johnson that it should be necessary to test each mud separately at the temperature of interest in a high temperature cell.

Beeson and Wright¹² produced a paper on the investigation of the mud loss, including solid particles, to formations. They discussed the entrance of whole mud, as well as filtrate, into pore channels of a size that exists in productive oil sands. The following conclusions could be drawn from their paper:

- (1) Their experimental data showed that a mud might give a negligible loss on filter paper, but give a large one on a permeable formation downhole.
- (2) The discrepancy between the gross loss on paper and that on the porous media was greater with unconsolidated sand than with consolidated rocks, even when the permeability of the latter was higher.
- (3) The discrepancies between the net filter loss on paper and on porous media increased with increase in spurt loss. Evidently the mud spurt plugged the cores to such an extent that the pressure drop within the core becomes significant, thereby reducing the drop across the cake, and reducing cake compaction.
- (4) The difference between the fluid loss on fine filter paper and on sand indicated that mud particles entered the pore channels prior to and during formation of the cake in the sand.

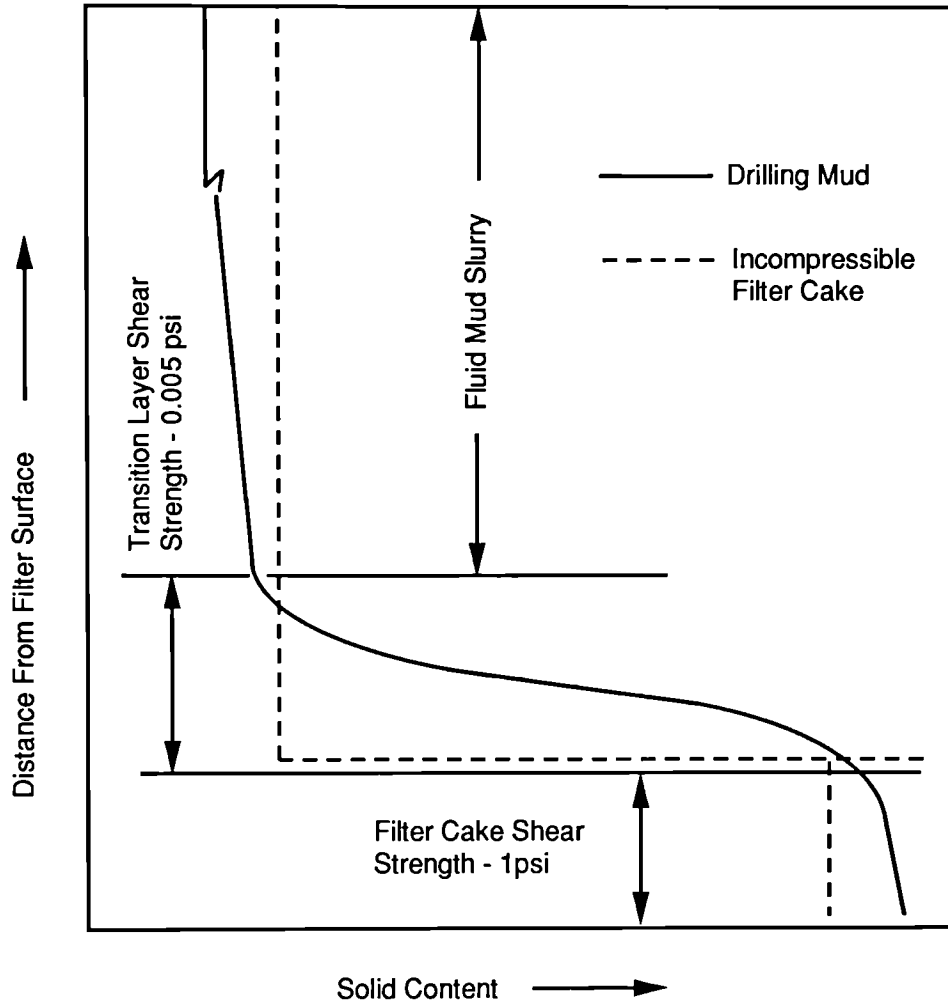
When accurate values of static cake thickness are required, the following method advised by von Engelhardt and Schindewelf⁹⁷ should be used: Only a limited amount of mud is put in the filter cell, and filtration is stopped at the moment all of the mud is used

up, so that only filter cake remains in the cell. The critical moment to stop filtration is determined by observing the filtrate volume at short time intervals, and concurrently plotting the volume versus the square root of the intervals. Filtration is stopped immediately when the curve departs from linearity. The total volume of mud filtered is calculated from the combined weight of the original mud. The cake volume is then obtained by subtracting the filtrate volume from the volume of mud filtered.

Ferguson and Klotz¹³ reported an outstanding piece of research on drilling fluids filtration in a paper published in 1954. They divided the filtration process of muds into three classes:

- (i) Static filtration — Mud does not circulate, filtration rate are controlled by cake performance. Cake thickness increases and filtration rate decreases continually with time;
- (ii) Dynamic filtration — Drilling mud circulates past the surface of the filter cake. Filtration rate is controlled by cake thickness. Cake thickness and filtrate flow rate become constant depending upon mud circulation and upon drilling string rotation;
- (iii) Filtration from beneath-the-bit while drilling — No filter cake forms beneath-the-bit. Filtration rate is controlled by plugging of the formation ahead of the bit by mud particles.

Their experiments were conducted on a large scale model wellbore which allowed the simulation at 500 psi of the radial flow of filtrate due to the above three types of filtration. They also reported a defined interface between filter cake and slurry, which is clearly shown in Figure(2-1.1). The figure showed the solids content as a function of distance from the filter cake surface for a classic incompressible filter cake and for a drilling mud filter cake. The interface between classic incompressible cake and slurry is defined sharply, but between drilling mud cake and mud slurry, it is not. It is believed that the solids concentration increases abruptly from the slurry to the cake in the former case, however, in the latter case, the interface between the cake and slurry has finite thickness,



Figure(2-1.1) Transition Layer Between Drilling Mud Filter Cake and Fluid Mud

and then the solids content increases gradually from the slurry to the cake through a transition region. They reported that the curves in Figure(2-1.1) as drawn here, are certainly qualitative, which apply to no particular mud. This transition region influences dynamic filtration and may account for the apparent equilibrium filter cake thickness observed in dynamic filtration, whereas shear strength of the cake is so high that hydrodynamic shear does not disturb it, shear strength of the upper part of the transition layer is only about 0.005 psi. This layer can therefore be removed by fluid flowing under a pressure gradient that is typical of mud flow. During dynamic filtration, this transition layer is swept away continually and cake thickness is limited even though fluid shear does not erode the dense part of the cake.

During experimental study, they obtained some excellent data on dynamic filtration rates in a small model well which duplicated field geometry. Holes were drilled in artificial sandstone blocks with 5¹/₄ inch and 5³/₈ inch bits. Figure(2-1.2) through (2-1.5) showed the change in dynamic filtration rates with time for four muds at various circulating velocities. The following conclusions were concluded:

- (1) Dynamic filtration rate starts high, about the same as the rate that would be predicted for static filtration. As dynamic filtration continues, the rate does not drop as rapidly as the static rate, and, after about 15 hours, the dynamic rate becomes constant or nearly constant, whereas static filtration rate continues to decrease.
- (2) The time to reach constant dynamic filter rates varied from 2 hours to over 25 hours, depending upon the type of mud and upon the flow velocity.
- (3) The equilibrium dynamic filtration rates do not appear to be related to the extrapolated API fluid loss for any of the muds. Moreover, muds with the lowest API filter loss, do not have the lowest equilibrium dynamic filtration rate.
- (4) The estimated amount of filtrate invasion as shown in Table 2.2 that would take place during the various stages of drilling and completing a hypothetical

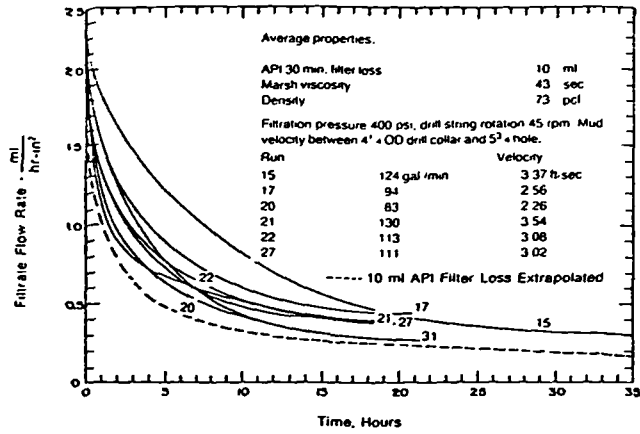
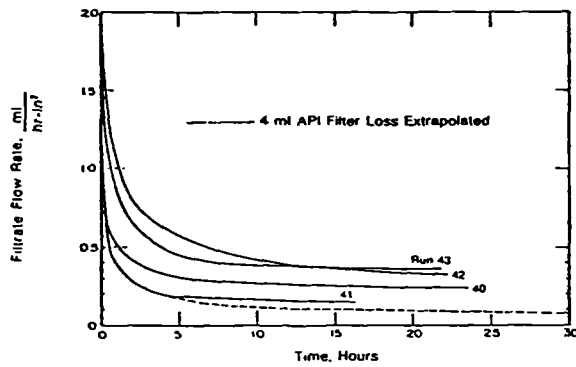


Figure (2 - 1.2) Dynamic filtration from bentonite mud.



Filtration pressure 200 psi, drill string rotation 90 rpm. Mud velocity between 4" x drill collar and 5" x hole.

Run	Velocity	Average properties:
40	92 gal/min 2.5 ft sec	API 30 min. filter loss 4 ml
41	40.5 1.1	Marsh viscosity 50 sec
42	125 3.4	Slover viscosity 25 cp
43	111 3.0	Density 75 pcf

Figure (2 - 1.3) Dynamic filtration from lime-starch mud.

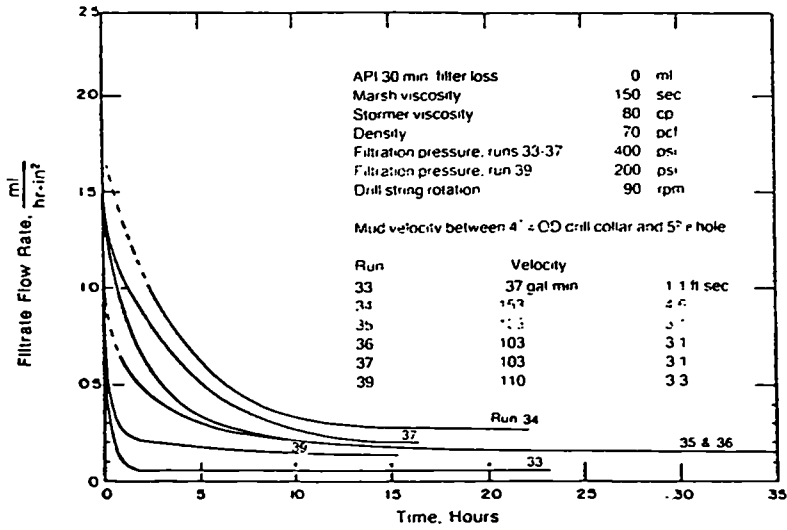
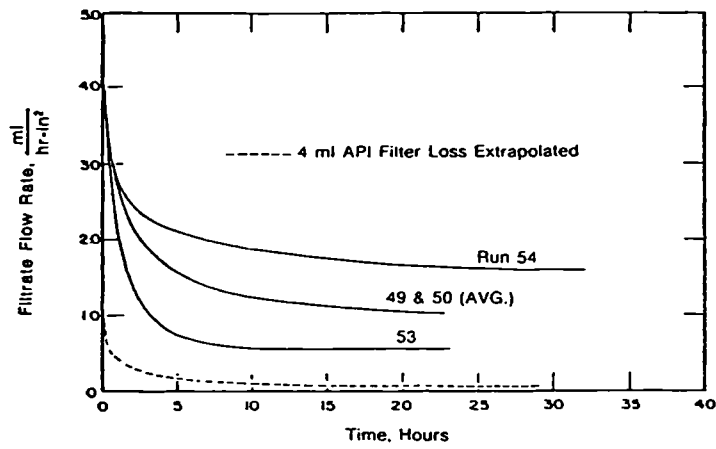


Figure (2 - 1.4) Dynamic filtration from oil base mud.



Average properties:

API 30 min. water loss
 Marsh Viscosity
 Stormer Viscosity
 Density

4 ml
 45 sec
 17 cp
 70 pcf

Filtration pressure 400 psi; drill string rotation 90 rpm; Mud velocity between 4" x OD drill collar and 5" r hole:

Run	Velocity
49 and 50	149 gal/min 5.0 ft/sec
53	62.5 2.1
54	286 9.6

Figure (2 - 1.5) Dynamic filtration from emulsion mud.

Table 2.2 Drilling Schedule and Filtration Invasion¹³

Operation	Time (hours)	Filtrate Volume (ml/in ²)	Invasion Radius (inches)	Invaded Zone Thickness (inches)
Drill through zone at 5 fph			7.3	3.5
Drill below zone at 5 fph	50	120	18.4	14.6
Round trip to replace bit	8	3.5	18.6	14.8
Drill below zone at 5 fph	50	61.5	21.1	17.3
Pull pipe, log well, run pipe	12	2.9	21.3	17.5
Condition hole to run casing:				
Circulating drilling mud	2	2.9	21.5	17.7
Pull drill pipe	4			
Run casing	12	2.9	21.7	17.9
Cementing casing, end of mud filtration:				
Total Mud Filtration	138	192	21.7	17.9

well, assuming a sand at 7,000 feet and a total depth of 7,500 feet showed that some 95% of the invasion would take place under dynamic conditions while drilling, and only 6% under static conditions while tripping and completing.

- (5) Mud particle bridging and plugging apparently limit the flow of filtrate from mud stream to formation even beneath-the-bit where no mud cake exists.

They compared the fluid loss behaviour of an incompressible and compressible filter cake using an analytical model, the filter cake was assumed to exist in thin layers. The permeability, K_i , of each layer was assumed to depend on the pressure gradient, P_i , in that layer at the time it was deposited, according to the equation:

$$K_i P_i^n = \text{Constant}$$

where

K_i, P_i were the permeability and the pressure gradient respectively upon layer "i" in the cake.

As cake thickness increases, while total filtration pressure remains constant, P_i becomes smaller and K_i larger, for each succeeding layer of the filter cake. The application of this to a composite cake leads to a filtration curve of cumulative filtrate volume V vs. the square root of filtration time \sqrt{t} which is concave. This does not agree with experimental observations. Feguson and Klotz therefore proposed a hypothesis that the filter cake comprised two layers. The lower layer was a filter cake consisting of deposited and packed solid particles, whilst the upper layer consist of a mud gel. This mud gel would have two properties:

- (a) The velocity of the gel would be greater than that of the solid particles contained in the gel, i.e. leakoff rate would be high through the cake where as the rate of the particles deposition would be substantially decreased. This would obviously only occur after the spurt loss period when the cake would slow down the mud filtrate velocity through the filtration surface and increase the gel strength.

- (b) The resistance to the flow, because of the gelled layer, would increase with time (gel strength formation being time dependent) and hence filtration rates would decrease. This decrease may counteract the concave filtration curve to give the straight line behaviour observed in experiments.

Havenaar¹⁴ presented the experimental filtration data at the bottom of the borehole and a good quantitative interpretation of the data using a formula derived from the following assumptions:

- (i) Each time a blade of a drag bit, or a cone of a roller bit, moves along the bottom of the hole, the mud cake is completely removed.
- (ii) A new mud cake is immediately formed on the freshly produced surface, and losses of whole mud into the formation are negligible (this is equivalent to an immediate plugging of the pores).
- (iii) The filtration of the mud at the bottom of the hole follows the classic law.

The equation for filtration through the bottom of the hole while drilling reported by Havenaar will be discussed in chapter three.

Table 2.3 compares filtration rates calculated by his equation with experimental data of Ferguson and Klotz¹³. The poor correlation obtained with oil base mud is probably because cakes of oil base muds are easily eroded, and Havenaar's equation neglects erosion by the mud jets.

In two related papers, Glenn and Slusser¹⁵ concluded from the experimental volume-time data obtained during exposure of filter paper or a consolidated porous medium to a mud under differential pressure that there could be three stages involved in an experiment. viz:

- (i) Mud spurt period — An initial period which mud particles bridged pores inside porous medium and initiated filter cake formation. Filtration rates were very high.
- (ii) Non-uniform cake thickness period — An intermediate period during which

Table 2.3 Comparison Between Calculated and Experimental Bottomhole Filtration Rates¹⁴

Muds	V ₃₀ (ml)	C (sec/cm ²)	Rate of Drilling (fph)	Bottom Hole Filtration Rate (Q = cm ³ /sec)	
				Calculated	Experimental
Field	10.1	7.2×10^4	11.3	1.6	3.7
Gel	10.5	6.7×10^4	11.6	1.6	3.6
Gel	10.5	6.7×10^4	6.2	1.6	2.5
Oil Base	0.2	1.8×10^8	32	0.04	0.52
Lime Starch	4.1	4.4×10^5	19	0.73	0.60
Lime Starch	4.1	4.1×10^5	43	0.73	0.6 — 4

filter cake build-up inside porous medium occurs and the differential pressure across the cake increases. Additional particles were “piled-up” behind the bridging particle or particles so that a “filter cake” was rapidly built up. Filtration rates were in continuous decline.

- (iii) Constant pressure filtration Period — A later stage in which pressure across filter becomes constant. Filtration rates were constant.

The following conclusions were reported:

- (1) The mud spurt loss increased with pressure differential for a given sample permeability and the mud spurt loss at a given pressure differential increased with increasing original sample permeability.
- (2) The bridging phenomenon and the presence of particles in the filtrate indicated that the mud spurt loss could depend upon the particle size (and shape) distribution of the mud, the pore entry size distribution of the porous medium.
- (3) Particles bridge pores inside porous media during the surge period and filter cake build-up inside porous media occurs during subsequent filtration.

Horner, *et al.*¹⁶ reported a laboratory study of the effects of physical and easily measured rheological properties, such as apparent viscosity, plastic viscosity, yield value, density and API fluid loss under beneath-the-bit and dynamic filtration conditions. Those conditions were:

Samples: Torpedo sandstone, 2 inch diameter, 4 inch length, 1500 to 2000 md permeability, 25% porosity;

Saturation Fluid: Distilled water;

Differential Pressure: 5 psi;

Flow rate: Approximately 6 gal./min.;

Drilling rate: 1.5 — 2.0 ft/hr;

Penetration: 3 inch;

Bit size and type: 1¹/₄ inch microbit.

The conclusions drawn from their work may be summarized as follows:

- (a) The lack of correlation between either the filtration rate beneath-the-bit or dynamic filtration rate and the API filter loss was ascertained by the experimental data.
- (b) Filtration rates beneath-the-bit, unlike filtration rates through the bore walls, are influenced by the permeability of the formation.
- (c) No relationship could be ascertained between beneath-the-bit and dynamic filtration and the rheological properties identified above.

In a paper concerned with the effect of borehole variables on drilling rate, Cunningham and EeNick¹⁷ reported experiments performed to determine the pressure drop across mud filter cakes. They reported that a pressure of 5000 psi was required to obtain 0.3 cc/min of filtrate rate through the core plus filter cake. After removing the cake, it required 50 psi to achieve the same filtration rate. Five thousandths of an inch was removed from the end of the core and the experiment repeated requiring only 2 psi to flow the same rate as before. The influence of these results is that the filter cake permeability is at least 3 orders of magnitude lower than the core and the internal filter cake formed is limited to a very close proximity to the core face.

The effects of elevated temperature on the filtration of drilling fluids was reported by Milligan and Weintritt¹⁸. They concluded that interpretation of data might be more involved than in the API filtration tests because some muds might undergo irreversible reactions or changes in composition while filtering at an elevated temperature. They also found that more filtration occurred at low differential pressures than at high differential pressure when mud was treated with a surfactant. This behaviour was explained that at high differential pressure the filter cake is more easily compacted than in the mud without the surfactant, which could keep the dispersed bentonite broken up into particles.

In 1961, Gatlin and Nemir¹⁹ reported an investigation of the effects of particle size distribution on bridging in lost circulation and filtration tests. They concluded that a

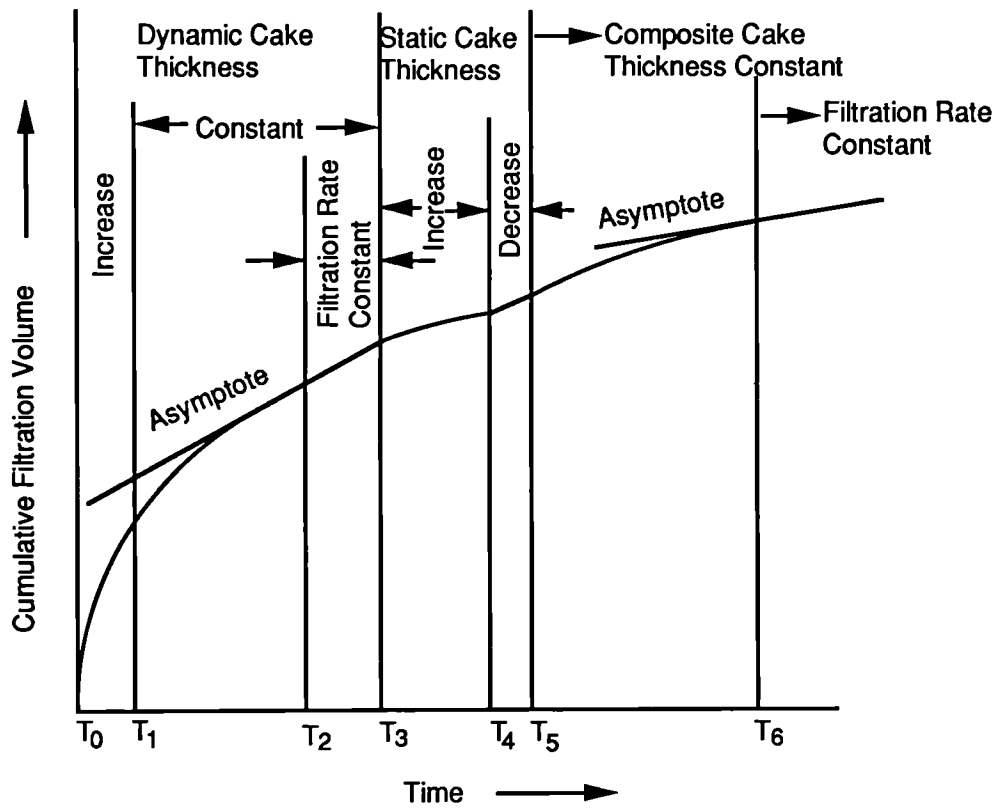
maximum density distribution of the “large” particles in commercial bentonite reduces the initial surge or “spurt loss” of a bentonite mud in the standard filter press test and the maximum density theory, which is based on inert particles, apparently does not hold for the linear portion of the filtration curve of a bentonite mud.

Krueger²⁰ reported a study aimed at evaluating the effect of various additives on dynamic fluid loss performance. His tests were conducted in a mud circulating system at a pressure of 500 psi and temperature of 170 °F. Dynamic filtration rates were obtained in each experiment under two different simulated wellbore conditions:

- (i) Filtration just above the bit through a new mud cake laid down dynamically on a freshly drilled formation;
- (ii) Filtration up hole through a mud cake formed by deposition of a static filter cake on top of the initial dynamically formed cake.

The lack of correlation between the API filter loss and the dynamic filtration rate reported by Ferguson and Klotz¹³ casts doubts upon the validity of the API test as a criterion for downhole filtration rates. Experimental work by Krueger substantiated these doubts. His results were presented as graphs of API static fluid loss versus the equilibrium dynamic fluid loss for muds with an increasing concentration of specific fluid loss control additives. The results showed that there was a different relationship between dynamic filtration rate and API filter loss for each agent.

Krueger also produced a typical curve for accumulated fluid loss vs. time which is shown in Figure(2-1.6). After about 6 to 10 hours, equilibrium conditions are reached and fluid loss rate becomes constant as indicated by the straight line portion of the curve. The slope of the portion of the curve in millilitres per hour is the dynamic fluid loss rate through the equilibrium dynamic mud cake laid down on newly exposed formation. The second portion of the curve represents the period during which circulation was stopped and the static mud cake allowed to build-up on top of the dynamic cake. The third portion of the filtration curve represents the period after circulation is re-started. Shearing action of the flowing mud stream is insufficient to wash off the mud cake, except for the weak



Figure(2-1.6) A Typical Plot of Cumulative Filtrate Volume Collected as a Function of Time For Sequential Filtration

surface structure (the “transition layer” defined by Ferguson and Klotz¹³) and a new equilibrium dynamic fluid loss rate is established. Because fluid loss is now restricted by the combination static-dynamic cake, the equilibrium dynamic fluid loss rate is much less than the previous rate which was limited by the dynamic cake alone.

In 1963, Outmans²¹ primarily concerned with the numerical modelling of static and dynamic filtration and developed a theoretical-empirical nonlinear diffusion equation describing the mechanisms of filtration through a compressible filter cake based upon four assumptions:

- (i) The fluid flow through a compressible porous medium is governed by Darcy's law.
- (ii) The rate of change in fluid content of an element of the porous medium is proportional to the rate of change of solid pressure between the particles.
- (iii) The solid particles are incompressible within the range of pressures considered.
- (iv) The total pressure on a surface normal to the line of flow is equal to the sum of the fluid pressure and the pressure between the particles (solid pressure) at that surface.

He suggested that dynamic filtration consists of three distinct stages as shown in Figure(2-1.6):

- (i) The first stages is the deposition of the particles in the form of “card pack” floc and is characterised by increasing cake thickness. This stage is represented by the time interval T_0 to T_1 .
- (ii) The second stage is characterised by filtration through a cake of constant thickness. Outmans suggested that during this phase the cake continues to compact but since the cake thickness is constant the rate of deposition and the rate of compaction must be equal. This phase is represented by the curve between times T_1 and T_2 .
- (iii) The third stage is characterised by equilibrium conditions in that the filtration rate, cake thickness and permeability are constant between times T_2 and T_3 .

The theory proposed by Outmans²¹ for the generation of an equilibrium filter cake on a basis of continuing compaction is markedly different from that suggested by Prokop¹⁰ of a sorting/classification mechanism due to mud flow through the surface of the cake leading to denser packing and constant permeability to thickness ratio. The curve produced by Outmans model²¹ is similar in shape to that produced experimentally by Krueger²⁰.

From the results, the following conclusions were presented:

- (1) The most effective fluid loss control agents under dynamic flow conditions were starch and the organic viscosity reducers, quebracho and complex metal lignosulfonate in clay-gel drilling fluid.
- (2) Experimental data confirmed the theoretical conclusion that a dynamic cake, once formed, is extremely difficult to erode.
- (3) It is also experimentally verified that the dynamic rate of filtration decreases when the drilling fluid becomes less viscous and also if the rate of circulation is reduced.

Darley²² designed an apparatus to measure the change of filtrate flow rate during the first second of the filtration process and reported that initial filtration rates depended upon the concentration of solids and particle size distribution in the mud. The results presented by Darley suggested that there was a critical size range for bridging in the surface pores. Larger or smaller particles did not cause bridging—the larger particles because they could not enter the pores and were swept away by the mud stream, the smaller particles because they could pass freely through the pores. However, once the pores were bridged by the right size particles, successively smaller ones were trapped, and a filter cake was established.

Bo *et al.*²³ extensively investigated the effect of particle-size distribution on the permeability of filter cakes and reported that the lack of the definition of “particle size” led to an anomalous correlation between particle size and filtration rate. They criticized the

“average particle size” concept and suggested the proper criterion should be particle-size distribution. Experimental work presented by them showed that widely different permeabilities and porosities (and hence filtration rates) could exist in beds of particles with the same overall size range but with different size distributions within that range.

In 1966, Bezemer and Havenaar²⁴ conducted dynamic filtration tests in two different type of apparatus. One of them consisted of a porous filter pipe through which the drilling mud was circulated, dynamic filtration rates and cake thickness were determined as a function of flow rate and time. The other was a simple filter apparatus where mud flow was similar to that in a rotational viscometer. Filtration pressure was limited to 100 psi.

From the results, the following observations were reported:

- (1) A state of equilibrium was eventually reached; i.e., both cake thickness and filtration rate attained constant values.
- (2) The rate of shear at the cake surface is a measure of the effect of mud flow on dynamic filtration. This means that borehole conditions of laminar mud flow can be simulated in laboratory filtration tests. Of the two arrangements used, the dynamic filter apparatus is clearly much more suited than the filter pipe.
- (3) The equilibrium filtration rate was found to be proportional and the equilibrium cake thickness inversely proportional, to the rate of shear at the cake surface for most types of mud investigated.
- (4) The erodability of the cake surface is independent of temperature and pressure. The equilibrium rate of filtration being independent of temperature, a reduction in the viscosity of the mud filtrate by raising the temperature is compensated by a increase in cake thickness. In a similar way, an increase in filtration pressure is mainly compensated by a reduction in cake permeability. In the limited range of filtration pressures and temperatures investigated, it was found that: (a) equilibrium filtration rate is not affected by filtration temperature and differential pressure; (b) equilibrium cake thickness increases with increasing filtration temperature (if the cake permeability remains unaffected by temperature,

equilibrium cake thickness is inversely proportional to mud filtrate viscosity);

(c) equilibrium cake thickness is hardly affected by filtration pressure.

- (5) Higher mud circulation rates resulted in higher equilibrium filtration rates and shorter time for the filtration process to reach equilibrium.

Young and Gray²⁵ conducted beneath-the-bit filtration during microbit drilling tests.

The following results were concluded:

- (a) The filtrate flow rate measured beneath-the-bit was found to be independent of borehole pressure and rock permeability.

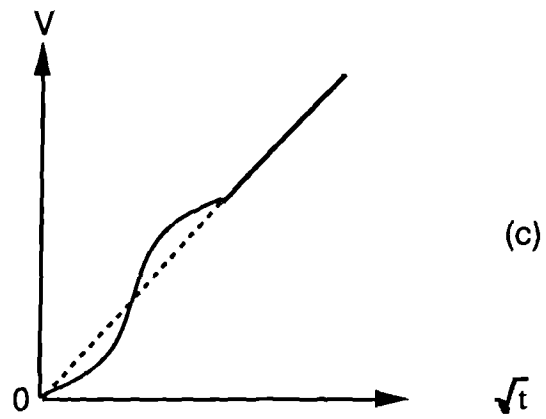
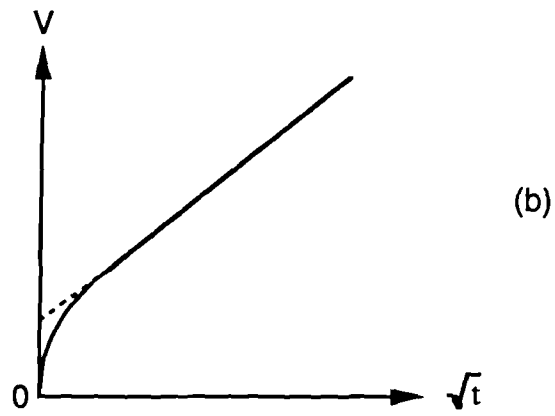
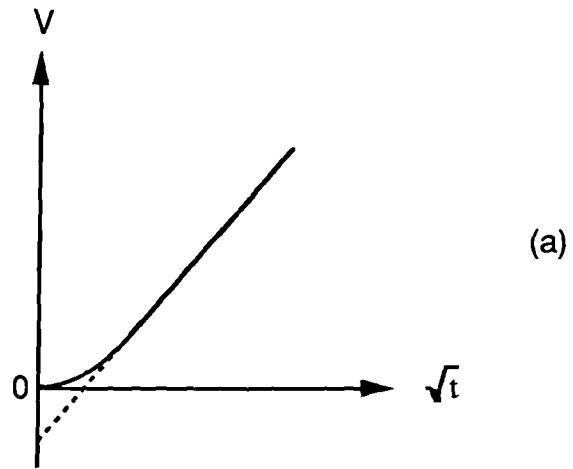
The filtrate flow rate beneath the bit using both low fluid loss mud and high fluid loss mud was constant as core length decreased, which was explained by a deposition of very low permeability of the filter cake.

- (b) An observed reduction in drilling rate is associated more with the reduction in mud cake permeability rather than spurt loss.

Considerable rock permeability damage was found beneath-the-bit in all samples tested, this damage was proportional to both borehole pressure and rock permeability. Extensive permeability reduction was found to about 1 cm beneath-the-bit in high-permeability rock drilled with water, and to less than 1/2 cm in those drilled with low fluid loss mud.

- (c) The API static fluid loss may be a good indicator of beneath-the-bit filtration rates.
- (d) The high differential pressure beneath-the-bit is dissipated over the first centimetre depth of the formation.

Barkman and Davidson²⁸ showed three characteristic shapes of the cumulative filtrate volume against the square root of the time curve. Experimental examples of each type of shape is presented in Figure(2-1.7). They considered the shape of curve that results in any particular case would depend upon the properties of the suspended solids and of the filter medium. When the suspended particles are larger than pores of the filter medium, no invasion takes place and the type of the curve shown in Figure(2-1.7a) results, and the



Figure(2-1.7) The Examples of Three Types of Filtration Curves

intercept of the straight-line portion at time zero is negative. When the suspended solids are much smaller than the pores of the filter medium, invasion takes place at least during the early part of the test. A positive intercept results, as shown by Figure(2-1.7b). The third type of curve, which has a characteristic S-shape, can also occur under some circumstances, as shown in Figure(2-1.7c).

Barrington and Smith³⁰ invented an apparatus for determining dynamic fluid loss trends as a patent, which provided a dynamic fluid loss testing cell comprising a cell wall, a detachable lid having an inlet for pressurising fluid, a detachable base having a drain, and a stirrer, the stirrer being journalled in the lid and being provided with an external drive.

Simpson³¹ presented data for filtration of drilling fluid under simulated downhole conditions, with confining pressures as high as 10,000 psi and temperatures up to 400 °F. He considered that the knowledge of the filtration rate (as an indication of depth of filtrate invasion) is important in controlling a drilling fluid to minimize productivity damage.

Following results were summarized:

- (i) The effect of very high total pressure on the filtration of a drilling fluid varies depending upon the temperature of the test. No simple calculation can be made to normalize the effect of pressure.
- (ii) Use of the filtration rate derived based on result of API high-temperature filtration test for calculation of depth of filtrate invasion can give much higher values than depths calculated from filtration rates measured under simulated downhole conditions.

Simpson³⁵ conducted filtration tests at downhole pressure and temperature upon a filter—a fused aluminium oxide material having a water permeability of about 500 md. The equipment was designed to permit filtration tests at pressures as high as 10,000 psi and at temperatures upto 400 °F. Tests were performed at three muds:

- (1) A water-base mud—potassium lignite surfactant system suitable for use at 300 °F;
- (2) A conventional invert oil-base mud—conditioned for low filtrate as measured by API test at 300 °F;
- (3) A low colloid oil-base mud—no colloidal solids other than oil-dispersible bentonite for suspension of solids and emulsifier for emulsification of water and oil-wetting of barite.

For the purpose of comparison with the customary filtrate values, the three muds were tested using the API high temperature procedure. The results showed that:

- (a) The conventional invert oil-base mud had a very low filtrate flow rate by the API test at 300 °F;
- (b) The water base mud had a satisfactory filtrate;
- (c) The filtrate for the low-colloid oil base mud was higher than would be ordinarily considered acceptable.

Testing at downhole pressure and temperature (500 psi, 300 °F) gave a different ranking for performance of the muds. The results showed that there was little change in the filtrates for the first two muds, but the filtrate for the low colloid oil base mud was much lower than that indicated by the API test when tested at downhole pressure and temperature, the low colloid oil base mud had a considerably lower filtrate than the water base mud. Simpson concluded from the results that the difference in performance indicated by the two test procedures might be explained by two factors:

- (1) Greater effect of pressure on the viscosity of oil as compared with water;
- (2) The difference in filter media used.

It is believed that the thin sheet of filter paper used in the API test does not provide pore spaces where internal filter cake might start to form. In contrast, the fused aluminum oxide filter cylinder is 0.75 inch thick and has interconnecting pore spaces more like those of permeable rock. A mud having a poor particle size distribution, but containing material

adsorbable by cellulose, might show an erroneously low filtrate on paper. Conversely, a mud containing solids that would seal the surface pores of permeable rock might have the solids stack on the surface of a sheet of paper and delay the formation of a low permeability filter cake.

Sharma *et al.*³⁶ examined the effect of various drilling fluid additives on water loss and the permeability of filter cakes. Permeability of filter cakes was measured before and after addition of chemicals. A straight line relationship was generally found to exist between water loss and mud cake permeability except in the case of presence of water loss reducing agents. Different additives affect values of the slope and the intercept in distinctive ways. Inert materials give rise to low slope values as compared to those obtained with electrolytes, whereas thinners produce intermediate slope values. Similar additives produce comparable slope and intercept values.

Peden *et al.*³⁷ conducted both dynamic and static filtration tests upon two inhibited water based muds. The dynamic filtration experiments were performed at the pressure of 100 psi and the room temperature on a filtration column, consisting of two concentric acrylic tubes of 6 ft length. The static experiments were conducted in a perspex core holder fitted with a mud sample chamber. The following specific results were proposed:

- (i) Annular velocity (shear rate) has a pronounced effect on dynamic fluid loss and the exact mechanism might be dependent upon the nature of the filter cake, specifically the size and shape of the constituent particles;
- (ii) The filtrate loss is highly dependent upon core permeability for dynamic filtration;
- (iii) Barytes in conjunction with more conventional fluid loss control additives greatly enhances filtration control;
- (iv) The presence of a range of particle size is crucial to effective fluid loss control.

Peden *et al.*³⁸ in the second one of a series of papers related to the borehole filtration reported an extensive investigation on filtration under dynamic and static conditions. The following observations and conclusions were made:

- (a) Spurt loss is directly dependent upon pressure;
- (b) The presence of bridging particles such as CaCO₃, Gypsum and Barytes substantially improves the ability of the mud to limit spurt loss and subsequently filtration rates.
- (c) The cake deposited under static conditions is largely eroded once circulation is restarted.
- (d) For static filtration an increase in concentration of barytes as the weighting material results in a reduction in fluid loss, an increase in cake thickness and an increase in cake permeability.

Wyant *et al.*³⁹ measured the dynamic fluid loss of oil base additives. The aim of his experiment was to correlate the DFL (dynamic fluid loss) with the static fluid loss, the sticking coefficient, and the FLCA (fluid loss control agent) concentration in oil muds. The DFL data (at 250 °F and 500 psi) were obtained with a developed cell shown in Figure(2-1.8), in which filtration occurs in an annulus around a central permeable core.

The following conclusions can be drawn from their paper:

- (i) The DFL decreases with decreasing static (API HT/HP) fluid loss.
- (ii) The major portion of each short term fluid loss reduction(both static and dynamic) was obtained by FLCA concentrations of about 4 lbs/bbl [11.4 Kg/m³]. The long term equilibrium dynamic filtration rate was not changed greatly by FLCA additions with the exception of the polymer based FLCA 2. Higher concentrations of this FLCA increased the DFL values.
- (iii) The DFL (both long term and short term) increased with increasing shear rate or fluid pulsation.
- (iv) Primary fluid loss control occurred at or slightly within the core surface rather than within the bulk filter cake.
- (v) A mechanistic theory, based on pore structure differences between natural sandstone and synthetic sintered stainless steel cores, was proposed to explain the consistent variations in DFL. Increasing permeability (from 200 to 600 md)

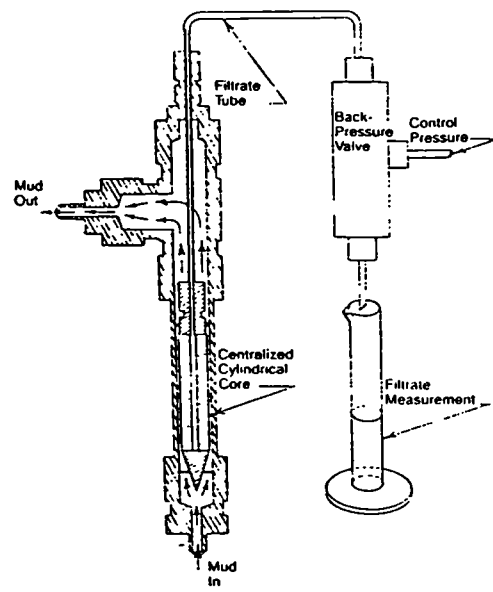


Figure (2 - 1.8) Dynamic filtration cell and filtrate collection system.

of Berea sandstone cores decreased the dynamic filtration, whereas increasing the permeability of synthetic sintered stainless steel cores (from 47 to 2,000 md) increased the DFL.

Vaussard⁴⁰ simulated the borehole conditions to measure the dynamic fluid loss. Tests were performed at a maximum pressure of 1070 psi and at maximum temperature of 300 °F. He and his coworkers observed no correlation between API static filtration and dynamic filtration under downhole conditions. Figure(2-1.9) showed the filtration simulator employed by them. Their findings were:

- (a) Dynamic filtration is independent of permeability, except in the case of synthetic filter media.
- (b) Filtration and cake formation depended upon 2 opposing phenomena: the deposition and erosion of solids. Erosion is facilitated if the solids are only slightly compressible. If solid arrangement occurs with difficulty, it results in a more fragile cake, which is less efficient in terms of filtration.
- (c) It is the overall physico-chemical equilibrium that allows good filtration control under borehole conditions, the difference between static and dynamic being in the first place the ease of erosion, and in the second place only, the cake permeability.
- (d) An efficient cake is one where solids have a high colloidal nature. This explains the filtration control difficulties, either by the prevention of cake structural organization in water base muds (excess of fine but only slightly colloidal solids and/or presence of aggregates between solids and additives is supposed to reduce filtration) or by the low colloidal nature of solids in oil base muds.
- (e) Only a slightly difference in filtration depending upon formation permeability might be observed at the beginning of dynamic filtration. This would disappear as soon as a stabilized cake is obtained.
- (f) The dynamic rate was reduced by a period of static filtration, but increased if the annular flow rate was increased-markedly so at the onset of turbulence, which occurred at about 1,800 l/min as shown in Figure(2-1.10).

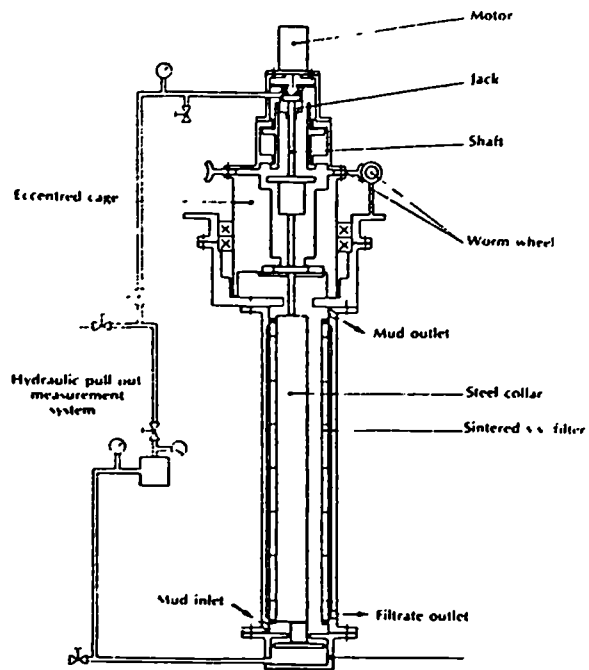


Figure (2 - 1.9) Filtration and sticking simulator.

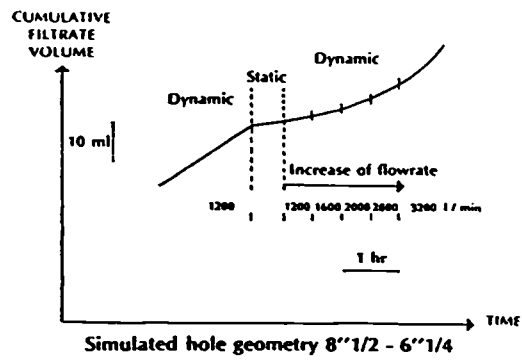


Figure (2 - 1.10) Filtration vs. flow changes.

- (g) There is considerably less spurt loss with polymer muds because the filtrates from the polymer systems are much more viscous and therefore have a much reduced spurt loss.

Bizanti⁴¹ reported an investigation on the relationship between static and dynamic filtration. The experiments were conducted upon the sandstones under dynamic and static conditions over three mud samples: water, water plus clay and water plus clay plus barytes. He also presented a regression analysis, performed between the fluid loss parameter ($q/D^2 V$) and Reynolds number (NR) and between the fluid loss parameter ($q/D^2 V$) and the modified Reynolds number ($NR \cdot \Delta P/\tau_y$). The following conclusions could be derived:

- (1) The greater the pressure drop, the greater the filtration volume;
- (2) The greater the mud density, the thicker the mud cake deposited;
- (3) An increase in Reynold number (NR) increases dynamic fluid losses.
- (4) From the regression analysis conducted on the experimental results, it is seen that the modified Reynolds number ($NR \cdot \Delta P/\tau_y$) correlates better with the fluid loss parameter ($q/D^2 V$) than with the Reynolds number (NR);
- (5) The pressure drop yield point ratio ($\Delta P/\tau_y$) has great effect on the fluid loss parameter ($q/D^2 V$) while the Reynolds number (NR) has less effect on the fluid loss parameter ($q/D^2 V$).

Hartmann *et al.*⁴² presented an analysis of mud cake structures formed under simulated borehole conditions. The tiny pieces of filter cake were shock-frozen and broken while immersed in the coolant. The specimens were then studied with scanning electron microcopy (SEM) in both freeze-dried and frozen-hydrated stages. The investigation covered filter cakes of four different drilling fluids with respect to fluid loss data, as well as thermal and chemical degradation. The following observations were obtained:

- (1) The honeycomb structures of bentonite contained in drilling fluids were found

in the resulting filter cakes. This may be induced by the edge-to-face attachment of the bentonite platelets.

- (2) The gel strength of the drilling fluid exerts a considerable influence on dynamic filter cake structures.
- (3) A structural orientation in the direction of flow for the drilling fluid within the filter cake can be observed only if the gel strength has diminished within the drilling fluid.
- (4) During chemical and/or thermal over stressing of the drilling fluid, the bentonite platelets lose their structure-forming property through coagulation.

Jamison and Fisk⁴³ invented an apparatus for testing fluid loss characteristics of a test fluid such as drilling mud under static and dynamic conditions. The apparatus having a filter medium cell which has a generally vertically disposed cylindrical wall, the apparatus further including a first chamber which is in open communication with the inner surface of the cylindrical wall and a second chamber which is in communication with the outer surface of the cylindrical wall, there being a generally vertically disposed rotatable shaft which is received internally of the cylindrical wall, the shaft being driven by a motor or the link, the apparatus being capable of providing a differential pressure across the cylindrical wall such that fluid will flow from the first chamber to the second chamber to the differential pressure and the liquid passing into the second chamber can be suitably measured and used to calculate fluid loss rate of the test fluid.

Zamora *et al.*⁴⁴ presented a paper on the development and application of three innovative devices for measuring important physical properties of water and oil-base muds. These three devices are:

- (i) *Automatic Shear Meter* shown in Figure(2-1.11)—which measures shear strength of a column of mud after static aging at temperature and pressure;
- (ii) *HTHP Dynamic Filtration Tester* shown in Figure(2-1.12)—which measures dynamic filtration at operating conditions upto 400 °F (204 °C) and 500 psi;
- (iii) *Filter Cake Penetrometer* shown in Figures (2-1.13) and (2-1.14)—which

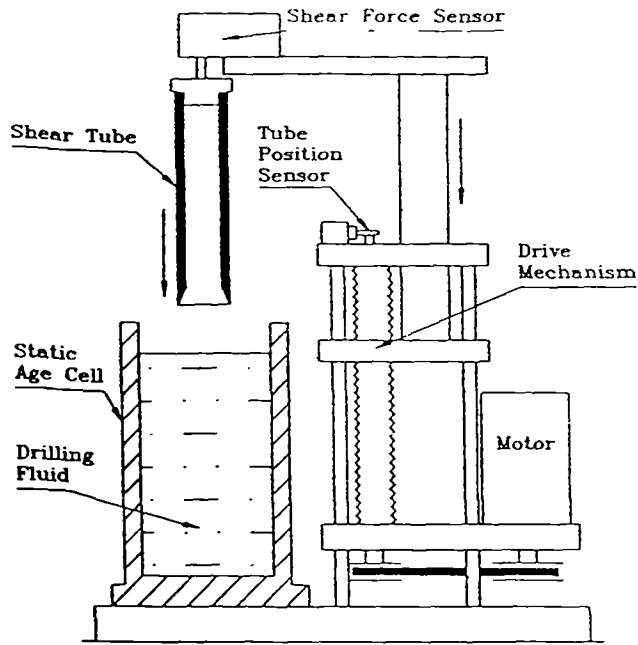


Figure (2 - 1.11) Automatic shearometer unit.

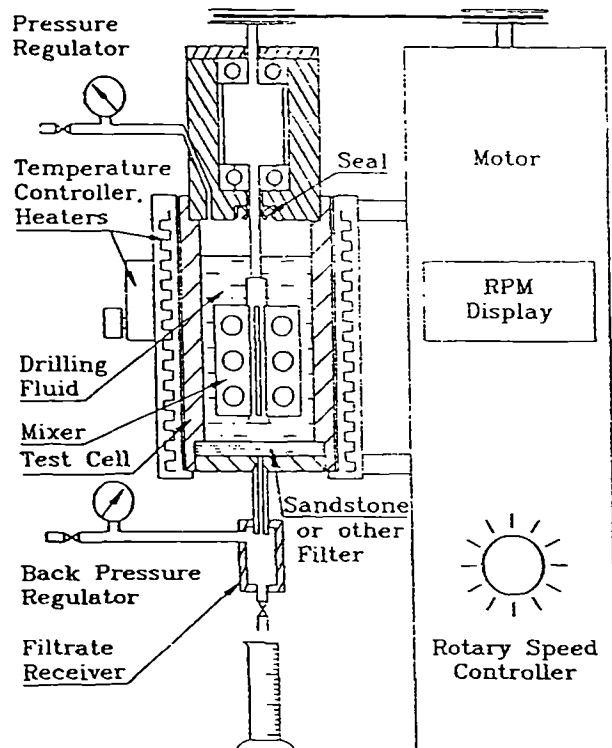


Figure (2 - 1.12) HTHP dynamic filtration tester.

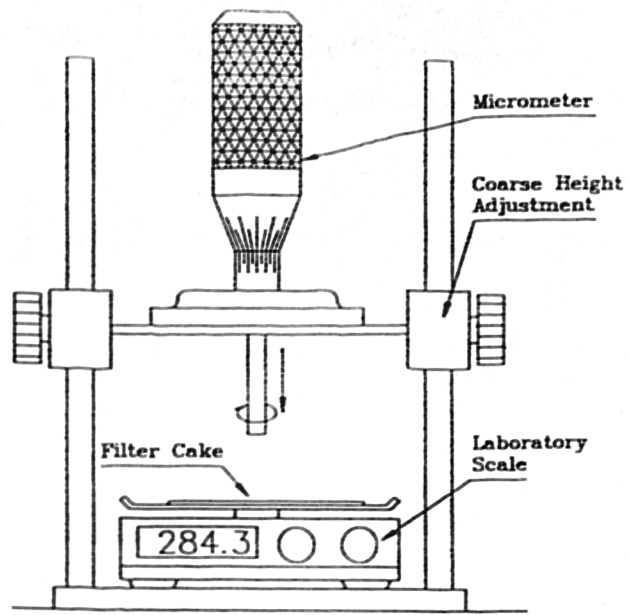


Figure (2 - 1.13) Manual filter-cake penetrometer.

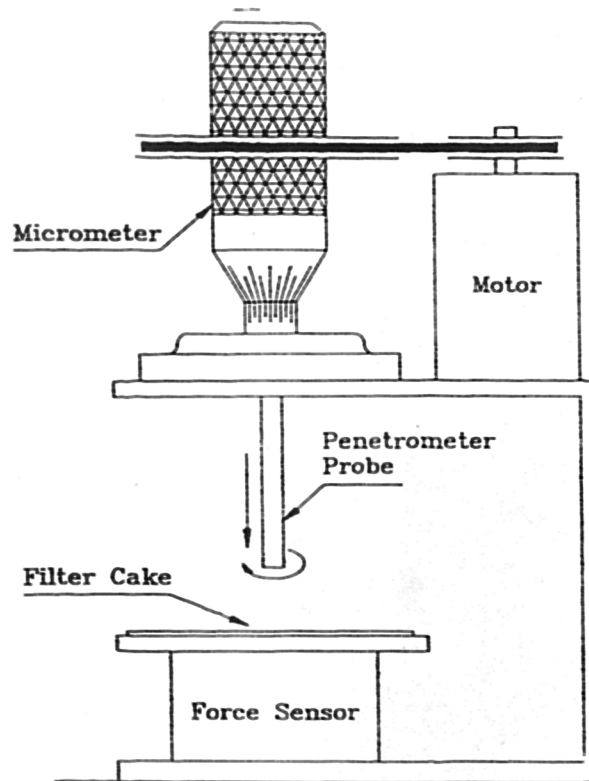


Figure (2 - 1.14) Motorized filter-cake penetrometer.

determines characteristics and thickness of filter cakes obtained from both low- or high-pressure, static or dynamic filtration test.

Fisk and Jamison⁴⁶ presented an experimental study on physical properties of three types of drilling fluids at high temperatures and pressures. Data were obtained with the dynamic HPHT test system which is capable of operating at pressures up to 20,000 psi and maximum temperatures to 650 °C and a laboratory dynamic filtration devices which temperature and pressure limits are 400 °F and 1,000 psi respectively. The results indicated:

- (a) Fluid penetration into the pore space is controlled by the shear forces and the size of the aggregates in the drilling fluid relative to the pore size of the formation;
- (b) The differential pressure causing the solids consolidation had a greater effect on the dynamic filtration rate than on the change in the filtrate viscosity, whereas total system pressure had a minimal effect on the dynamic filtration rates of the oil and the water based fluids at all temperatures;
- (c) Dynamic, radial, filter loss values increase linearly with time at constant shear and differential pressure for all systems investigated;
- (d) Shear prevents the penetration and bridging of the particles which cause the dynamic filtration rate to increase with shear. If the fluid particles are much smaller than the size of pores in the formation, the particles can penetrate and bridge the pores in the formation and reduce the dynamic filtration rates, even at fairly high fluid velocities;
- (e) Oil and water based drilling fluids that contain clays form compressible filter cakes.

Fordham *et al.*⁴⁵ reported an investigation on the variation of key parameters describing the dynamic fluid loss behaviour of two water-base drilling fluids, baryte-weighted and unweighted in an annular flow dynamic filtration cell shown in Figure(2-1.15) designed to provide well controlled laminar flows over a wall shear rate typical of

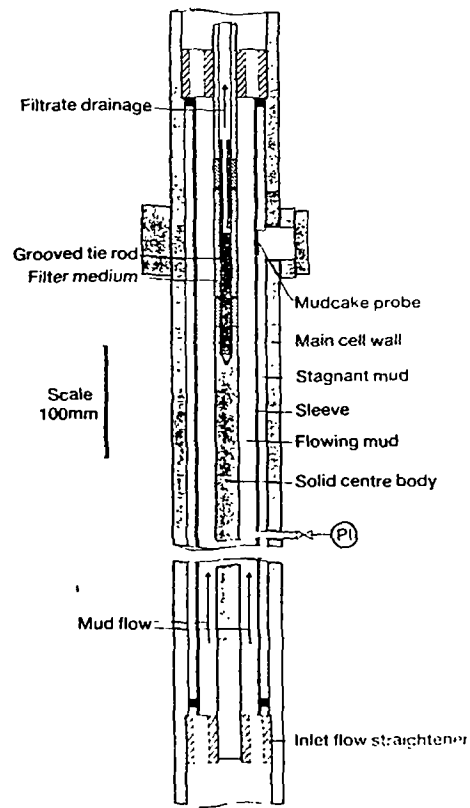


Figure (2 - 1.15) The annular flow dynamic filtration cell (section).

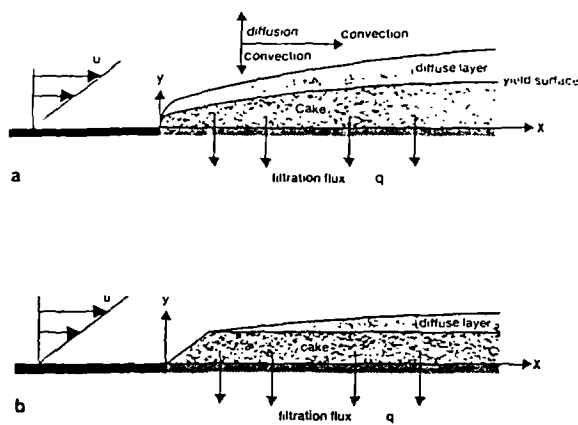


Figure (2 - 1.16) (a) Basic ideas of convection-diffusion models and (b) basic ideas of particle adhesion models.

those in the wellbore during drilling. From the experimental results, they obtained that the fluid loss might be described by three key parameters: one describing the early (“quasi-static”) behaviour, a second describing the late (“dynamic”) behaviour of near-constant fluid loss rate and thirdly a timescale for the transition between these two regimes. The following conclusions were reported:

- (i) Fluid loss in the “quasi-static” phase is only weakly affected by shear;
- (ii) Fluid loss in the “dynamic” phase varies with the tested mud systems according to (approximately) the 0.6 power of the wall shear rate;
- (iii) The irreversible deposition of mud cake under dynamic conditions reported by others was also observed.

In addition to the above, two fundamental models of dynamic filtration were also discussed. One of them is Convection-diffusion balance model shown in Figure(2-1.16a) which based on the mechanism that the control of dynamic fluid loss is a balance between convective transport of mud particles towards the filtration surface by the filtration flux, and the diffusion of particles away from the surface. The other is the Particle adhesion model shown in Figure(2-1.16b) which is supported by the hypothesis that particles stick at the cake surface, in a manner that depends on both the filtration rate and on the colloidal interactions between particles; Once stuck, such particles are unable to diffuse away from the cake.

Arthur and Peden⁴⁷ reported the results of an experimental programme to investigate the influence of mud composition, pressure and temperature on the properties of filter cakes formed during static filtration. The tests were conducted upon three water based muds at pressures upto 4.2 MPa and temperature upto 93 °C. The filter medium were filter papers. The spurt loss, cumulative fluid loss, cake thickness and porosity were measured and, the cake resistance and compressibility were also calculated using a modified equation. The following results were presented:

- (1) Spurt loss (at 2 seconds) was a power function of pressure with the exponent varying between 0.05 and 0.25 for all the muds tested.

- (2) It is found that the Larsen's relationship which proposes that the increase in the fluid loss is due solely to the decrease in the filtrate viscosity may be used to provide reasonably good estimates of the fluid loss when the test temperature is not greatly different from the temperature of interest.
- (3) The cumulative fluid loss, cake resistance and compressibility were unaffected by the grade of filter paper(filter medium).
- (4) The drilling fluid filter cake are highly compressible under pressure. This was illustrated by experimental data.

Plank and Gossen⁴⁸ investigated the effects caused by temperature, electrolytes and polymers on filtration control in which they studied fluid loss polymers such as starch, polyanionic cellulose (PAC) and a synthetic high temperature stable polymer in drilling mud filter cakes using SEM photography to visualize the freeze-dried API filter cakes. The following conclusions were presented:

- (a) Bentonite in drilling fluids forms a card-house gel structure in the filter cake;
- (b) The average pore size of a mud filter cake is influenced by temperature, electrolytes and polymers;
- (c) Starch polymer forms characteristic bridges within filter cake pores;
- (d) PAC is adsorbed onto the edges of clay platelets and forms few bridges;
- (e) The synthetic HT-polymer reveals typical polymer fingers extending into the pore space.
- (f) Addition of calcium does not change the appearance of starch and the HT-polymer. PAC forms conglomerates (precipitated Ca-PAC).
- (g) API filtrate data correspond well with temperature and electrolyte solubility of polymers observed under the SEM.

2.2 THE EFFECTS OF INDIVIDUAL WELLBORE VARIABLES UPON STATIC AND DYNAMIC FILTRATION PERFORMANCE

As can be seen from the foregoing review, much effort has been directed towards the investigation of the fluid loss characteristics of drilling muds. The complexity of the borehole filtration has been shown. It is therefore meaningful to identify the effects of individual variables upon this process. The variables discussed will include, absolute and differential pressure, temperature, mud constituents and properties, annular velocity and hydrodynamic parameters, formation characteristics, mechanical erosion of the filter cake and sequential filtration.

2.2.1 The Effect of Absolute Pressure and Differential Pressure

A large number of published papers studied the effect of pressure differential rather than the absolute pressure upon the drilling fluid filtration.

ABSOLUTELY PRESSURE:

Simpson^{31,35} identified the effect of total pressure on compressible mud filtrates, e.g., oil base muds. At 200 °F, the viscosity of diesel is of the order of 2.4 cp at 100 psi and is increased to 4.9 cp at 10900 psi. However the effects of absolute pressure would be to alter the rheological properties of the mud and the effects of this on the hydrodynamic shear in dynamic filtration are unknown. In addition the behaviour of chemical molecules either individually or in groups e.g., polymer, is not well understood and it is possible that molecular shape and size would be affected thus changing the filter cake characteristics.

Fisk and Jamison⁴⁶ concluded that the total system pressure had a minimal effect on

the dynamic filtration rates of the oil and the water base fluids at all temperatures.

PRESSURE DIFFERENTIAL:

If the filter cake were of constant permeability then the volume of filtrate obtained would be proportional to the square root of pressure differential according to Darcy's law, and a log-log plot of filtrate volume versus pressure should yield a straight line with a slope of 0.5. Actually, this condition is never met because mud filter cake is to a greater or lesser extent compressible, so that the permeability is not constant, but decreases with increase in pressure⁴.

Jones and Babson¹ observed that the filtration rate and the thickness of the mud cake deposited were little affected by the variation in pressure above 500 psi. This would suggest a balance between deposition due to increasing differential pressure and compaction of the cake with a resulting decrease in cake permeability.

An exponential relationship between the cumulative filtration volume and the pressure drop was obtained by Larsen⁴. For their muds tested, the exponent varied between 0 and 0.24 and depended largely on the size and shape of the particles composing the cake. The exponent varies from mud to mud⁹⁵, but is always less than 0.5.

The mud spurt loss increased with increase in pressure, and this might be attributed to the increase in velocity of the mud solids at the instant of application of pressure¹².

The pressure drop across the rock sample had little effect upon the filtrate volume beneath-the-bit¹⁶.

The equilibrium filtration rate at a constant value of the rate of shear was independent of the filtration pressure²⁴. In the case of incompressible filter cakes, the equilibrium cake thickness h_{eq} is proportional to filtration pressure. In the case of compressible mud cakes, little or no increase in cake thickness was observed. This might be explained that an increase in filtration pressure is mainly compensated by a reduction in cake permeability.

In conclusion it would appear that most investigators although not all, observed that the equilibrium dynamic filtration rate was unaffected by differential pressure^{21,24}. A balance between compaction and increased deposition rate with increasing differential pressure would explain these observations.

2.2.2 The Effect of Temperature

Increase in temperature may increase the filtrate volume in several ways. In the first place, it reduces the viscosity of the filtrate, and therefore, if changes in the cake structure and properties do not occur with changing temperature, then the cumulative filtrate volume will be inversely proportional to the square root of the viscosity. The viscosity of the water and of 6% brine are shown over a range of temperatures in Table 2.4⁹⁵. It is evident that changes in temperature may have a substantial effect on filtrate volume because of changes in filtrate viscosity.

Change in temperature may also affect filtrate volume through changes in the electrochemical equilibria which govern the degree of flocculation and aggregation, thus altering the permeability of the filter cake. As a result of such effects, filtrate volumes may be higher or lower than predicted from Larsen's equation but usually they are higher^{5,18}.

Chemical degradation of one or more components of the mud is a third mechanism by which high temperatures can affect filtrate properties. Many organic filtration control agents start to degrade significantly at temperatures above about 212 °F(100 °C), and the rate of degradation increases with further increase in temperature until filtration properties can not be adequately maintained⁹⁵.

The increase in fluid loss at elevated temperatures was generally higher than would have been predicted by the viscosity corrected for the change in temperature^{5,11}. Temperature affects the size of particles in a mud¹².

Table 2.4 The Viscosity of Water and 6% Sodium Chloride Brine at Various Temperatures⁹⁵

Temperature (°C)	Temperature (°F)	Viscosity of Water (cp)	Viscosity of Brine (cp)
0	32	1.792	—
10	50	1.308	—
20.2	68.4	1.000	1.110
30	86	0.801	0.888
40	104	0.656	0.733
60	140	0.469	0.531
80	176	0.356	0.480
100	212	0.284	—

Dynamic equilibrium filtration rate is independent of temperature change²⁴. The explanation is that if the temperature increases, and accordingly the filtrate viscosity is reached, the filtrate rate will increase giving rise to increased deposition of cake solids and increasing cake resistance (thickness). Accordingly the balance is maintained. It is unlikely that this will be true for all muds as the solids content would vary depending upon mud type and properties.

2.2.3 The Effect of the Properties of Filter Medium

Logically it can be reasoned that the filtration rate will depend upon a number of variables connected with the filter medium which defines the resistance of the medium and parameters which will cause it to change, e.g.:

- (i) the size and distribution of the pores of the filter medium;
- (ii) the size and distribution of the grains of the reservoir rock;
- (iii) the physico-chemical nature of the suspended particles in the invading filtrate.

If the particle size in the mud is such that particles are capable of penetrating deeply into the porous rock resulting in plugging, then the filtrate loss may be lower in a high permeability formation which permits this transport and plugging. However in a low permeability in which it can not occur, an external filter cake will only be formed due to bridging. If the particle size distribution of the mud is such that it provides good bridging for all permeabilities then the fluid loss will appear to be independent of filter medium permeability. Finally if the cake formed is highly permeable then filtrate could be dependent upon the formation permeability.

From the above discussion it is apparent that it is difficult to distinguish the effects of

formation permeability/pore size characteristics and the size and distribution of particles in the mud. It is therefore not surprising that conflicting conclusions have been reached by the researchers on this subject.

Williams and Cannon³ inferred from their work that the filtration properties of muds are governed by the amount and size of solids in the mud and are therefore independent of formation permeability.

Larsen⁴ reports data which support his claim that the filtration rates he obtained were independent of the filter bed materials used, namely compressed sand, natural sandstone or filter paper.

Byck⁷ measured fluid loss and the permeability of cakes deposited on a range of filter materials with different muds, and concluded that:

- (i) fluid loss does not depend upon the formation permeability but does depend upon the amount and nature of the mud solids
- (ii) filter cake permeability does not depend upon the formation permeability;

Nowak and Krueger⁹ suggested that filtrate flow was controlled primarily by particle plugging. Their results indicated that in general the cumulative filtrate volume seemed to be inversely proportional to the core permeability for most cases although the exact behaviour depended on the mud type. In some cases, this was due to higher spurt loss and in others to higher filtration rates. These experiments were performed with dynamic filtration. In addition, for static filtration with cores within a permeability range of 744-896 md, both spurt loss and cumulative filtrate were inversely proportional to core permeability.

Dickey and Bryden⁹² observed internal bridging by semi colloidal particles which were transported into the pore space where they bridged thus plugging pore throats and preventing further filtration.

Simposon³¹ in his experiments at simulated downhole conditions observed higher

dynamic fluid losses with low permeability cores(0.5 md) than with high permeability cores of 50 md. Since he observed that the cores possessed the same static fluid loss it would appear that in the case of the 50 md core, an internal filter cake was deposited thus limiting filtration.

In conclusion, it would seem that the effects of the porous medium upon filtration can not be isolated from the effects of the mud constituents upon dynamic filtration. The capability to produce low permeability particulate bridges will control fluid loss and this depends upon both porous media and mud particulate properties.

However, for beneath-the-bit filtration, since a filter cake does not permanently exist, it would be expected that filtration would depend upon permeability^{16,25}.

2.2.4 The Effect of the Mechanical Erosion of Dynamically Deposited Cakes

It can be imagined that simulation of the effects of mechanical attrition of the cake would be very difficult due to one or more of the following:

- (i) the rotation of the drill string causing contact with the filter cake particularly due to hole deviation, dog legs in the hole, inflexion in the drill string and packed hole assemblies comprising drill collars and stabilisers;
- (ii) retraction of the bit to add a single.

Nowak and Krueger⁹ used an experimental cell which allowed:

- (a) a jet of mud to be continuously jetted on the face of the 1" diameter cores used for the filtration studies;
- (b) a scraper to be reciprocated across the face of the core at a rate of 10 strokes per minute.

Unfortunately they did not differentiate between the effects of these two mechanisms. Their tests were conducted with oil based, emulsion and clay water based muds. The results indicated that the cumulative filtrate volume after 100 minutes of filtration was increased by a factor of 10 when circulation and jetting was carried out with dynamic filtration for the clay water and emulsion based muds. The results for the oil based mud showed a smaller degree of increase. They also concluded that the effects of scraping were less significant when both internal and external filter cakes existed.

In a subsequent paper Krueger and Vogel⁸⁵ using the same cell as described above, without the effects of the jetting on the core surface, observed that for the clay water mud there was still a 10 fold increase in the cumulative fluid loss after 100 minutes for dynamic filtration performed with the cake scraper compared to that without scraping. For the oil based mud the increase was of the order of two times for the dynamic fluid loss with the addition of scraping.

It is impossible to generalise on the degree of scraping in a real borehole or on the fraction of the borehole wall affected e.g. whilst the retraction of the bit might affect the entire circumference of the borehole, when adding singles and during each round trip, the effects of rotation in a dog leg might effect only specific sections along the length of the borehole and small fractions of the borehole circumference.

It would therefore be impossible to generalise on the effects of this in the prediction of filtration and invasion although clearly they could be substantial.

2.2.5 The Effect of Annular Hydraulics on Dynamic Fluid Loss

Although a number of researchers have studied dynamic filtration, few have attempted to evaluate the relationship between the hydraulics in the annular space and dynamic fluid loss.

The following variables are involved in this relationship:

- (i) Annular fluid circulation velocity;
- (ii) Fluid shear rate/shear stress on the surface of the cake;
- (iii) Reynold number in the annulus which covers the turbulent or laminar flow in the annulus.

These variables are related to each other and almost all the researchers did not consider any difference between any of them.

It was indicated that the dynamic filtration rate was proportional to the square root of the volumetric mud flowrate^{6,13} and the erosion rate of the cake in inches/minute was approximately proportional to the square of the circulation velocity¹⁰.

Perhaps the greatest contribution by Ferguson and Klotz¹³ to this particular subject was the proposed qualitative model for the filter cake formed under dynamic conditions. They argued that for cake erosion to occur, the hydrodynamic shear of the circulating mud must exceed the cake shear strength. Since the shear strength of filter cakes was in the range of 0.3-15 psi it would be necessary for the pressure gradient in the circulating mud to be of the order of 3-150 psi/ft to ensure that erosion of the cake took place.

Peden *et al.*³⁸ reported that the statically deposited filter cake could be largely eroded during the mud circulation.

Bizanti⁴¹ found that an increase in Reynold's number (NR) increases dynamic fluid losses.

Beck *et al.*⁸⁶ had measured the hydrodynamic shear rates of the muds and a value of 0.003 psi/ft was typical. Accordingly Ferguson and Klotz¹³ argued that erosion of the cake could not take place. They proposed a model comprising a conventional filter cake on the borehole wall and a transition zone of low shear strength between the cake and the mud. The dynamic cake properties were therefore influenced by the erosive action of the mud stream on this transition zone since this would control the particle size, the

particulate concentration and thickness of the transition zone.

2.2.6 The Effect of Mud Properties and Constituents

Most of the published research in this area has been directed at understanding the relation between the size distribution of particulates in muds and the control of filtration through the establishment of a filter cake of low permeability.

Cake permeability is, however, influenced by the kind of colloid as well as by the amount and particle size. For instance, filter cakes of bentonite suspensions in fresh water have exceptionally low permeabilities because of the flat, filmy nature of the clay platelets, which enables them to pack tightly normal to the direction of flow.

Gates and Bowie⁸ in 1942 attempted to correlate mud filtration properties against the particle size distribution in the mud and reported the following results:

- (i) Optimal filtration control was provided by muds having a relatively uniform particle size distribution.
- (ii) The best filtration control was provided by a mud composed of 65% colloids, 30% silt-size particles and 5% sand-size particles.
- (iii) Poorest filtration control was observed in muds having a very low concentration of colloids.

This point, regarding the contribution of colloids to fluid loss control, was earlier suggested by Sawdon⁸⁷.

Krumbein and Monk⁸⁸ investigated the effect of particle size and size distribution on the permeability of sand packs and concluded that:

- (i) Cake permeability was minimised by increasing the width of the particle size range.

- (ii) Cake permeability decreases with a reduction in the mean particle size.

Bo *et al.*²³ concluded that cake porosity was affected by particle size and size distribution in a way analogous to the effects on permeability reported above⁸.

Cake permeabilities have been measured for drilling fluids at a variety of pressures giving values in the range 0.2×10^{-3} - 250×10^{-3} md^{3,5,7,8}. The range of values indicates the influence of the mud type.

The initiation of filter cake deposition and the consequent control of spurt loss is dependent upon mud particulates bridging off against the pore throats of the porous media. This bridging can take place inside or outside the porous media¹⁵. Darley²² who confirmed that the significance of the colloidal fraction on fluid loss control has suggested from experimental measurements that this initial bridging process is accomplished in less than a second for many drilling fluids. The rapid control of the fluid loss has been attributed to the presence of the larger bridging particles in the drilling fluid by several authors^{15,19,83}, by investigating the effect of additions of sized particles to the mud to control spurt loss for rocks in the permeability range of 70-350 md and for which particles in the range of 1-6 μm were effective. The addition of the 21 μm particles did not effect bridging and hence control of the spurt.

It is obvious that the mechanical bridging process and spurt loss will therefore be characterised by the relationship between the mud particle and mean formation pore size as indicated by the results of Beeson and Wright¹². Darley²² in a paper discussing productivity impairment suggests that the presence of a mixture of particle sizes with a range 2-150 μm will bridge most formations. It has been reported that invasion due solely to the spurt loss period can extend to a depth of 1" in consolidated sandstones^{15,22,25,89}.

Abrams⁸⁹ from experiments with sand packs and cores, suggested that particles with a medium diameter of about 1/3 of the media pore size would bridge. Smaller particles would be required to fill in the interstitial spaces between the bridging particles thus lowering the permeability and subsequent filtration rate. However, universal application

of this concept is difficult in view of the variations in the pore size distribution of most reservoirs and the dynamic change in mud solid sizes whilst drilling. In addition McGuire and McFall⁹⁰ questioned the validity of the 1/3 bridging rule when applied to CaCO₃/HEC suspensions.

Krueger²⁰ investigated the effect of several fluid loss additives on the dynamic fluid loss characteristics of drilling fluids. The materials tested were CMC, complex metal lignosulphonate, starch, polyacrylate and quebracho. Krueger reported his results by plotting equilibrium dynamic fluid loss rates against the relevant API static fluid loss for increasing concentrations of these additives in various muds. For the clay gel based mud, Optimum fluid loss control did not necessarily occur with the maximum addition of these agents and was greatly influenced by the initial cake structure for sequential filtration.

Horner *et al.*¹⁶ found no correlation between the rheology of the mud and the dynamic fluid loss. Prokop¹⁰ suggested that the rheology is only significant in that it influences the flow regime in the annulus for dynamic filtration.

As yet no significant research has been reported on the influence of particle shape on fluid loss control although the need has been identified¹⁶. The use of the scanning electron microscope has highlighted both the complex structure of mud additives⁹¹, and the potential use of this technique for evaluating filter cakes³².

The dependence of the fluid loss upon the interrelation between the characteristics of the porous media and the fluid is most complex and, in any modelling process account will have to be taken of the statistical nature of these parameters. This will make the prediction of fluid loss a most difficult task to accomplish.

2.2.7 The Sequential Filtration

In real drilling operations, borehole filtration actually occurs as a sequence of dynamic

and static filtration periods as outlined earlier. This means that the latter stages of filtration will take place through a composite cake.

Figure(2-1.6) illustrates a typical filtration curve for a sequence of dynamic-static-dynamic filtration^{13,20}. The initial dynamic filtration period(T_0 - T_3) results in an equilibrium filtration rate being achieved which depends upon the properties of the dynamically deposited filter cake. The next phase of the curve corresponds to the period of static filtration(T_3 - T_4) which occurs when circulation is stopped. During this time the filter cake thickness will start to increase again and accordingly the rate of filtration will be drastically reduced resulting in little increase in the cumulative filtrate collected^{26,27}. The structure of the cakes deposited during these two phases is markedly different as confirmed by SEM studies³². This static cake may also affect the subsequent filtration which takes place once circulation is restarted. The third phase(T_4 - T_6) shown in Figure(2-1.6) is after restarting dynamic filtration and it can be seen that the new dynamic equilibrium filtration rate ultimately achieved is less than the initial value and since no change in the hydrodynamic conditions is assumed, the total resistance to filtration has increased because of the cake deposited in the static phase. This infers that upon restarting circulation the hydrodynamic shear is insufficient to reach the static filter cake except for the gelatinous outer layer. This confirms the theory proposed by Ferguson and Klotz¹³.

It is therefore clear that in the modelling of borehole filtration for realistic drilling conditions, the model must account for sequential filtration^{21,49,84}. However the shear strength of the filter cakes deposited during static filtration, their thickness and the hydrodynamic conditions are likely to be highly variable depending upon the mud deposition conditions and the borehole.

Chapter Three

NUMERICAL MODELING OF THE FILTRATION OF DRILLING FLUIDS

In this chapter, a literature survey of cake filtration theory prevailing in chemical engineering industry over past several decades is reported. Emphasis in this survey is placed on the empirical analysis of constant pressure filtration because the filtration phenomenon of drilling fluids mostly occurs under constant pressure. The filtration equations used for predicting drilling fluid loss are also reviewed. Based on these results, a developed filtration equation for drilling fluid loss under borehole conditions is presented.

Dimensional analysis of dynamic equilibrium filtrate flow of drilling fluid is included in this chapter as well.

3.1 LITERATURE SURVEY ON CAKE FILTRATION THEORY

3.1.1 The Behaviour of Fluids Flowing Through Porous Medium

Filtration through porous medium was compared with flow through a large number of capillary tubes, and on this assumption the rate of filtrate flow would follow Poiseuille's law⁵⁰ which was developed from experimental data:

$$\text{Rate of Flow} = \frac{\pi r^4 \Delta P}{8 \mu l} \quad (3-1.1)$$

where:

ΔP — the differential pressure at the ends of tube;

r — the internal radius of the tube;

l — the length of the tube;

μ — the coefficient of viscosity.

In 1856, Darcy⁵¹ showed that the flow of water through a fixed soil bed varied as follows:

$$\text{Rate of Flow} = \frac{K \Delta P}{\mu L} \quad (3-1.2)$$

where:

L — length of filter bed;

K — the permeability constant for different soil which is defined as a lumped parameter that characterises the bed. This parameter depends upon the size, shape and packing arrangement of the particulates that comprise the bed.

3.1.2 The Flow Through the Filter Cake

3.1.2.1 Direct Filtration Measurement

Examination of earlier (1910-1930) published papers on cake filtration, in which the investigators^{52,53,54,55,56,57} concentrated their efforts in obtaining relationships between flow rate, applied pressure, and cake thickness using large-scale filtration equipment,

revealed a power struggle between the two trends over what the fundamental filtration equation should be. One of trends was those^{53,55} in favour of Darcy's law, and the other^{52,54,56,57} rejected Darcy's law.

In 1912, Almy and Lewis⁵² first rejected Darcy's law and derived from experiments a mathematical formula of filtration for any particular sludge:

$$q = \frac{1}{A} \frac{dV}{dt} = K \frac{P_a^m}{V^n} \quad (3-1.3)$$

Where:

t — time;

q — filtrate flow rate;

A — cross-section area;

P_a — applied pressure of filtration;

V — cumulative volume of filtration;

$K, m,$ and n — constants for any one experiment;

dV/dt — the rate of discharge of liquid through the cake.

They concluded that the rate of flow of a liquid through a filter cake was not as a rule directly proportional to the pressure and inversely proportional to the thickness of cake but the flow rate was proportional to P^m and the resistance was proportional to V^n , where m, n accounted for deviations from parabolic behaviour. They also found that K was inversely proportional to the viscosity. This was contrary to the experimental result that K should be directly proportional to the viscosity.

In 1916, Sperry⁵³ reported the following rate equation in favour of Darcy's law and Poiseuille's law:

$$\frac{dV}{dt} = \frac{P_a}{R_c + R_m} = \frac{P_a}{rL + R_m} \quad (3-1.4)$$

and considered that cake resistance, R_c , was proportional to the thickness of cake, L ,

and L was proportional to filtration volume, V , viz:

$$L = \frac{sV}{D} \quad (3-1.5)$$

The result supported the parabolic filtration equation:

$$t = \frac{sr}{2DP_a} V^2 + \frac{R_m}{P_a} V \quad (3-1.6)$$

Where:

- D — the rate of deposition;
- r — resistance of material;
- s — solid percentage concentration;
- R_c — resistance of filter cake deposited;
- R_m — is the resistance of filter medium.

Sperry's equation was deduced from theoretical rather than experimental considerations. These had been prompted by the analogy between the filtration process and the flow of ground water. Since for the latter, Poiseuille's law had been shown to hold, Sperry postulated that Poiseuille's law was also the basic law of filtration. Upon this theoretical basis, he was able to derive a general equation in which the rate of flow was considered to be strictly proportional to the first power of P and V .

In 1921, Baker⁵⁴ analysed the rate equations reported by either Almy and Lewis⁵² or Sperry⁵³, and severely criticized Sperry's work that the power constant of pressure m is 1.0. He employed a similar analogy as Sperry did but disagreed with him by postulating that the rate of flow was proportional to indefinite powers (m and n) of pressure and volume, in accordance with the conclusions made by Almy and Lewis. He also considered the resistance proportional to V^n .

On this basis he secured an equation of the form:

$$\frac{dV}{dt} = \frac{C' A^2 P_s^m}{V^n} \quad (3-1.7)$$

where:

C' — proportionality constant, depending upon the nature of the sludge.

It should be noted here that A^2 is used, and not A .

In an exchange of letters in 1921, Sperry⁵⁵ and Baker⁵⁶ criticised each other's work severely. Baker's equation was criticized because:

- (i) it did not take the filter medium resistance into account;
- (ii) it did not explicitly include the mass fraction of solids in the slurry and the rate of deposition.
 c early ✓

On the other hand, Sperry's equation was criticized because:

- (i) it held only for incompressible sludge;
- (ii) it could not be used for constant rate filtration;
- (iii) it did not explicitly include the filter area term.

In 1926, Weber and Hershey⁵⁷ ignored Sperry's work and Darcy's law, and produced the simulated rate equation by analogy with Ohm's law:

Ohm's Law:

$$\text{Current} = \frac{\text{Voltage}}{\text{Resistance}} \quad (3-1.8)$$

$$\text{Resistance} = \text{Specific Resistance} \times \frac{\text{Length}}{\text{Area}} \quad (3-1.9)$$

Filtration analogy:

$$\frac{\mu}{A} \frac{dV}{dt} = \frac{P_s}{R_c + R_m} \quad (3-1.10)$$

$$R_c = \alpha \frac{W_s}{A} \quad (3-1.11)$$

where:

W_s — solids weight as laid on the filter medium.

If letting C = the weight of solids as laid on the filter per volume of filtrate, C was simply considered constant for any one suspension. Then:

$$W_s = CV \quad (3-1.12)$$

Inserting equation(3-1.12) into (3-1.11) and rearranging:

$$R_c = \alpha CV/A \quad (3-1.13)$$

Neglecting filter medium resistance temporarily, then:

$$q = \frac{1}{A} \frac{dV}{dt} = \frac{P_s}{\mu R} = \frac{P_s}{\mu R_c} = \frac{P_s A}{\alpha \mu CV} \quad (3-1.14)$$

It was ascertained that the above equation applied reasonably well to rigid, noncompressible sludges. It would hold fairly well for either constant pressure or constant velocity filtration.

In 1933, Ruth *et al.*⁵⁸ first analysed the existing theories in detail. Then they introduced cumulative drag stress as the agent which causes solid movement and cake compressibility.

Simply assuming the variables on both sides of equation(2-1.14) except V and t are constant, By rearrangement and integration, the following equation was obtained:

$$V^2 = Kt \quad (3-1.15)$$

where:

$$K = \frac{PA^2}{\mu\alpha C} \quad (3-1.16)$$

The irregularities observed in the V^2 vs. t plots at the beginning of filtration prompted them to modify the above equation. They found that the above anomalous behaviour was due to the resistance of the filter medium. If this resistance would be expressed in the units of cake resistance and considered as an integral part of the filtration cycle, the relation between volume and time should be shown to be parabolic throughout the whole course of the filtration. The following equation was suggested by them to correlate with the actual filtration data:

$$(V + V_0)^2 = K(t + t_0) \quad (3-1.17)$$

where:

V_0 — was regarded as a measure of the resistance that existed previously to the instant filtrate began to appear at the measuring device. It might be considered as the resistance of a layer of solids and filter medium.

t_0 — a corresponding shift in the time axis.

It is clear that whatever might be the actual nature of V_0 and t_0 , equation(3-1.17) had been verified to predict better filtration data than equation(3 -1.15).

By differentiating equation(3-1.17), they obtained:

$$\checkmark \text{ ee notes } \rightarrow \frac{dt}{dV} = \frac{2}{K}V + \frac{2V_0}{K} \quad (3-1.18)$$

This equation was used to calculate cake resistance but not septem resistance, because they did not think that the equation was valid for the initial portion of constant pressure filtration as postulated above.

Ruth *et al.*⁵⁸ also proposed the concept of average specific cake resistance:

$$\alpha_{avg} = \frac{P_a}{\int_0^{P_a} \frac{dP}{\alpha}} \quad (3-1.19)$$

which is constant for compressible cakes and showed that parabolic behavior was independent of cake compressibility.

In 1935, Ruth⁵⁹ extended the above work based on Weber and Hershey⁵⁷, in which the assumption of equation(3-1.12) could be obtained from a macroscopic mass balance:

$$\text{Weight of Slurry} = \text{Weight of Wet Filter Cake} + \text{Weight of Filtrate}$$

or symbolically:

$$\frac{W_s}{s} = \frac{W_s}{s_c} + \rho_f V \quad (3-1.20)$$

where:

ρ_f — the density of filtrate;

s, s_c — the solids fraction in slurry and filter cake respectively.

Comparing equation(3-1.12) with equation(3-1.20), then

$$C = \frac{\rho_f s}{1 - ms} \quad (3-1.21)$$

Where:

$m = 1/s_c$, and is the ratio of weight of wet filter cake to dry filter cake.

Combining equation(3-1.10) with equation(3-1.11) and inserting C from equation(3-1.21) into it, then:

$$\frac{\mu}{A} \frac{dV}{dt} = \frac{P_a}{\alpha \frac{CV}{A} + R_m} = \frac{P_a}{\frac{\alpha \rho_f s}{(1 - ms)A} V + R_m} \quad (3-1.22)$$



For a constant pressure filtration, integration of equation(3-1.22) by considering C , α and R_m constant produced a general equation—the well known Ruth's filtration equation:

$$t = \frac{\alpha_{avg} \mu \rho_f S}{(1 - ms) P_s A^2} V^2 + \frac{\mu R_m}{P_s A} V \quad (3-1.23)$$

It should be noted that α was replaced by α_{avg} before integration because Ruth⁵⁹ thought α_{avg} is constant through out the filtration process.

In 1938, Carman⁶⁰ extensively studied cake filtration and concluded that the Darcy's law is applicable to filtration. He modified Kozeny's equation into the form:

$$q = \frac{1}{A} \frac{dV}{dt} = \frac{\epsilon^3}{(1 - \epsilon) k S_0^2} \frac{\Delta P}{\mu L} \quad (3-1.24)$$

which is one of the most widely used equations—Kozeny-Carman Equation.

where:

ϵ — porosity of the cake;

k — Kozeny's constant;

S_0 — Specific surface of solids, i.e., surface area per unit volume of solid.

According to Darcy'law, the permeability coefficient should be:

$$K = \frac{\epsilon^3}{(1 - \epsilon) k S_0^2} \quad (3-1.25)$$

Comparing equation(3-1.14) with equations(3-1.24), (3-1.25) and inserting the following relationship:

$$W_s = LA(1 - \epsilon) \rho_s = CV \quad (3-1.26)$$

then:

$$\alpha = \frac{1}{\rho_s(1-\epsilon)K} \quad (3-1.27)$$

In equation(3-1.23), both sides are divided by V:

$$t/V = \frac{\alpha_{avg}\mu\rho_f s}{(1-ms)P_a A^2} V + \frac{\mu R_m}{P_a A} \quad (3-1.28)$$

Therefore, when t/V is plotted versus V , the slope is related to the average cake resistance α_{avg} and the intercept is proportional to the septem resistance R_m .

Contrary to the predictions of the theory, however, t/V versus V plot does not give a straight line in most cases. This prompted the investigators to deduce a mechanism through internal variations in filter cakes. The device used in the simulation of internal profiles is called the Compression-Permeability Cell (CPC). It was Ruth⁶⁷ who first suggested the use of the CPC in the simulation of internal profiles. He showed that the results from simulations and experiments agree to $\pm 10\%$ when average filtration resistances are compared.

3.1.2.2 Simulation of Filter Cake Compressibility

Ruth⁶⁷ suggested that the compression is caused by a pressure on the solids, set up as a result of the drag of the liquid as it flows fractionally through the cake. He presumed that the drag was transmitted cumulatively through the cake without loss as shown in Figure(3-1.1). Then assuming that the area of contact between the particles is negligible, the following balance can be written:

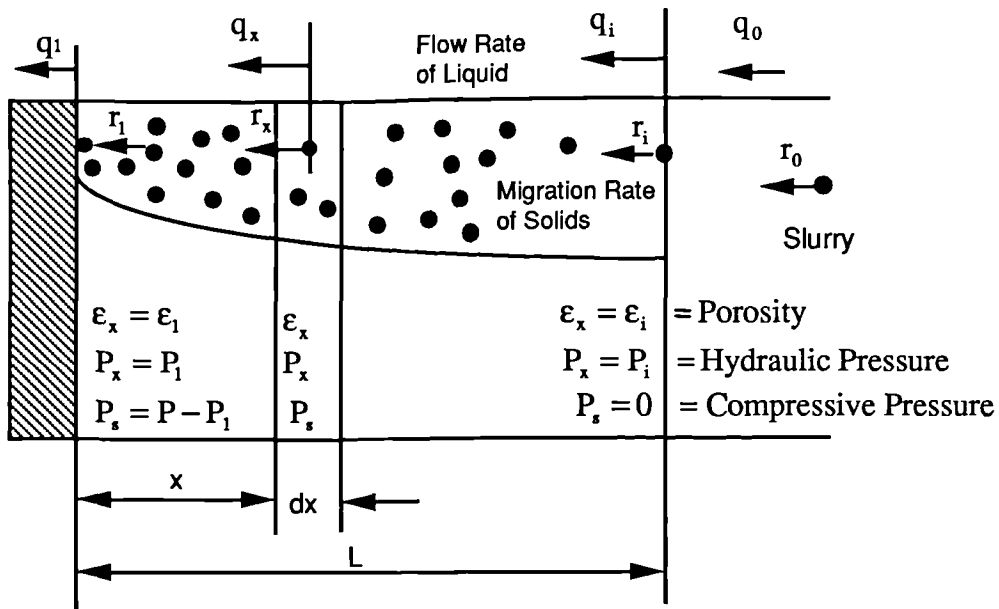
$$P_a = P_s + P_x \quad (3-1.29)$$

Where:

P_a — Filtration pressure;

P_s — Pressure on solids at x ;

P_x — Hydraulic pressure at distance x from the medium.



Figure(3-1.1) Schematical Diagram of Important Parameters in Cake Formation

The CP cell which was constructed by Ruth⁶⁷ was a small apparatus, in which a shallow bed of solids could be subjected to a mechanically applied stress.

Porosity and pressure distributions are the key variables for the description of the internal structure of compressible cakes. The functions describing compressibility phenomena are not only nonlinear, but appear to be non-analytical. As a result, it becomes necessary to relate porosity and specific resistance to P_s with empirical functions.

The earliest empirical equation from the CP cell which was used to represent variation in α was:

$$\alpha = (\text{constant}) \cdot (P_s)^n \quad (3-1.30)$$

This form has the serious problem that α approaches zero as P_s approaches zero, which is contrary to experience.

An improvement was made by Tiller^{69,70} who proposed that:

$$1 - \epsilon = BP_s^\beta \quad P_s \geq P_i \quad (3-1.31)$$

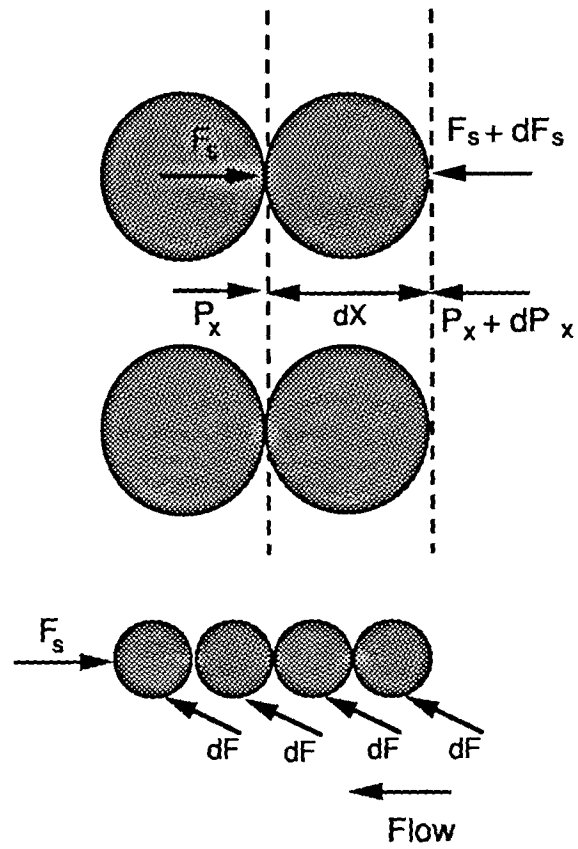
$$1 - \epsilon = 1 - \epsilon_i = BP_i^\beta \quad P_s \leq P_i \quad (3-1.32)$$

where P_i is some low pressure, below P_i the porosity reaches a limiting value ϵ_i which represents the porosity of a cake laid down under virtually zero pressure.

In order to relate the porosity in a filter cake to the porosity in the CP cell, It is assumed that the porosities in the cake and cell are equal when the solid compressive pressure in the filter, as indirectly calculated by $P_s = P - P_x$, equals the compaction pressure in the CP cell as shown in Figure(3-1.2).

Like porosity, variation of the specific filtration resistance with compressive stress is empirically represented in the form:

$$\alpha = aP_s^n \quad P_s \geq P_i \quad (3-1.33)$$



Figure(3-1.2) Compressive Force Due to Frictional Drag

$$\alpha = \alpha_i = aP_i^n \quad P_i \leq P_i \quad (3-1.34)$$

This modification leads to quite useful practical formulae in many cases, but results in errors because it is equivalent to assuming cakes to be incompressible in the low pressure region where rates of change are largest, in fact.

In 1953, Rietema⁶¹ evaluated the porosity at various heights in a filter cake by measuring the electrical resistance between gauge pins in a cake of spherical PVC (polyvinyl chloride) particles of 5-12 μ in diameter. He observed a minimum in the porosity distribution and called it *Retarded Packing Compressibility* (RPC), in which a form of Retarded Packing Compressibility was found where the first layers of cake do not compress gradually but only after a critical cake thickness was reached and this critical cake thickness can be reduced by the addition of a deflocculant. The results were ignored because they conflicted with filter cake simulations which require a monotonic porosity distribution.

Grace⁶⁸ also described the application of the CP technique to the study of the properties of a wide range of compressible filter cakes and conclusively demonstrated that CP data can simulate filtration to within $\pm 10\%$ when average filtration resistances are compared.

He introduced a modified definition of average specific cake resistance based on Ruth's definition⁵⁸:

$$\alpha_{avg} = \frac{\Delta P_c}{\int_0^{\Delta P_c} \frac{dP_s}{\alpha}} \quad (3-1.35)$$

where:

ΔP_c — Pressure differential across the filter cake,

α_{avg} is a function of time if the septem resistance is not negligible.

In 1958, Kottwitz and Boylan⁷¹ successfully predicted average cake resistance using Compression-Permeability test data. They introduced an alternative definition of average cake resistance:

$$\alpha_{mean} = \frac{\int_0^{\Delta P_c} \alpha dP_s}{\Delta P_c} \quad (3-1.36)$$

and concluded that predictions made by using above expression were in some cases better than predictions made by using equation(3-1.35). In other cases the predicted values of average specific cake resistance by both methods were in good agreement. In all cases, however, the α_{avg} values were lower than the laboratory filtration specific resistance.

In 1960, Tiller and Cooper⁸⁰ introduced the concept that average porosity is not constant but that it decreases and squeezes liquid out of the cake causing the exit flow to exceed the entrance flow. Subsequently, a correction factor, J_T was introduced by Tiller and Huang⁷² into the definition of the average cake resistance to account for the internal flow rate variation. Figure(3-1.1) listed the important parameters in cake formation. The correction factor:

$$(\alpha_{avg})_T = J_T(\alpha_{avg}) \quad (3-1.37)$$

$$J_T = \frac{q_{avg}}{q_i} \quad (3-1.38)$$

where:

q_{avg} — average value of q_x ;

q_i — value of q_x at interface of medium and cake;

α_{avg} — average value of α uncorrected for variation of flow rate;

J_T — correction factor for filtration resistance, ratio of average flow rate to rate at medium, dimensionless.

J_T would be evaluated from CP data. The average resistance was then a function of P_a , s and dV/dt and is no longer constant as Ruth⁵⁸ initially postulated.

Baird and Perry⁶³ confirmed Rietema's results⁶¹ and demonstrated that RPC is a function of critical cake length and applied pressure. He also criticized filter cake simulation because it can not take into account the dynamic effect of fluid flow on the developing cake structure and porosity.

Shirato *et al.*⁷⁴ further developed an empirical exponential function for the distribution of solids stress in a CP cell arising from side-wall friction in 1968. The results showed that neglecting side-wall friction in a CP cell leads to significant error in estimating filtration characteristics and that CP porosities and resistances are not uniform as previously assumed.

In 1969, another correction factor, J_s was introduced by Shirato *et al.*⁶⁴ into the definition of the average cake resistance to account for the relative velocity between the solid and liquid:

$$\alpha_{avg} = J_s(\alpha_{avg}) \quad (3-1.39)$$

$$J_s = \int_0^1 \left[1 - \frac{(\epsilon_x - \epsilon_{avgx})(m-1)}{(1-\epsilon_x)\epsilon_{avg}(1-ms)} \cdot s \cdot \left(\frac{x}{L}\right) \right] d\left(\frac{W_x}{W}\right) \quad (3-1.40)$$

where:

ϵ_{avg} — average porosity for entire cake, dimensionless;

ϵ_x — local value of porosity at distance x from the medium,
dimensionless;

ϵ_{avgx} — average porosity for the portion of cake between medium and
distance x , dimensionless;

α_{avg} is theoretically the average specific resistance of a compressible bed with the slurry concentration equal to zero. If slurry concentration were actually zero, there would

be no additional solids deposited. In practice, α_{avg} is a good approximation of the average filtration resistance when the slurry is dilute.

J_s is always less than unity and dependent on slurry concentration and pressure drop across cake. J_s is evaluated from CP data.

Tiller *et al.*⁷⁷ presented simplified wall friction theory for CP cells and derived the empirical expression given earlier by Shirato⁷⁴. They itemized the variations in CP methodology that have a significant effect on CP results.

Tiller *et al.*⁷⁷ also presented the qualitative stress profiles for cakes in CP cells, especially with regard to the interaction of various solid particulates and different coating materials for CP cell walls.

In 1973, Tiller and Green⁷⁸ further found that the methodology of the CP cell is further complicated by the fact that it is virtually impossible to obtain accurate values of resistance and porosity from CP cells at low pressure.

Willis *et al.*⁶⁶ introduced a novel filter chamber that measures the accumulative drag experienced by the septum. They measured P_c/σ and found the ratio equal to the average porosity rather than unity. They suggested that cakes are incompressible up to a critical cumulative drag stress. The parabolic filtration equation was shown to be independent of cake compressibility where cake compressibility is determined a priori from axial distributions.

For constant applied pressure axial filtration, incompressible cakes exhibit a linear pressure distribution while compressible cakes exhibit a non-linear pressure distribution. Based on this latter definition Willis *et al.*⁶⁶ categorized filter cakes a Priori according to their axial pressure distributions and showed that cakes with linear pressure profiles are indeed very rare. Further cakes with either a linear or non-linear pressure distribution are described best by the parabolic correlation.

Wronski *et al.*⁶² observed deviations from Ruth's equation and proposed a model of

average specific cake resistance of the form:

$$\alpha_{\text{avg}} = a + b \left(\frac{dt}{dV} \right) \quad (3-1.41)$$

to correct the errors caused by Ruth's equation.

Tiller *et al*¹⁰⁷ proposed another form for the porosity variation with P_s :

$$1 - \varepsilon = (1 - \varepsilon_L) \cdot \left(1 + \frac{P_s}{P_{\text{arb}}} \right)^\beta \quad (3-1.42)$$

where

P_{arb} — an arbitrary parameter used to make the equation dimensionless.

Similarly:

$$\alpha = \alpha_L \left(1 + \frac{P_s}{P_{\text{arb}}} \right)^n \quad (3-1.43)$$

Above equations provides a continuous function over the entire compressive pressure range.

In 1980, Willis and Tosun⁷³ developed a rigorous cake filtration theory based on the multiphase equations of change and they found the least permeable part of the cake at the cake-septem interface controls the filtrate rate. The internal variations in porosities and specific cake resistances can be obtained directly from filtration data alone and do not required a CPC simulation.

In 1982, Tosun and Willis⁷⁵ verified the validity of the “power law” approximation equations which states that the average specific cake resistance and average cake porosity can be expressed by a power law relationship with the pressure on solid and concluded that these equations should not be used.

Tosun and Willis⁷⁶ then realized that the classification of filter cakes as compressible

and incompressible is unnecessary. The parabolic behaviour could be achieved by proper septum selection. Subsequently, they⁷⁹ further concluded that the average cake porosity is independent of time and filter cake geometry.

Bierck *et al.*⁸¹ also found that average cake porosity is constant.

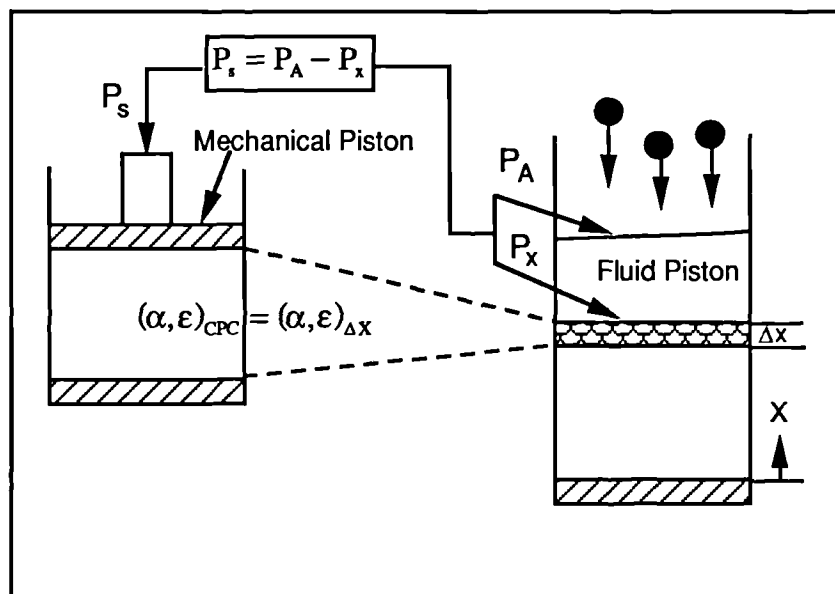
3.1.3 Summary of Cake Filtration Theory

Presented above is a careful examination of the literature in the chronological order of events over the past 60 years. The papers surveyed are of significance which represented the current direction of cake filtration mechanisms research⁶⁵. It is clear that there were two distinct approaches which, one of them was based on direct filtration measurements, dominating the early development (1912-1933), the other one was based on filter cake simulation using the compression-permeability (CP) concept, dominating the more recent (1946-1980) efforts in filtration investigations.

Through the first approach in filtration investigation postulated above, it is evident that the equation developed by Ruth⁵⁸ in 1935 is still considered to be the basic cake filtration equation. The second approach, which has been recognised by those interested in the progress of research in solid-liquid separation that the CPC simply does not work⁶⁵, are presented because it is believed that this knowledge should be useful to understand filtration phenomenon more deeply.

The simulation of filtration using CPC depends on two postulates:

- (i) When the difference between the applied pressure and the pressure at any point within the cake is equal to the applied pressure in CP cell, the porosity and the specific cake resistance obtained from this device are equal to the porosity and the specific cake resistance of the differential volume element as shown in Figure(3-1.3).



Figure(3-1.3) Simulation of Filtration by Using
Compression Permeability Cell

- (ii) The local porosity and specific cake resistance can be uniquely expressed as a function of the compressive pressure P_s .

Unfortunately, there is no evidence in the literature that quantitative investigations have been undertaken to investigate these highly questionable postulations. These postulations have received tacit acceptance. Besides, due to the serious methodology problems encountered with the operation of the CPC, such as side-wall friction, the data obtained from the CPC have never been able to predict actual filtration data⁶⁵.

3.2 LITERATURE REVIEW OF FILTRATION EQUATIONS OF DRILLING FLUIDS

Most of the research on the theoretical modelling of drilling fluids filtration were based on Darcy's law and the first published paper was given by Williams and Cannon³ who predicted the static filtration of drilling muds. The integrated form of their equation was:

$$\frac{V}{A} = \sqrt{M_w t + C_w^2} - C_w \quad (3-2.1)$$

in which

$$M_w = \frac{2\Delta P_c^{1-s}}{\mu \nu R' (1-s)} \quad (3-2.2)$$

$$C_w = \frac{A \rho' f(\Delta P_c)}{\nu R' \Delta P_c^s} \quad (3-2.3)$$

where

subscript w represents Williams

t — time

A — filtration area

μ — filtrate viscosity

V — cumulative filtrate volume

s — a compaction function of the cake

R' — a function of resistivity of the cake

ΔP_c — filtration pressure drop across cake

v — ratio of volume of filter cake to volume of filtration

$\rho'f(P)$ — a function of the resistance of the filtration medium

ρ' — resistance coefficient of filtration medium and sludge contained therein

They found from the experimental results that:

- (1) s , the compressibility function varied from 0.80 to 0.87 for the usual unweighted mud. Addition of weighted material ordinarily lowers this value. Chemical treatment affects s very little.
- (2) R' , the resistance coefficient of the filter cake, appeared to depend upon the specific nature of the solid phase, the particle size distribution and the state of aggregation of the solid phase.
- (3) v , cake volume/filtrate volume ratio, usually remains within a narrow range.

No fixed rule for evaluation of $\rho'f(P)$ was found, Generally, $f(P)$ seems to be an exponential function.

The equation(3-2.1) which was only applicable to static filtration was slightly later extended to the dynamic filtration of muds in a second paper by Williams⁶. He found that the filtration rate during dynamic condition became constant after a short time and this constant rate attained in any particular test depended on the pressure, rate of mud circulation, and mud properties. Williams thereafter proposed the following equation from the experimental results to express the equilibrium filtration rate:

$$q_{\text{eq}} = \frac{1}{A} \left. \frac{dV}{dt} \right|_{\text{eq}} = C_w' \sqrt{QM_w} \quad (3-2.4)$$

where

Q — axial mud flow rate;

M_w — determined in equation(3-2.1)

C_w' — empirical constant

Equation(3-2.1) was also extended from laboratory filter to the borehole radial flow case by Williams⁶. The form for the borehole radial filtration was:

$$V + \left(\frac{\pi r_0^2 L}{v} - v \right) \cdot \ln \left(1 - \frac{vV}{\pi r_0^2 L} \right) + \frac{4\pi L \rho' f(\Delta P_c)}{R' \Delta P_c^s} = \frac{4\pi L \Delta P_c^{1-s}}{\mu R' (1-s)} \quad (3-2.5)$$

Larsen⁴ developed a static filtration equation for incompressible cake from Darcy's law:

$$V = K_L \sqrt{\frac{P_s R_L t}{\mu}} \quad (3-2.6)$$

where:

$$R_L = \frac{V_{\text{filtrate}}}{V_{\text{cake}}} \text{ Ratio of filtrate volume /volume of deposited solid}$$

K_L — constant for specific mud.

The above equation was then modified by Larsen⁴ to consider the deviation which occurs during the initial stage of the filtration as follows:

$$V = K_L' \sqrt{t} + e \quad (3-2.7)$$

Larsen further investigated the validity of the above equations by varying the applied differential pressure. It can be seen from equation(3-2.6) that V should be proportional to the square root of the differential pressure, however, the experimental results showed that

a more general relationship was valid:

$$V = k_L P^x \quad (3-2.8)$$

where $x < 0.5$ and could be evaluated from the log-log plot of volume versus pressure.

Further, Larsen also studied the effect of temperature on the cumulative filtrate volume and proposed that:

$$\frac{V(T_2)}{V(T_1)} = \sqrt{\frac{\mu(T_1)}{\mu(T_2)}} \quad (3-2.9)$$

where V and μ are the cumulative filtrate volume and filtrate viscosity at temperature T_1 and T_2 respectively.

Ferguson and Klotz¹³ presented a modification of the classic cake filtration equation to express static filtration upon a dynamic filtration cake. It was assumed that the static filtration follows the classic law:

$$V^2 = C_F t \quad (3-2.10)$$

Then they used following equation:

$$(V + V_0)^2 = C_F (t + t_0) \quad (3-2.11)$$

to express the static filtration upon a dynamic filter cake in which the resistance of the dynamic cake is represented as the resistance of fictitious static filter cake that was deposited in t_0 hours with a flow of V_0 ml/in² of filtrate. However, this modified equation did not follow the experimental static filtration data for two reasons that they reported:

- (i) As the drill string, including a rock bit, was pulled and the linear run, part of dynamic cake was scraped from the wellbore so that part of the static cake deposited on a clean sand face and part on a dynamic cake;
- (ii) The equation is derived for filtration through a plane filter whereas filtration in a

well occurs on the inner surface of a cylinder.

They then presented an equation to calculate the filtration volume that flows through the well wall after part of wall has been scraped clean by a bit:

$$V = \psi V_s + (1 - \psi) V_u \quad (3-2.12)$$

where

V_s — volume of filtrate that flows through the scraped portion of well wall

V_u — volume of filtrate through the unscraped portion

ψ — the fraction of the well wall that is scraped clean

V_s changes with time according to equation(3-2.10) whereas V_u changes according to equation(3-2.11). The total volume of the filtration volume is:

$$V = \psi \sqrt{C_F t} + (1 - \psi) \left[\sqrt{C_F t + C_F t_0} - V_0 \right] \quad (3-2.13)$$

Ferguson and Klotz also presented following equation to cover the difference between the filtration volume from plane filter and from cylindrical filter:

$$\left(\frac{V_p}{Zr} \right)^2 = \left(\frac{1}{2} - \frac{V_c}{2r} \right) \left[\ln \left(1 - \frac{2V_c}{Zr} \right) \right] + \frac{V_c}{Zr} \quad (3-2.14)$$

where

r — the well radius

Z — ratio of filtrate volume to cake volume

V_p — volume of filtrate collected on plane filter

V_c — volume of filtrate collected on cylindrical filter

Glenn and Slusser¹⁵ used the classic static filtration equation to evaluate the filtration characteristics of drilling muds in the form:

$$\frac{t}{V} = M_G V + N_G \quad (3-2.15)$$

where

M_G — a coefficient defined by physical characteristics of the mud filter cake and conditions imposed during filtration

N_G — a constant defined by the fluid flow characteristics of septum.

In equation(3-2.15), t and V are both cumulative values, and include respectively the spurt time t_{sp} and spurt volume V_{sp} . They considered that the septum resistance are very small compared to cake resistance. It was then neglected without appreciable error. If t_{sp} and V_{sp} are subtracted from t and V respectively, equation(3-2.15) becomes:

$$t'/V' = M'_G V' \quad (3-2.16)$$

where

$$t' = t - t_{sp} \quad (3-2.17)$$

$$V' = V - V_{sp} \quad (3-2.18)$$

M'_G = a number defining the filtration characteristics of the mud filter cake.(increases from zero to a value which is constant for the constant pressure filtration period.)

Outmans²¹ reported for the first time a theoretical study on dynamic filtration modelling. The filtration curve produced by him of the various stages is shown in Figure(2-1.6). From T_1 to T_2 the thickness of the cake remains constant, but the filtration rate continues to decrease. He explained that the filter cake continue to compact (presumably, the rate of deposition equals the rate of compaction). At time T_2 , equilibrium conditions are reached, and both the filtration rate and the cake thickness remain constant. The equilibrium filtration rate is then given by the equation:

$$q|_{\infty} = \frac{1}{A} \frac{dV}{dt} \Big|_{\infty} = \frac{K_1 (\tau_f)^{-v+1}}{\mu \delta (-v+1)} \quad (3-2.19)$$

where

K_1 — the cake permeability at 1 psi pressure

$-v+1$ — a function of the cake compressibility

τ — the shear stress exerted by the mud stream

δ — the thickness of the cake subjected to erosion

f — the coefficient of internal friction of the cake's surface layer

Bezemer and Havenaar²⁴ used another form of the classic static filtration equation:

$$\frac{dV}{dt} = \frac{1}{2} C_B t^{-\frac{1}{2}} \quad (3-2.20)$$

to evaluate the experimental data. In their dynamic filtration tests, it was found that the relationship between equilibrium filtration rate and rate of shear at the cake surface could be given by:

$$\left. \frac{1}{A} \frac{dV}{dt} \right|_{eq} = q_{eq} = C'_B \gamma \quad (3-2.21)$$

where

eq — subscript referring to equilibrium conditions

γ — rate of shear at the cake surface

Combination of above equations with Darcy's law for a flat cake gives:

$$\gamma h_{eq} = \frac{K \Delta P}{\mu C'_B} \quad (3-2.22)$$

where

K — Cake permeability

h_{eq} — filter cake thickness after equilibrium attained

Chelton²⁹ adapted Darcy's law as follows:

$$K = \frac{q\mu L}{AP} \quad (3-2.23)$$

where

L = length

q = flow rate

P = pressure

K = permeability

A = filter medium cross section

μ = viscosity of the flowing fluid

at constant pressure:

$$\frac{1}{A} \left(\frac{dV}{dt} \right) = \frac{P}{\mu(L/K)} \quad (3-2.24)$$

He thought the term $[L/K]$ represents resistance to flow. In a filter press, the resistance to flow is made up of the resistance of the filter medium and the filter cake and thereafter:

$$L/K = L_c/K_c + L_f/K_f \quad (3-2.25)$$

where

L_c, K_c — length and permeability of filter cake, and

L_f, K_f — length and permeability of filter medium.

Therefore

$$\frac{1}{A} \frac{dV}{dt} = \frac{P}{\mu[L_c/K_c + L_f/K_f]} \quad (3-2.26)$$

The permeability of the filter cake K_c may depend upon pressure, temperature, and the type of solids in the fluid, but can be assumed to be independent of the quantity of

filtrate. The length of filter cake L_c should be proportional to the amount of solids deposited in the cake, or proportional to $[V/A]$, and thereafter:

$$\frac{d(V/A)}{dt} = \frac{P}{\mu(\alpha V/A + r)} \quad (3-2.27)$$

where

α — a function [of pressure, temperature and type of solids] representing the specific cake resistance.

r — L_f/K_f constant resistance of the filter medium to flow

Separating the variables and integrating:

$$\frac{Pt}{V/A} = \left(\frac{\mu\alpha}{2}\right)V/A + \mu r \quad (3-2.28)$$

Plotting $Pt/V/A$ vs. V/A should yield a straight line with an intercept of μr and slope of $\mu\alpha/2$. The specific cake resistance α is related to the pressure as follows:

$$\alpha = \alpha' P^s \quad (3-2.29)$$

$$\log \alpha = s \log P + \log \alpha' \quad (3-2.30)$$

a plot of $\log \alpha$ vs. $\log P$ yields a straight line with a slope of s , and an intercept at $P=1$ of α' .

Hassen⁴⁹ proposed a series of equations to predict the static and dynamic filtration as follows:

Static filtration rate declines with time according to classic law:

$$q = C_1 t^{-0.5} \quad (3-2.31)$$

where

C_1 — static filtration rate constant

Integrating above equation then the value of static filtration increases with time much as described in equation:

$$V = C_2 t^{0.5} + C_3 \quad (3-2.32)$$

where

C_2 — static filtration volume constant

C_3 — spurt loss volume

It is clear that $C_2 = 0.5 C_1$

Equation(3-2.31) and (3-2.32) represent filtration under constant temperature and pressure conditions. In order to include the effect of temperature, it is compensated for by a factor as shown in equation(3-2.33):

$$q_2 = q_1 \exp\left[\frac{B (T_2 - T_1)}{2 T_2 T_1}\right] \quad (3-2.33)$$

where

B — viscosity constant for newtonian fluid

He believed that the effect of temperature caused by the change of filtrate viscosity.

The effect of pressure on filtrate flow rate were considered as described in equation(3-2.34):

$$q_2 = q_1 \left(\frac{\Delta P_2}{\Delta P_1}\right)^p \quad (3-2.34)$$

where

p — pressure correction exponent for filter cake.

If the filter cake is incompressible, the p is 0.5. In fact, in most cases, the p is less

than 0.5. He found the extreme case, $p = 0$, such as Wyoming bentonite in fresh water slurry that has a very compressible filter cake. The typically good mud has a power of 0.1 to 0.2.

Hassen used the following equation to describe the dynamic non-equilibrium period:

$$q = C_4 t^{-0.5} + \gamma C_5 \quad (3-2.35)$$

where

C_4 — non-equilibrium shear rate multiplier

C_5 — dynamic non-equilibrium constant

γ — fluid shear rate

C_4 is approximated by C_1 for water base mud, but may be up to 6 times larger for emulsion muds. The dynamic equilibrium period was described by

$$q = C_6 t_{eq}^{-0.5} + \gamma C_7 \quad (3-2.36)$$

where

C_6 — dynamic equilibrium constant

C_7 — equilibrium shear rate multiplier

t_{eq} — time at which dynamic equilibrium is attained

Here C_6 is approximated by C_4 .

The constant C_5 and C_7 are a function of how mechanically stable a filter cake is.

Hassen also proposed a equation to calculate the depth of filtration invasion resulting from the above:

$$\text{Depth} = r \left[\left(1 - \frac{X}{E} \right) + \frac{q}{\phi U E} \right]^{1/2} - r \quad (3-2.37)$$

where

- r — Radius of wellbore
- ϕ — Formation porosity
- U — Drilling penetration rate
- E — Fluid displacement efficiency of filtrate
- X — Fraction of filtrate through hole bottom removed by drill bit

Fordham *et al.*⁴⁵ suggested, based on the experimental data, the following equation to predict dynamic fluid loss of drilling mud:

$$V = (\pi D_1 L) \cdot S \cdot t^{1/2} \quad t \ll t_c \quad (3-2.38)$$

$$V = (\pi D_1 L) \left[S \cdot t_c^{1/2} + q_{\infty} t \right] \quad t \gg t_c \quad (3-2.39)$$

where

- S — sorptivity;
- D_1 — annulus inner diameter;
- L — filter core axial length
- q_{∞} — dynamic filtration rate per unit area
- t_c — some timescale for the transition to the dynamic phase.

They concluded that the fluid loss can be described by three key parameters: One describing the early (“quasi-static”) behaviour, a second describing the late (“dynamic”) behaviour of near-constant fluid loss rate, and thirdly a timescale for the transition between these two regimes.

By simply matching the filtration rate at time $t = t_c$ in model equation(3-2.38) and (3-2.39), it can be derived:

$$t_c = \frac{S^2}{4q_{\infty}} \quad (3-2.40)$$

An empirical correlation:

$$q_{\infty} \approx Q_{\infty} \left(\frac{\gamma_w}{\Gamma_d} \right)^m \quad (3-2.41)$$

where

γ_w — shear rate at channel wall

Γ_d — scaling shear rate (arbitrary value)

m — exponent in dynamic fluid loss correlation

Q_{∞} — Pre - factor in dynamic fluid loss correlation

was obtained when they plot dynamic fluid loss rates q_{∞} against wall shear rates corrected for rheological and geometry effects in log-log form.

where m takes a value between 0.59 and 0.69. and if Γ_d (an arbitrary scaling shear rate) is taken at 100 s^{-1} , Q_{∞} is approximately $0.15 \mu\text{ms}^{-1}$ for their mud systems.

The relation (3-2.40) combined with the correlation (3-2.41) implies a similar power law correlation for t_c :

The correlation:

$$t_c = \varphi \left(\frac{\Gamma_d}{\gamma_w} \right)^{2m'} \quad (3-2.42)$$

where

φ — pre - factor in transition time correlation

m' — exponent in transition time correlation

models the data satisfactorily, with m' taking the values from 0.62-0.71, similar to m in equation(3-2.41) as expected.

t_c thus varies inversely with wall shear. t_c is between about 5 hours and 20 minutes in their experiments.

Arthur and Peden⁴⁷ used the equation:

$$t' = a_2 V'^2 + a_1 V' + t_0 \quad (3-2.43)$$

where

$$a_2 = \frac{\mu \alpha_{avg} \rho_f s}{2(1 - ms) A^2 \Delta P} \quad (3-2.44)$$

$$a_1 = \frac{\mu (R_m + R_{sp})}{A \Delta P} \quad (3-2.45)$$

t' and V' possess the same meaning as they are in equation(3-2.17) and (3-2.19).

t_0 represents the correction value of the initial non-constant pressure across cake filtration.

They used an expression for average cake resistance of compressible filter cakes:

$$\alpha_{avg} = \frac{\alpha_0 \Delta P_c^n}{1 + n} \quad (3-2.46)$$

and average porosity and permeability which directly calculated from the definition:

$$\epsilon_{avg} = \frac{(m - 1) \frac{\rho_s}{\rho_f}}{1 + (m - 1) \frac{\rho_s}{\rho_f}} \quad (3-2.47)$$

$$K_{avg} = \frac{1}{\alpha_{avg} (1 - \epsilon_{avg}) \rho_s} \quad (3-2.48)$$

They also found that the spurt loss V_{sp} is non-linear function of pressure of the form:

$$V_{sp} = a \Delta P^b \quad (3-2.49)$$

and confirm the Larsen's relationship.

3.3 DEVELOPMENT OF GENERAL FILTRATION EQUATION OF DRILLING FLUIDS

3.3.1 External Mass Balance

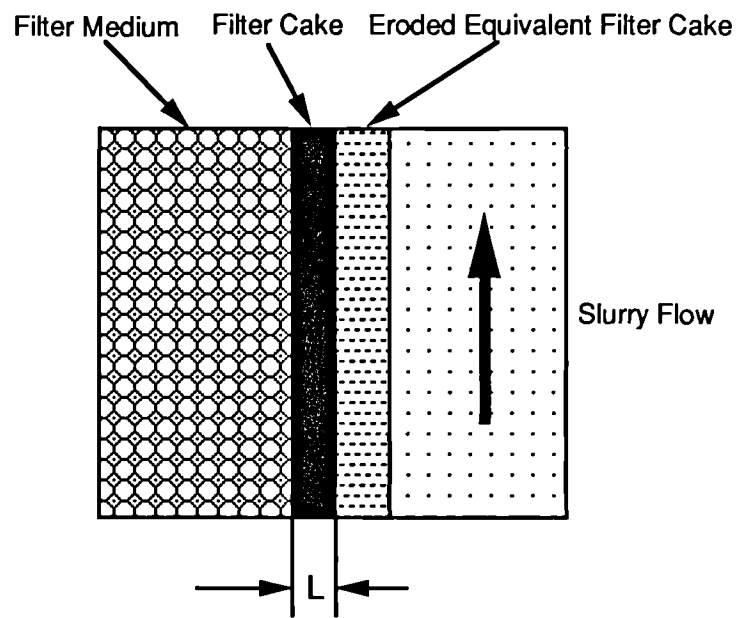
The mathematical treatment of drilling fluids filtration is based on the following concepts:

- (i) The weight of eroded solids from the cake is proportional to the duration of circulation and the shear stress on the filter cake surface if mud is circulating, and filter cake area;
- (ii) Filter cake build-up is a continual process of deposition and erosion, and these actions occur simultaneously;
- (iii) Flow through the filter cake is laminar. Because the pore sizes in the cake and filter medium are small, and the liquid velocity through the pore is low, the filtrate flow may then be considered laminar;
- (iv) The filter cake is incompressible. In fact, the mud cake is compressible and this will be discussed in chapter five;
- (v) The filter medium resistance is constant throughout the whole filtration process. This assumption requires that the process is no-bridging filtration.

In Figure(3-3.1), if the eroded mass of solid is expressed in terms of equivalent filter cake mass, the external mass balance can also be used.

since:

$$W = W_c + W_e \quad (3-3.1)$$



Figure(3-3.1) The Relationship between Filter Cake and Cumulative Deposited Cake

where:

W_c — filter cake weight per unit area (Kg/m^2)

W_e — eroded solid weight per unit area (Kg/m^2)

W — cumulative deposited solids (filter cake) weight per unit area (Kg/m^2)

According to above concepts, we may express W_e as:

$$W_e = K_\tau \cdot \tau \cdot t \quad (3-3.2)$$

or

$$W_e = B \cdot t \quad (3-3.3)$$

where:

t = time (sec)

B = dynamic filtration coefficient ($\text{Kg/m}^2 \cdot \text{sec}$)

τ = shear stress on the filter cake surface (N/m^2)

K_τ = dynamic filtration erodability coefficient ($\text{Kg/N} \cdot \text{sec}$)

K_τ is defined as the eroded solid mass per unit of shear stress on a unit of filter cake surface area in a unit of time

Writing external mass balance:

$$\frac{W}{s} = \frac{W}{s_c} + \rho_f \frac{V}{A} \quad (3-3.4)$$

Solving equation(3-3.4) for W ,

$$W = \frac{\rho_f s}{1 - ms} \frac{V}{A} \quad (3-3.5)$$

where:

$$m = \frac{1}{s_c}$$

Substituting W_e , W in equation(3-3.3) and equation(3-3.5) for W , W_e in equation(3-3.1), we may obtain W_c :

$$W_c = \frac{\rho_f s}{1 - ms} \frac{V}{A} - Bt \quad (3-3.6)$$

Now we can write Darcy's law:

$$q = \frac{1}{A} \frac{dV}{dt} = \frac{\Delta P}{\mu R} = \frac{\Delta P}{\mu(R_c + R_m)} \quad (3-3.7)$$

where

$$R_c = \alpha W_c \quad (3-3.8)$$

Combining equation(3-3.6) with equation(3-3.8) and inserting the resultant R_c into equation(3-3.7), and rearranging:

$$\frac{dt}{dV} = \frac{\mu \alpha \rho_f s}{\Delta P A^2 (1 - ms)} V - \frac{\mu \alpha B}{\Delta P A} t + \frac{\mu R_m}{\Delta P A} \quad (3-3.9)$$

This is a first order nonhomogeneous linear differential equation if all the terms on the right hand side, except t and V , are assumed to be constant with time, and solving for t vs. V with the boundary condition:

$$\text{if } t=0, \text{ then } V=0$$

we can get the relation between cumulative filtrate volume and time and this will be discussed next.

3.3.2 Solution of Differential Equation of Filtration

A first order differential equation is said to be linear if it can be written:

$$y'+p(x)y=r(x) \quad (3-3.10)$$

The characteristic feature of this equation is that it is linear in y and y' , whereas p and r on the right may be any given function of x . If right-hand side $r(x)$ is zero for all x in the interval in which we consider the equation (written $r(x)=0$), The equation is said to be homogeneous, otherwise it is said to be nonhomogeneous. For the nonhomogeneous first-order linear differential equation(3-3.10), we have the general solution:

$$y(x) = e^{-h} \left[\int e^h r(x) dx + C \right], \quad h = \int p(x) dx \quad (3-3.11)$$

where the choice of the value of the constant of integration in $\int p(x) dx$ is immaterial.

Now we can write our problem equation(3-3.9) in the form of nonhomogeneous first-order linear differential equation as follows:

$$\frac{dt}{dV} + \kappa_2 t = \kappa_1 V + \kappa_3 \quad (3-3.12)$$

Where:

$$\kappa_1 = \frac{\mu \alpha_{avg} \rho_f S}{\Delta P A^2 (1 - ms)} \quad (3-3.13)$$

$$\kappa_2 = \frac{\mu \alpha_{avg} B}{\Delta P A} \quad (3-3.14)$$

$$\kappa_3 = \frac{\mu R_m}{\Delta P A} \quad (3-3.15)$$

It should be noted that α was replaced by α_{avg} for integration because α_{avg} is assumed

to be constant through out the whole filtration.

Comparing equation(3-3.12) with equation(3-3.11), the general solution of equation (3-3.12) is then given by:

$$t = e^{-\int \kappa_2 dV} \left[\int e^{\int \kappa_2 dV} (\kappa_1 V + \kappa_3) dV + C \right] \quad (3-3.16)$$

Simplifying equation(3-3.16), we obtain:

$$\begin{aligned} t &= e^{-\kappa_2 V} \left[\int e^{\kappa_2 V} (\kappa_1 V + \kappa_3) dV + C \right] \\ &= e^{-\kappa_2 V} \cdot \left[\frac{\kappa_1}{\kappa_2^2} \cdot (\kappa_2 V - 1) \cdot e^{\kappa_2 V} + \frac{\kappa_3}{\kappa_2} \cdot e^{\kappa_2 V} + C \right] \\ &= \frac{\kappa_1}{\kappa_2} V + \frac{\kappa_3}{\kappa_2} - \frac{\kappa_1}{\kappa_2^2} + C \cdot e^{-\kappa_2 V} \end{aligned} \quad (3-3.17)$$

Applying the initial condition, $V=0$, when $t=0$ to above equation, we could get the integration constant::

$$C = \frac{\kappa_1}{\kappa_2^2} - \frac{\kappa_3}{\kappa_2} = \frac{\kappa_1 - \kappa_2 \kappa_3}{\kappa_2^2} \quad (3-3.18)$$

Hence, inserting C from equation(3-3.18) into equation(3-3.17), the general solution of our initial value problem is obtained:

$$t = \frac{\kappa_1}{\kappa_2} V - \frac{\kappa_1 - \kappa_2 \kappa_3}{\kappa_2^2} [1 - e^{-\kappa_2 V}] \quad (3-3.19)$$

By inserting $\kappa_1, \kappa_2, \kappa_3$ from equation(3-3.13), (3-3.14), (3-3.15) into equation(3-3.19), we get:

$$t = \frac{\rho_f s}{(1 - m_s) B A} V - \left(\frac{\Delta P \rho_f s}{(1 - m_s) \mu \alpha_{avg} B^2} - \frac{R_m}{\alpha_{avg} B} \right) \cdot \left(1 - e^{-\frac{\mu \alpha_{avg} B V}{\Delta P A}} \right) \quad (3-3.20)$$

Equation(3-3.20) is the general equation of filtration.

Letting:

$$C_1 = \frac{\rho_f s}{(1 - ms)AB} \quad (3-3.21)$$

$$C_2 = \left(\frac{\Delta P \rho_f s}{(1 - ms)\mu\alpha_{avg} B^2} - \frac{R_m}{\alpha_{avg} B} \right) \quad (3-3.22)$$

$$C_3 = \frac{\mu\alpha_{avg} B}{\Delta P A} \quad (3-3.23)$$

Then equation(3-3.20) becomes:

$$t = C_1 V - C_2 (1 - e^{-C_3 V}) \quad (3-3.24)$$

3.3.3 Applications of General Filtration Equation

3.3.3.1 Erodability of Dynamically Deposited Cake

Differentiating equation(3-3.24) on both sides with respect to time:

$$1 = C_1 \frac{dV}{dt} - C_2 C_3 e^{-C_3 V} \frac{dV}{dt} \quad (3-3.25)$$

Rewriting above equation:

$$\frac{dV}{dt} = \frac{1}{C_1 - C_2 C_3 e^{-C_3 V}} \quad (3-3.26)$$

When $t \rightarrow \infty$, $V \rightarrow \infty$, then $e^{-C_3 V} \rightarrow 0$, $\left. \frac{dV}{dt} \right|_{t \rightarrow \infty} = \left. \frac{dV}{dt} \right|_{V \rightarrow \infty} \rightarrow \frac{1}{C_1}$,

So that:

$$q_{eq} = \frac{1}{A} \frac{dV}{dt} \Big|_{eq} = \frac{1}{AC_1} = \frac{(1-ms)B}{\rho_f s} \quad (3-3.27)$$

q_{eq} is then defined as the dynamic equilibrium filtration rate.

Combining equation(3-3.2) with (3-3.3), it is obtained:

$$B = K_\tau \cdot \tau \quad (3-3.28)$$

Inserting equation(3-3.28) into equation(3-3.27), we obtain:

$$q_{eq} = \frac{(1-ms)K_\tau \tau}{\rho_f s} \quad (3-3.29)$$

Equation(3-3.29) represents the relationship between the dynamic equilibrium filtration rate and shear stress on the filter cake surface. From equation(3-3.29), we can get:

$$K_\tau = \frac{\rho_f s}{(1-ms)\tau AC_1} \quad (3-3.30)$$

3.3.3.2 Static Filtration Equation

If letting $B=0$ in equation(3-3.20), then

on the left hand side:

$$\lim_{B \rightarrow 0} t = t \quad (3-3.31)$$

on the right hand side:

$$\begin{aligned} & \lim_{B \rightarrow 0} \left\{ \frac{\rho_f s}{(1-ms)B} \frac{V}{A} - \left(\frac{\Delta P \rho_f s}{(1-ms)\mu \alpha_{avg} B^2} - \frac{R_m}{\alpha_{avg} B} \right) \cdot \left(1 - e^{-\frac{\mu \alpha_{avg} B V}{\Delta P A}} \right) \right\} \\ & = \frac{\rho_f s \mu \alpha_{avg}}{2 \Delta P A^2 (1-ms)} V^2 + \frac{\mu R_m}{\Delta P A} V \end{aligned} \quad (3-3.32)$$

hence:

$$t = \frac{\rho_f s \mu \alpha_{avg}}{2 \Delta P A^2 (1 - ms)} V^2 + \frac{\mu R_m}{\Delta P A} V \quad (3-3.33)$$

letting:

$$a_2 = \frac{\rho_f s \mu \alpha_{avg}}{2 \Delta P A^2 (1 - ms)} \quad (3-3.34)$$

$$a_1 = \frac{\mu R_m}{\Delta P A} \quad (3-3.35)$$

then

$$t = a_2 V^2 + a_1 V \quad (3-3.36)$$

this is the classic static filtration equation.

3.4 THE DIMENSIONAL ANALYSIS OF DYNAMIC FILTRATION OF DRILLING FLUIDS

3.4.1 The Buckingham Π Theorem⁹⁸

In a physical problem including n quantities in which there are m dimensions, the quantities can be arranged into $n-m$ independent parameters. Let $A_1, A_2, A_3, \dots, A_n$ be the quantities involved, such as pressure, viscosity, velocity, etc. All the quantities are known to be essential to the solution, and hence some functional relation must exist.

$$F(A_1, A_2, A_3, \dots, A_n) = 0 \quad (3-4.1)$$

If Π_1, Π_2, \dots represent dimensionless groupings of the quantities A_1, A_2, A_3, \dots then with m dimensions involved, an equation of the form:

$$\Phi(\Pi_1, \Pi_2, \Pi_3, \dots, \Pi_{n-m}) = 0 \quad (3-4.2)$$

exists.

The method of determining the Π parameters is to select m of the A quantities, with different dimensions, that contain among them the m dimensions, and to use them as repeating variables together with one of the other A quantities for each Π . For example, let A_1, A_2, A_3 contain M, L and T , not necessary in each one, but collectively. Then the first Π parameter is made up as:

$$\Pi_1 = A_1^{X_1} A_2^{Y_1} A_3^{Z_1} A_4 \quad (3-4.3)$$

the second one as

$$\Pi_2 = A_1^{X_2} A_2^{Y_2} A_3^{Z_2} A_5 \quad (3-4.4)$$

and so on, until

$$\Pi_{n-m} = A_1^{X_{n-m}} A_2^{Y_{n-m}} A_3^{Z_{n-m}} A_n \quad (3-4.5)$$


In these equations the exponents are to be determined so that each Π is dimensionless. The dimensions of the A quantities are substituted, and the exponents of M, L , and T are set equal to zero respectively. These produce three equations in three unknowns for each Π parameter, so that the X, Y and Z exponents can be determined, and hence the Π parameter.

3.4.2 The Application of Π Theorem to the Dynamic Filtration

So far as the Π theorem is concerned, filtration flows are similar to those for which

the Π theorem holds. However, due to the complexities of filtration mechanism, few researchers have attempted to apply dimensional analysis to it. One of the most significant limitations of the application of the Π theorem is that the quantities selected should represent all the main factors of the problem.

Based on this fundamental principle, dynamic equilibrium filtration is chosen as the problem to which the Π theorem will be applied. Hence the dynamic filtration equilibrium rate must be a function of a number of variables which are listed as follows:

- (1) Differential pressure across the filter cake, ΔP_c (psi)
- (2) Viscosity of filtrate, μ (cp) 
- (3) Filter cake thickness, h (mm)
- (4) Filter cake permeability, K_c , (m^2)
- (5) Annular mud flow velocity, V_{ANN} , (m/s)
- (6) Temperature, T , ($^{\circ}C$)

In addition to the above, the following parameters are also variables which will affect the dynamic equilibrium filtrate flow rate, however these variables can be reduced or ignored when using Π theorem:

- (7) Absolute pressure, P_{ab} , (psi)

The absolute pressure will only affect the viscosity of the mud and filtrate.

- (8) Shear rate, γ , and shear stress, τ

The shear rate and shear stress are functions of annular velocity V_{ANN} and mud viscosity μ_m , if a specific model of mud type is determined.

- (9) Mud density, ρ_m , and solids density, ρ_s

The flow of fluid through porous medium is not like that through pipes or conduits. The dominant filtration forces are capillary and applied hydraulic pressure. The weight of the particulates themselves are too small relative to the forces mentioned above. So ρ_m, ρ_s

are often ignored.

(10) Gravitational Acceleration, g

There are five forces associated with filtration mechanism⁹⁹, they are : the inertial force, the viscous force, the pressure force, the gravity force and the interfacial force. However the interfacial force and the gravity force are relatively negligible compared to the others. We can then neglect g and consider that the dominant effect factors of filtration are pressure and viscosity, not gravity.

(11) Filter Cake Pore Size Function (Size, Shape, Distribution)

(12) Mud Particle Function (Size, Shape, Distribution)

Both (11) and (12) are very important items which play a dominant role in the filtration. However, it is assumed that filter cake pore size and mud particle only affect the cake thickness h_c and cake permeability K_c . It should be noted that the use of statistical methods⁹⁹ rather than dimensional analysis is simple.

(13) Time, t

When equilibrium is reached, all the variables occur independent of time, hence the time t is omitted.

(14) Filtration Area, A

If the item q_{dc} is defined by

$$q_{dc} = \frac{1}{A} \left. \frac{dV}{dt} \right|_{dc} \quad (3-4.6)$$

we can then eliminate the variable of area.

After that, a general equation can be made:

$$F(q_{dc}, \Delta P_c, \mu_m, \mu_f, h_c, K_c, V_{ANN}, T) = 0 \quad (3-4.7)$$

In order to make the equation simpler, it is assumed that the filtration takes place at the constant temperature. Rearranging above equation as follows:

$$F\left(q_{de}, \frac{\Delta P_c}{h_c}, \mu_m, \mu_f, K_c, V_{ANN}\right) = 0 \quad (3-4.8)$$

By using the Π theorem, and selecting $\frac{\Delta P_c}{h_c}$, K_c , μ_f as the independent variables (repeating variables), the dimensionless equation can be obtained:

$$\Phi(\Pi_1, \Pi_2, \Pi_3) = 0 \quad (3-4.9)$$

where

$$\Pi_1 = \frac{q_{de}}{\frac{K_c \Delta P_c}{\mu_f h_c}} \quad (3-4.10)$$

$$\Pi_2 = \frac{\mu_m}{\mu_f} \quad (3-4.11)$$

$$\Pi_3 = \frac{V_{ANN}}{\frac{K_c \Delta P_c}{\mu_f h_c}} \quad (3-4.12)$$

Substituting Π_1, Π_2, Π_3 into equation(3-4.9)

$$\Phi\left(\frac{q_{de}}{\frac{K_c \Delta P_c}{\mu_f h_c}}, \frac{\mu_m}{\mu_f}, \frac{V_{ANN}}{\frac{K_c \Delta P_c}{\mu_f h_c}}\right) = 0 \quad (3-4.13)$$

Writing equation(3-4.13) in another form:

$$q_{de} = V_{ANN} \cdot \phi \left(\frac{q_{de}}{K_c \Delta P_c}, \frac{\mu_m}{\mu_f h_c} \right) \quad (3-4.14)$$

Equation(3-4.14) would apply to both compressible and incompressible cake dynamic filtration.

For incompressible filter cakes, both h_c and K_c will not change once equilibrium is reached, hence Darcy's law can be used, thus

$$q_{de} = \frac{1}{A_y} \frac{dV}{dt} \Big|_{de} = \frac{K_c \Delta P_c}{\mu_f h_c} \quad (3-4.15)$$

so the dimensionless equation becomes

$$q_{de} = V_{ANN} \cdot \phi \left(\frac{\mu_m}{\mu_f}, 1 \right) \quad (3-4.16)$$

If assuming that the viscosity of mud and filtrate do not change or the parameters which affects them such temperature, pressure do not change, equation(3-4.16) will be simplified as

$$q_{de} = \text{Constant} \times V_{ANN} \quad (3-4.17)$$

in which constant is only the function of μ_f, μ_m .

Equation(3-4.17) is very similar to that reported by Bezemer and Havenaar²⁴ who found from the experimental results that equilibrium filtrate flow rate is proportional to the rate of shear on the cake surface.

For a compressible filter cake, the equation(3-4.14) will also hold, however, $\frac{q_{de}}{K_c \Delta P_c}$

$\frac{\mu_m}{\mu_f h_c}$

should be determined by experiments, which use $\phi \left(\frac{q_{de}}{K_c \Delta P_c}, \frac{\mu_m}{\mu_f} \right) = \frac{q_{de}}{V_{ANN}}$, since both h_c

and K_c are variables.

Chapter Four

THE EXPERIMENTAL EQUIPMENT AND PROCEDURES

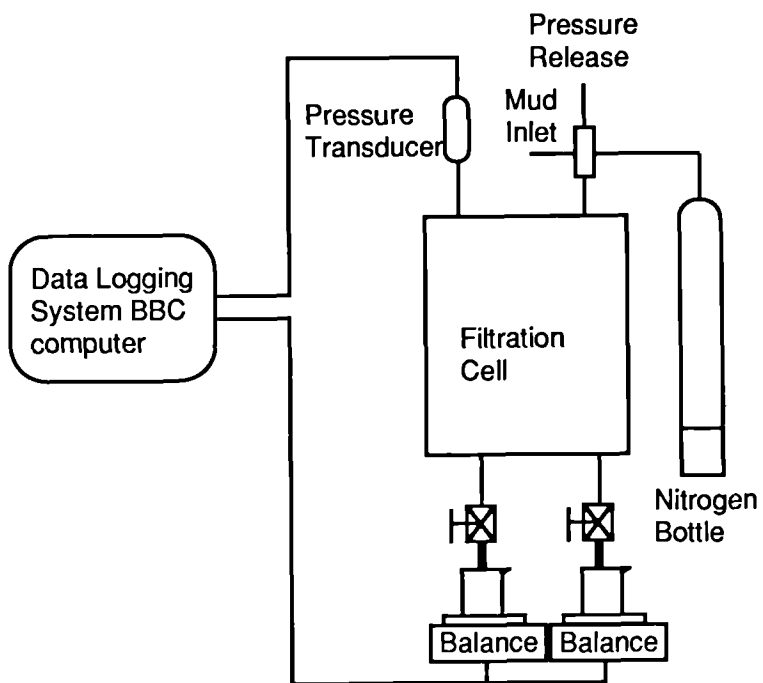
The object of this chapter is to describe the static and dynamic experimental facilities and procedures. It is necessary to point out that the static experiments are covered because it was initially hoped that the dynamic filtration might be predicted using static experimental filtration data in a filtration numerical model as has been discussed in chapter three. A number of static filtration tests were therefore conducted, prior to commencing dynamic filtration tests and those filter cake characteristics, such as average specific cake resistance α_{avg} , cake wet/dry mass ratio m and cake thickness h , which were obtained will be used for the dynamic filtration modeling in chapter eight.

4.1 STATIC FILTRATION

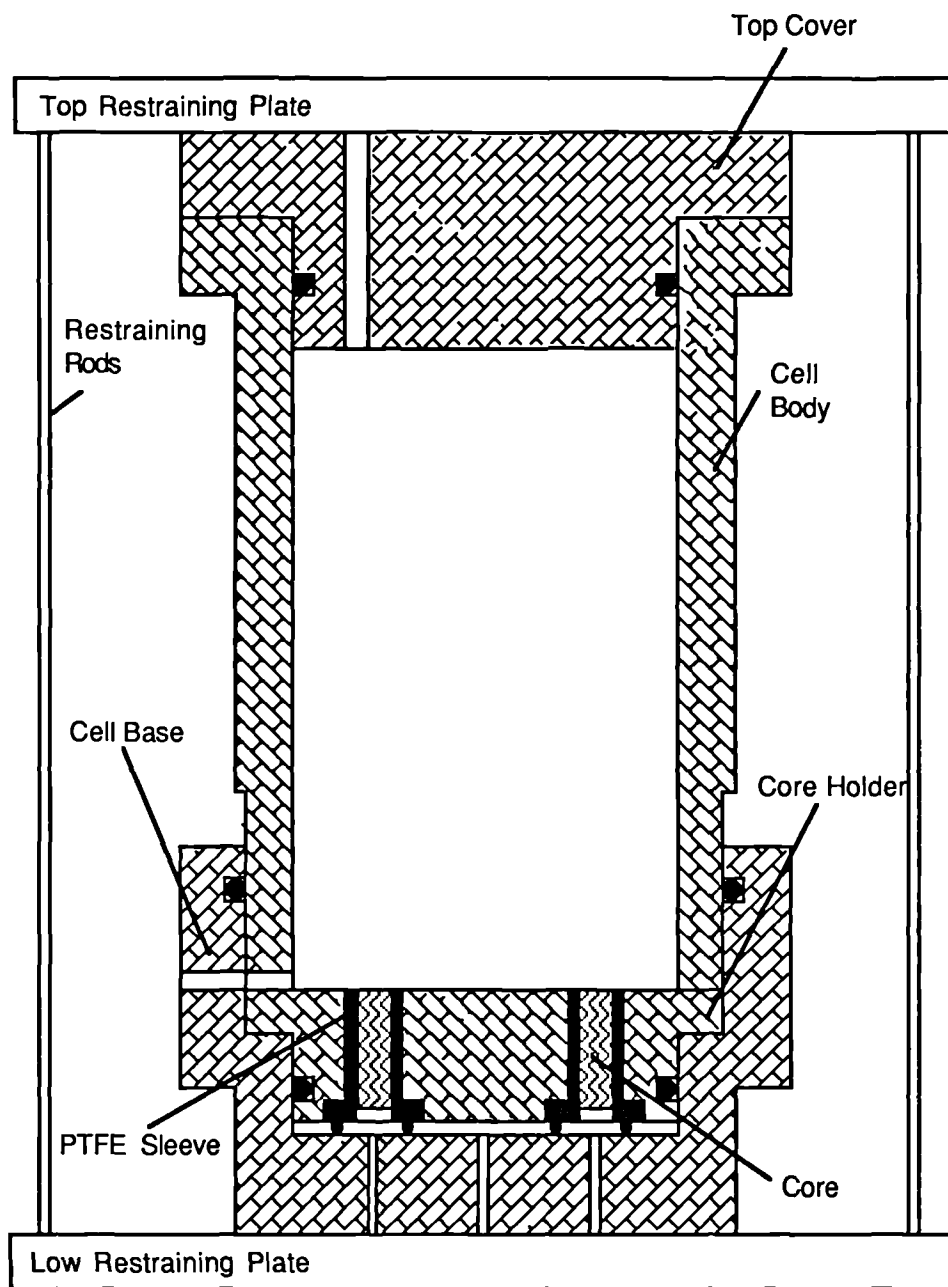
4.1.1 Description of the Modified Static Filtration Cell

The modified static filtration cell was originated from a cell which was previously used for static filtration with filter papers. Its schematic diagram is showed in Figure(4-1.1) and Figure(4-1.2) shows the cross section of the cell. The cell is made up of 5 main parts:

- (1) the cell base;



Figure(4-1.1) Schematic of Room Temperature Filtration Cell and Associated Equipments



Figure(4-1.2) A Schematic Drawing of Cross Section of Static Filtration Cell

- (2) the core holder;
- (3) the cylindrical body;
- (4) the top cover;
- (5) the system of restraining plates.

The core holder consists of 4 core-location holes which have an inside diameter of about 35 mm. The PTFE sleeve which has an outer diameter of approximately 35 mm and an inner diameter of 25 mm is used between the hole and core so that the leakage of mud around the core is prevented. The length of the hole is approximately 1.5 inch.

4.1.2 Muds Tested for Static Filtration

Two mud systems were used in this study, viz:

- (1) Seawater/KCL/Polymer mud
- (2) Freshwater Gypsum-Ferrochrome Lignosulphonate mud

All are commonly used in the North Sea and elsewhere⁹⁴. The compositions of the two muds are listed in Table 4.1. A very brief description of the main components and their function is given in Table 4.2.

4.1.3 Mud Preparation

The list of components in Table 4.1 is the order in which the chemicals were added. For the Seawater/KCL/polymer mud, the Seawater was made up to the composition shown in Table 4.3. The components were added in the order shown in Table 4.1, whilst stirring, and the mud left overnight and then remixed before use. The caustic soda and

Table 4.1 Composition of the Two Basic Muds Used

Mud System 1: Seawater/KCL/Polymer

Component	Concentration
Seawater	0.965 bbls
Caustic Soda	1.0 lbs/bbl
Sodium Carbonate (Soda Ash)	1.0 lbs/bbl
Potassium Chloride(KCL)	30 lbs/bbl
Drispac	1.0 lbs/bbl
XC Polymer	1.0 lbs/bbl
Barite	70 lbs/bbl

Mud System 2: Freshwater/Gypsum-Lignosulphonate

Component	Concentration
Freshwater	0.967 bbls
Wyoming Bentonite	20 lbs/bbl
Caustic Soda	0.75 lbs/bbl
Gypsum	4.0 lbs/bbl
Ferrochrome Lignosulphonate	3.0 lbs/bbl
LV CMC	2.0 lbs/bbl
Barite	70 lbs/bbl

Table 4.2 Brief Description of Mud Components

Components	Brief Descriptions
Wyoming Bentonite	Mainly sodium montmorillonite clay used to impart rheological properties to the mud and to control fluid loss by the formation of thin filter cakes of low permeability
Ferrochrome Lignosulphonate	A sub-colloid used to deflocculate the colloidal clay particles
Gypsum	Calcium sulphate, added as a source of soluble calcium to inhibit clay swelling
LV CMC	Low Viscosity Carboxymethyl Cellulose, a polymeric fluid loss additive which gives very little, if no, rise in viscosity
Drispac	polyanionic cellulosic polymer, a more refined cellulose which gives viscosity and fluid loss control
XC Polymer	Xanthan Gum Biopolymer, mainly used as a thickener to give viscosity but is less affected by Ca^{++} and Mg^{++} ions than Drispac
Potassium Chloride	Added as a soluble source of potassium to prevent shales/clays swelling

Table 4.3 Composition of Simulated North Sea Water

Compound	Concentration (lbs/bbl)
$\text{CaCl}_2 \cdot 6\text{H}_2\text{O}$	0.790
$\text{MgCl}_2 \cdot 6\text{H}_2\text{O}$	3.863
KCL	0.296
NaCl	8.091
Na_2SO_4	1.478

soda ash were added to treat out Ca⁺⁺ and Mg⁺⁺ ions present in the Seawater, which have a detrimental effect on the polymer.

For the Freshwater/Gypsum-Lignosulphonate mud, the Wyoming bentonite was added directly, slowly to the tap water whilst stirring with a salveson mixer. The mixture was then left for 18-24 hours to allow the bentonite to pre-hydrate. The caustic soda, dissolved in a small quantity of water, was then added whilst stirring, resulting in the mixture getting extremely thick. At this point, part of the required amount of lignosulphonate in effort to thin down the mud would be added before carrying on with the additions as they are listed.

After the addition of the LV CMC the mud thickened slightly but this was temporary. and if left, mixing in the next day it 'broke' back to a reasonable viscosity.

4.1.4 Core Preparation

The filter media used were sandstone cores which were drilled from natural clashach block. All cores tested in this study were 1" in diameter, about 1" in thickness and had permeabilities between 50 and 5000 md.

4.1.5 Experimental Procedure

The static filtration tests were carried out through following steps:

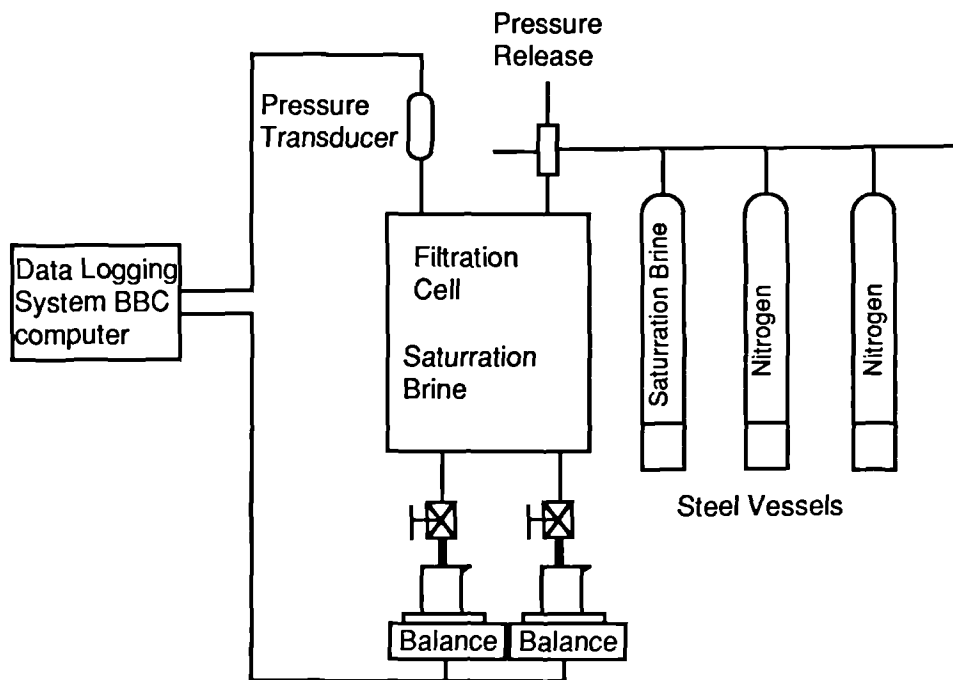
Preliminary work and core saturation: To ensure that no leakage of mud around the core was occurred, a PTFE sleeve was used. The core was inserted into the sleeve before the sleeve with the core was pressed into the core holder. The core holder was then put

onto the cell base when the bronze disc had already been inserted below each core and the four “O” rings had been added between core holder and cell base as well, which made sure that the filtrate went through the outlet individually. The body of the cell was carefully lowered onto the core holder and the top cover was placed in position. The end plate was then located on the restraining rods and the bolts were tighten.

In order to purge the air inside the core, below it and the outlet tubing, a vacuum pump was used and the brine(NaCl_2 45,000 ppm and CaCl_2 4,500 ppm) which is most similar to the underground fluid in reservoir, was then allowed to flow through the core. Once saturation was completed, the outlet valve was then closed.

Measurement of initial fluid permeability of the core: Figure(4-1.3) shown the schematic of permeability measurement. The fluid of measurement was saturation brine which has viscosity in range of 1.09-1.24 μp . A small scale pressure transducer(3.5 bar) was used in stead of the big scale one(35 bar) due to low applied constant pressure so that a more accurate pressure value was obtained. Two big vessels were employed to store Nitrogen to keep the filtration cell under constant pressure even the liquid volume declined very rapidly when the measurement of permeability was processing. To make sure that the permeability value obtained was available, the cumulative volume vs. time was noted by balances and logged by computer as longer as required. Subsequently, permeability was calculated according to Darcy's law. The brine in the cell was then drained off once permeability measurement was completed.

Filtration data logging: After the bolts were untighten and end plate was removed, the top cover of filtration cell was carefully lifted and the inside surface was dried by tissue paper before a freshly mixed mud to be tested was slowly dropped into the cell. The top cover, end plate and bolts were then put back in position The nitrogen inlet line, pressure gauge and pressure transducer (35bar) were then connected to the cell and two clean beakers placed on the balances and the balances zeroed individually. With the outlet valve closed the cell was then pressurized to the required filtration pressure. Filtration test was then commenced by opening the outlet (electrical) valves and simultaneously running the



Figure(4-1.3) Schematic of Liquid Permeability Measurement

program. Filtrate weights and pressure were automatically measured as a function of time with the electronic balances and pressure transducers, and transmitted into BBC computer and then saved on the floppy disk. The data on the BBC floppy disks can be transferred through KERMIT to VAX mainframe or any other computers such as, IBM personal, or Macintosh etc. for further processing.

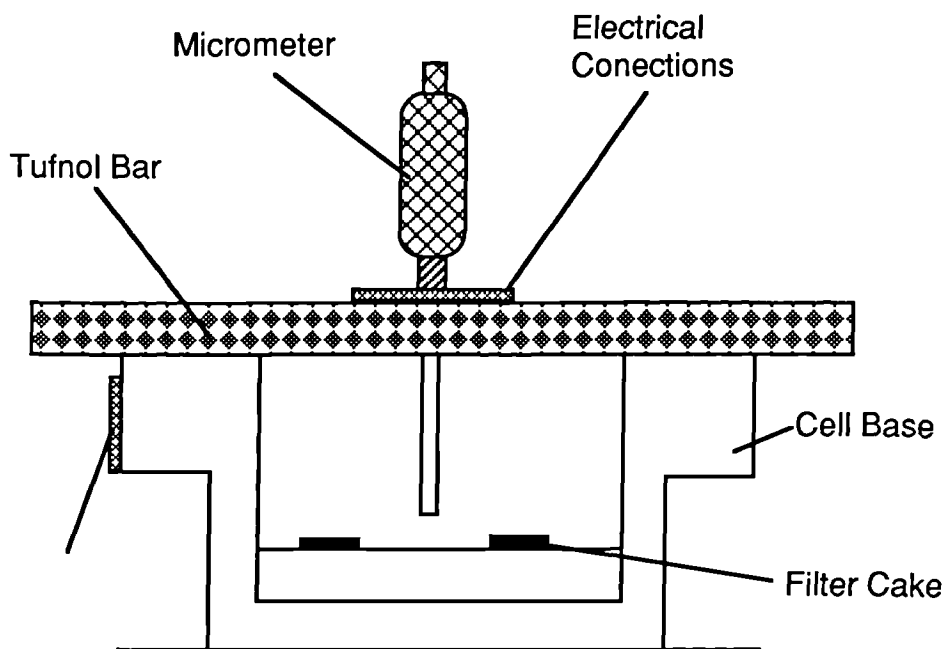
Filtration test was stopped after about two hours(or any time as required) by stopping the program and closing the outlet (electrical) valves and the pressure was then released. After that, the mud was drained off and the bolts, the end plate and top cover were removed.

The cell body was then carefully separated from the base and any excess mud lying on the surface of the cake was then gently washed off using tap water. Since the electrical circuit connected to the depth gauge touches any electrical conductor, any excess water lying on the surface of the cake was removed using a hot air blower for about 20 to 30 seconds.

The depth gauge was then placed over the cake surface and the gauge lowered until the buzzer sounded. The depth reading was noted and the whole procedure repeated 8-9 times to obtain an average value of the depth from the top of the cell base to the cake surface.

The filter cake was then carefully removed and put into a weighted glass plate which would be weighted, dried by putting into the humidity oven for one day, then reweighted. After that, the depth gauge was placed over the core surface and the gauge lowered until the buzzer sounded. The depth reading was noted and the whole procedure repeated 8-9 times to obtain an average value of the depth from the top of the cell base to the core surface. By subtracting the initial average depth with filter cake from the average depth without the filter cake, the average cake thickness could be obtained. Figure(4-1.4) shows the schematic of the micrometer arrangement for measuring filter cake thickness.

Finally the cell was cleaned.



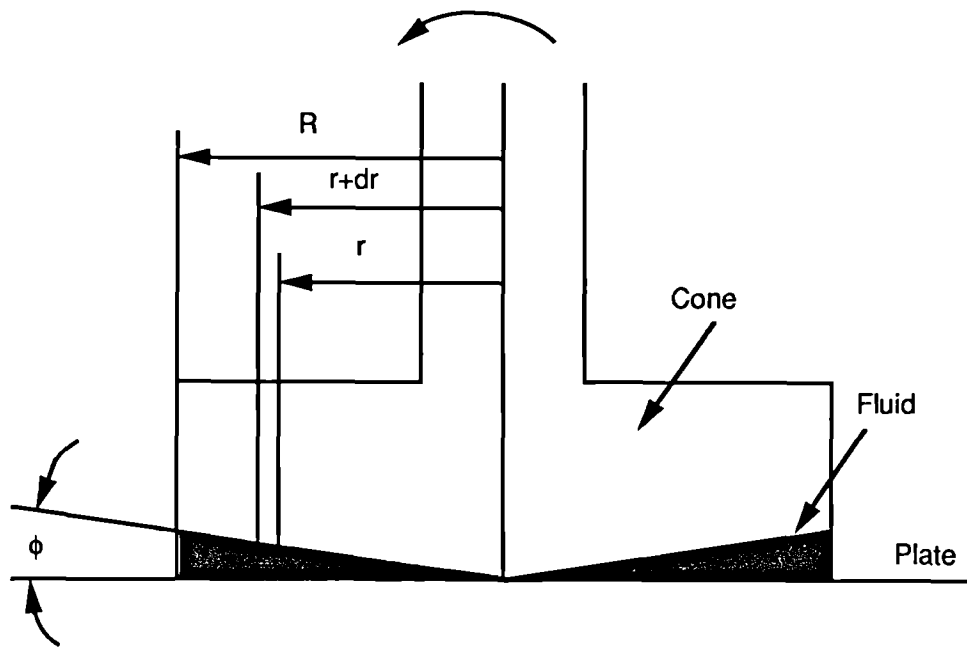
Figure(4-1.4) Schematic of Micrometer Arrangement for Measuring Filter Cake Thickness

4.2 DYNAMIC FILTRATION

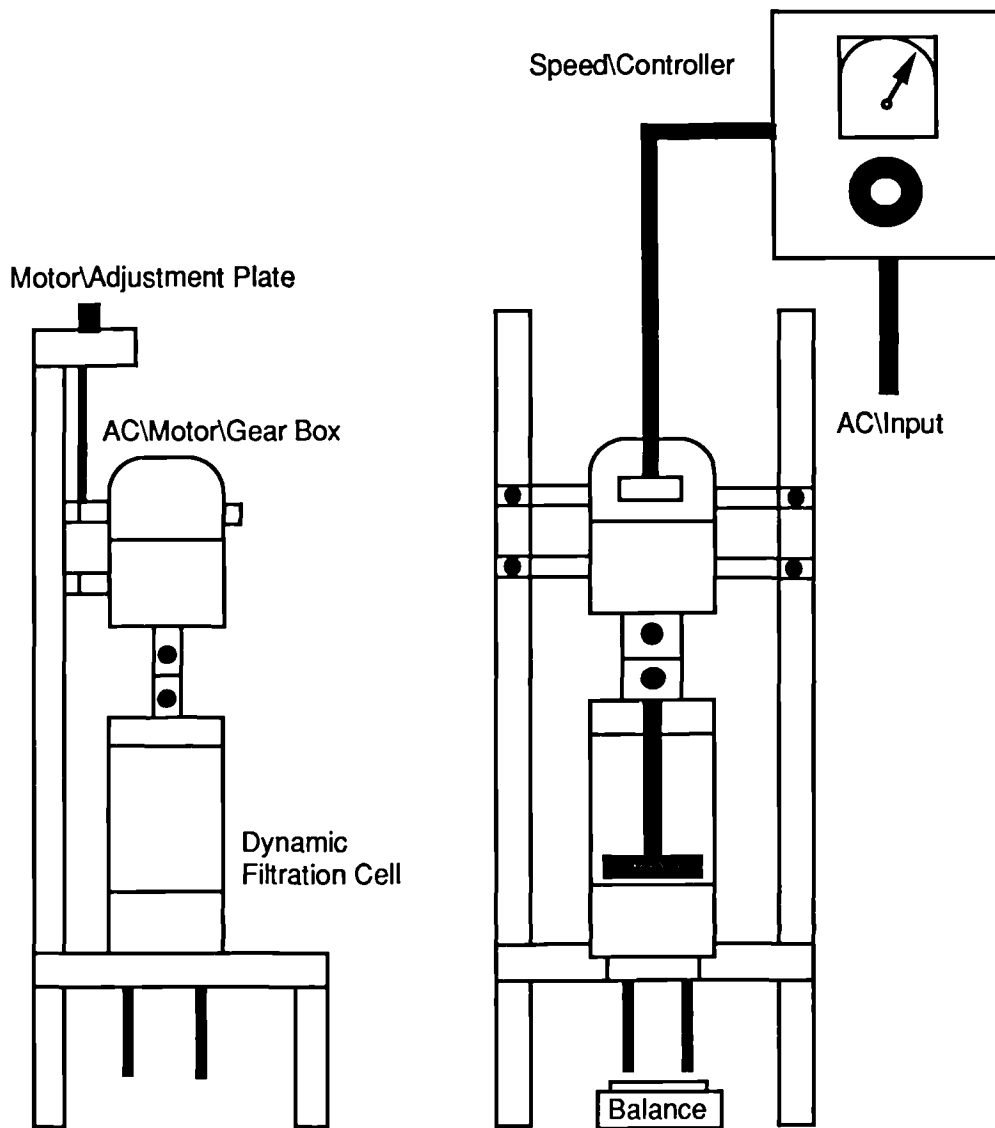
4.2.1 Experimental Rig and Procedure

The new dynamic filtration cell was designed based on the static filtration cell which has been discussed earlier in this chapter. The concept of the design is to simulate a cone-and-plate viscometer, shown schematically in Figure(4-2.1), which consists essentially of a stationary flat plate, upon which is placed a puddle of the liquid(mud) to be tested, and an inverted cone, which is lowered into the puddle until its apex just contacts the plate. If the angle between the conical and flat surface is kept small, say about two degrees, the magnitude of shear stress and shear rate is very near constant throughout the fluid.

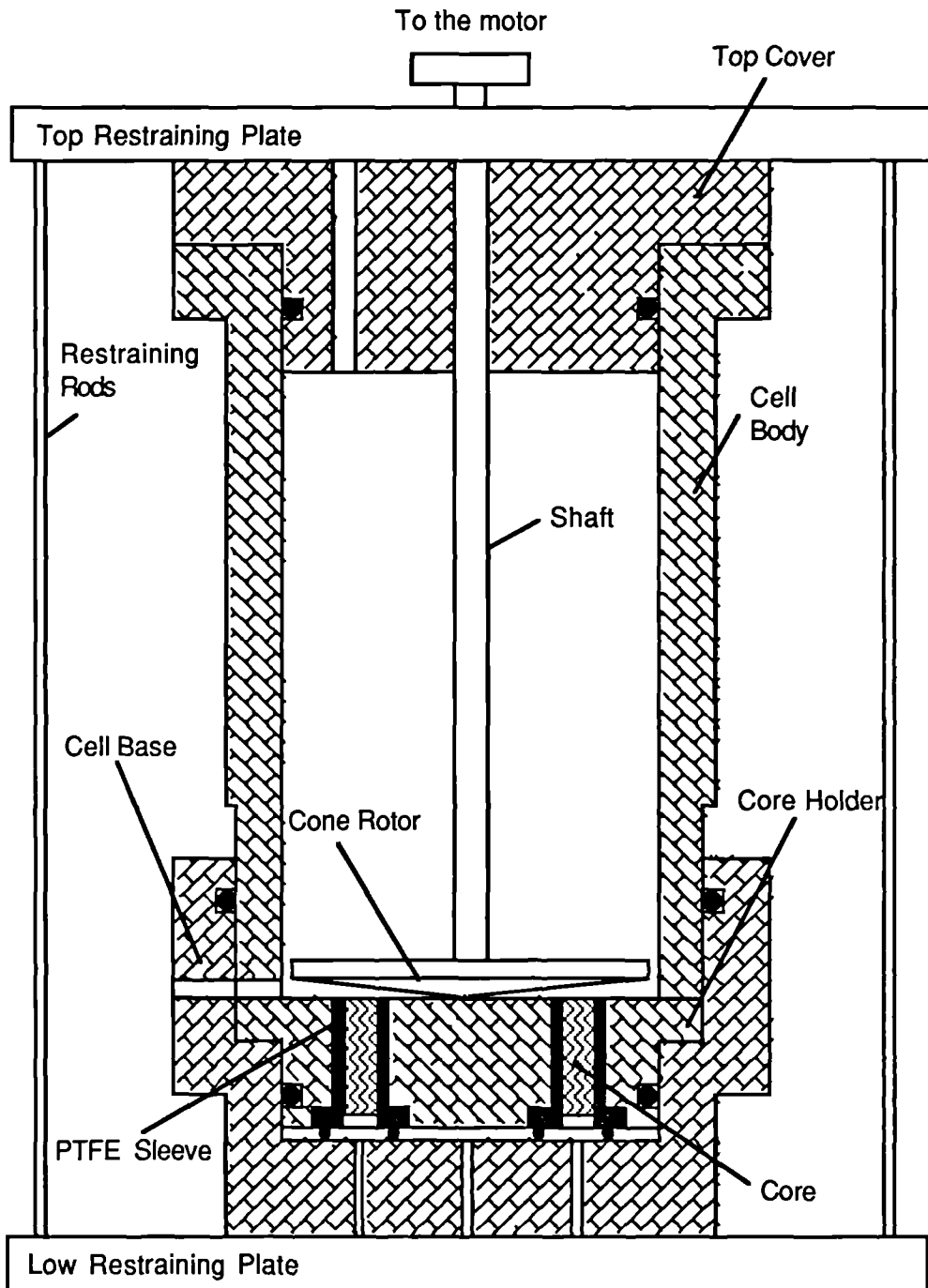
A schematic of assembled dynamic filtration rig and associated equipments is shown in Figure(4-2.2) and Figure(4-2.3) shown the cross section of the new dynamic filtration cell. The new cell is very similar to the static filtration cell showed in Figure(4-1.1) with exception of the difference between the top covers which the new one consists of a cover with cone-rotor and shift. The dynamic filtration experiment tests were therefore completed under a similar procedure as static filtration conducted. For the equipment, the top cover were replaced by the cone-rotor-shift cover which connected to a motor. The experiment was conducted as same as static experiment discussed before but run the motor to a required shear rate prior to pressurising of the cell.



Figure(4-2.1) Schematic Diagram of the Cone-and-Plate Viscometer.



Figure(4-2.2) A Schematic of Assembled Dynamic Filtration Rig



Figure(4-2.3) A Schematic Drawing of Dynamic Filtration Cell

4.2.2 The Determination of the Shear Rate and Rotational Speed from Equivalent Annular Velocity

Simulation of 8¹/₂" — 6¹/₂" annulus conditions, with good working mud flows (laminar flow) using power law model the shear rate on the wall is given by:

$$\gamma = \frac{4V_{ANN}(2 + \frac{1}{n})}{d_2 - d_1} \quad (4-2.1)$$

where

n — the behaviour index of the mud, usually 1.0 — 0.4

V_{ANN} — annular circulating velocity, usually 0.5 — 1.30 m/s

d_2 — the diameter of well bore, 5³/₈" — 8¹/₂"

d_1 — the diameter of drilling pipe, 3" — 6¹/₄"

It should be noted that these values are only approximately covered in drilling engineering.

The maximum and minimum rate of shear were then determined:

$$\gamma_{max} = 294.80 \text{ (1/s)} \text{ and } \gamma_{min} = 75.6 \text{ (1/s)}$$

As it is shown in Figure(4-2.1), if the cone rotates at a constant speed of N rps, the linear velocity at r is $2\pi rN$. The gap height at r is $r \tan\phi$. The magnitude of the shear rate at r is therefore:

$$\gamma = \frac{2\pi rN}{r \cdot \tan\phi} = \frac{2\pi N}{\tan\phi} \text{ (1/s)} \quad (4-2.2)$$

The shear rate is evidently constant over the range $0 \leq r \leq R$ so that shear stress τ_{xy}

must also be constant over this range. In practice, the angle Φ_0 between the conical and flat surface is kept small, say, about one and half degree so that strong secondary flows can be prevented.

It is clear that measurement of the rotational speed permits the calculation of the shear rate. Converting above shear rates to the rotational speed:

$$N_{\max} \approx 100 \text{ rpm and } N_{\min} \approx 25 \text{ rpm}$$

4.3 THE ADVANTAGES OF THE MODIFIED FILTRATION CELL

The following advantages of new modified filtration cell might be drawn:

- (1) The four cores whether or not they are synthetic or natural can be used simultaneously.
- (2) It is possible to conduct both static and dynamic filtration.
- (3) Four electronic balances can be used (even only two have been used so far) to measure the cumulative filtration volume/weight at any moment and these readings with those from the pressure transducers can automatically be logged by BBC computer.

Chapter Five

PRESENTATION OF STATIC FILTRATION EXPERIMENTAL RESULTS

This chapter presents the results of static filtration experiments conducted for two mud systems.

5.1 MUDS TESTED AND THEIR PROPERTIES

One of the purposes of static filtration tests is to produce relevant data to allow the prediction of the dynamic filtration properties of drilling muds. The experiments did not consider the effects of the components of the muds on the static filtration behaviours. Nevertheless, the muds used were based muds and only solids concentrations were changed which is directly related to the filter cake characteristics. Details are showed in Table 5.1 and Table 5.2 which list the compositions of Seawater/KCL/ Polymer & Freshwater/Gypsum/Lignosulphonate muds respectively. The corresponding rheological properties and specific weight of those two muds were presented in Table 5.3 and Table 5.4. It should be noted that the rheological data were calculated using the Bingham plastic model. Each mud was tested at pressures of 100, 200, 300, 400, 500 psi.

When converting filtrate mass to volume the density of the filtrate was measured and for this mud it was found to be equal to 1014 Kg/m^3 . Also the filtrate viscosity was measured by a low shear viscometer and it was found to be between 1.09-1.24 cp.

Table 5.1 Composition of the Tested Seawater/KCL/Polymer Mud

Components	Concentration tested			
	(lbs/bbl)			
Caustic Soda (NaCl)	1			
Soda Ash (Na ₂ CO ₃)	1			
Potassium Chloride (KCl)	30			
Drispac	1			
XC Polymer	1			
Barite (BaSO ₄)	50	70	140	210

Table 5.2 Compositions of the Tested Freshwater/Gypsum-Lignosulphonate Mud

Components	Concentration tested			
	(lbs/bbl)			
Wyoming Bentonite	20			
Caustic Soda (NaOH)	0.75			
Gypsum (CaSO ₄)	4			
Ferrochrome Lignosulphonate	3			
LV CMC	2			
Barite (BaSO ₄)	0	70	140	210

Table 5.3 The Properties of Seawater/KCL/Polymer Mud

Component	Concentration (lbs/bbl)	Apparent Viscosity (cp)	Plastic Viscosity (cp)	Yield Point (lbs/100 ft ²)	Mud Weight (lbs/gal.)
Barite	50	22.00	12.50	19.00	9.75
	70	25.00	15.50	19.00	10.00
	140	30.00	22.00	16.00	11.10
	210	35.50	26.00	19.00	12.00

Table 5.4 The Properties of Freshwater/Gypsum/Lignosulphonate Mud

Component	Concentration (lbs/bbl)	Apparent Viscosity (cp)	Plastic Viscosity (cp)	Yield Point (lbs/100 ft ²)	Mud Weight (lbs/gal.)
Barite	0	42.50	31.50	22.00	8.65
	70	51.25	39.00	24.50	9.90
	140	53.75	41.00	25.50	10.95
	210	65.25	48.50	33.50	12.00

5.2 EXPERIMENTAL RESULTS OF STATIC FILTRATION

5.2.1 Spurt Loss

The relationship reported by Arthur⁹⁴ which the spurt loss is an exponential function of pressure was not found in this study. Figure(5-2.1) shows the spurt loss as a function of pressure and barite concentration. The experimental data demonstrated that the spurt loss would depend more upon the relation between filter medium characteristics and slurry constituents than upon the applied pressure alone. Extensive discussion on this problem will be made in the chapter six.

5.2.2 Effect of ~~Pressure and~~ Barite Concentration upon Cumulative Filtrate Volume

Figure(5-2.2) to (5-2.5) show the cumulative filtrate volume as a function of time and pressure for a range of barite concentrations. It is clearly demonstrated that the effects of pressure and barite concentration upon cumulative filtrate volume are significant. An increase in pressure or barite concentration generally results in an increase in cumulative filtrate volume. This may be explained by that, at high barite concentration, the filter cakes become less compressible and thus increases the filter cake permeability.

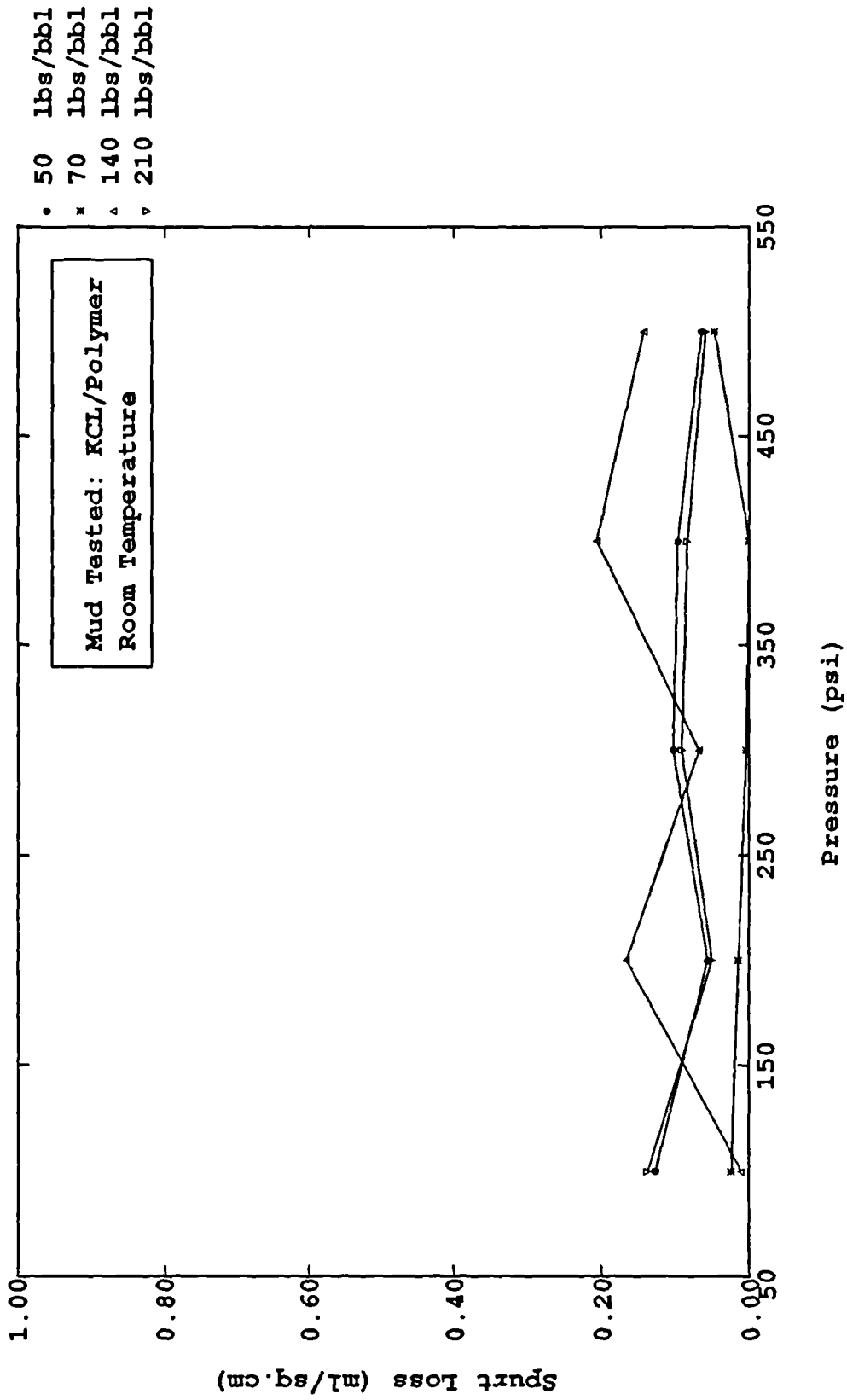


Figure (5 - 2.1) Spurt Loss as Function of Pressures and Barite Concentrations in Static Filtration Test

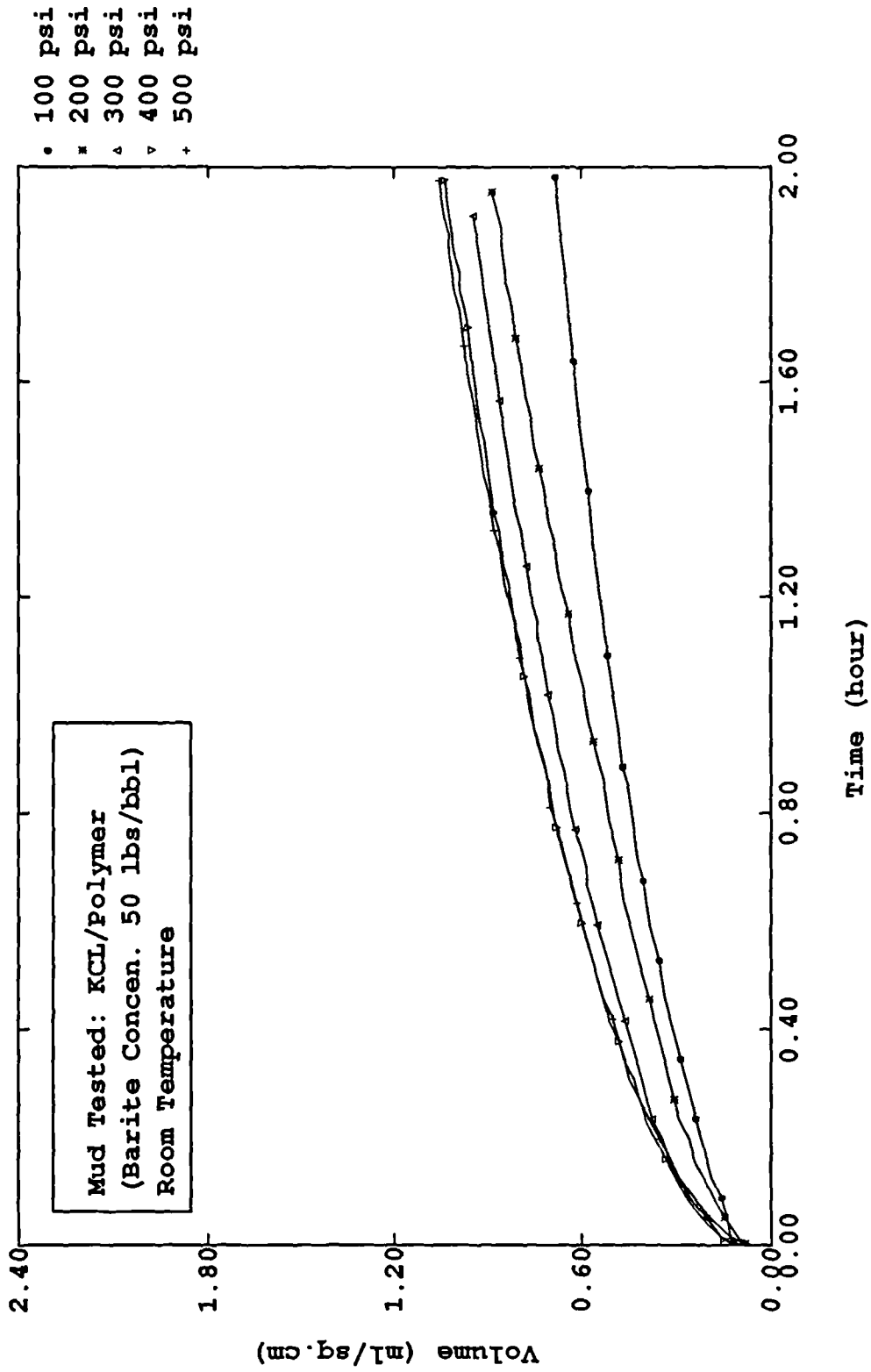


Figure (5 - 2.2) Cumulative Filtrate Volume Per Unit Area as Function of Time in Static Filtration Tests

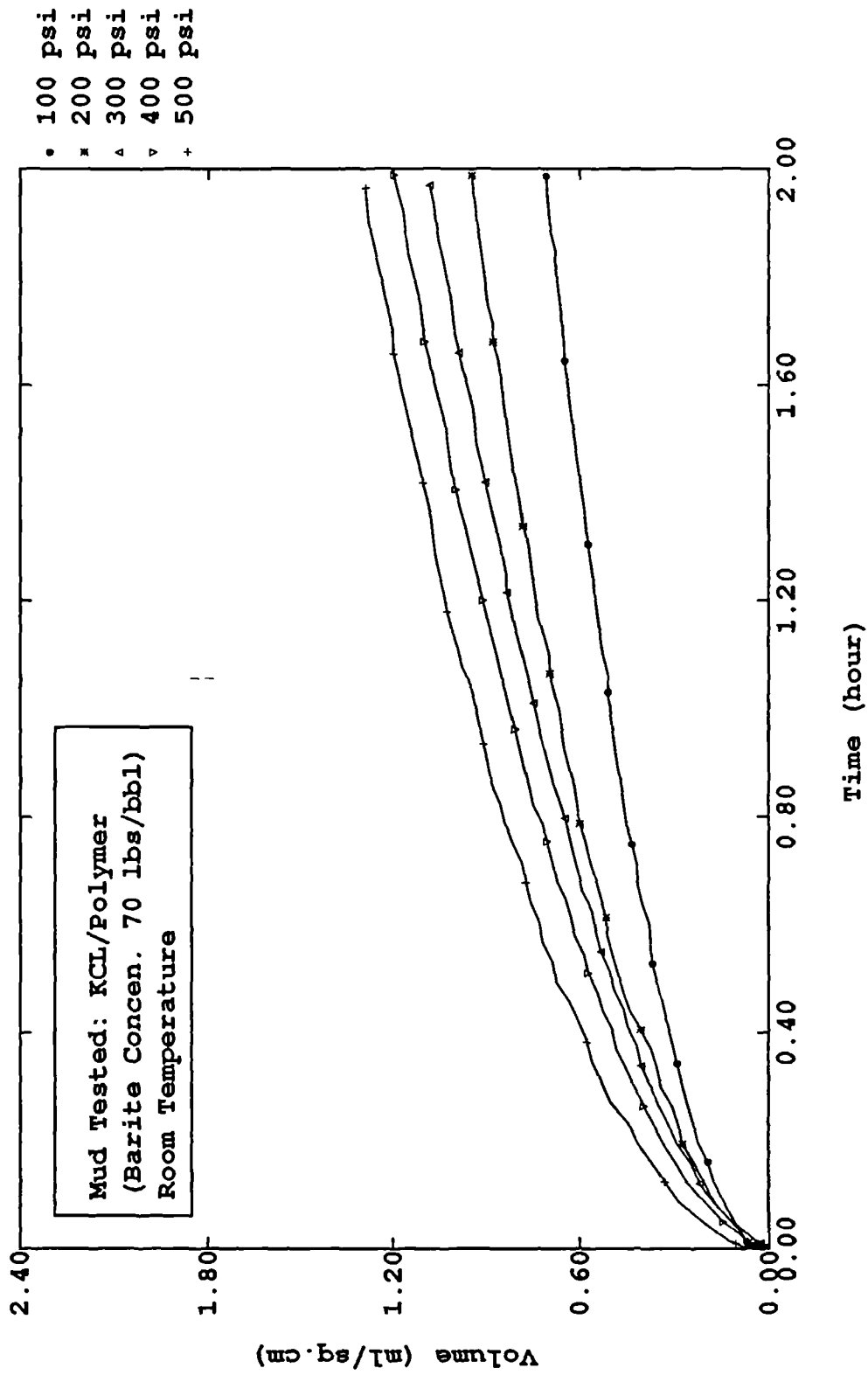


Figure (5 - 2.3) Cumulative Filtrate Volume Per Unit Area as Function of Time in Static Filtration Tests

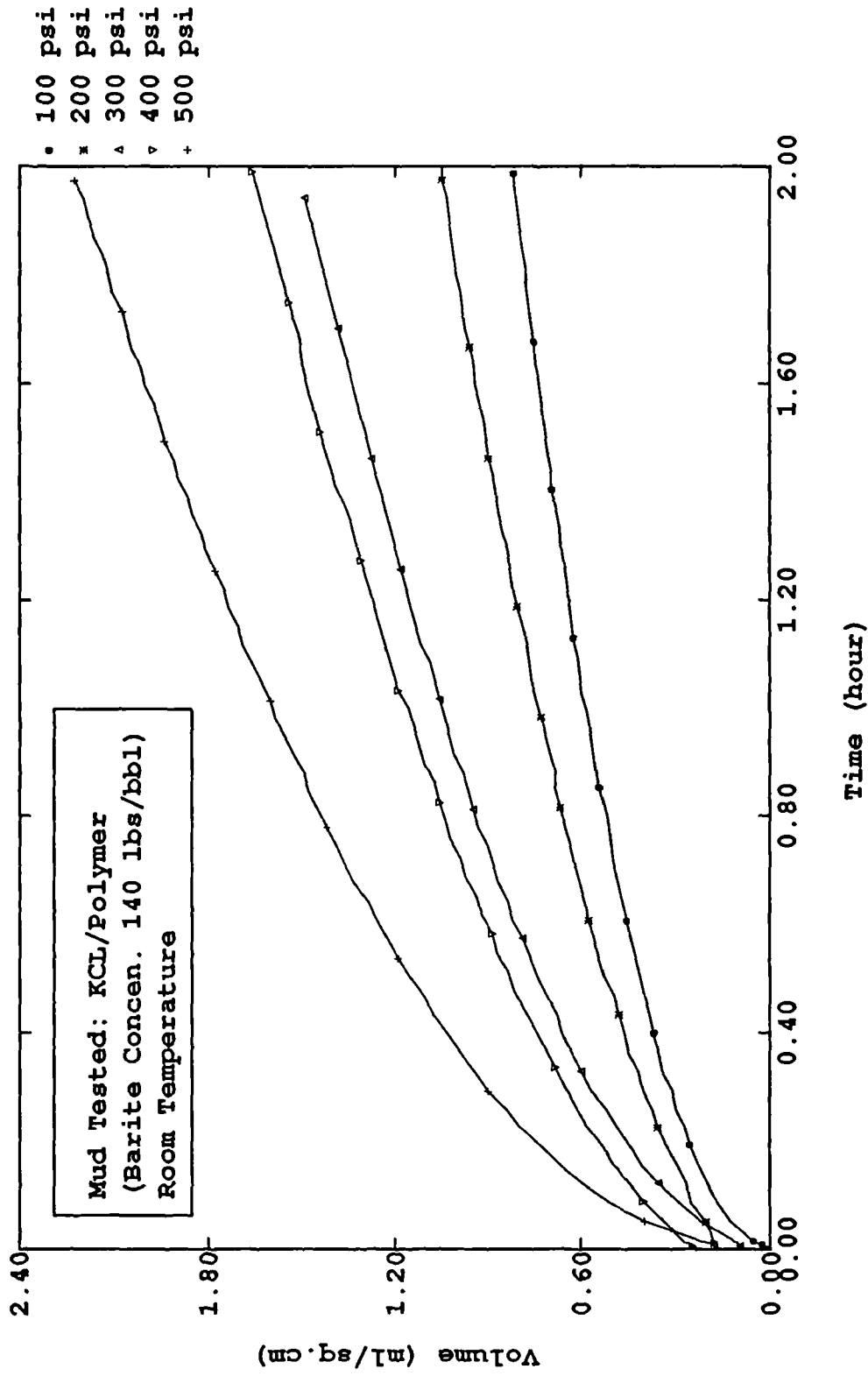


Figure (5 - 2.4) Cumulative Filtrate Volume Per Unit Area as Function of Time in Static Filtration Tests

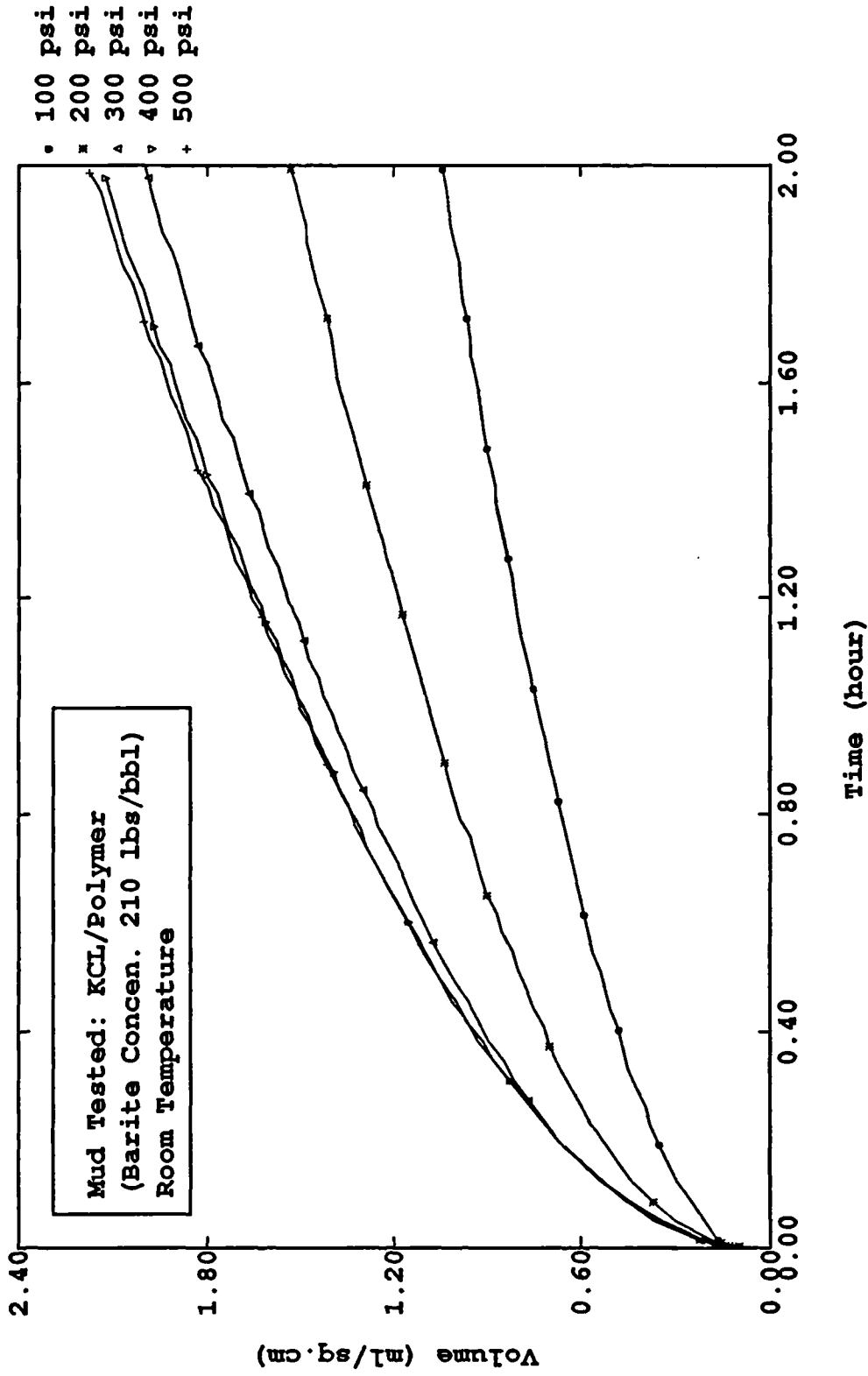


Figure (5 - 2.5) Cumulative Filtrate Volume Per Unit Area as Function of Time in Static Filtration Tests

5.2.3 Effect of Pressure and Barite Concentration upon Filter Cake Thickness

Figure(5-2.6) shows the measured filter cake thickness as a function of pressure and barite concentration. In general, when pressure or barite concentration increases, the filter cake thickness will increase. However, the effect of pressure on cake thickness is not so significant when the barite concentration is less than 70 lbs/bbl for which an increase in pressure does not make apparent change in filter cake thickness. This suggests that the filter cakes formed in a low barite concentration, say 50 lbs/bbl, are more compressible than those formed at a high barite concentration. It is assumed that, for compressible filter cakes, two opposing actions exist: one increases the filter cake thickness by piling-up solid particles, the other decreases the filter cake thickness by compacting. The two actions compensate for each other and create no pronounced change in filter cake thickness with increase in pressure. For incompressible cakes, however, the filter cakes would vary with the pressure apparently, e.g., filter cake thickness should be proportional to the square root of pressure because no compaction exists.

5.2.4 Effect of Pressure and Barite Concentration upon Wet to Dry Cake Mass Ratio (m)

Figure(5-2.7) shows the ratio of measured mass of wet to dry cake (m) as a function of pressure and barite concentration. Generally, m declines with increase in pressure and barite concentration. At low barite concentration in the mud, say 50 lbs/bbl, 70 lbs/bbl, m changes significantly with increase in pressure. This corresponds with the above results that the filter cakes formed under those conditions are more compressible. However, at

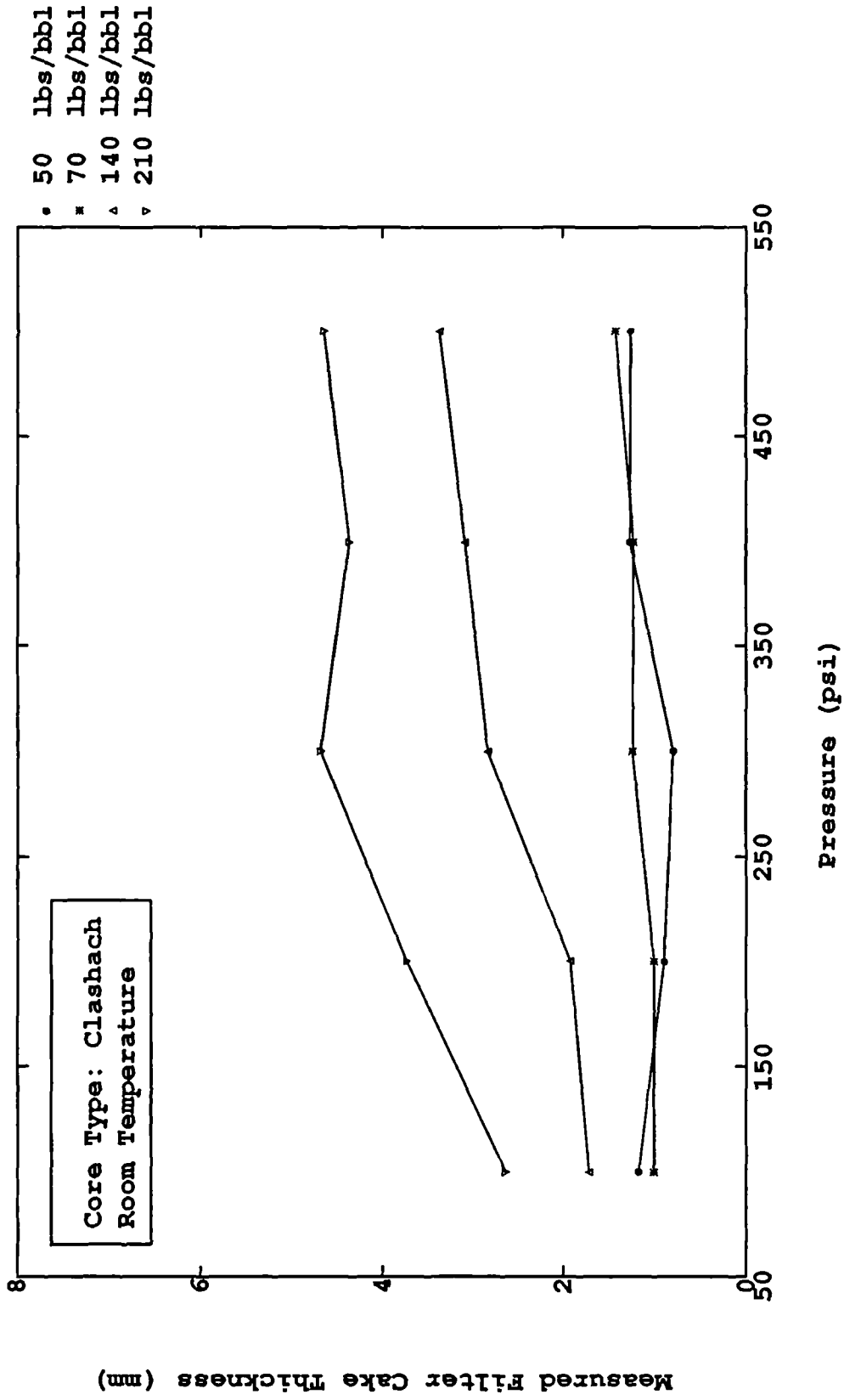


Figure (5 - 2.6) Measured Filter Cake Thickness For KCl/Polymer Mud as Function of Pressures and Barite Concen.

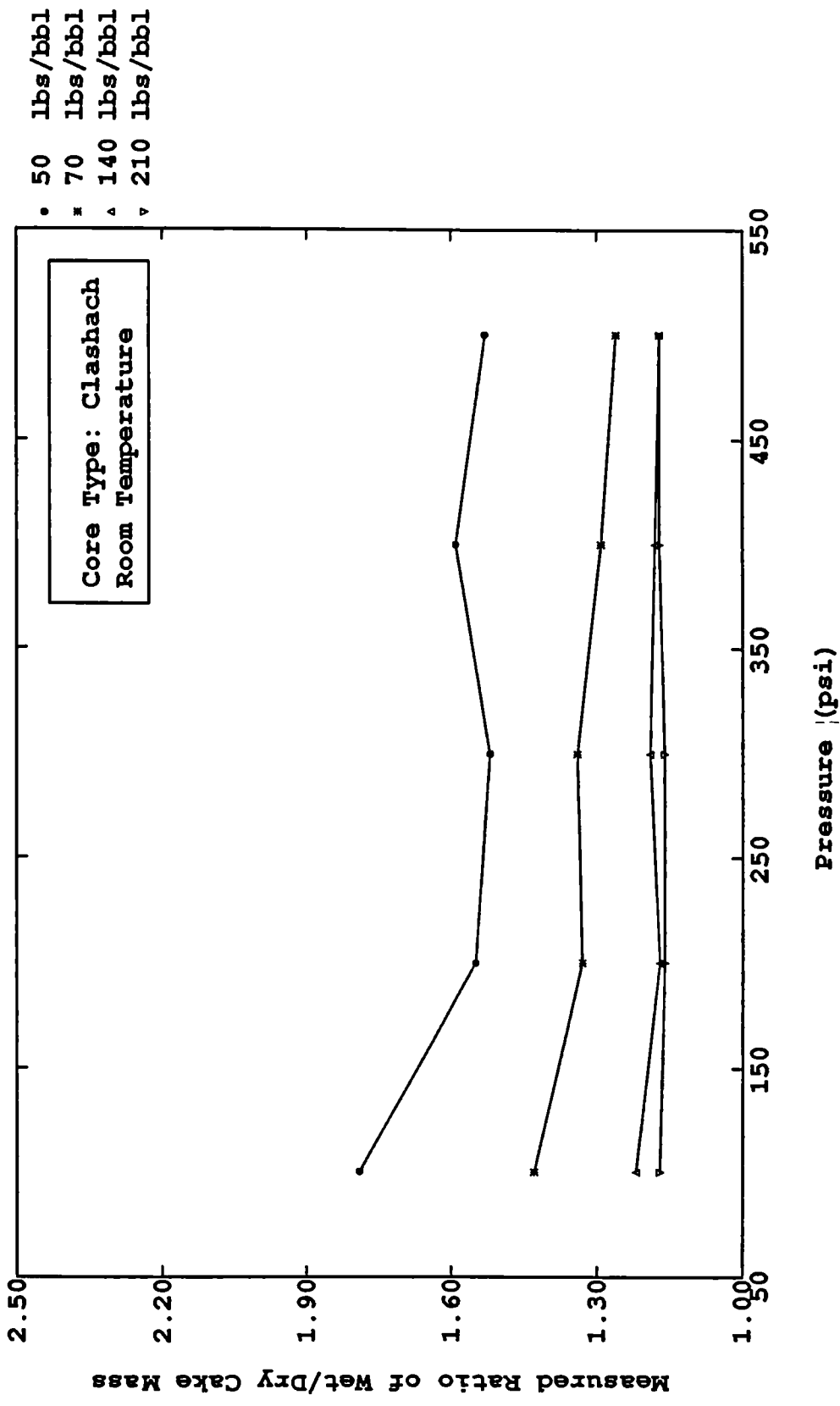


Figure (5 - 2.7) Measured Ratio of Wet/Dry Cake Mass For KCl/Polymer Mud as Function of Pressures and Barite Concen.

high barite concentration, “m” seems not to change very much when the pressure changes from 100 psi to 500 psi. This further supports the view that filter cakes deposited at this condition should be less compressible. Comparing with Figure(5-2.6), it should be noted that m varied very little with changing pressure for mud with a high barite concentration. This supports the results discussed previously.

5.3 THEORETICAL MODELLING OF STATIC FILTRATION EXPERIMENT

5.3.1 Derivation of Static Filtration Equation

In chapter three, equation(3-3.33) was derived and it has been widely used as a basic law of static filtration in the history of drilling fluids. This equation, however, is only valid under conditions that the filter cake is incompressible and the filter medium resistance could be neglected. The requirement of the incompressible filter cakes is necessary because it ensures that the average specific cake resistance α_{avg} , in stead of the local specific cake resistance α , could be used. The assumption that the filter medium resistance is negligible is important because the differential pressure across the cake is constant under this condition. In fact, in drilling engineering, the filter cake formed from the muds is compressible⁹⁵. It is understood that the pressure differential across the cake at the initial stage of the filtration process increases from zero to maximum while the pores of the filter medium are plugged and bridged, and/or the first layer of filter cake is forming. It is clear therefore that the assumption of constant pressure filtration is approximate. The equation would need to be modified before it can be used for predicting drilling fluid filtration.

Equation(3-3.33) can also be derived from equation(3-3.9).

Letting $B = 0$, then equation(3-3.9) becomes:

$$\frac{dt}{dV} = \frac{\mu\alpha\rho_f s}{\Delta PA^2(1-ms)} V + \frac{\mu R_m}{\Delta PA} \quad (5-3.1)$$

If the filter cake is incompressible, we can then integrate the above equation, which gives equation(3 -3.33). For a compressible filter cake, Kozicki *et al.*⁹⁶ modified the basic filtration equation to allow for the variation in α_{avg} and ϵ_{avg} in the initial stages of filtration. The above equation is then rewritten to include a correction term yielding the correct values of dt/dV in the initial period:

$$\frac{dt}{dV} = \frac{\mu\alpha\rho_f s}{\Delta PA^2(1-ms)} V + \frac{\mu R_m}{\Delta PA} + F(V) \quad (5-3.2)$$

where

$$F(V) \neq 0, \quad 0 \leq V \leq V_i$$

$$F(V) = 0, \quad V \geq V_i$$

in which V_i is the volume of filtrate collected before parabolic behaviour is reached and α_{avg} and m are the constant values reached subsequent to the initial non-parabolic period.

The assumption that the formation is a no bridging porous medium may lead to erroneous analysis of the borehole filtration. Glenn *et al.*¹⁵ subtracted the spurt volume and the spurt time from the data of cumulative filtrate volume vs. time. Filtration then commences with solids already deposited in the pores and on the surface of the filter medium. This process may reduce a lot of errors encountered at initial filtration stages. Designating the added resistance of the solids deposited during the spurt period as R_{sp} ,

Equation(5-3.2) becomes:

$$\frac{dt'}{dV'} = \frac{\mu\alpha_{avg}\rho_f S}{\Delta PA^2(1-ms)} V' + \frac{\mu(R_m + R_{sp})}{\Delta PA} + F(V') \quad (5-3.3)$$

in which the new integrating limits:

$$t' = 0, V' = 0$$

$$t' = t - t_{sp}, V' = V - V_{sp}$$

Separating the variables in equation(5-3.3) and integrating:

$$\begin{aligned} \int_0^{t-t_{sp}} dt' &= \frac{\mu\alpha_{avg}\rho_f S}{\Delta PA^2(1-ms)} \int_0^{V-V_{sp}} V' dV' + \frac{\mu(R_m + R_{sp})}{\Delta PA} \int_0^{V-V_{sp}} dV' \\ &+ \int_0^{V'} F(V') dV' \end{aligned} \quad (5-3.4)$$

which gives:

$$t' \Big|_0^{t-t_{sp}} = \frac{\mu\alpha_{avg}\rho_f S}{2\Delta PA^2(1-ms)} V'^2 \Big|_0^{V-V_{sp}} + \frac{\mu(R_m + R_{sp})}{\Delta PA} V' \Big|_0^{V-V_{sp}} + t_0 \quad (5-3.5)$$

where $\int_0^{V'} F(V') dV'$ is represented by t_0

Simplifying the above equation:

$$t - t_{sp} = \frac{\mu\alpha_{avg}\rho_f S}{2\Delta PA^2(1-ms)} (V - V_{sp})^2 + \frac{\mu(R_m + R_{sp})}{\Delta PA} (V - V_{sp}) + t_0 \quad (5-3.6)$$

Kozicki *et al.*⁹⁶ defined t_0 as the effective time of commencement of filtration since when $t = 0, V = 0$. Comparing equation(5-3.6) with equation(3-3.36), then:

$$t' = t_0 + a_1 V' + a_2 V'^2 \quad (5-3.7)$$

where:

$$t' = t - t_{sp}$$

$$V' = V - V_{sp}$$

This is the modified static filtration equation.

The possibility of a negative value for t_0 was considered by Kozicki *et al.*⁹⁶ and they concluded that since:

$$m_i \geq m_m$$

and

$$[\alpha_{avg}]_i \leq [\alpha_{avg}]_m$$

where the subscript i and m refer to the initial and main stages of filtration respectively. It is possible for t_0 and $F(V)$ to be negative, depending on the relative values of m_i , m_m , $[\alpha_{avg}]_i$, and $[\alpha_{avg}]_m$.

Equation(5-3.7) is then used to fit experimental data points V - t using the least-squares method and coefficients t_0 , a_1, a_2 are obtained.

Equation(5-3.7) can be rewritten:

$$\frac{t' - t_0}{V'} = a_1 + a_2 V' \quad (5-3.8)$$

It is clear that plot of $\frac{t' - t_0}{V'}$ vs. V' should yield a straight line.

Inserting a_1 , a_2 , into the equations(3-3.34) and (3-3.35), the average specific cake resistance, effective filter medium resistance could be determined.

From equations(3-3.34) and (3-3.35):

$$\alpha_{avg} = \frac{2\Delta P A^2 (1 - ms)}{\mu \rho_f s} \cdot a_2 \quad (5-3.9)$$

$$R_{\text{meff}} = \frac{\Delta PA}{\mu} \cdot a_1 \quad (5-3.10)$$

5.3.2 Application of Static Filtration Equation to Experimental Data

5.3.2.1 Average Specific Cake Resistance and Effective Filter Medium Resistance

Table 5.5 and Table 5.6 listed the coefficients of static filtration experiments for Seawater/KCL/Polymer and Freshwater/Gypsum/Lignosulphonate mud respectively. The coefficients were observed by fitting experimental data points $V-t$ to a second order of polynomial.

In order to further investigate the static cake characteristics, equations(5-3.9) and (5-3.10) would be employed. So far, all variables in equation(5-3.9) except s (solid fraction in slurry) are known. s can be determined as follows: (Assuming Freshwater/Gypsum-Lignosulphonate base mud as an example)

According to definition:

$$\begin{aligned} s &= \frac{\text{Mass of Solid in Slurry}}{\text{Mass of Slurry}} \\ &= \frac{(70 + 20) \text{ lbs / bbl} \times 1.0 \text{ bbl}}{9.90 \text{ lbs / gal} \times 1.0 \text{ bbl}} \\ &= 0.2165 \end{aligned}$$

Figures(5-3.1) to (5-3.4) are plots of $(t - t_{\text{sp}} - t_0)/(V - V_{\text{sp}})$ vs. $(V - V_{\text{sp}})$ as function of pressure and solid concentration. The straight lines through the plots were produced by the equation $y = a_1 + a_2x$ in which y represents the $(t - t_{\text{sp}} - t_0)/(V - V_{\text{sp}})$

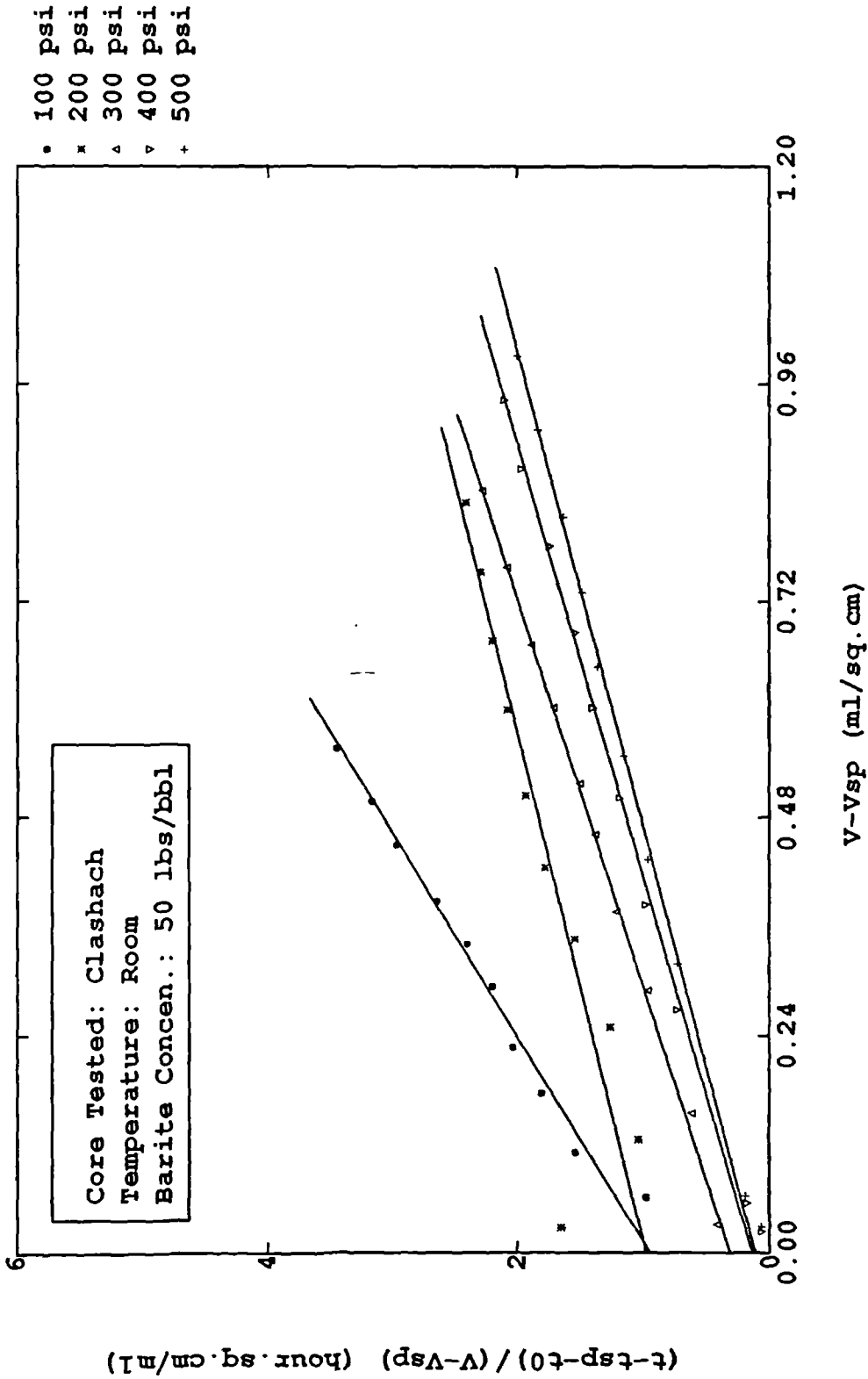


Figure (5 - 3.1) $(t-t_0-t_{sp}) / (V-V_{sp})$ vs. $(V-V_{sp})$ Plotting Under Various Differential Pressures for Seawater/KCl/Polymer Mud in Static Filtration

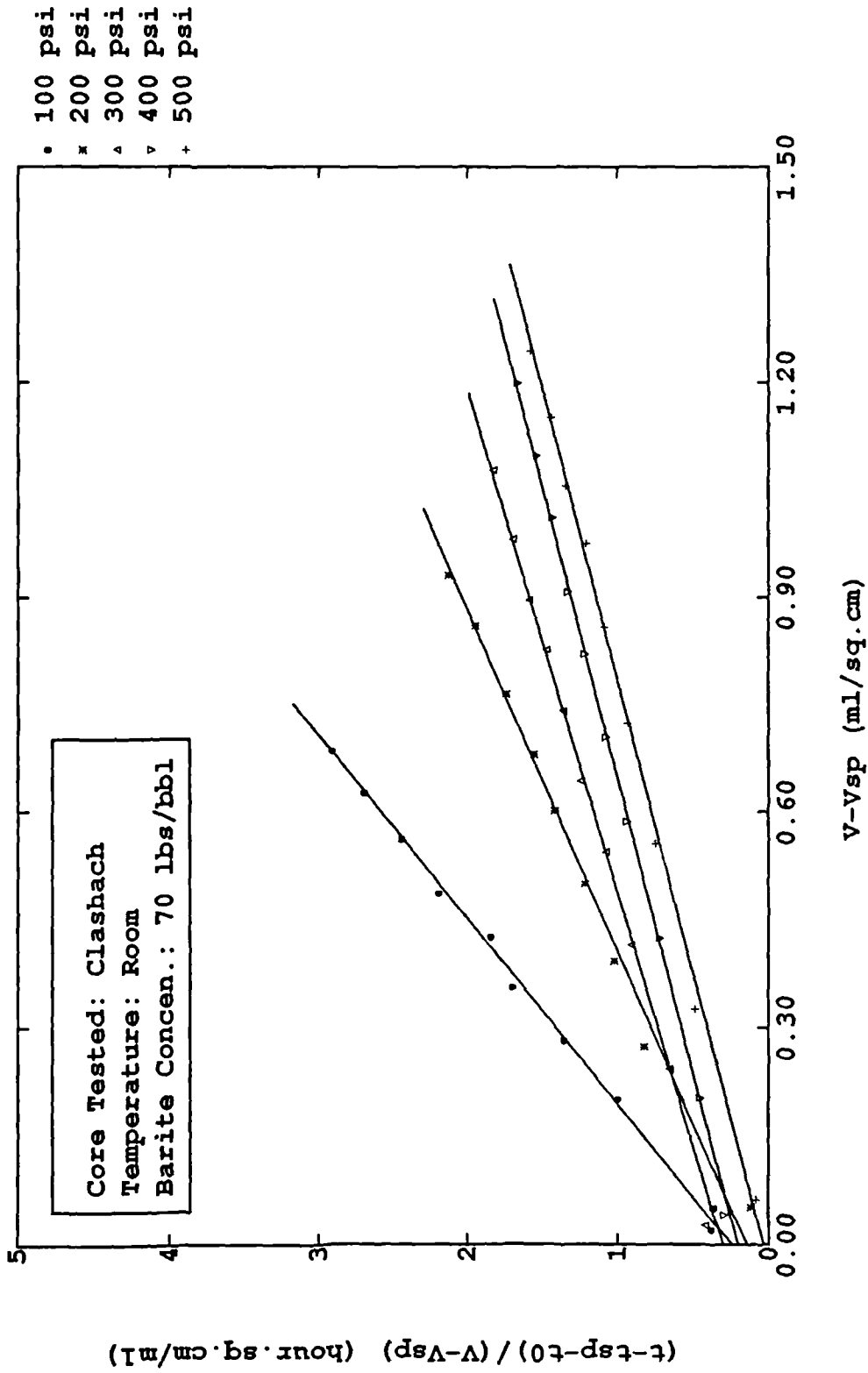


Figure (5 - 3.2) $(t-t_0-t_{sp}) / (V-V_{sp})$ vs. $(V-V_{sp})$ Plotting Under Various Differential Pressures for Seawater/KCl/Polymer Mud in Static Filtration

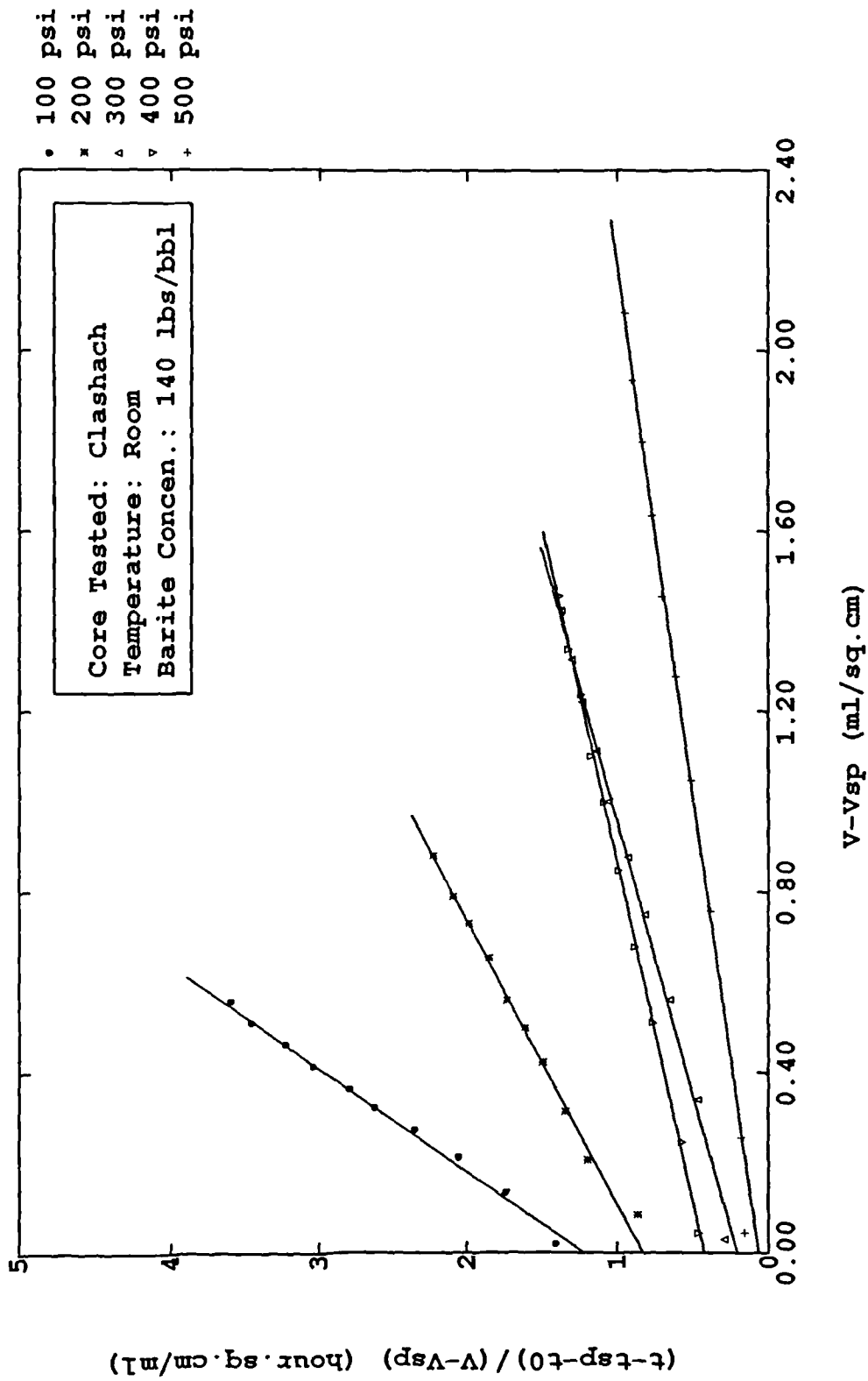


Figure (5 - 3.3) $(t-t_0-t_{sp}) / (V-V_{sp})$ vs. $(V-V_{sp})$ Plotting Under Various Differential Pressures for Seawater/KCl/Polymer Mud in Static Filtration

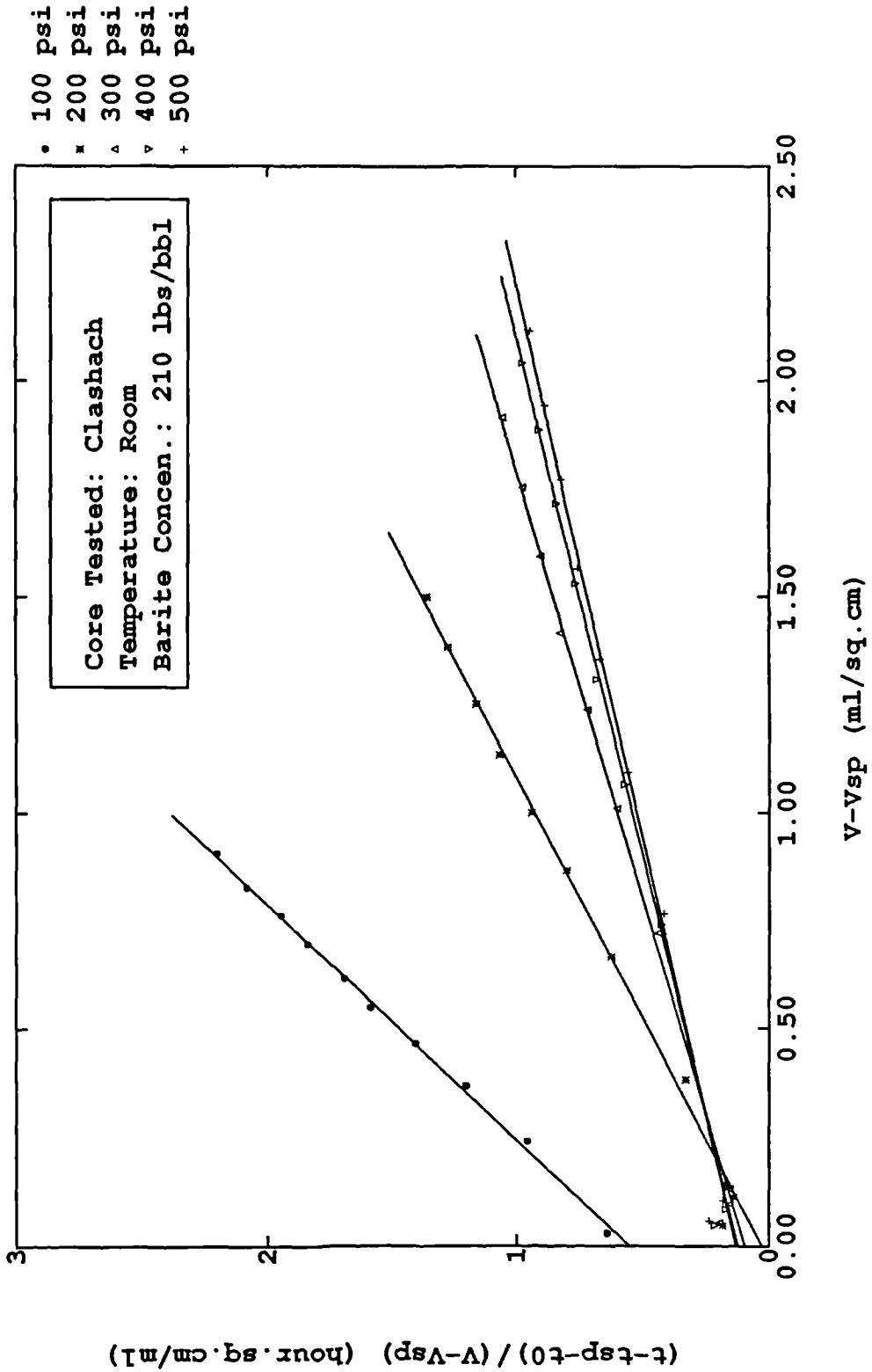


Figure (5 - 3.4) $(t-t_{sp}-t_0)/(V-V_{sp})$ vs. $(V-V_{sp})$ Plotting Under Various Differential Pressures for Seawater/KCl/Polymer Mud in Static Filtration

**Table 5.5 Regression Coefficients of Static Filtration Experiments
(Seawater/KCL/Polymer Mud)**

Barite Concentration (lbs/bbl)	Solids Fraction of Slurry (%)	Applied Pressure (psi)	$V_{sp} \times 10^{-2}$ (ml/cm ²)	a_2 (min/ml ²)	a_1 (min/ml)	t_0 (min)
50	12.40	100	12.631	10.364	11.168	3.842
		200	5.658	4.214	11.268	-2.246
		300	10.263	5.445	3.709	-0.500
		400	9.670	4.851	1.636	0.064
		500	6.513	4.407	1.346	0.087
70	16.90	100	2.434	9.111	2.816	-0.155
		200	1.447	4.913	1.725	0.356
		300	0.395	3.333	3.562	0.006
		400	0.000	2.868	2.412	-0.277
		500	4.737	2.869	0.410	0.231
140	30.26	100	1.099	10.264	14.206	-0.869
		200	16.578	3.729	9.787	0.612
		300	6.820	1.938	2.421	-0.177
		400	20.591	1.564	4.923	-0.860
		500	14.210	0.993	0.781	0.204
210	41.89	100	13.618	4.307	0.489	-0.273
		200	5.066	2.110	0.248	-0.277
		300	9.144	1.179	1.101	-0.365
		400	8.355	0.972	1.459	-0.408
		500	5.921	0.912	1.542	-0.612

Table 5.6 Regression Coefficients of Static Filtration Experiments (Freshwater/Gypsum/Lignosulphonate Mud)

Barite Concentration (lbs/bbl)	Solids Fraction of Slurry (%)	Applied Pressure (psi)	$V_{sp} \times 10^{-2}$ (ml/cm ²)	a_2 (min/ml ²)	a_1 (min/ml)	t_0 (min)
70	22.14	100	0.889	57.074	39.685	-2.449
		200	0.000	58.621	18.295	-1.818
		300	3.216	48.298	13.464	-0.874
		400	3.947	60.467	10.617	-1.025

axis, and x represents $(V - V_{sp})$ axis, where a_1 and a_2 are coefficients corresponding to the data. It is clear that substantial agreement between modified equation and the experimental data points exists. It is further seen that most of the values of $(t - t_{sp} - t_0)/(V - V_{sp})$ and $(V - V_{sp})$ fall on a straight line.

Figure(5-3.5) shows the calculated average specific cake resistance as a function of barite concentration and pressure. It is clear that the average specific cake resistance declines when the barite concentration increases and it will increase when the pressure increases. However, the figure also illustrates that the average specific cake resistance varies considerably with the pressure when the barite concentration in the mud is low, say 50 lbs/bbl. The average specific cake resistance remains in a very narrow range when the barite concentration is high, say 210 lbs/bbl. This is not contradictory to the conclusion discussed earlier in this chapter. Since we have already noted the effects of pressure and barite concentration upon the filter cake thickness and ratio of measured mass of wet to dry cake, it is therefore easy to understand that at the high barite concentration, the filter cake is less compressible and thus results in no pronounced effect of pressure upon average specific cake resistance.

Figure(5-3.6) shows the effective filter medium resistance as a function of pressure and barite concentration. The data points are very scattered and no specific relationship was found for this mud under static filtration but it worth noting that the effective filter medium resistance is in the same order of magnitude as the filter cake resistance.

5.3.2.2 Average Cake Porosity and Permeability

According to the definition of m :

$$m = \frac{\text{Wet Filter Cake Mass}}{\text{Dry Filter Cake Mass}}$$

$$= \frac{\rho_s(1 - \epsilon_{avg}) \cdot LA + \rho_f \epsilon_{avg} LA}{\rho_s(1 - \epsilon_{avg}) \cdot LA}$$

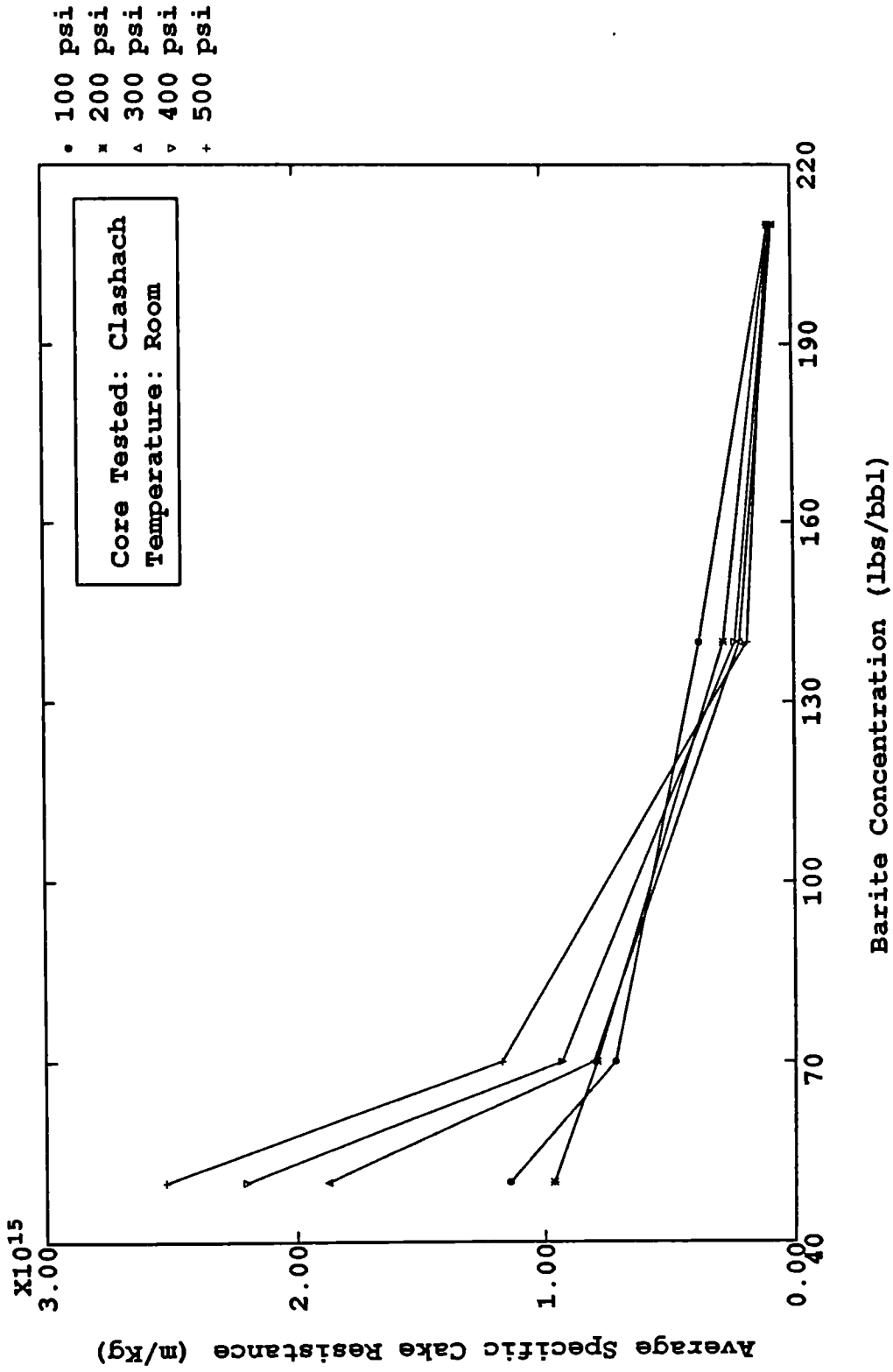


Figure (5 - 3.5) Average Specific Cake Resistance as Function of Barite Concentration and Pressure for Seawater/KCL/Polymer Mud in Static Filtration

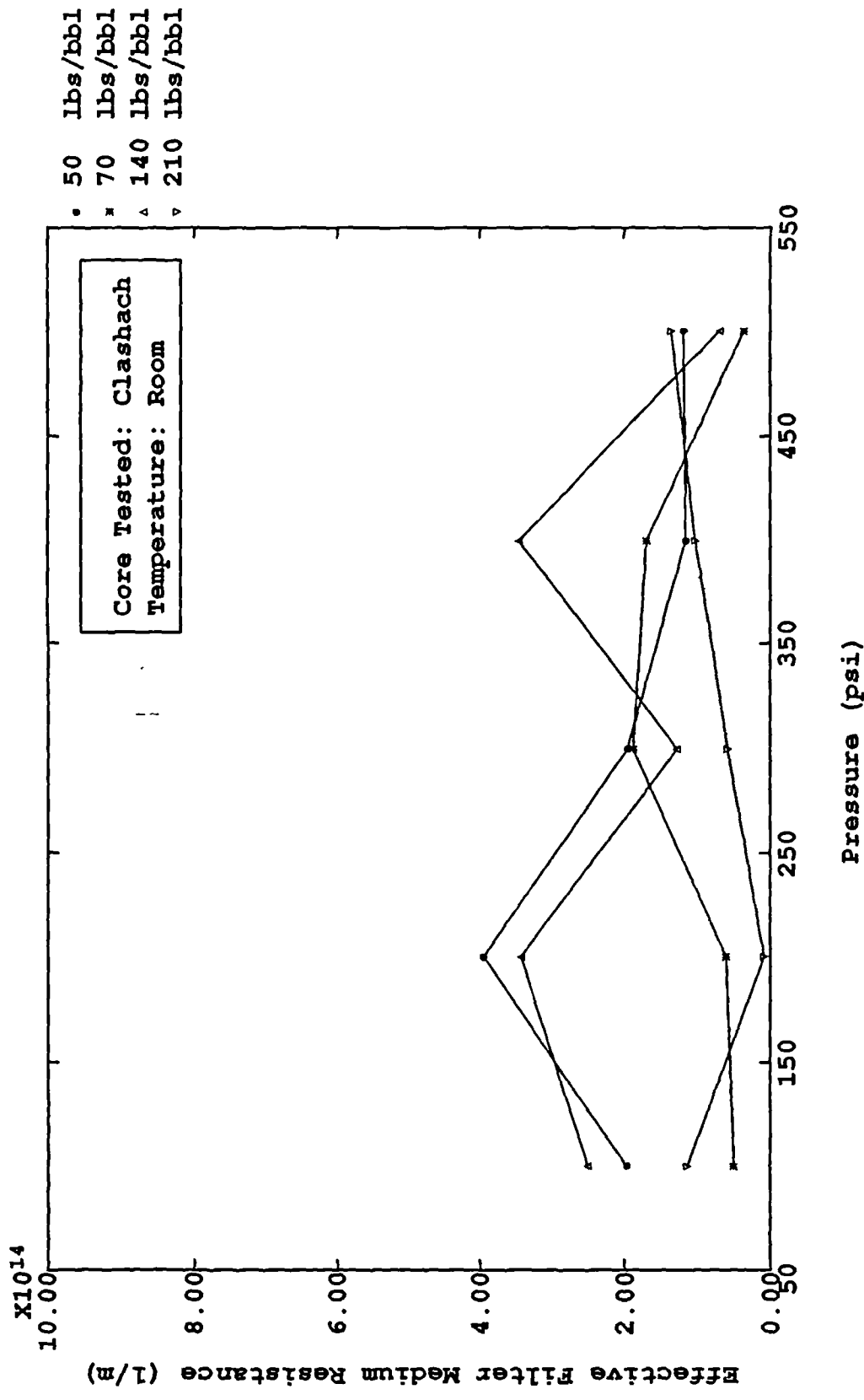


Figure (5 - 3.6) Effective Filter Medium Resistance as Function of Pressure and Barite Concentration for Seawater/KCl/Polymer mud in Static Filtration

$$= \frac{\rho_s(1 - \epsilon_{avg}) + \rho_f \epsilon_{avg}}{\rho_s(1 - \epsilon_{avg})} \quad (5-3.11)$$

Rearrange:

$$\epsilon_{avg} = \frac{(m-1)}{(m-1) + \frac{\rho_f}{\rho_s}} \quad (5-3.12)$$

From equation(3-1.27):

$$K_{avg} = \frac{1}{\rho_s(1 - \epsilon_{avg})\alpha_{avg}} \quad (5-3.13)$$

Above equations can be used to determine the average cake porosity and average cake permeability if the ratio of wet to dry filter cake mass, the density of the filtrate and solids can be obtained. It is important to note that the solid density as appears in the above equation should be determined by the true density because the filter cake is made up of several types of solids, such as, bentonite, barite, and polymer, for example in Freshwater/Gypsum-Lignosulphonate mud system. It is therefore necessary to describe the calculation method for the true solid density of the mud consisting of several kind of solids as follows.

Assuming the Freshwater/Gypsum-Lignosulphonate base mud as an example which the compositions are listed in Table 4.1. First, we use the following densities:

Bentonite	2300 kg/m ³
Barite	4300 kg/m ³
LV CMC	1600 kg/m ³

Whether or not the polymer should be included is questionable. However, there are many investigators^{48,94} who found that the polymer exists in the filter cakes. In this study, we will neglect the effects of polymer upon the filter cake true solids density

because it will make little difference when the effects of the polymer on calculation of mixed solids density is considered.

The density of above example should approximately be:

$$\rho_s = \frac{20}{90} \times 2300 + \frac{70}{90} \times 4300 = 3855.6 \text{ Kg/m}^3$$

If we include the polymer in calculation, it would be:

$$\rho_s = \frac{20}{92} \times 2300 + \frac{70}{92} \times 4300 + \frac{2}{92} \times 1600 = 3879.2 \text{ Kg/m}^3$$

The error caused by neglecting the polymer should be:

$$\Delta\% = \left| \frac{3855.6 - 3879.2}{3855.6} \right| \times 100 = 0.62\%$$

The error is very small and it is accurate enough for engineering practice.

Figure(5-3.7) shows the average cake porosity as a function of barite concentration and pressure. The curves are very similar to those plotted in Figure(5-2.7) because all the parameters affecting m (ratio of measured mass of wet to dry cake) will also influence the porosity.

Figure(5-3.8) shows the average cake permeability as a function of barite concentration and pressure. The average cake permeability was found to be between 0.3×10^{-6} and 5.2×10^{-6} darcies.

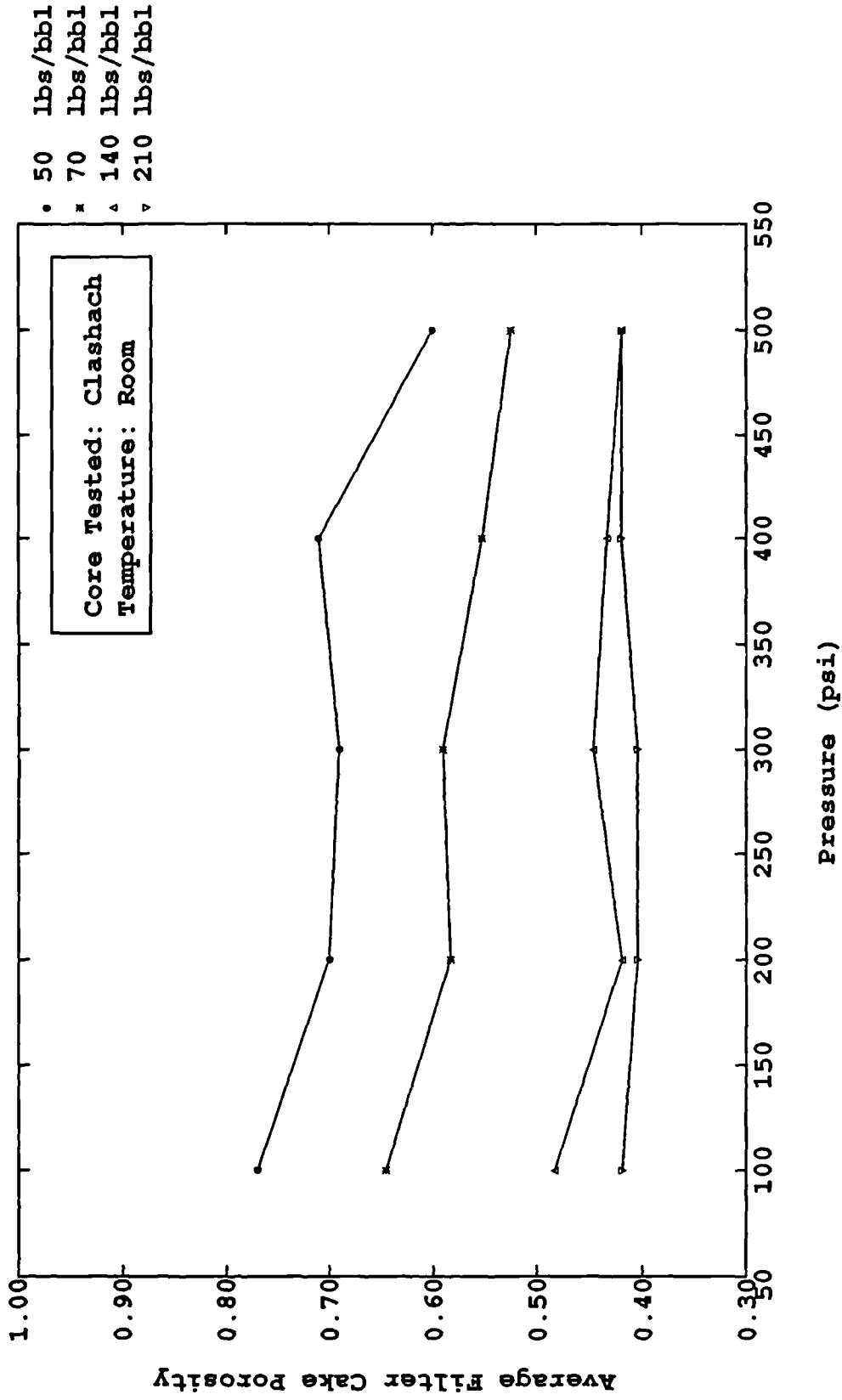


Figure (5 - 3.7) Average Filter Cake Porosity as Function of Pressure and Barite Concentration for Seawater/KCl/Polymer mud in Static Filtration

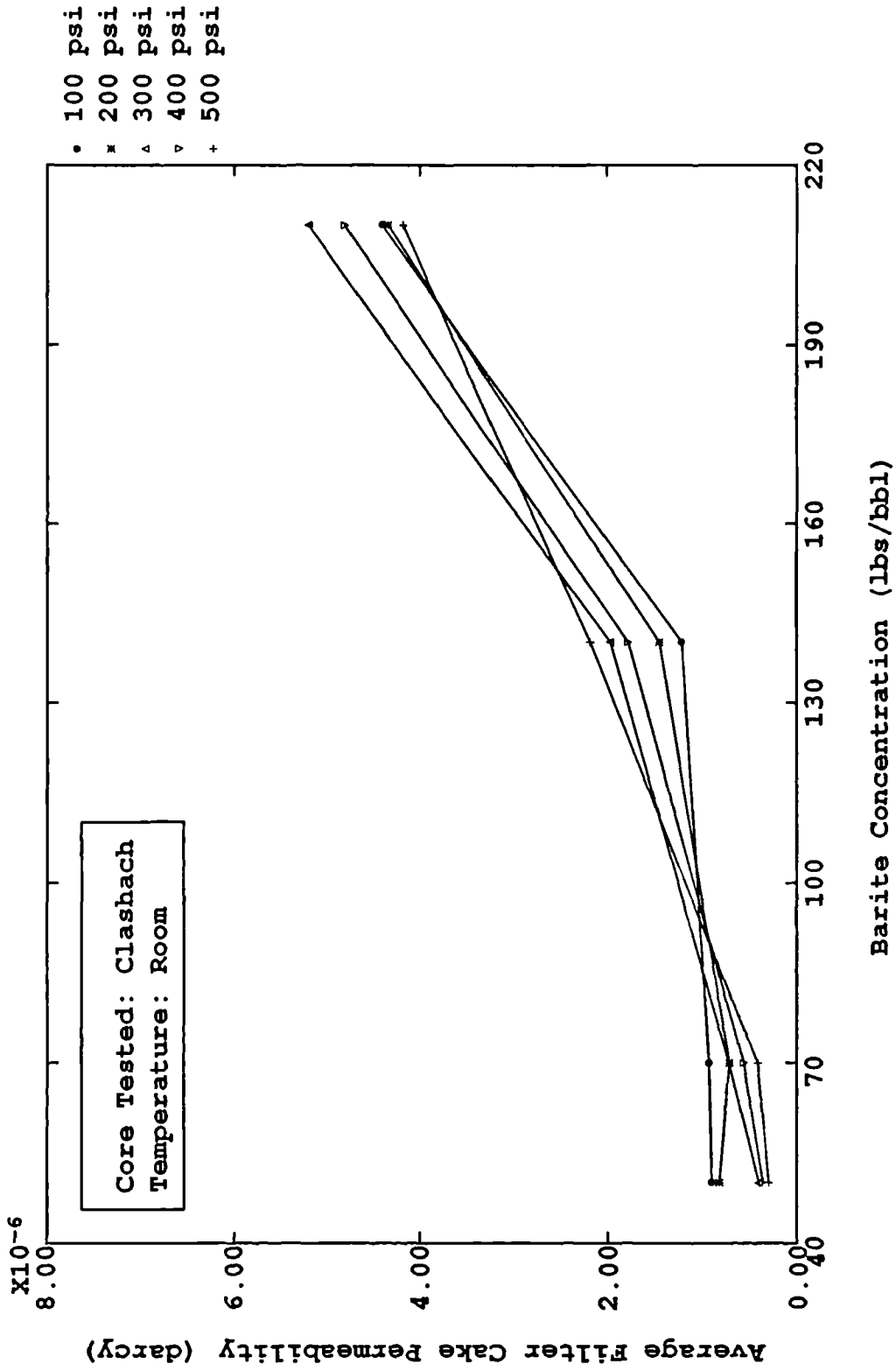


Figure (5 - 3.8) Average Filter Cake Permeability as Function of Barite Concentration and Pressure for Seawater/KCL/Polymer Mud in Static Filtration

Chapter Six

PRESENTATION OF DYNAMIC FILTRATION EXPERIMENTAL RESULTS

This chapter presents the results of dynamic filtration experiments.

6.1 MUD SYSTEMS TESTED AND THEIR PROPERTIES

In order to compare the parameters obtained from static and dynamic experiments, the same mud systems as were utilised for static tests were used. The muds were a Seawater/KCL/Polymer base mud and Freshwater/ Gypsum/Lignosulphonate base mud for which the compositions are listed in Table 5.1 and Table 5.2 and properties in Table 5.3 and Table 5.4. It should be noted that no attempts were made to perform dynamic filtration tests for a mud with a high solids (barite) concentration because due to the equipment utilized in this study, the filter cake could not be allowed to form more than 1 mm. The solid fraction, s , was calculated in the same way as in chapter five. The viscosity of filtrate was found to be 1.09-1.24 cp for Seawater/KCL /Polymer base mud and 1.1-1.25 cp for Freshwater/Gypsum/Lignosulphonate base mud. In this study, the viscosity of filtrates in all calculations was assumed to be equal to 1.195 cp for convenience.

6.2 EXPERIMENTAL RESULTS

6.2.1 Spurt Loss and Cumulative Filtrate Volume

Unlike static filtration experiments, the filter cake characteristics such as thickness, ratio of wet/dry cake mass etc., could not be obtained during dynamic filtration tests because dynamic filter cakes formed in the experiments were so thin that they were impossible to measure accurately using the method reported in chapter four. The attempts to measure filter cakes thickness suggested that the thickness of most cakes formed under our experimental conditions were less than 1.00 mm. The spurt loss and the cumulative filtrate volume were recorded. Every test was conducted for at least 8 hours. According to the result of plots of cumulative filtrate loss vs. time, it is clear that the test time of 8 hours was adequate to ensure that the dynamic filtration reached equilibrium. As pointed out in chapter 5, the spurt loss under static conditions was found to have no relationship with the tested variables, which contradicts with the results^{47,94} that the spurt loss is an exponential function of the pressure. This may be explained by the difference between the filter mediums utilised. Arthur *et al.*^{47,94} used filter papers as filter medium whereas in these experiments the filter medium was natural sandstone core which may have a very random surface pores size distribution and liquid permeability. It is understood that the spurt loss is a function of a large number of variables such as, pressure, mud solids concentration and solids size distribution, filter medium pore size and size distribution, filter medium permeability, shear rate, etc. Therefore, it is possible for the above contradictory to exist. Simpson³⁵ explained that thin filter paper does not provide pore spaces where internal filter cake might start to form compared to the natural core.

Figures(6-2.1) and (6-2.2) show the spurt loss under dynamic conditions as a

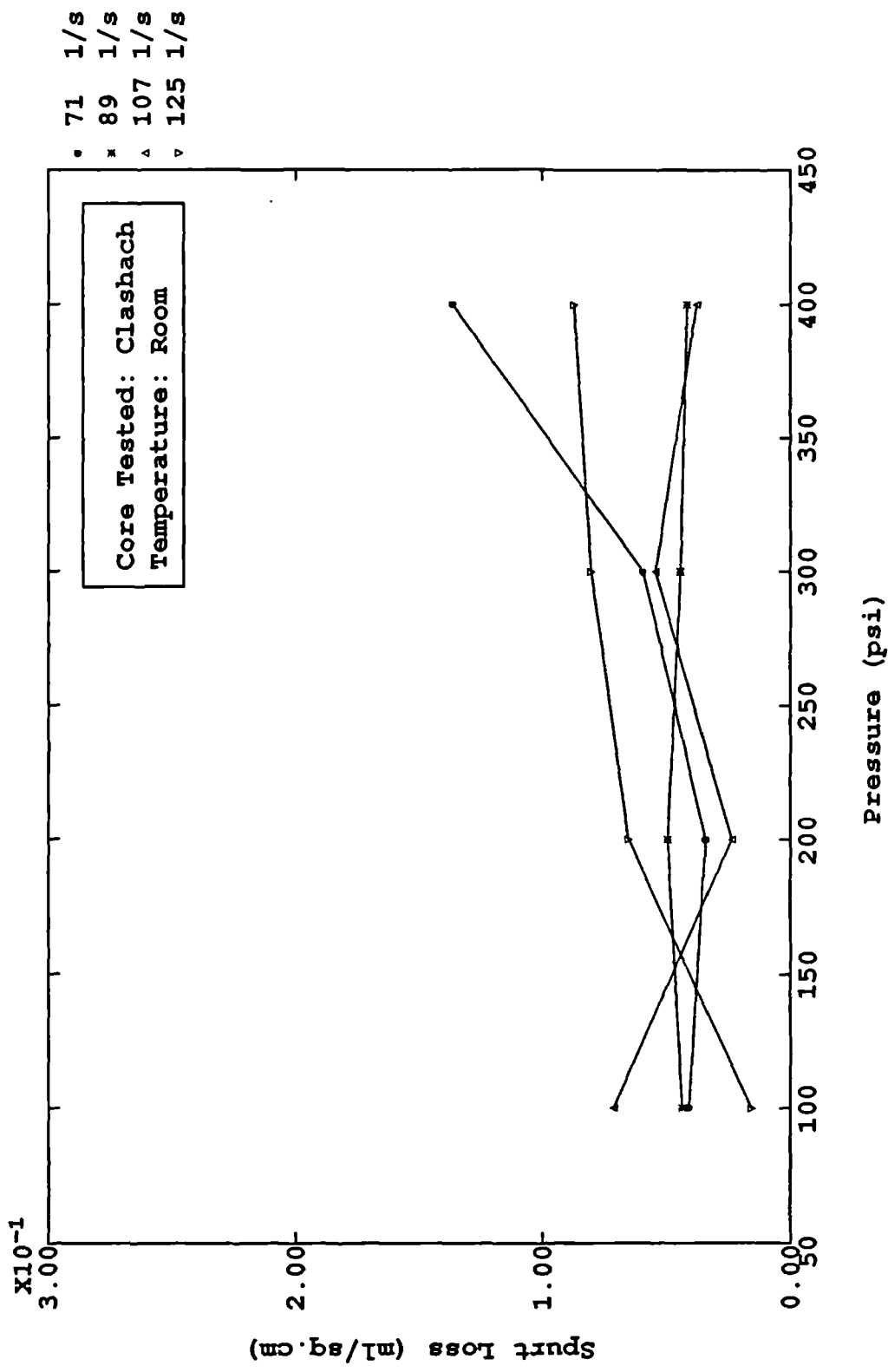


Figure (6 - 2.1) Spurt Loss as Function of Pressure and Shear Rate for Seawater/KCL/Polymer Mud in Dynamic Filtration

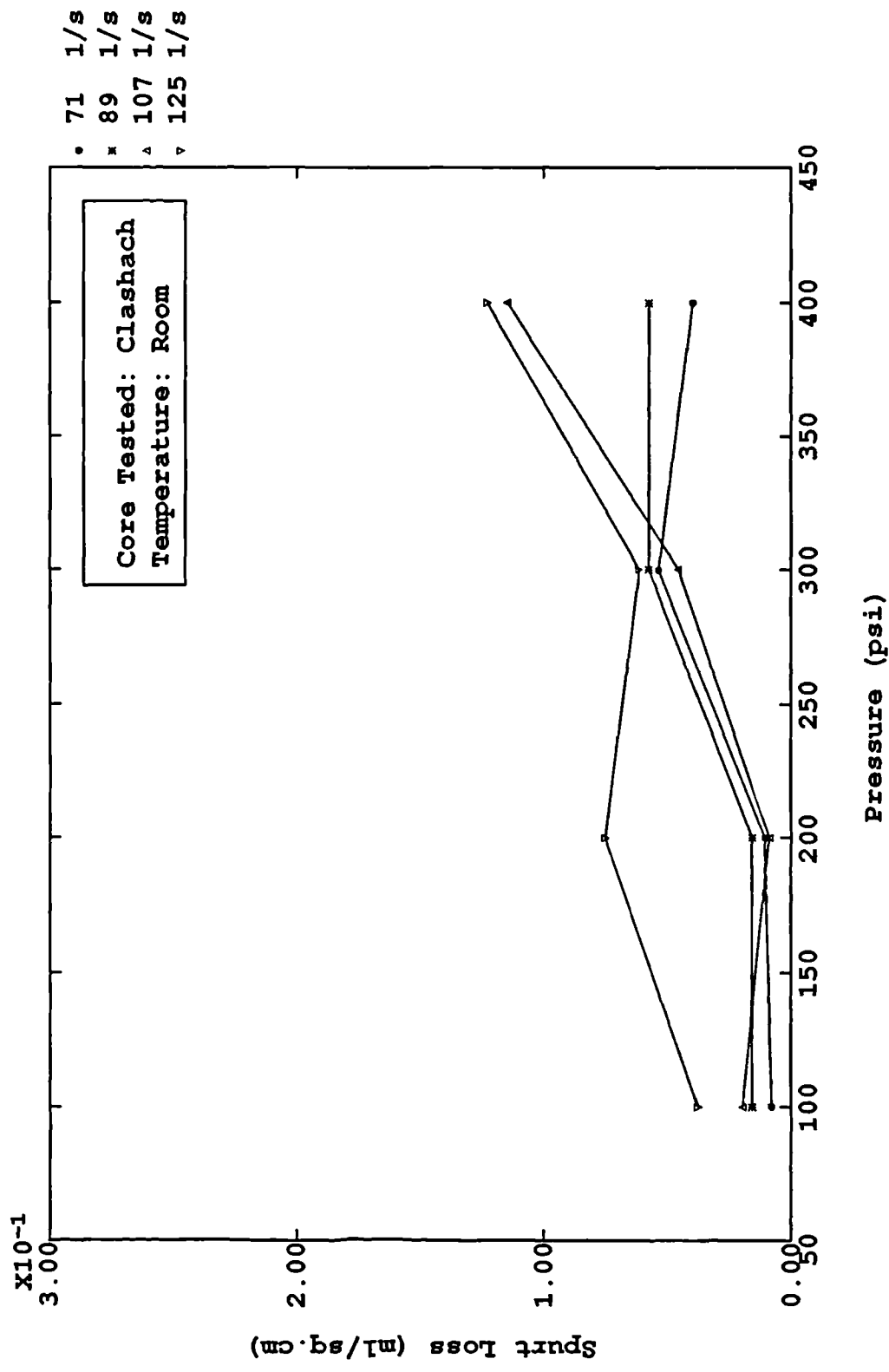


Figure (6 - 2.2) Spurt Loss as Function of Pressure and Shear Rate for Freshwater/Gypsum/Lingonosulphonate Mud in Dynamic Filtration

function of pressure and shear rate for two different muds. It is difficult to define whether or not an effect of pressure upon spurt loss exists under conditions where there is a shear stress on the surface of core.

Figures(6-2.3) and (6-2.4) show the cumulative filtrate volume at 8 hours as a function of shear rate and pressure in dynamic filtration. It can be understood from these figures that, the cumulative filtrate volume at 8 hours for Seawater/KCL/Polymer mud decreases slightly with increasing shear rate, for Freshwater/Gypsum/Lignosulphonate mud, however, this volume increases with increasing shear rate. This can be explained if the effect of shear rate is considered as two actions: the erosion and the sorting. The mud stream can continuously erode the freshly deposited cake and under this condition, the cumulative filtrate volume will increase rapidly and then reach an equilibrium when the shear rate increases from zero to maximum. On the other hand, when the filtration process continues, the particles sorting will increase the filter cake resistance and in this case, the cumulative filtrate volume will decline slowly and then reach an equilibrium whilst the shear rate approaches to maximum from zero. The above two actions affect the cumulative filtrate volume simultaneously. Considering the range of the shear rates of the above two figures, it is clear that the difference can be produced by these two mud systems.

Figures(6-2.5) to (6-2.10) present plots of dynamic cumulative filtrate volume versus time for various differential pressures and shear rates. Figure(6-2.11) shows cumulative filtrate volume as a function of time at low pressure and various shear rates. As with spurt loss, the effect of pressure and shear rate upon the cumulative filtrate volume are not very clear.

In general, increasing pressure would increase compaction of the filter cake which would lead to an increase in filter cake resistance and thus reduce filtrate volume if the filter cake is compressible. On the other hand, an increase in pressure could increase the driving force and thus should increase the filtrate volume according to darcy's law. For static filtration, the effect due to compaction of the cake on the filtrate volume may be less

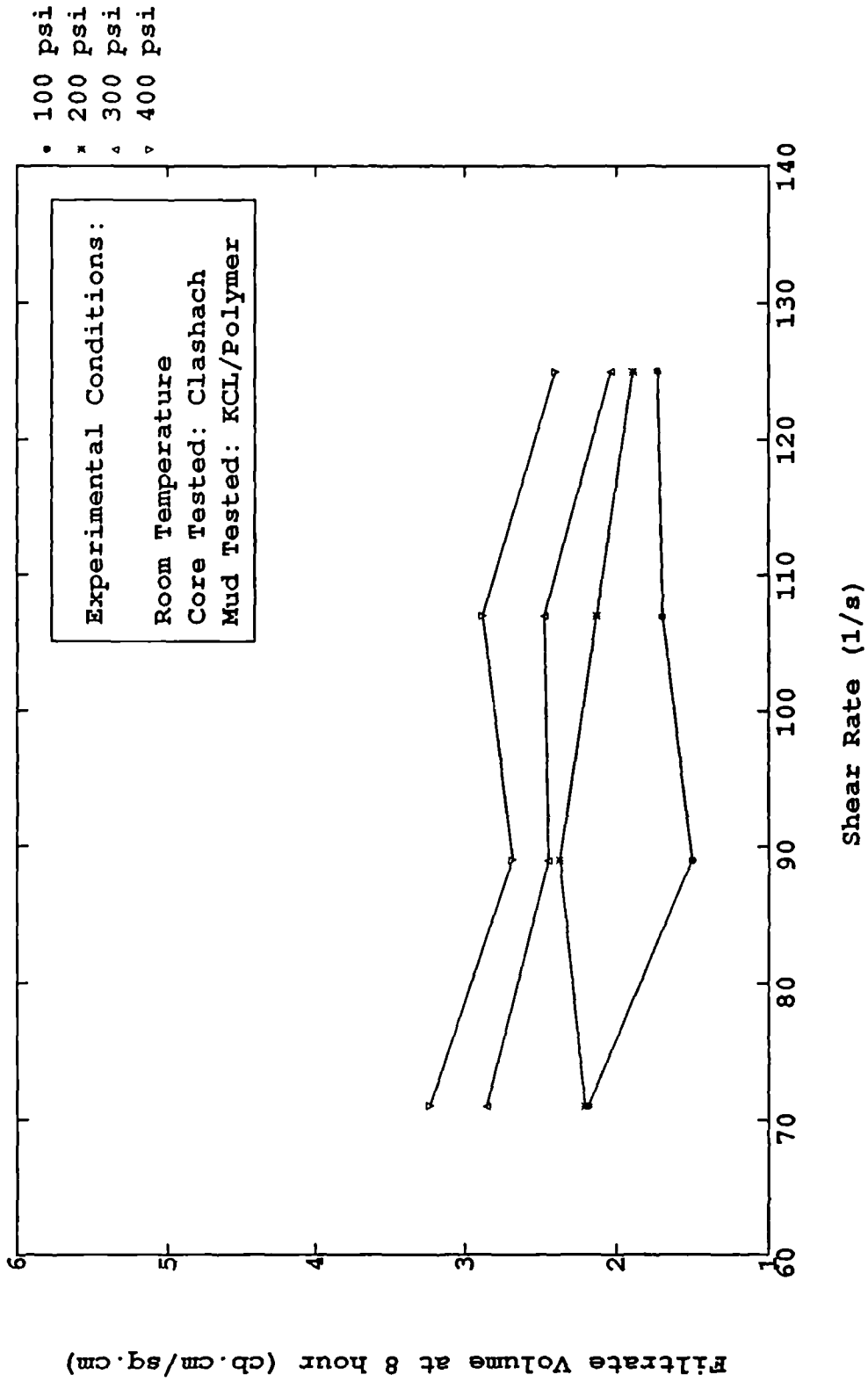


Figure (6-2.3) Cumulative Filtrate Volume at 8 hour as Function of Shear Rate and Pressure for KCL/Polymer Base Mud in Dynamic Filtration

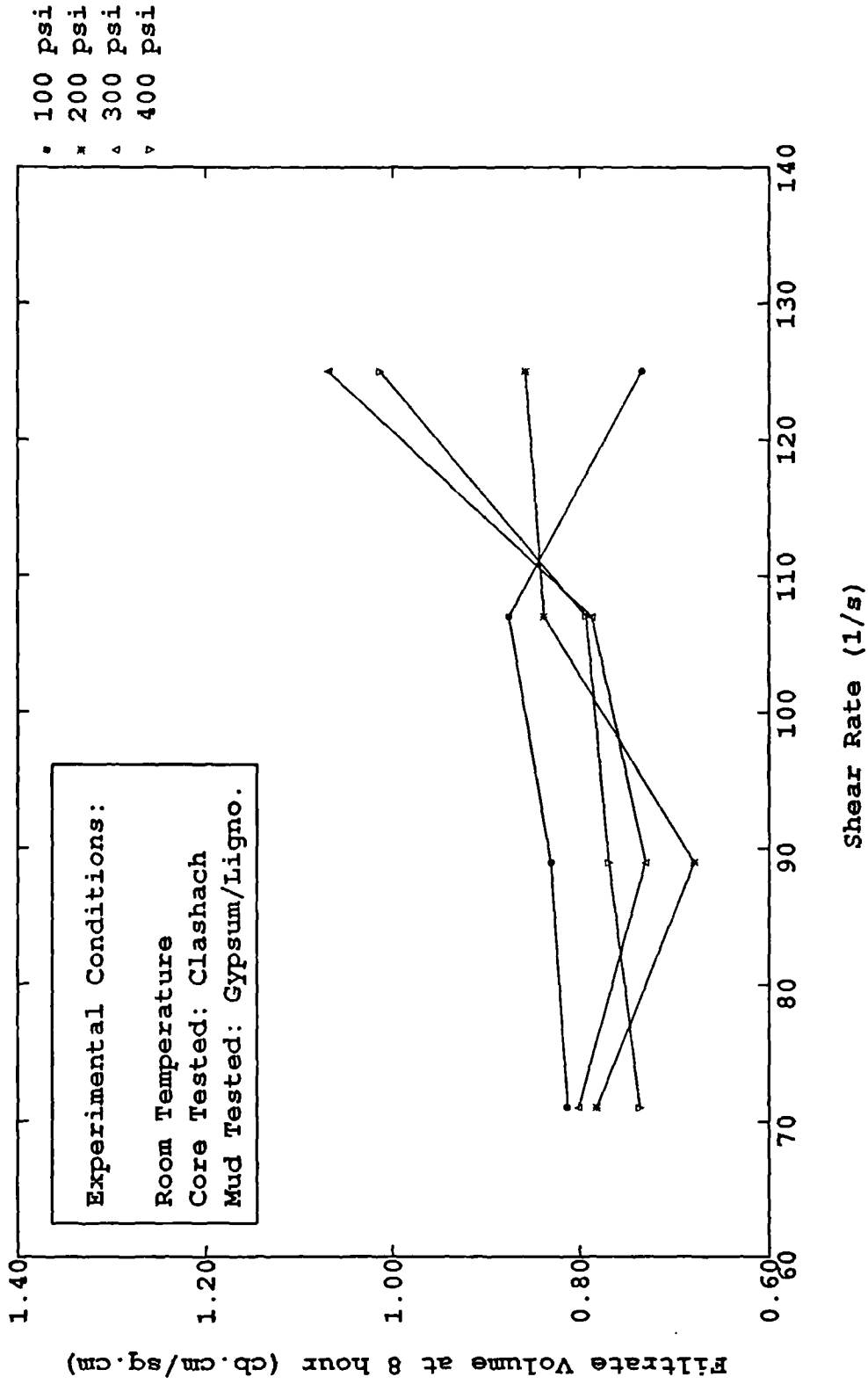


Figure (6-2.4) Cumulative Filtrate Volume at 8 hour as Function of Shear Rate and Pressure for Gypsum/Lignosulphonate Base Mud in Dynamic Filtration

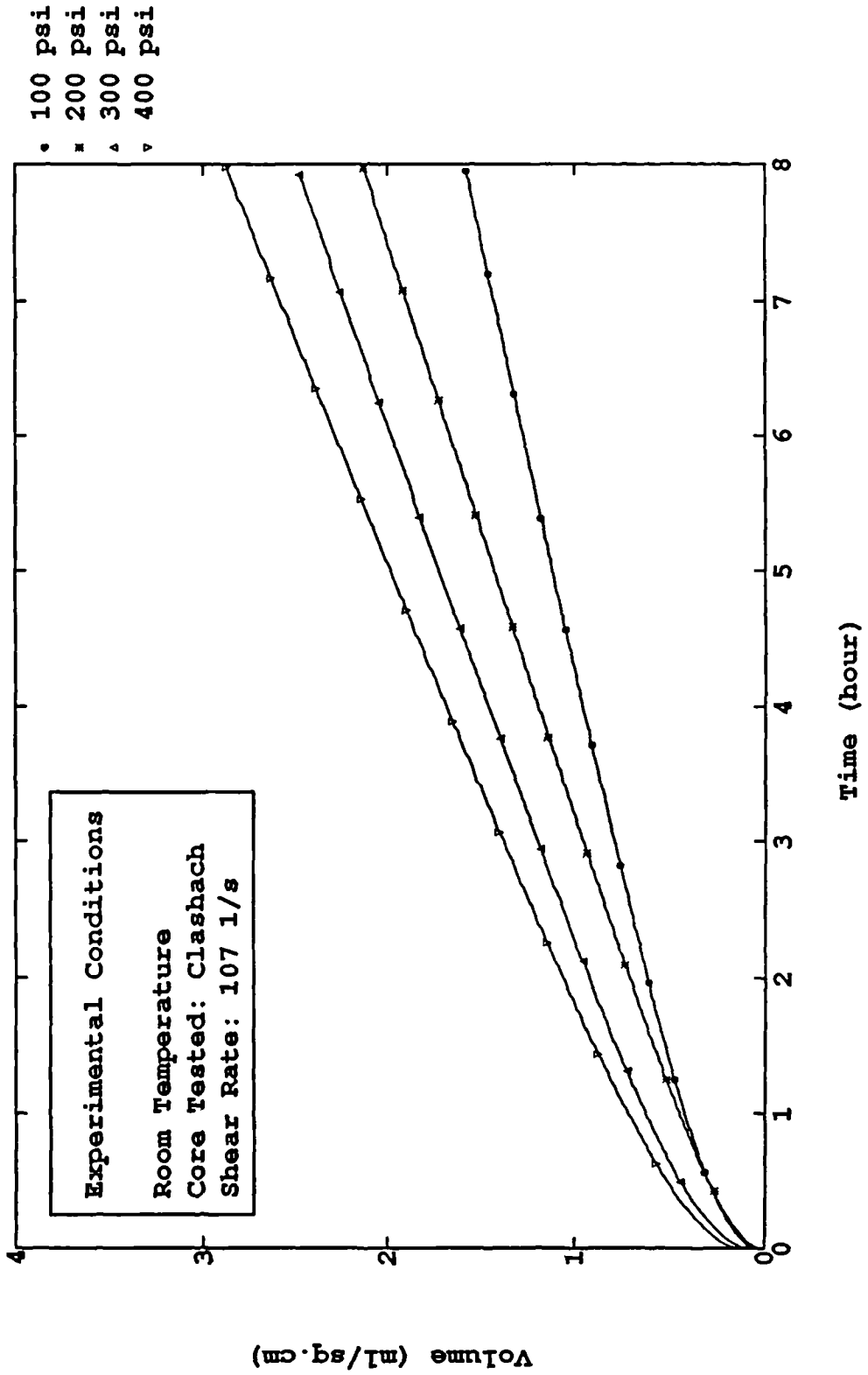


Figure (6 - 2.5) Cumulative Filtrate Volume Per Unit Area as Function of Time for Seawater/KCl/Polymer Mud in Dynamic Filtration

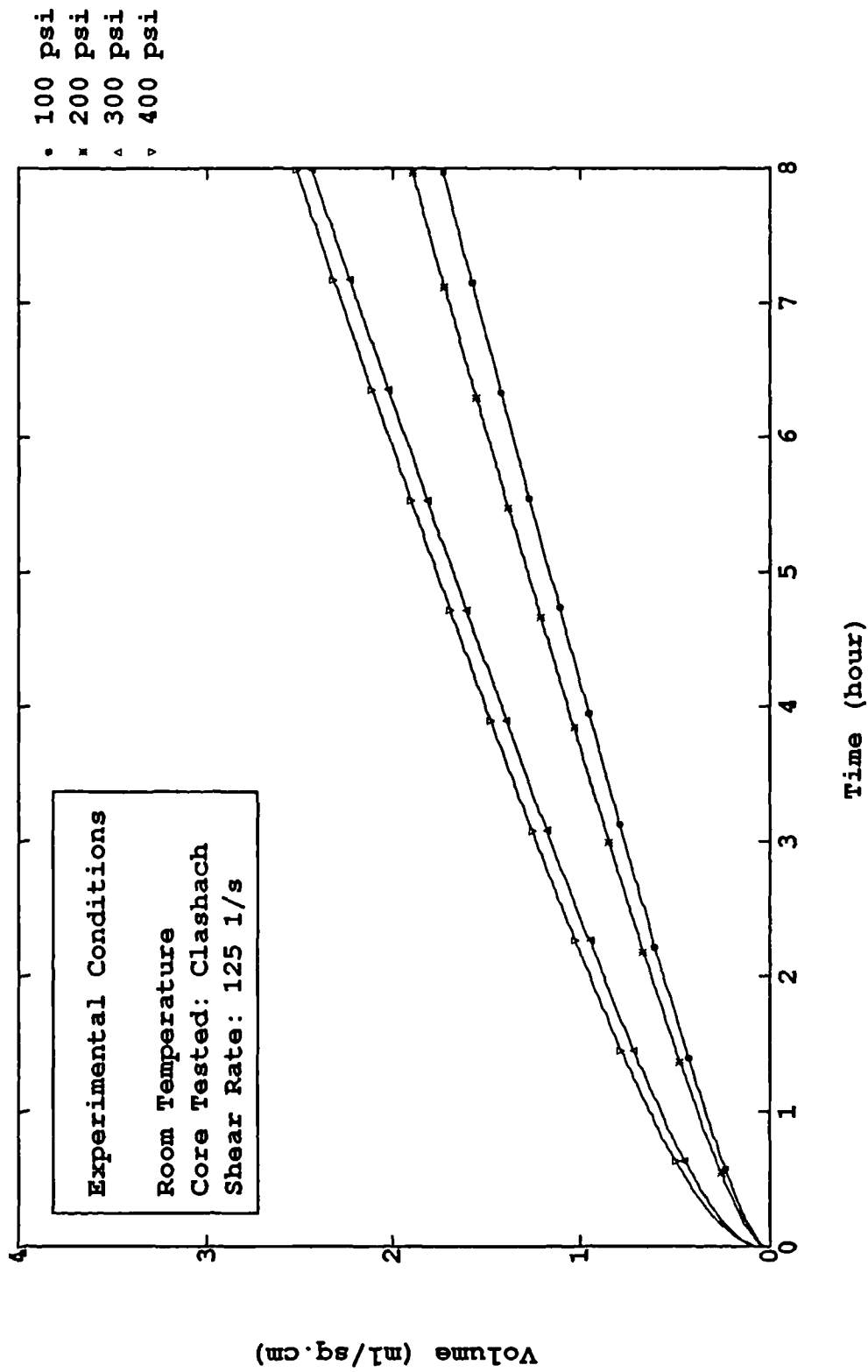


Figure (6 - 2.6) Cumulative Filtrate Volume Per Unit Area as Function of Time for Seawater/KCl/Polymer Mud in Dynamic Filtration

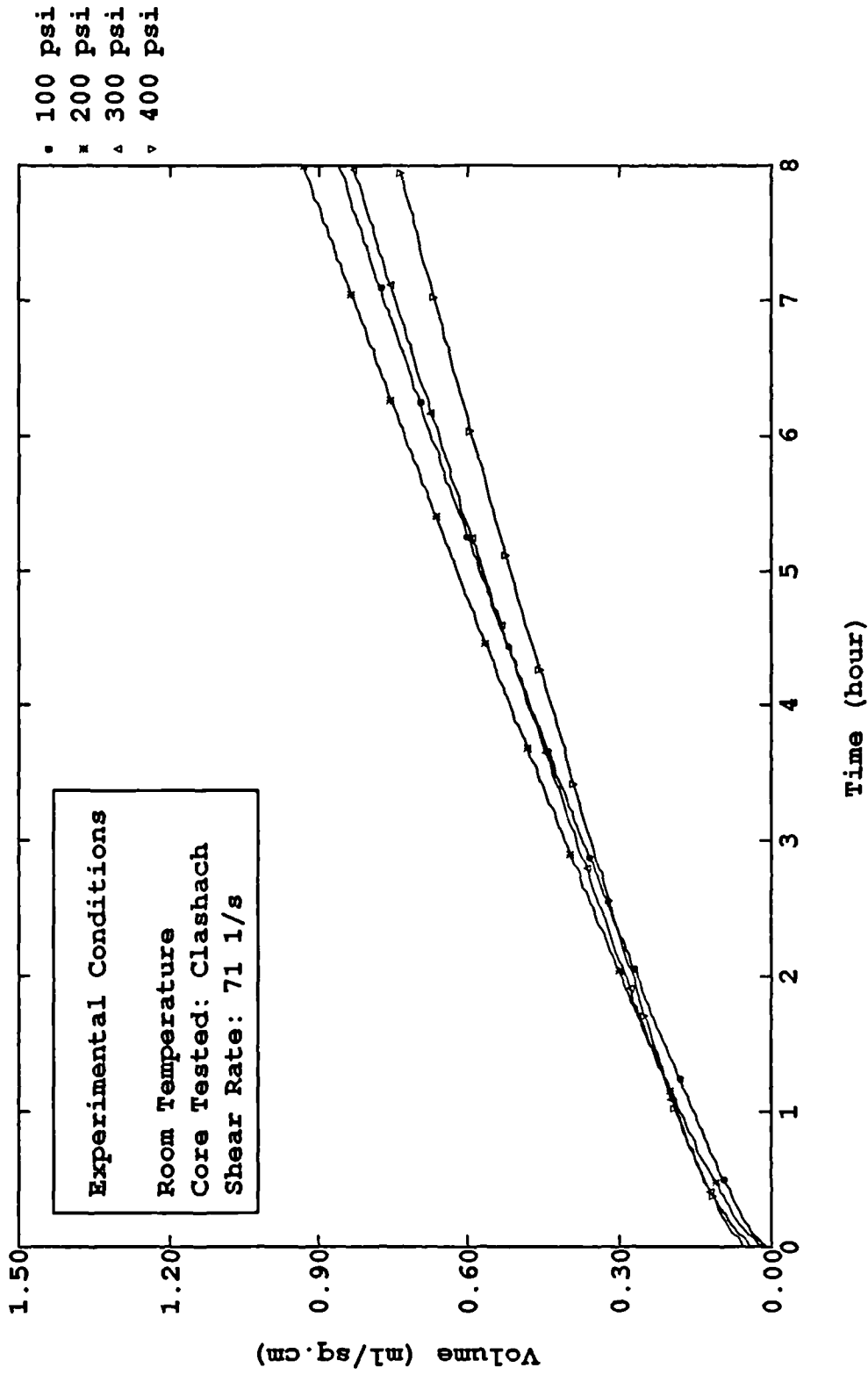


Figure (6 - 2.7) Cumulative Filtrate Volume Per Unit Area as Function of Time for Gypsum/Lignosulphonate mud in Dynamic Filtration

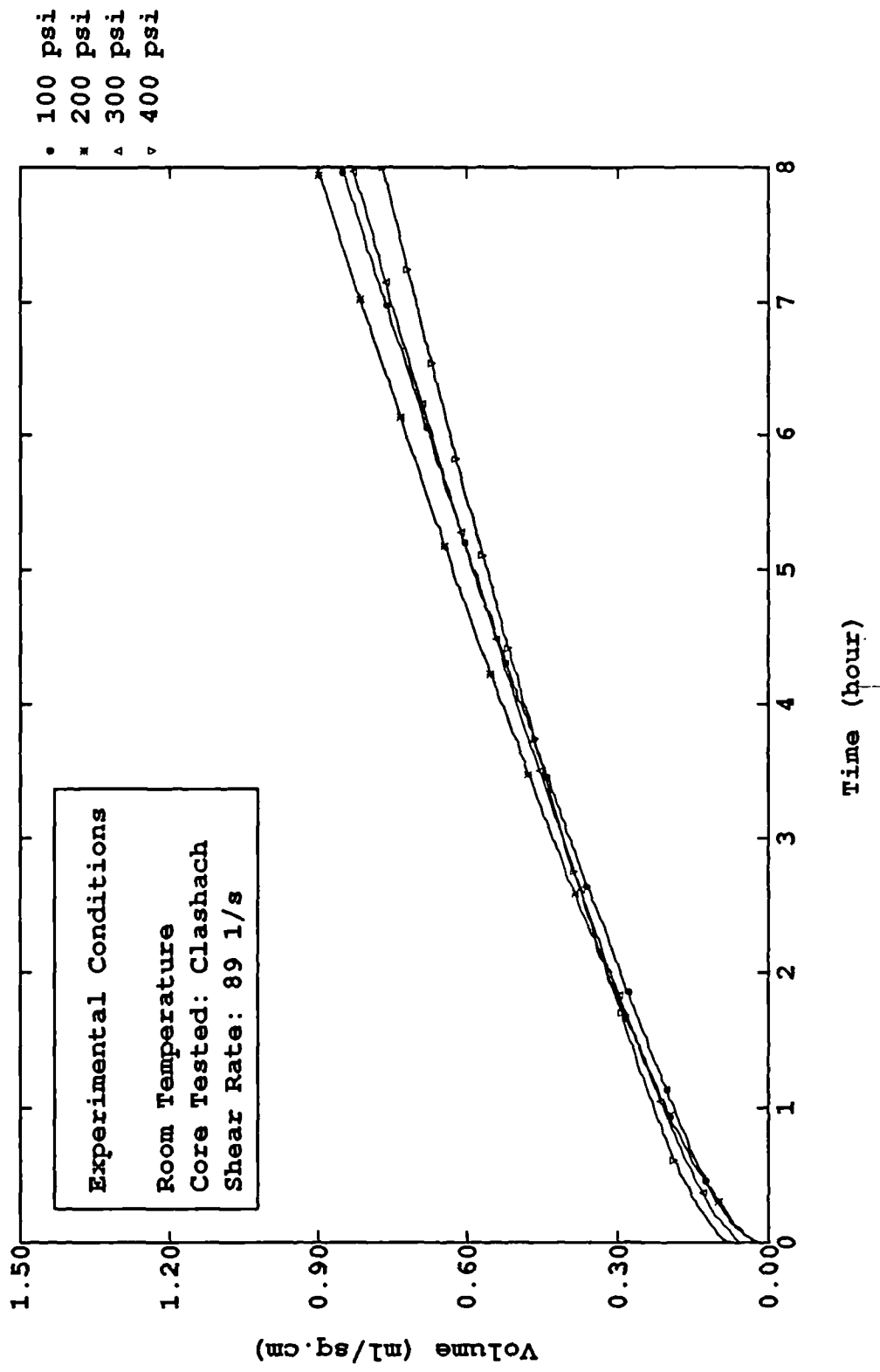


Figure (6 - 2.8) Cumulative Filtrate Volume Per Unit Area as Function of Time for Gypsum/Lignosulphonate mud in Dynamic Filtration

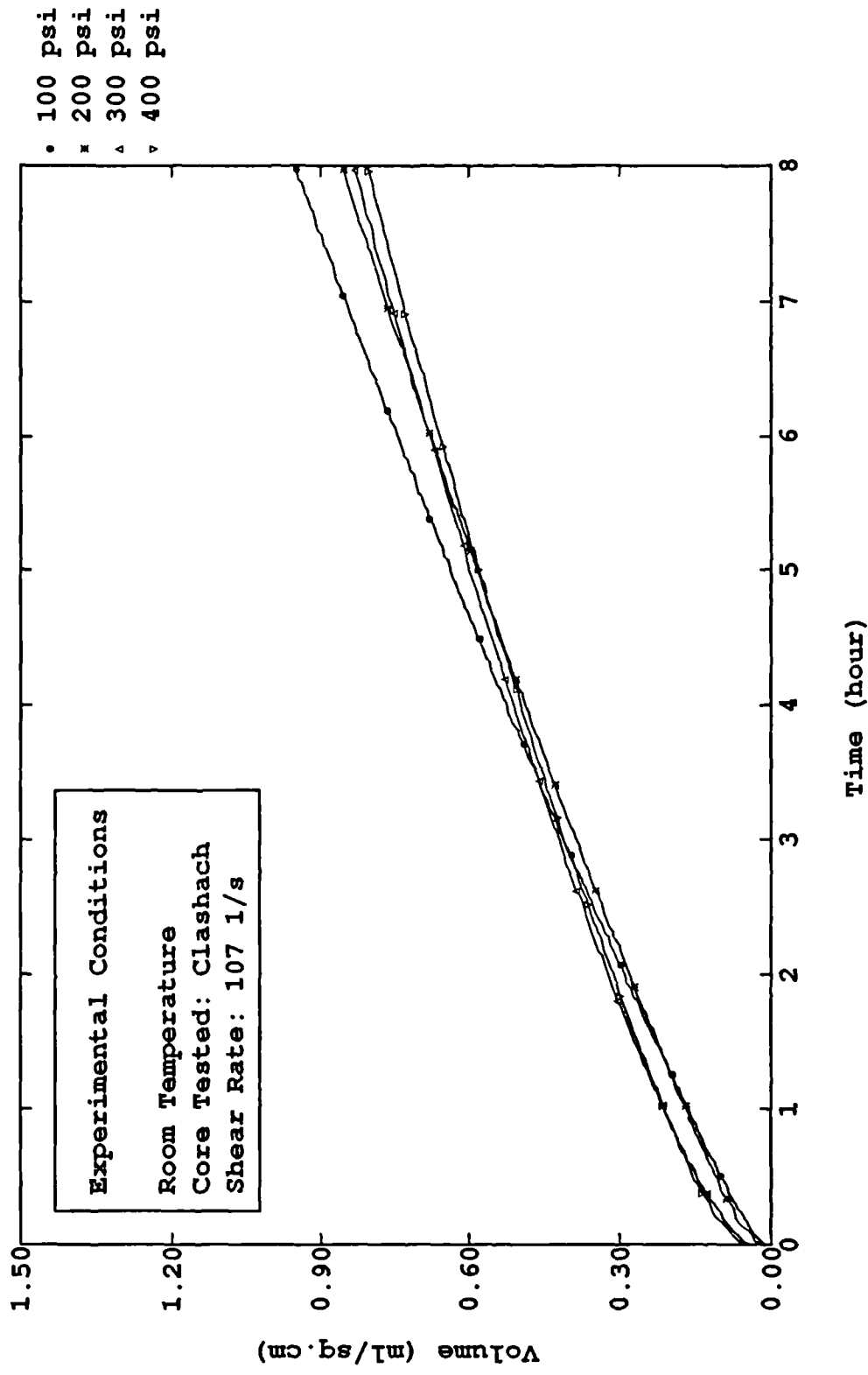


Figure (6 - 2.9) Cumulative Filtrate Volume Per Unit Area as Function of Time for Gypsum/Lignosulphonate mud in Dynamic Filtration

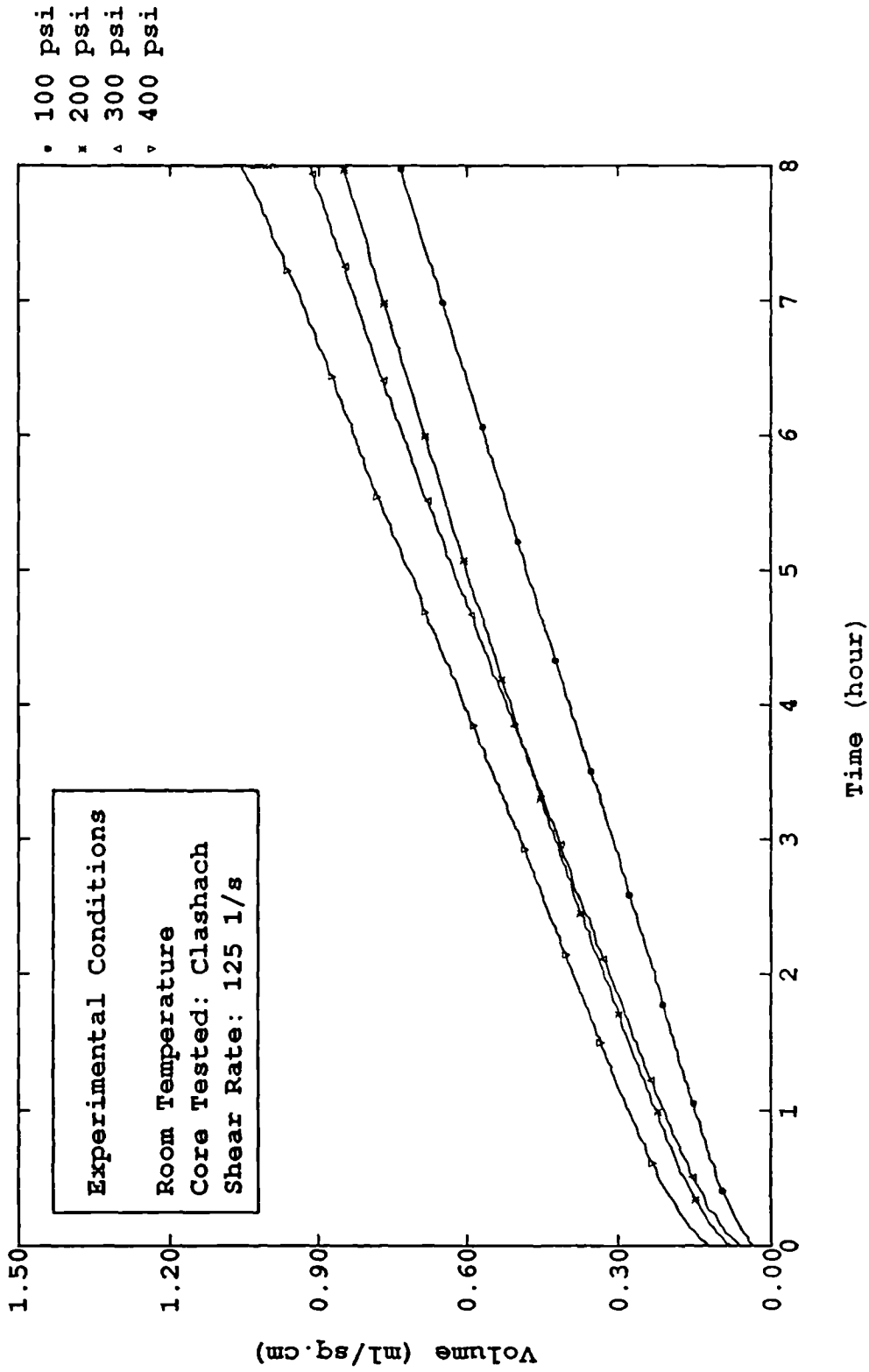


Figure (6 - 2.10) Cumulative Filtrate Volume Per Unit Area as Function of Time for Gypsum/Lignosulphonate mud in Dynamic Filtration

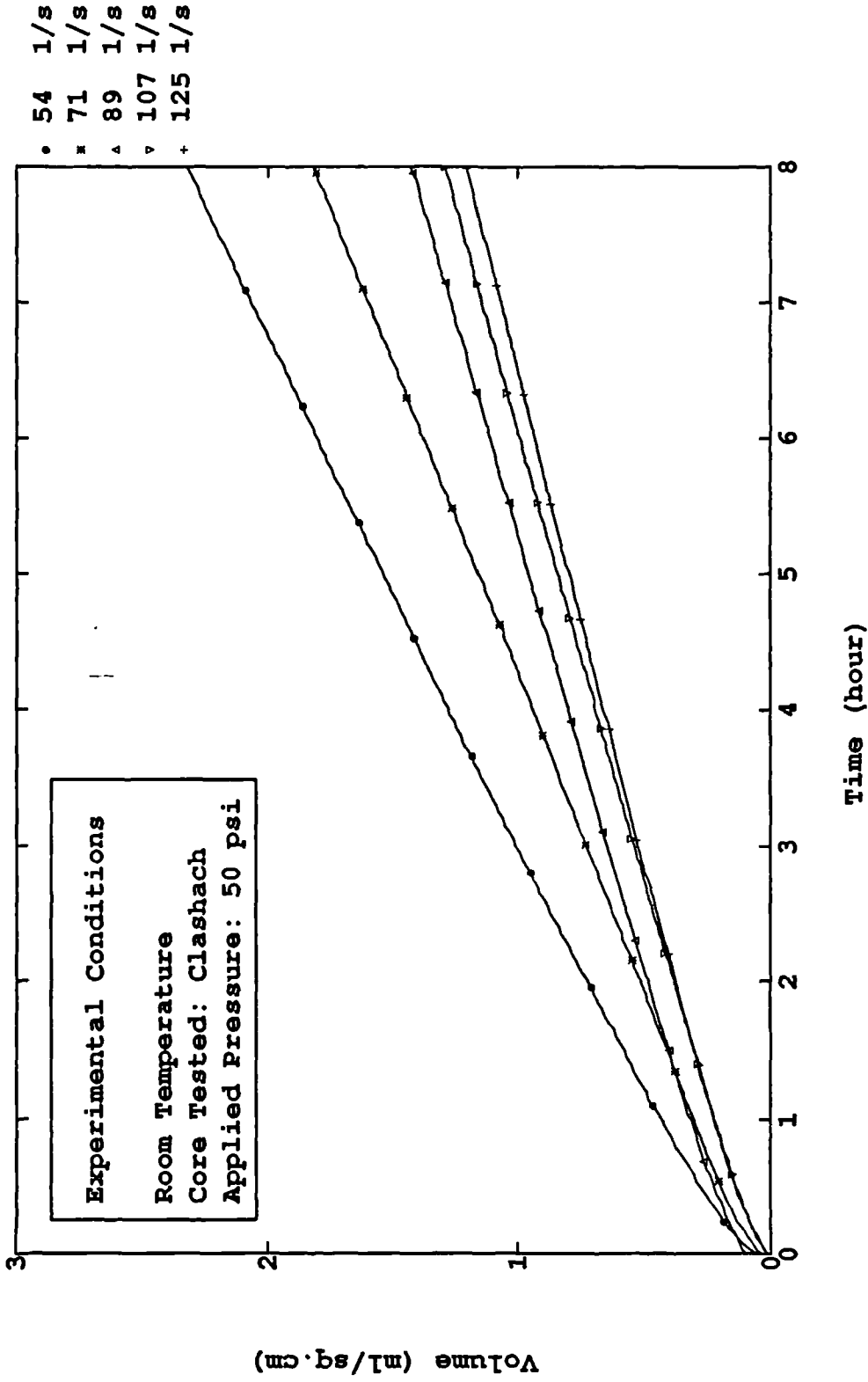


Figure (6 - 2.11) Cumulative Filtrate Volume Per Unit Area as Function of Time for Seawater/KCL/Polymer Mud in Dynamic Filtration

than that caused by pressure as driving force. In dynamic filtration, however, the shear stress/shear rate on the filter cake surface may affect the compaction of the filter cake which may lead to a more compacted and subsequently a higher resistance cake. A suitable shear rate could make the particles deposit properly, causing them to more easily plug and thus create a very high filter medium resistance. When the shear rate continue to increase, the transition layer¹³ of the filter cake would be eroded more and more, which would prevent the deposition of more filter cake.

From the plots, it is observed that the effect of pressure upon cumulative filtrate volume under shear conditions is not a simple exponential function as Larsen⁴ reported.

6.2.2 Derivation of Dynamic Filtration Equation

Similar to the derivation of the static filtration equation, the dynamic filtration equation is not difficult to derive based on the general equation developed in chapter three. Rewriting equation(3-3.12) in the form:

$$\frac{dt'}{dV'} + \kappa_2 t' = \kappa_1 V' + \kappa_3 + F(V') \quad (6-2.1)$$

where t' , V' and $F(V')$ are defined as in equation(5-3.3)

Integrating the above equations, then:

$$t' \Big|_0^{t'-V'} = \left\{ e^{-\int \kappa_2 dV'} \left[\int e^{\int \kappa_2 dV'} (\kappa_1 V' + \kappa_3 + F(V')) dV' + C \right] \right\} \Big|_0^{V'-V_p}$$

$$= \left\{ \frac{\kappa_2}{\kappa_1} V' + \frac{\kappa_3}{\kappa_2} - \frac{\kappa_1}{\kappa_2^2} + C \cdot e^{-\kappa_2 V'} + e^{-\kappa_2 V'} \int_0^{V'} e^{\kappa_2 V'} \cdot F(V') \cdot dV' \right\} \Big|_0^{V'-V_p}$$

(6-2.2)

Simplifying:

$$t - t_{sp} = \frac{\kappa_1}{\kappa_2} (V - V_{sp}) - \frac{\kappa_1 - \kappa_2 \kappa_3}{\kappa_2^2} (1 - e^{-\kappa_2 (V - V_{sp})}) + e^{-\kappa_2 (V - V_{sp})} \int_0^{V'} e^{\kappa_2 V'} \cdot F(V') \cdot dV' \quad (6-2.3)$$

Designating:

$$t_0 = e^{-\kappa_2 (V - V_{sp})} \int_0^{V'} e^{\kappa_2 V'} \cdot F(V') \cdot dV' \quad (6-2.4)$$

and replacing $\kappa_1, \kappa_2, \kappa_3$, by equations(3-3.13) through (3-3.15) in equation(6-2.3), the dynamic filtration equation for drilling fluids becomes:

$$t - t_{sp} = \frac{\rho_f s}{(1 - ms)B} \frac{V - V_{sp}}{A} - \left(\frac{\Delta P \rho_f s}{(1 - ms) \mu \alpha_{avg} B^2} - \frac{R_m}{\alpha_{avg} B} \right) \cdot \left(1 - e^{-\frac{\mu \alpha_{avg} B V - V_{sp}}{\Delta P A}} \right) + t_0 \quad (6-2.5)$$

This can be simplified to:

$$t' = C_1 V' + C_2 (1 - e^{-C_3 V'}) + t_0 \quad (6-2.6)$$

in which C_1, C_2, C_3 were defined in equations(3-3.21) to (3-3.23).

The equations(6-2.5) and (6-2.6) are the general equations for drilling fluid dynamic filtration as utilized in this study.

6.2.3 Application of Dynamic Filtration Equation

By fitting the dynamic filtration experimental data points V' vs. t' to equation(6-2.6) using the least squares method, then the coefficients C_1, C_2, C_3, t_0 could be determined. Because the equation(6-2.6) is nonlinear for the unknowns t' and V' , it would take a

large amount of time to write a program for calculating the coefficients by fitting experimental data. A short program in FORTRAN 77 utilising a NAG subroutine which solves the nonlinear regression problems was developed in this study.

It would be very important to note that the NAG subroutine (E04HEE) used in this study is a comprehensive modified Gauss-Newtonian Algorithm for finding an unconstrained minimum of a sum of squares of M nonlinear functions in N variables ($M \geq N$), That is:

$$\text{Minimize: } F(\underline{X}) = \sum_{i=1}^M [f_i(\underline{X})]^2 \quad (6-2.7)$$

where

$$\underline{X} = (X_1, X_2, \dots, X_N)^T \text{ and } M \geq N.$$

The function $f_i(\underline{X})$ are often referred to as residuals.

Before it is used, the equation(6-2.6) should be rearranged:

Let:

$$f_i(\underline{C}) = 1 - \frac{C_1 V' - C_2 (1 - e^{-C_3 V'}) + C_4}{t'} \quad (6-2.8)$$

It should be noted that t_0 is replaced by C_4 for convenience.

Input the data points V' , t' , a call to the NAG subroutine may result in the solution point which ensures that the $F(\underline{C})$ is minimum. The subroutine program for this regression is delivered in Appendix I.

Table 6.1, Table 6.2 and Table 6.3 list the regression results—coefficients of dynamic filtration experiments for Seawater/KCL/Polymer mud and Freshwater/Gypsum/Lignosulphonate mud, respectively. It is necessary to note that the spurt loss of each test is determined by taking the value of the filtrate volume at the fourth second of the experimental process. If the value at fourth second inside a data file recorded during

**Table 6.1 Regression Coefficients of Dynamic Filtration Experiments
(Seawater/KCL/Polymer Mud)**

Shear Rate (1/s)	Applied Pressure (psi)	V_{sp} $\times 10^{-2}$ (ml/cm ²)	C_1 (min/ml)	C_2 (min)	C_3 (1/ml)	C_4 (t_0) (min)	Relative Standard Deviation (%)
71	50	2.348	56.126	33.485	1.638	0.004	0.079
	100	4.079	51.132	66.939	0.739	-0.001	0.067
	200	3.415	50.064	75.722	0.605	-0.008	0.115
	300	5.920	40.194	62.059	0.564	0.074	0.040
	400	13.618	39.981	142.298	0.273	0.042	0.061
89	50	10.262	76.364	30.349	1.384	0.367	0.753
	100	2.763	86.747	172.628	0.399	0.047	0.035
	200	4.934	47.383	50.866	0.842	-0.003	0.075
	300	4.424	46.597	71.229	0.594	-0.014	0.059
	400	8.390	45.364	158.435	0.278	-0.005	0.009
107	50	0.955	72.037	32.761	2.161	0.007	0.140
	100	7.105	81.808	145.538	0.500	0.019	0.048
	200	2.368	50.490	60.258	0.798	-0.109	0.049
	300	8.684	47.648	97.157	0.478	0.052	0.110
	400	15.196	40.357	76.124	0.474	0.085	0.273
124	50	2.348	56.126	33.485	1.638	0.004	0.079
	100	1.974	58.394	38.506	1.368	-0.204	0.057
	200	3.158	53.817	41.045	1.113	-0.185	0.061
	300	8.001	47.003	82.191	0.504	0.013	0.404
	400	8.684	47.303	105.924	0.409	0.266	0.039

**Table 6.2 Regression Coefficients of Dynamic Filtration Experiments
(Freshwater/Gypsum/Lignosulphonate Mud)**

Shear Rate (1/s)	Applied Pressure (psi)	V_{sp} $\times 10^{-2}$ (ml/cm ²)	C_1 (min/ml)	C_2 (min)	C_3 (1/ml)	C_4 (t_0) (min)	Relative Standard Deviation (%)
71	100	0.789	114.44	27.11	3.292	-0.173	0.07
	200	1.067	107.37	33.39	3.019	-0.037	0.08
	300	5.329	131.77	42.84	1.800	-0.476	0.23
	400	3.947	162.76	95.18	1.405	-0.767	0.16
89	100	1.579	127.15	65.61	1.889	0.204	0.04
	200	1.579	117.00	62.16	1.712	-0.030	0.24
	300	5.723	146.80	99.13	1.018	-0.327	0.14
	400	5.723	165.33	105.95	1.241	-0.005	0.02
107	100	1.335	101.508	20.054	3.153	-0.084	0.081
	200	0.890	124.92	57.87	2.085	-0.004	0.80
	300	4.539	142.90	102.29	1.096	-0.017	0.12
	400	5.526	146.264	87.069	1.373	0.259	0.071
124	100	3.750	144.25	23.23	4.167	0.356	0.23
	200	7.499	129.48	44.92	2.545	-0.056	0.24
	300	6.118	117.26	33.92	2.530	0.305	0.05
	400	12.240	115.31	38.10	2.276	0.483	0.10

**Table 6.3 Regression Coefficients of Dynamic Filtration Experiments
(Freshwater/Gypsum/Lignosulphonate Mud)**

Shear Rate (1/s)	Barite Concent. (lbs/bbl)	V_{sp} $\times 10^{-2}$ (ml/cm ²)	C_1 (min/ml)	C_2 (min)	C_3 (1/ml)	C_4 (t_0) (min)	Relative Standard Deviation (%)
107	0	4.539	118.11	53.85	2.157	0.058	0.27
	70	0.890	124.92	57.87	2.085	-0.004	0.80
	140	3.750	132.78	71.56	1.588	-0.462	1.07
	210	4.342	118.20	49.30	1.799	-0.139	1.10

experiment is unavailable, V_{sp} is then calculated from the nearest two points around the time of 4 seconds using linear interpolation. The fitting errors are calculated using the general formula of Relative Standard Deviations as follows:

$$\text{Relative Standard Deviation(\%)} = 100 \times \sqrt{\frac{\sum_{i=1}^M \left(\frac{V_{i\text{-theory}} - V_{i\text{-experiment}}}{V_{i\text{-theory}}} \right)^2}{M - 1}} \quad (6-2.9)$$

where

$V_{i\text{-theory}}$ — theoretically calculated from the regressed equation

$V_{i\text{-experiment}}$ — experimental recorded data

M — total data point involved in regression.

So far, we have discussed the method that obtains the dynamic filtration equation's coefficients. It is therefore useful to analyse the filter cake characteristics based on the above results.

From equations(3-3.21) to (3-3.23), we can write:

$$\alpha_{\text{avg}} = \frac{(1 - ms)\Delta PA^2 C_1 C_3}{\mu \rho_f s} \quad (6-2.10)$$

$$R_{\text{meff}} = \frac{\Delta PA}{\mu} (C_1 - C_2 C_3) \quad (6-2.11)$$

$$B = \frac{\rho_f s}{(1 - ms) A C_1} \quad (6-2.12)$$

Inserting equation(3-3.28) into equation(6-2.12), and rearranging:

$$K_{\tau} = \frac{\rho_f \cdot s}{(1 - m_s)\tau AC_1} \quad (6-2.13)$$

Equations(6-2.10), (6-2.11), (6-2.13) are then used to obtain the average specific cake resistance, effective filter medium resistance, and filter cake dynamic erodability.

Before the above equations are used, we have to clarify the rheological properties of the mud and then the shear stress on the filter cake could be determined. Assuming that all muds tested are Bingham plastic and their rheological properties can be modeled by:

$$\tau = \tau_0 + \mu_p \gamma \quad (6-2.14)$$

The constants τ_0 , μ_p in the above equation could be determined from the Fann viscometer readings. The practical units are:

$$\tau_0 \rightarrow \text{lbs}/100\text{ft}^2$$

$$\mu_p \rightarrow \text{cp} \rightarrow 1.0 \times 10^{-3} \text{ N} \cdot \text{s}/\text{m}^2$$

In SI units, equation(6-2.14) should be rewritten:

$$\tau = 0.4788 \times \tau_0 + 1.0 \times 10^{-3} \times \mu_p \times \gamma$$

where

τ — shear stress (N/m^2)

τ_0 — yield point ($\text{lbs}/100 \text{ ft}^2$)

μ_p — plastic viscosity (cp)

γ — shear rate (s^{-1})

Table 6.4 lists the shear stress values acting on the filter cake surface on the assumption that the muds tested can be considered as Bingham Plastic fluids.

Figures(6-2.12) and (6-2.13) show the average specific dynamic cake resistance as a function of pressure and shear rate for Seawater/KCL/Polymer mud and Freshwater

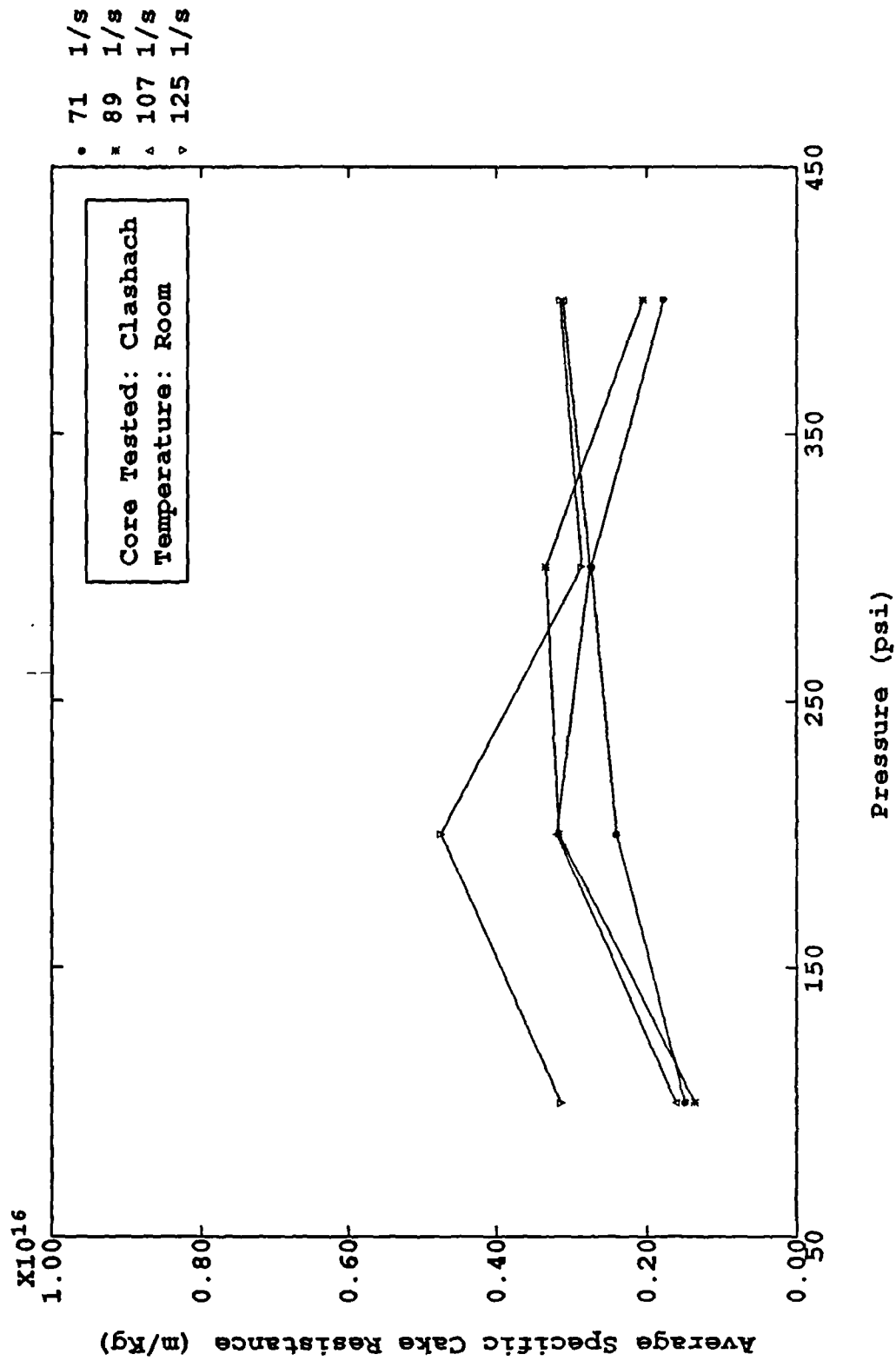


Figure (6 - 2.12) Average Specific Cake Resistance as Function of Pressure and Shear Rate for Seawater/KCl/Polymer Mud in Dynamic Filtration

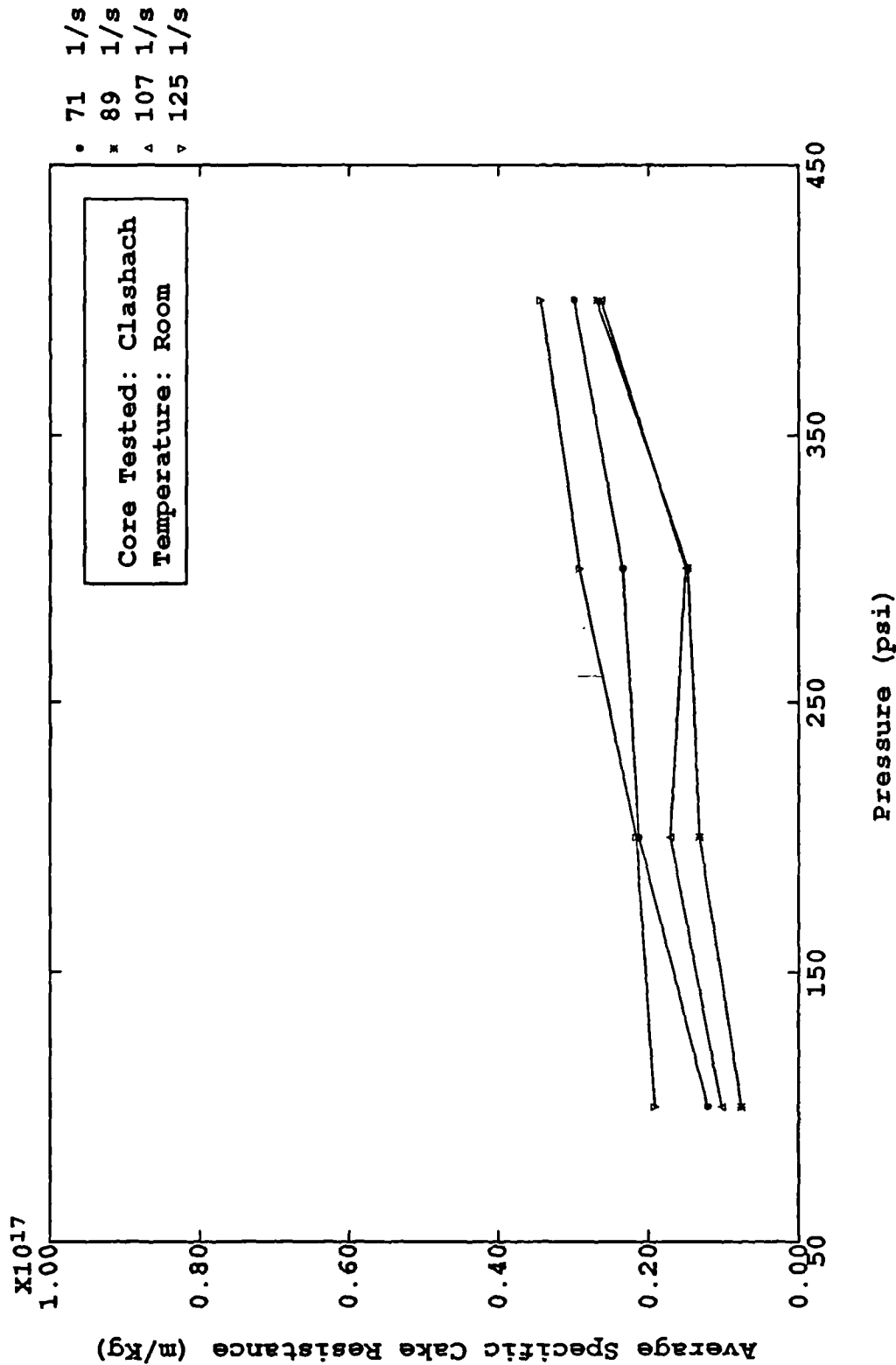


Figure (6 - 2.13) Average Specific Cake Resistance as Function of Pressure and Shear Rate for Freshwater/Gypsum/Lignosulphonate Mud in Dynamic Filtration

Table 6.4 The Shear Stress Acted on Filter Cake Surface for Different Muds (N/m²)

Mud Type	Barites Concentration (lbs/bbl)	Shear Rates (1/s)			
		71	89	107	125
Seawater KCL/Polymer	50	9.985	10.210	10.436	10.647
	70	10.198	10.477	10.756	11.019
	140	9.223	9.619	10.015	10.389
	210	10.943	11.411	11.879	12.321
Gypsum Lignosulphonate	0	12.770	13.337	13.904	14.440
	70	14.500	15.202	15.904	16.567
	140	15.120	15.858	16.596	17.293
	210	19.483	20.356	21.229	22.054

Gypsum/Lignosulphonate mud respectively.

For Seawater/KCL/Polymer mud, the average specific resistance is a complicated function of pressure which is obviously influenced by the shear rate. The average specific cake resistance seems to increase with increasing pressure until a critical pressure is reached, and then decreases.

For Freshwater/Gypsum/Lignosulphonate mud, it is clear that the average specific cake resistance increases with the pressure, however, the effect of the shear rate upon the average specific cake resistance is also very significant but no relationship between them could be obtained. This may be explained if we consider that the range of shear rate values was very narrow.

Figures(6-2.14) and (6-2.15) show the effective filter medium resistance as a function of pressure and shear rate.

For Seawater/KCL/Polymer mud, the effective filter medium resistance seems to increase a little bit with an increase in pressure, but the effect of shear rate is not clear.

For Freshwater/Gypsum/Lignosulphonate mud however, it is apparent that the effective filter medium resistance increases with increasing pressure and the more interesting thing is that the range of pressures can be divided into three zones: In the first and third zone, representing the pressures of 0-200 and 300-400 psi, the effective filter medium resistance seems not change. In the second zone, representing the pressure of 300-400 psi, the effective filter medium resistance increases rapidly. The author considers that the above results may be explained by the following: because the effective filter medium resistance consists of the filter medium resistance, the internal cake(formed inside the pore space of the core surface) resistance, and the resistance of the first layer of the filter cake deposited on the core surface until the spurt time comes to the end. In the above three resistances, the filter medium resistance can be neglected comparing to the other two. The internal filter cake resistance could be very big if the value of pressure, the shear rate and the particle size distribution are suitable. Therefore, it is assumed that the

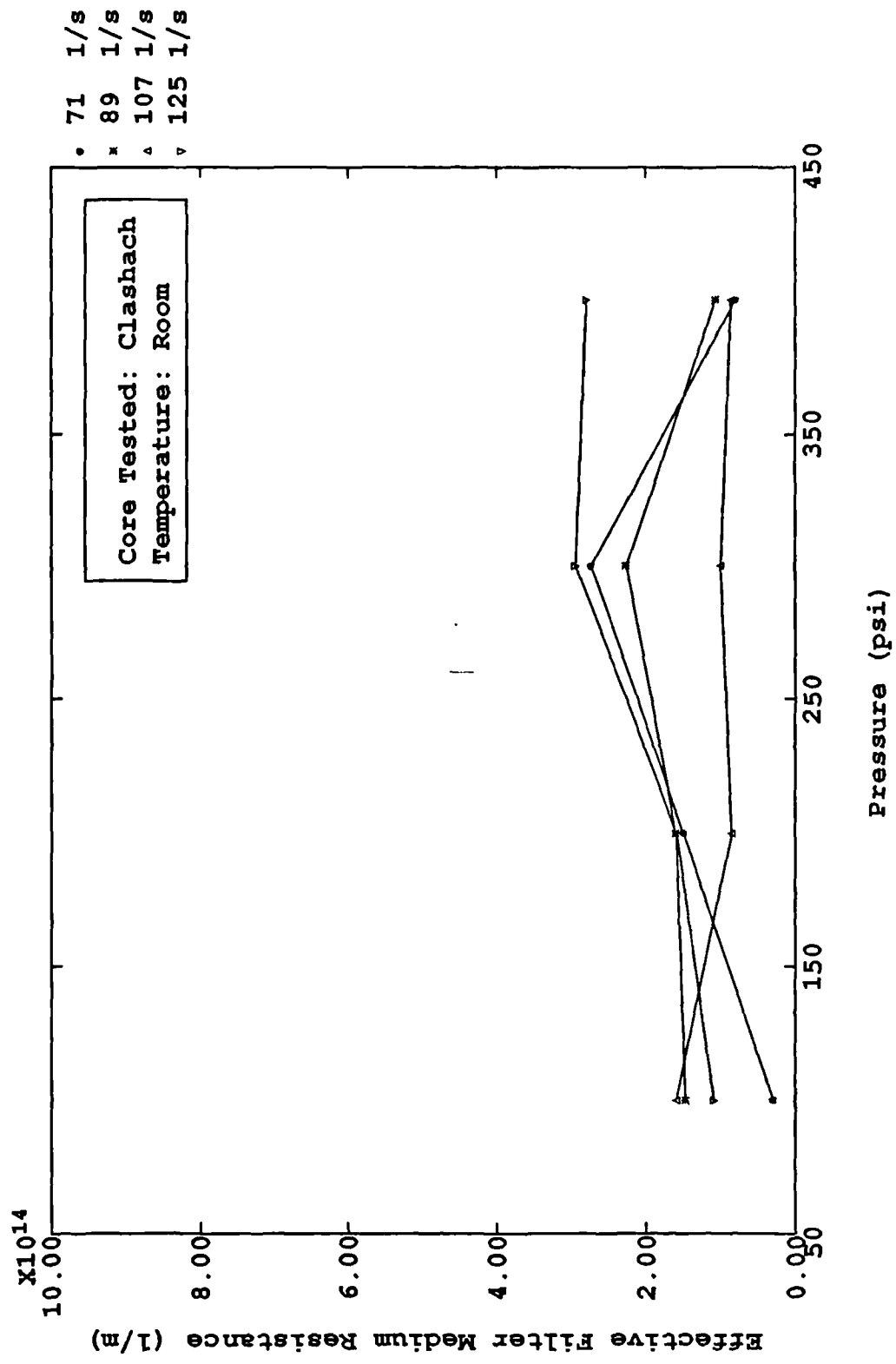


Figure (6 - 2.14) Effective Filter Medium Resistance as Function of Pressure and Shear Rate for Seawater/KCL/Polymer mud in Dynamic Filtration

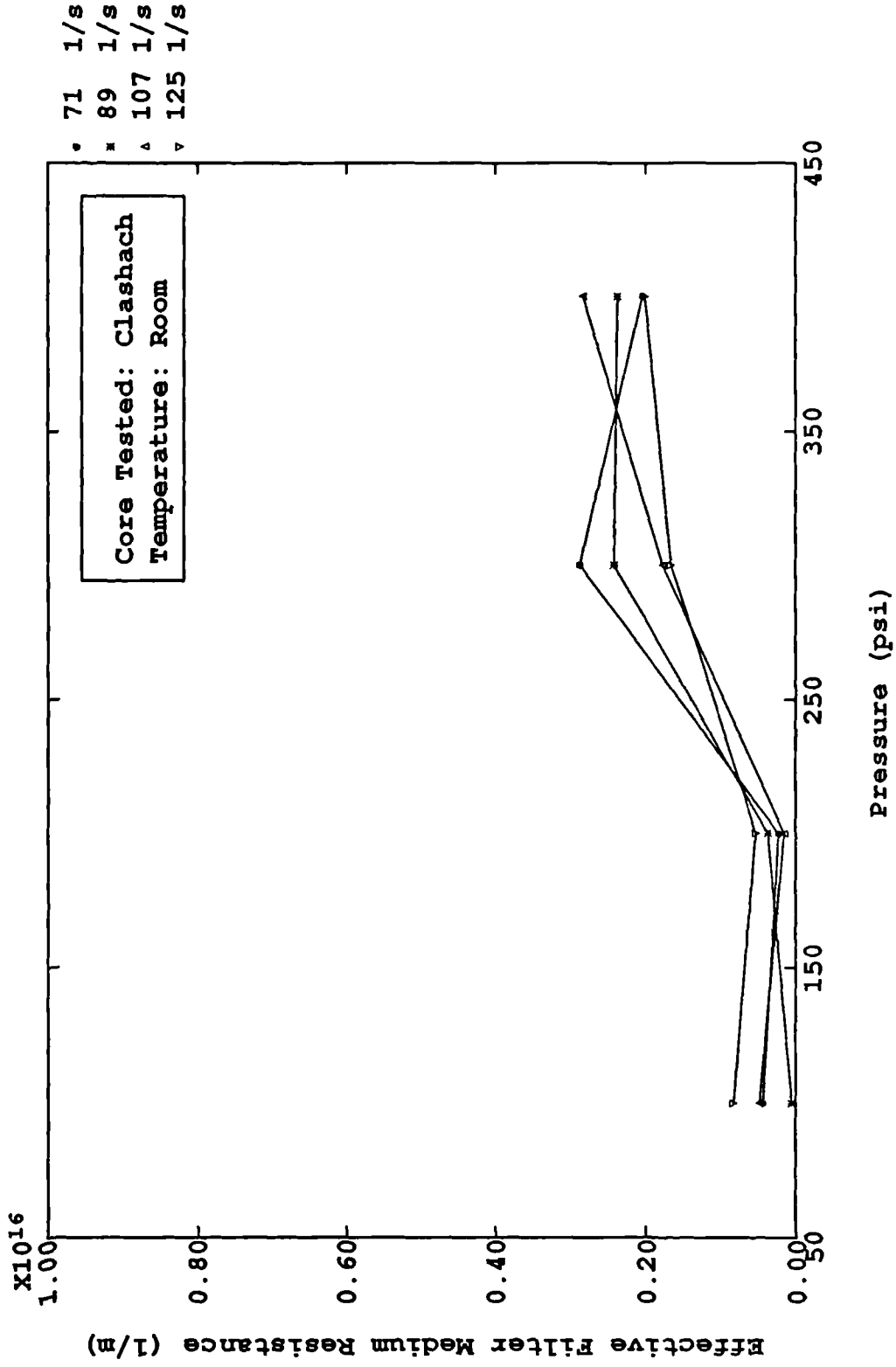


Figure (6 - 2.15) Effective Filter Medium Resistance as Function of Pressure and Shear Rate for Freshwater/Gypsum/Lignosulphonate Mud in Dynamic Filtration

pressure of 300-400 psi should be suitable for the internal filter cake to form for that mud at those shear rate range.

Figures(6-2.16) and (6-2.17) show the erodability of dynamically deposited cakes as a function of pressure and shear rate for Seawater/KCL/Polymer mud and Freshwater /Gypsum/Lignosulphonate mud respectively. Comparing those two figures for two mud types, it is clear that the erodabilities of filter cakes for Freshwater/Gypsum/Ligno-sulphonate mud are about three times smaller than those for Seawater/KCL/Polymer mud. This may be explained by the effect of bentonite on the mud cake structure. The mud with bentonite forms the flat plate cake and this cake is more compressible.

Equation(3-3.27) was utilised to secure the dynamic filtration equilibrium flow rate. Figures(6-2.18) and (6-2.19) show the dynamic equilibrium filtrate flow rate as a function of pressure and shear rate respectively. The erodability of the filter cakes are directly related to the dynamic equilibrium filtrate flow rate, nevertheless, quite similar curves as shown in Figures(6-2.18) and (6-2.19) compared to those in Figures(6-2.16) and (6-2.17) are obtained.

Equation(5-3.13) is used to calculate the average dynamic filter cake permeability. Figures(6-2.20) and (6-2.21) show the average dynamic filter cake permeability as a function of pressure and shear rate for two base muds.

6.3 RESULTS OF SEQUENTIAL FILTRATION EXPERIMENTS

Figure(6-3.1) shows the cumulative filtrate volume as a function of time in sequential filtration for Seawater/KCL/Polymer mud. Figure(6-3.2) shows the corresponding filtrate flow rate as a function of time. The tests conducted consisted of 4 hours of dynamic filtration as a first phase. At the end of the first phase, the dynamic filtration was already reached equilibrium. A static filter cake was then deposited upon the dynamic filter cake

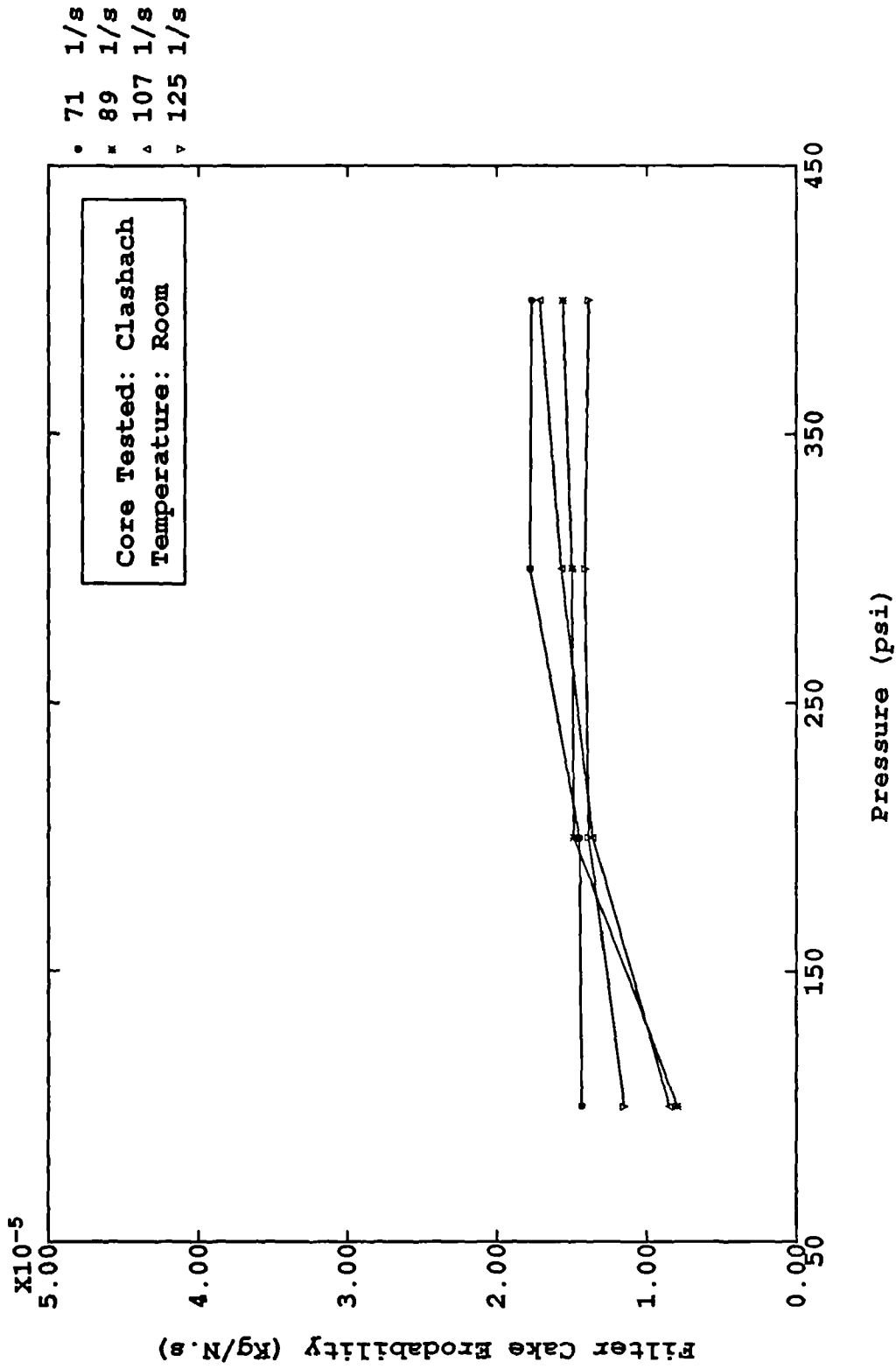


Figure (6 - 2.16) Filter Cake Erodability as Function of Pressure and Shear Rate for Seawater/KCl/Polymer Mud in Dynamic Filtration

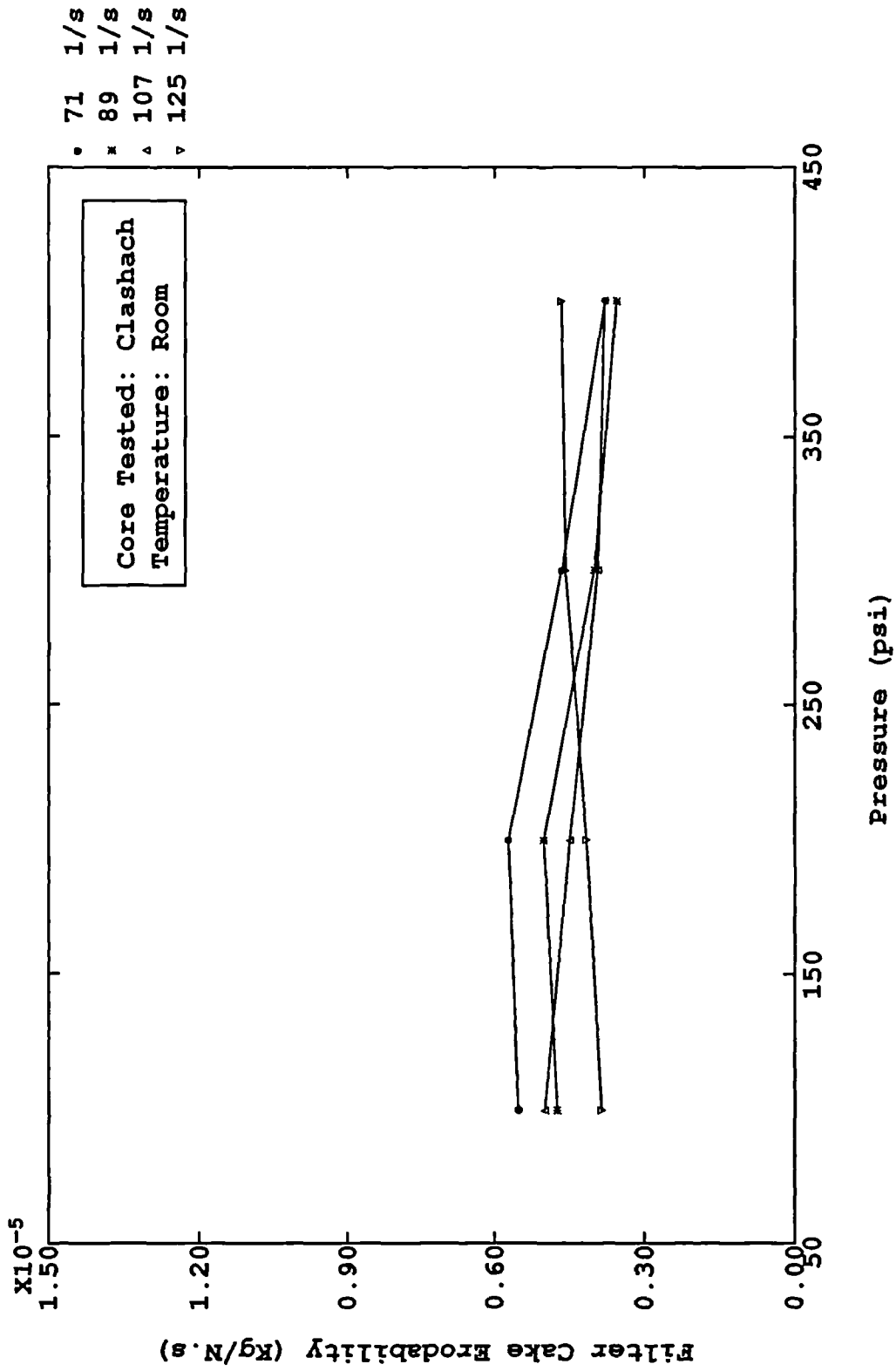


Figure (6 - 2.17) Filter Cake Erodability as Function of Pressure and Shear Rate for Freshwater/Gypsum/Lignosulphonate Mud in Dynamic Filtration

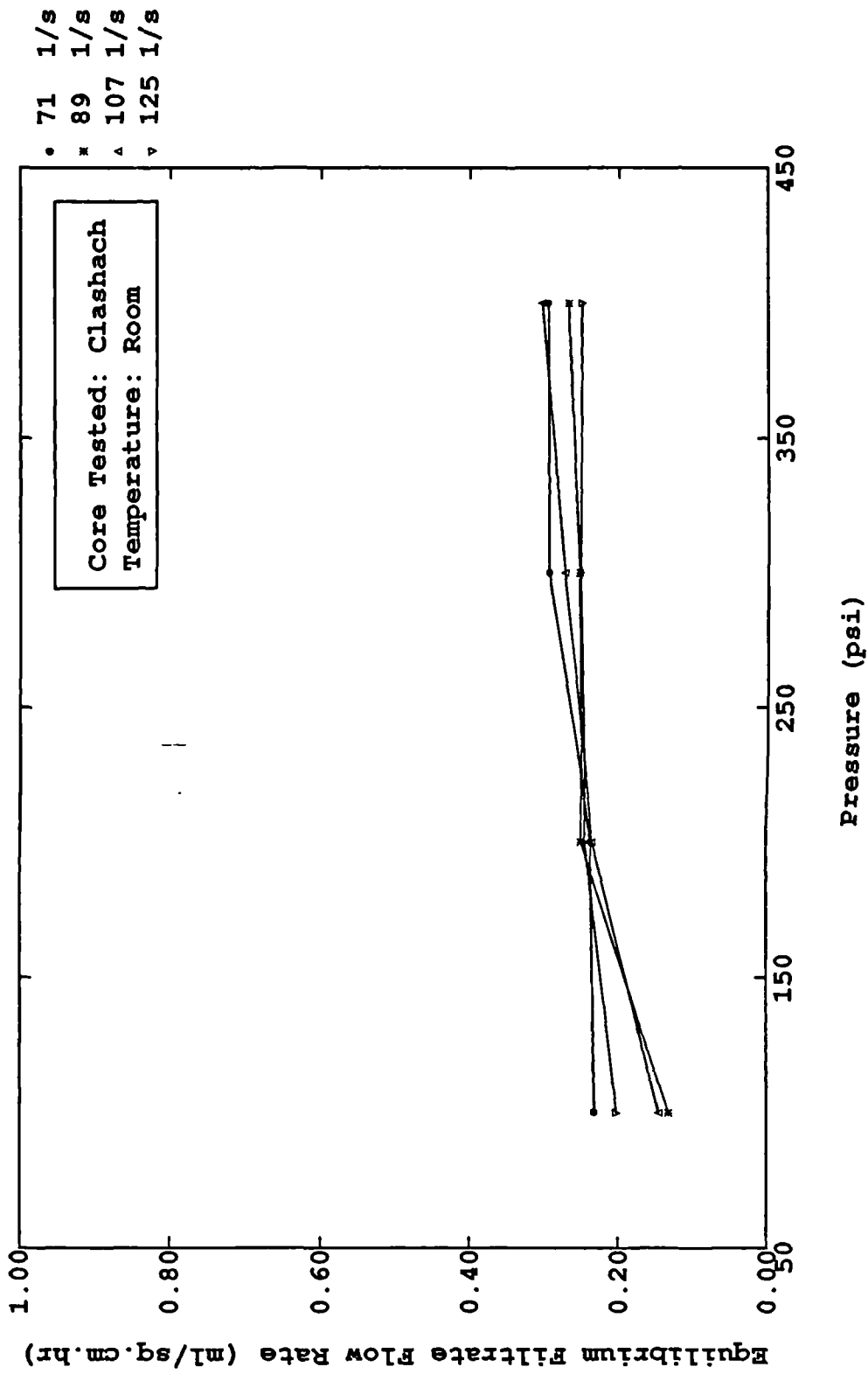


Figure (6 - 2.18) Equilibrium Filtrate Flow Rate as Function of Pressure and Shear Rate for Seawater/KCL/Polymer Mud in Dynamic Filtration

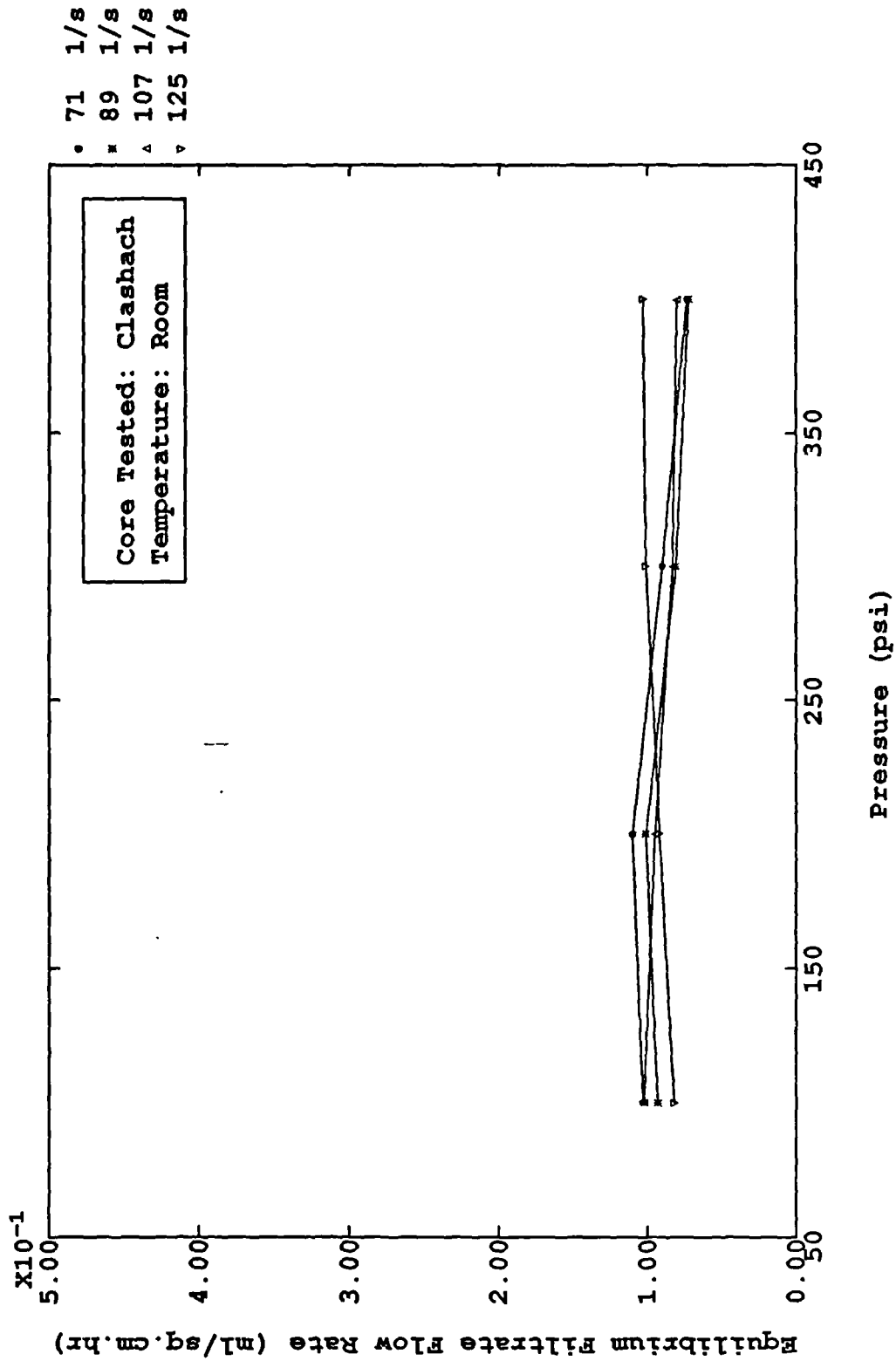


Figure (6 - 2.19) Equilibrium Filtrate Flow Rate as Function of Pressure and Shear Rate for Freshwater/Gypsum/Lignosulphonate Mud in Dynamic Filtration

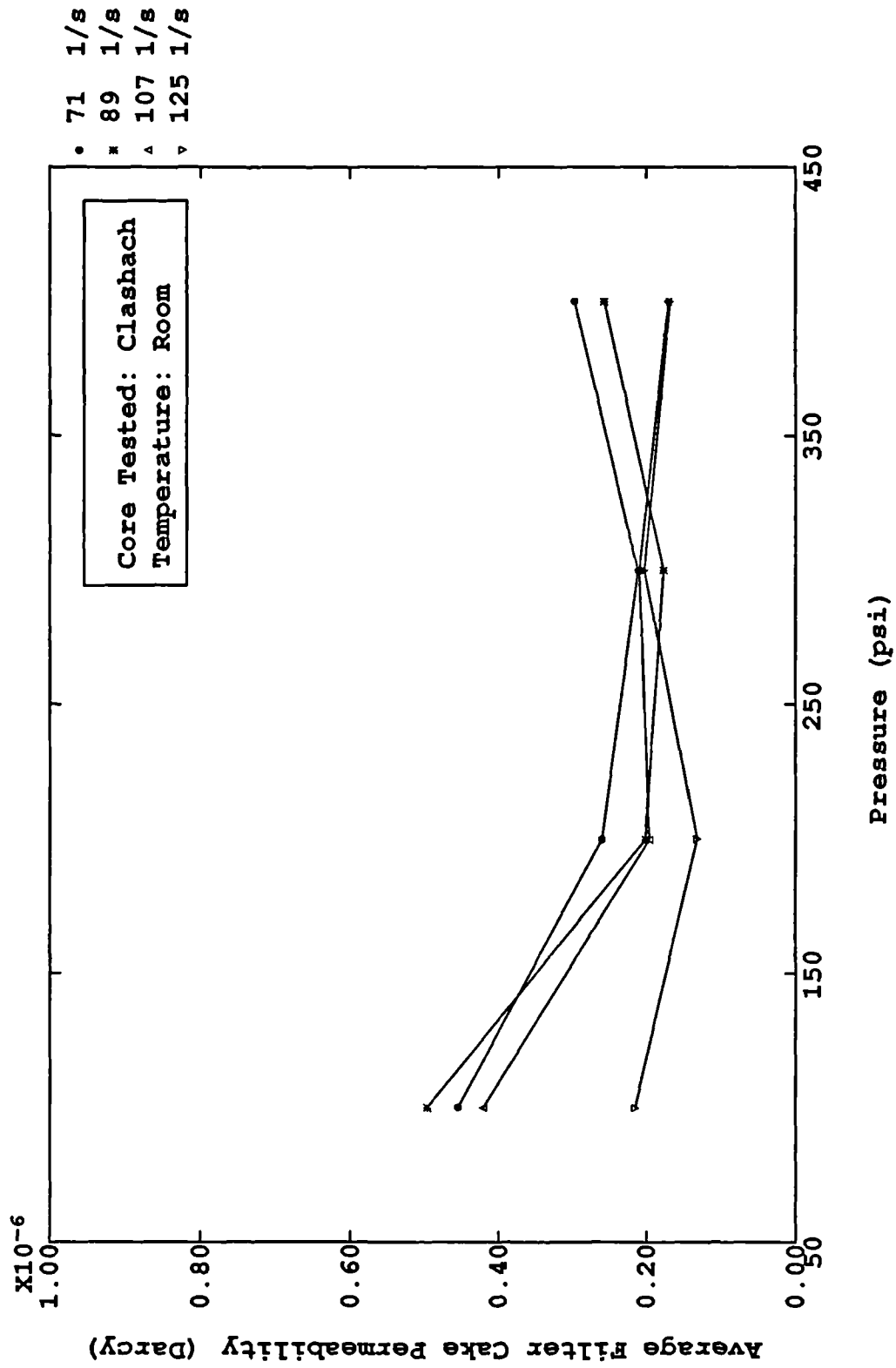


Figure (6 - 2.20) Average Filter Cake Permeability as Function of Pressure and Shear Rate for Seawater/KCl/Polymer Mud in Dynamic Filtration

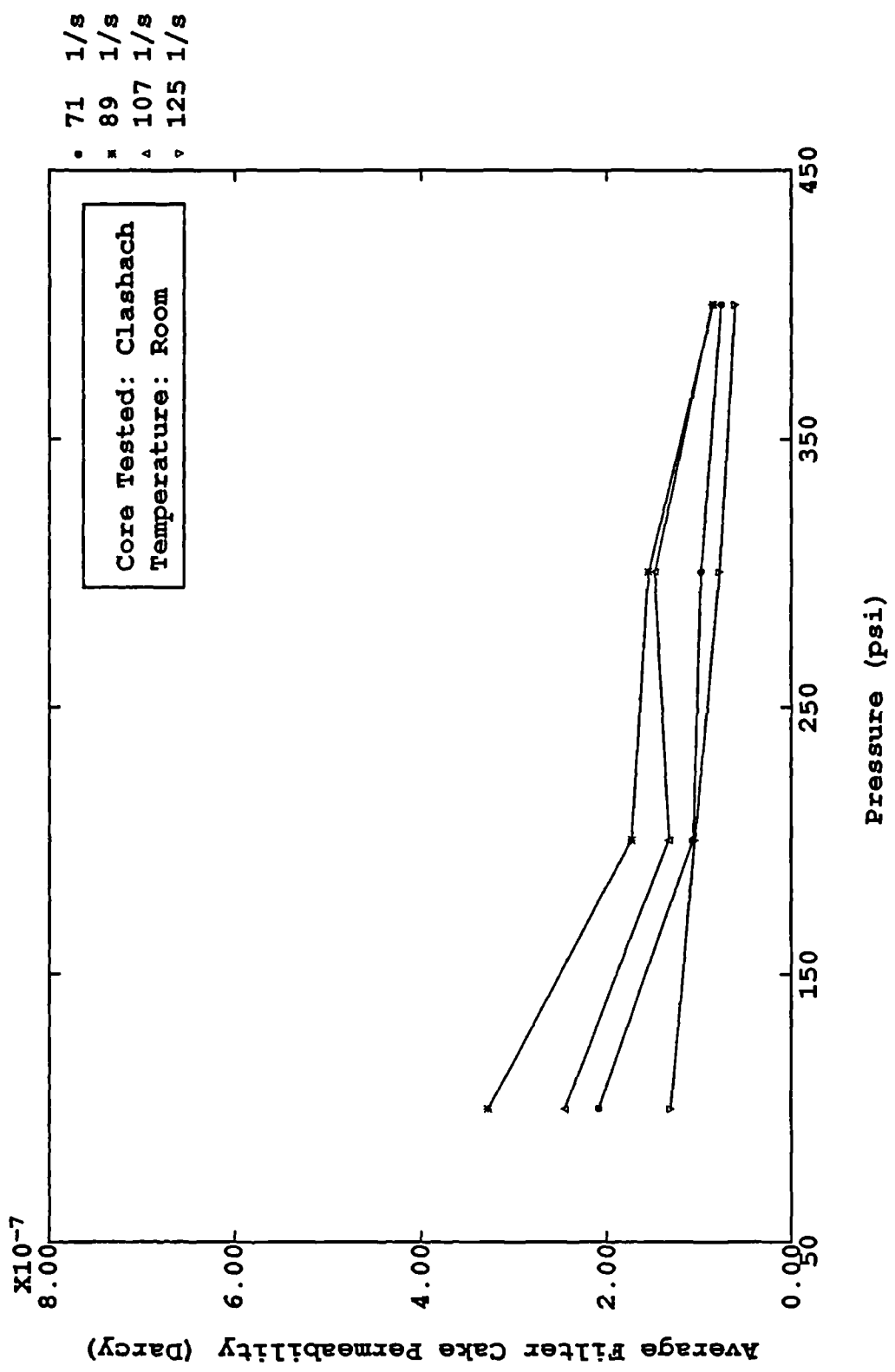


Figure (6 - 2.21) Average Filter Cake Permeability as Function of Pressure and Shear Rate for Freshwater/Gypsum/Lignosulphonate Mud in Dynamic Filtration

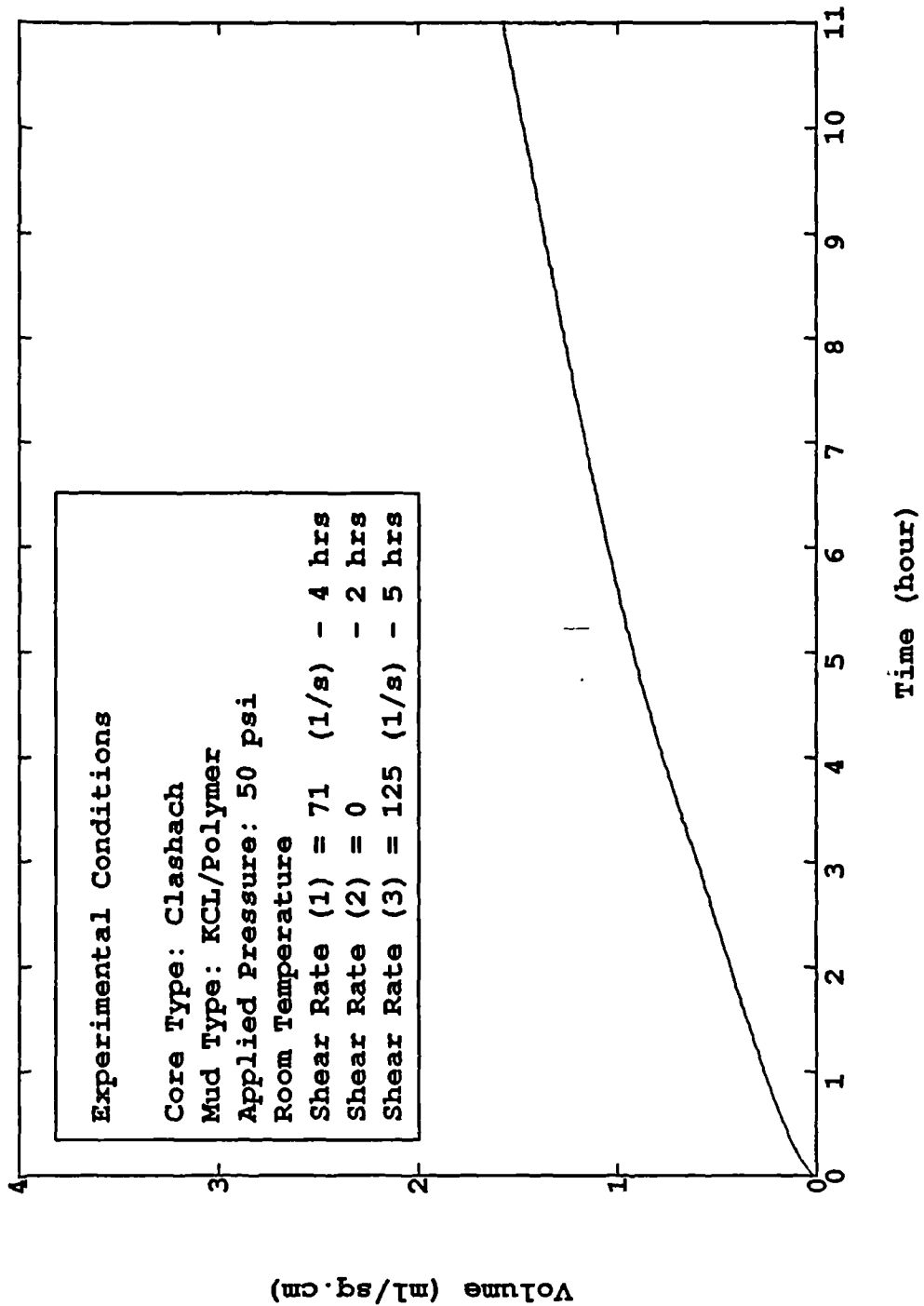


Figure (6-3.1) Cumulative Filtrate Volume Per Unit Area as Function of Time in Sequential Filtration Tests

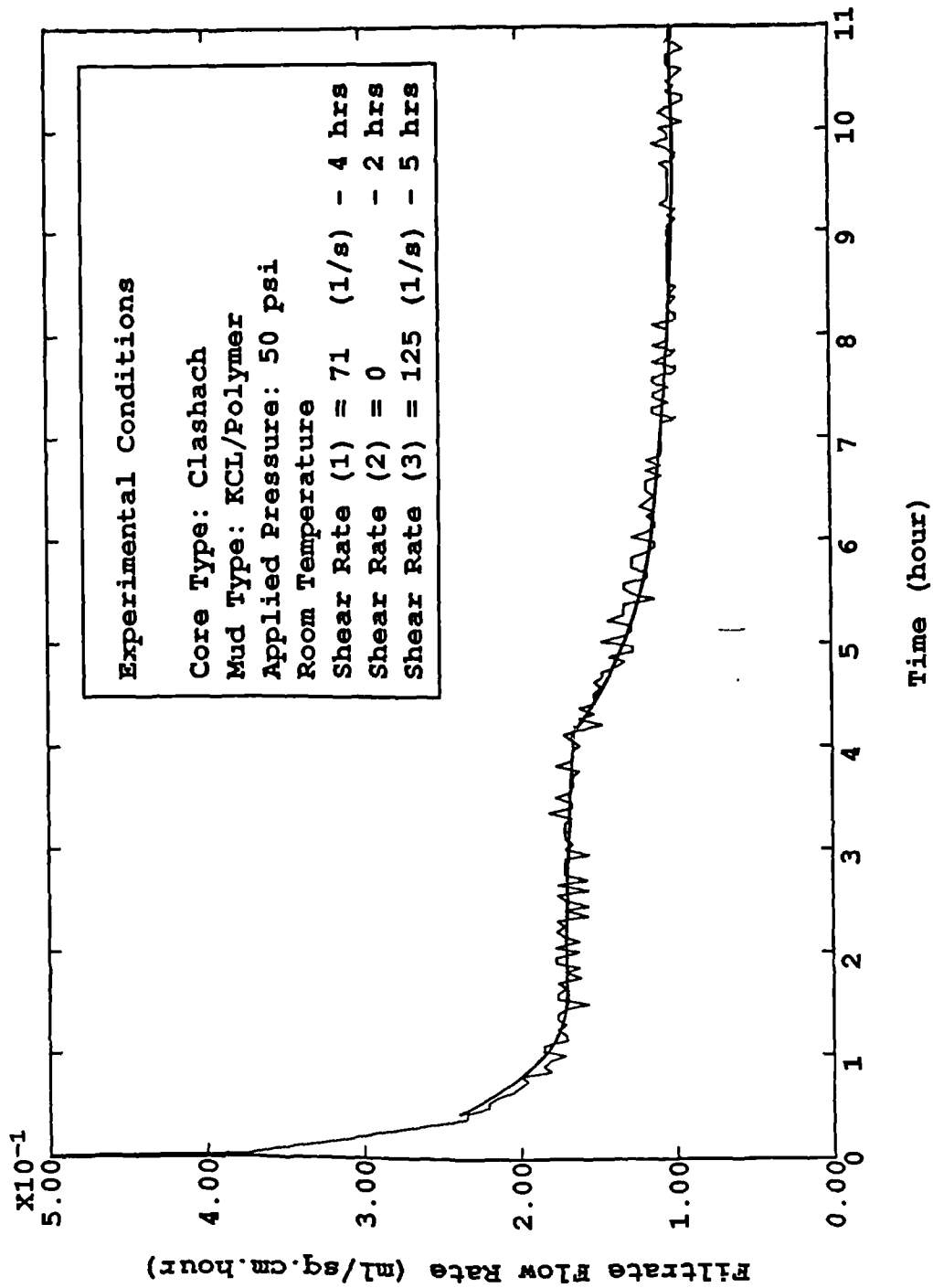


Figure (6-3.2) Filtrate Flow Rate as Function of Time in Sequential Filtration Tests.

for a period of 2 hours. Then the filtration was continued in the third phase by restart dynamic filtration at a shear rate higher than that in the first phase. The third phase lasted 5 hours which was enough to reach equilibrium again.

Figures(6-3.3) and (6-3.4) show the cumulative filtrate volume and filtrate flow rate as a function of time in a sequential filtration for Freshwater/Gypsum/Lignosulphonate mud. A similar filtration process was carried out and a similar filtration curve was obtained.

So far, we can conclude that in a sequential filtration, the static filter cake deposited upon a dynamic filter cake could not be removed by the mud shear even if the shear rate is higher than that in the first phase. It is interesting that the filtration reached equilibrium and filtrate flow rate attained constant values in the first phase, after depositing a static filter cake in the second phase in which the filtrate flow rate declines according to equation(5-3.7). However, the filtration in the third phase still took a short period of time to reach equilibrium even at a relatively higher shear rate than that in the first phase, and it is useful to emphasize that at this stage, the filtrate flow rate does not go up again, but remains constant. This supports the conclusion drawn above that the static filter cake deposited upon dynamic filter cake in sequential filtration would not be removed.

More sequential filtration tests were conducted to verified the above results which are postulated in Figures(6-3.5) to (6-3.8).

Figure(6-3.5) and (6-3.6) are plotted on cumulative filtrate volume and filtrate flow rate as a function of time. The smooth curve in Figures are produced by dynamic filtration equation(6-2.6) which coefficients are obtained by fitting the equation to the first four hour data. It is very clear that both cumulative volume and filtrate rate are in substantial agreement with the experimental data. From the 5th to 6th hour, the filtration process was static and the cumulative volume and filtrate flow rate then drops down because the static filter cake is forming. After 6 hours, the shear stress acts again and at this time, the cumulative volume increases proportional to the time, but the filtrate flow rate keeps constant. Figures(6-3.7) and (6-3.8) are the similar tests which further confirm this

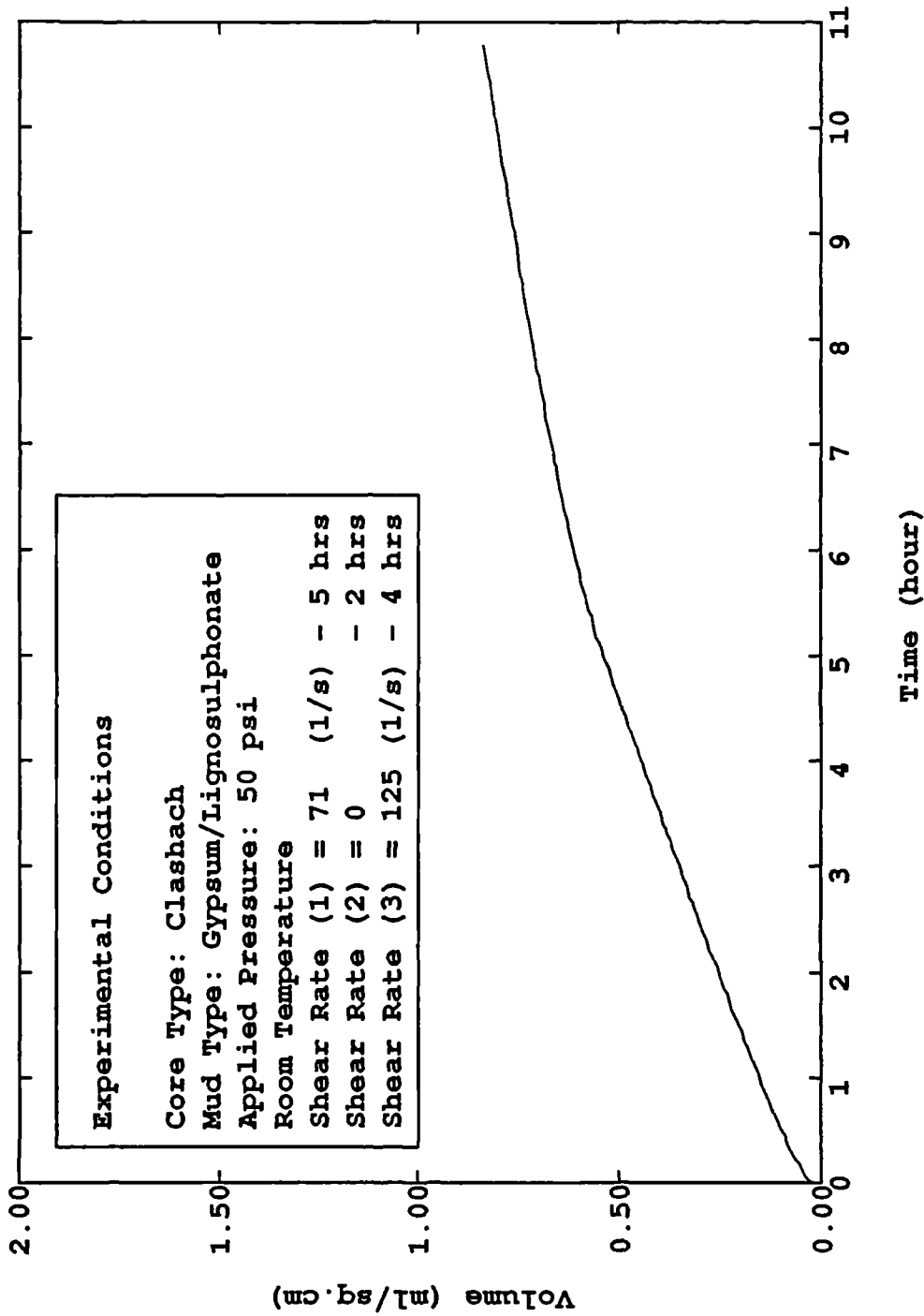


Figure (6-3.3) Cumulative Filtrate Volume Per Unit Area as Function of Time in Sequential Filtration Tests

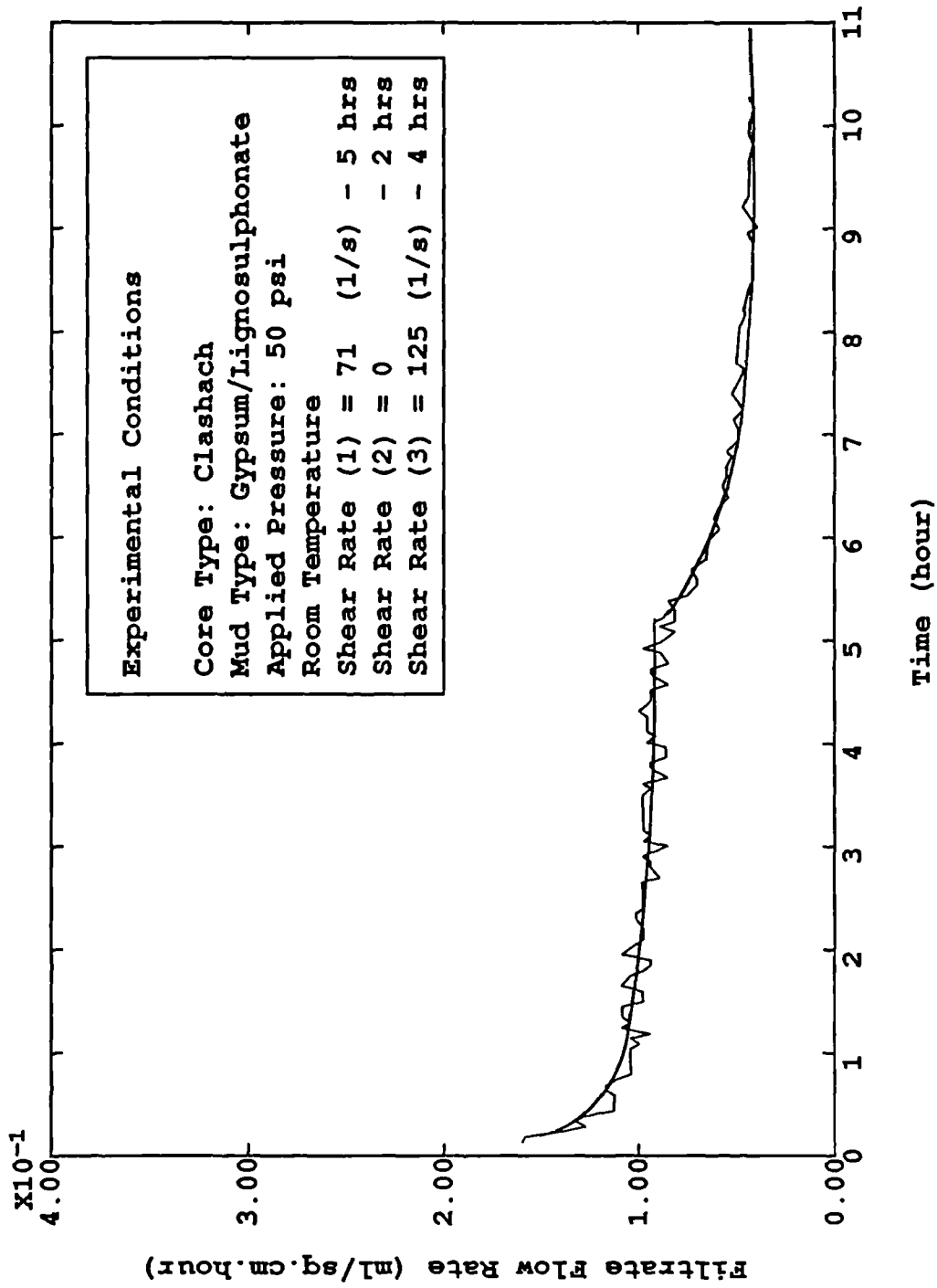


Figure (6-3.4) Filtrate Flow Rate as Function of Time in Sequential Filtration Tests .

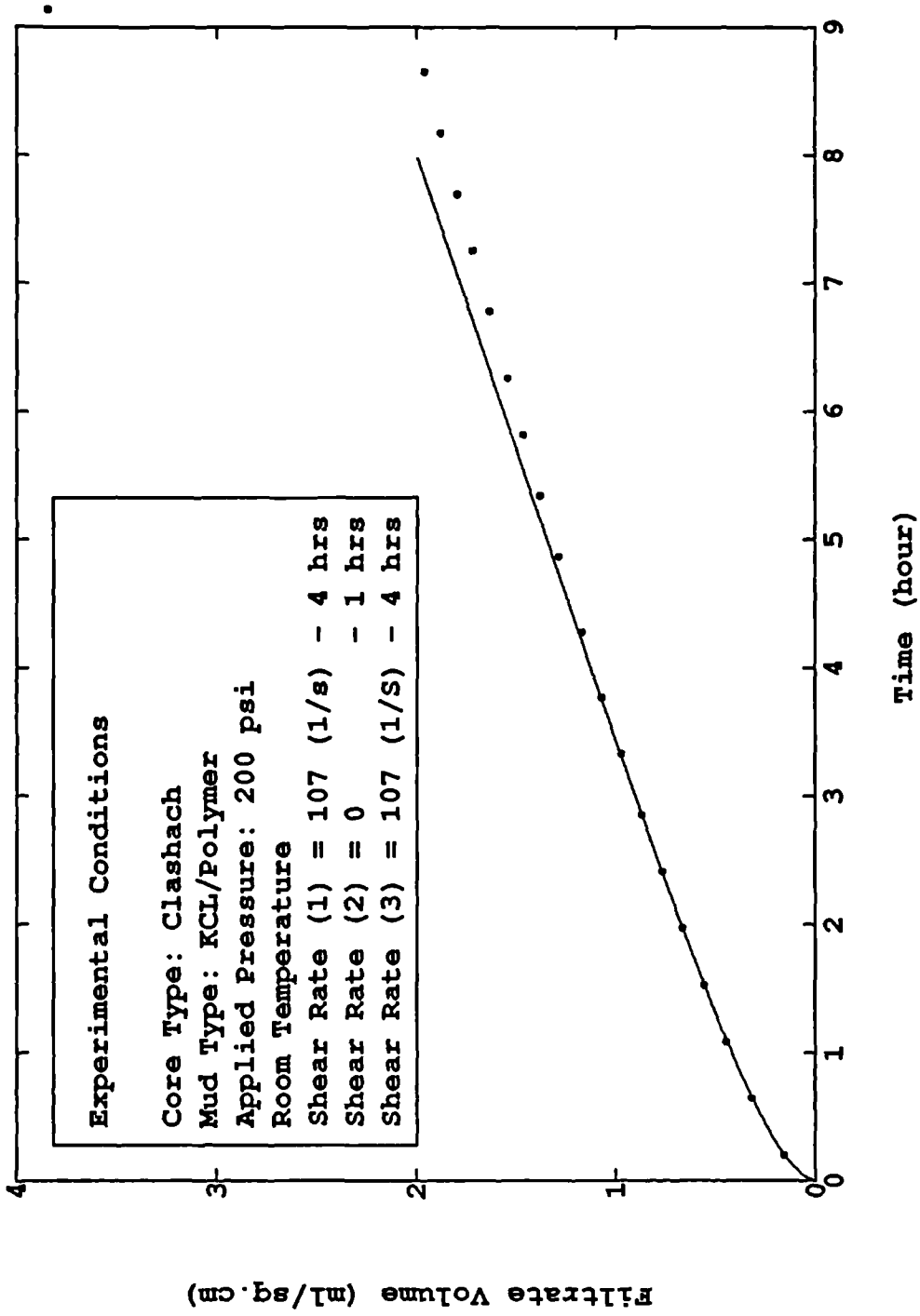


Figure (6-3.5) Cumulative Filtrate Volume per unit area as Function of Time in Sequential Filtration Tests

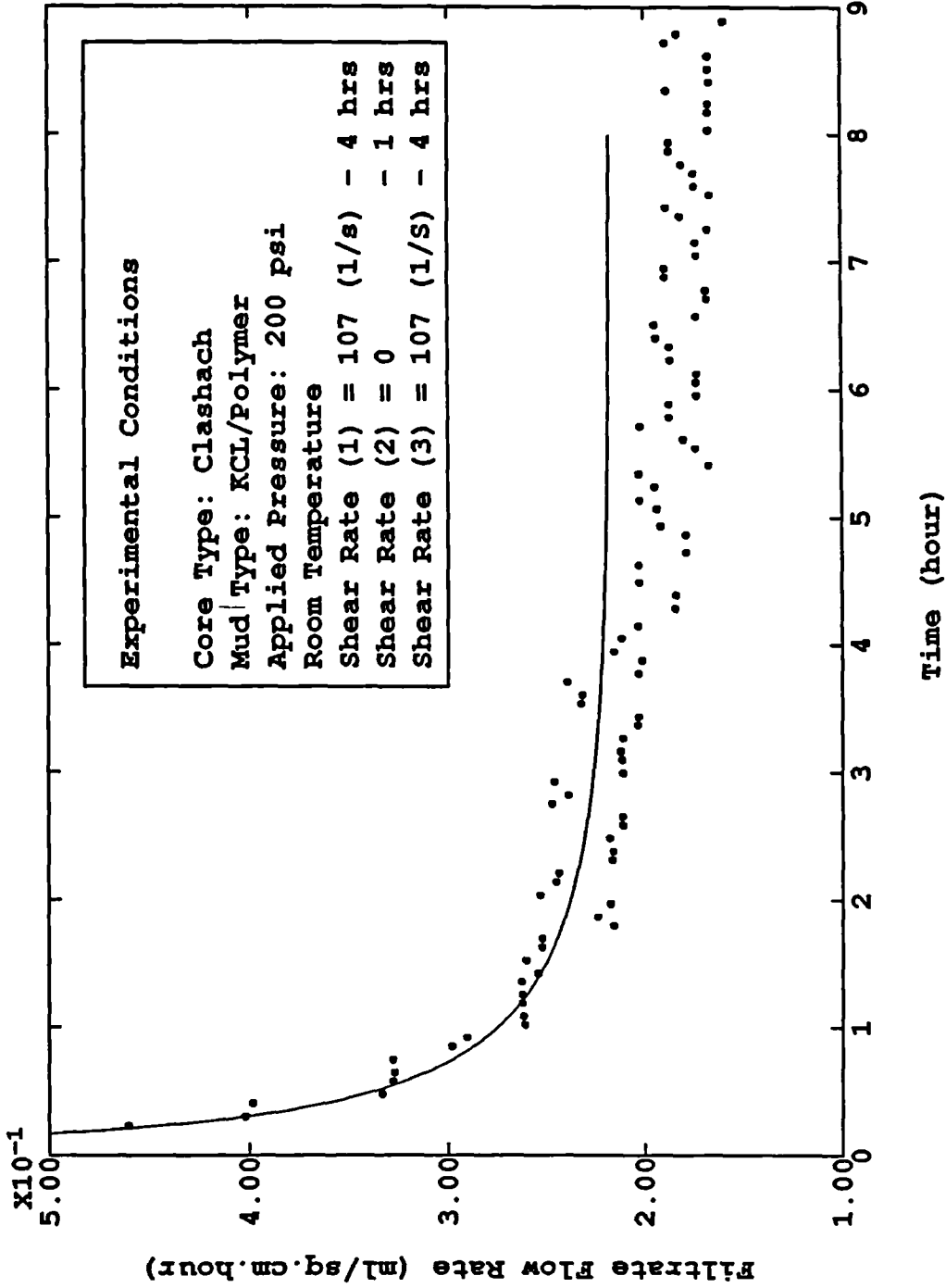


Figure (6-3.6) Filtrate Flow Rate as Function of Time in Sequential Filtration Tests .

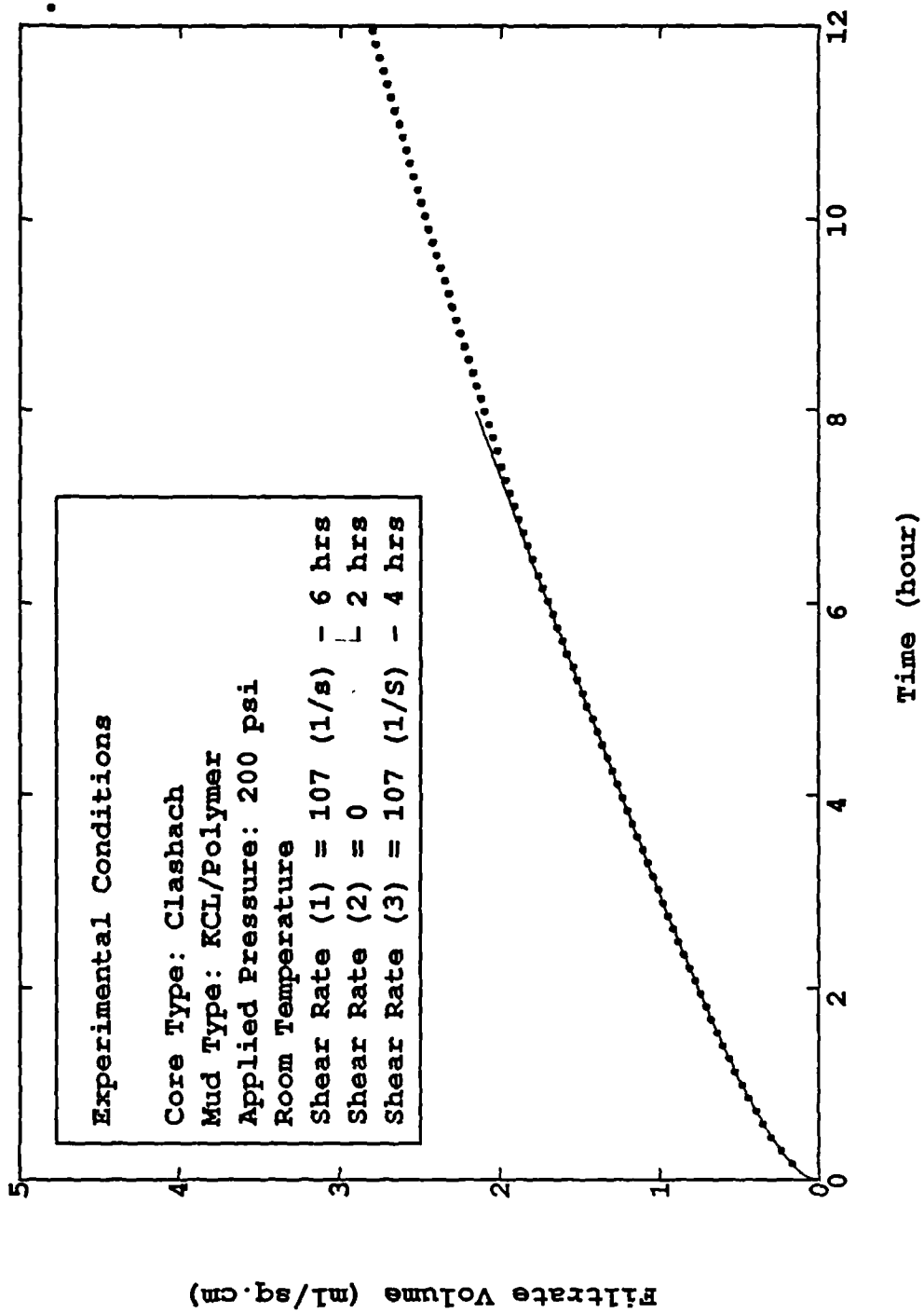


Figure (6-3.7) Cumulative Filtrate Volume per unit area as Function of Time in Sequential Filtration Tests

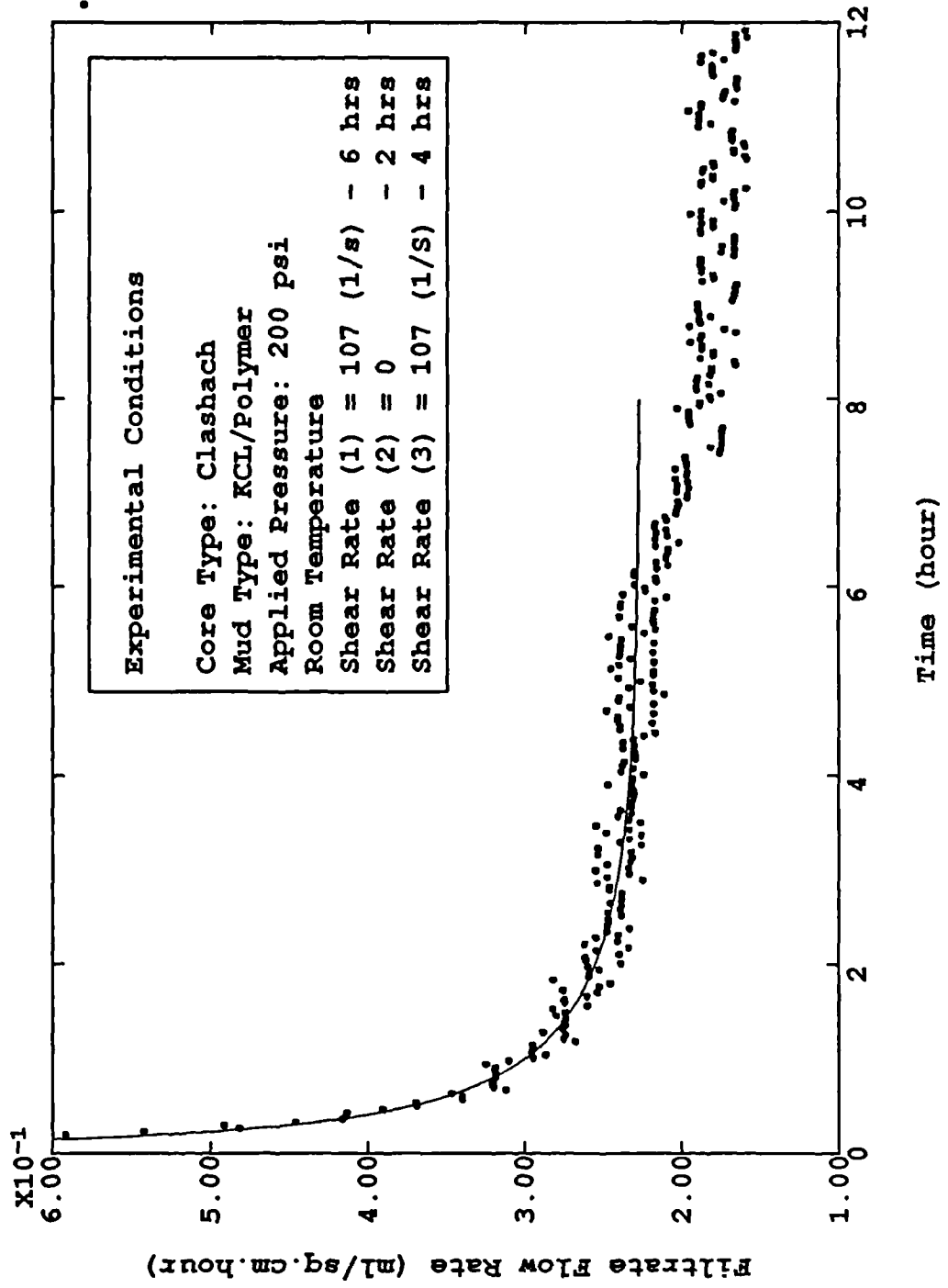


Figure (6-3.8) Filtrate Flow Rate as Function of Time in Sequential Filtration Tests

sequential filtration process.

Those the application of shear stress could not remove static cakes, would increased shear stress erode the dynamically deposited cake? The following experiments could answer this question.

Figures(6-3.9) to (6-3.12) show the cumulative filtrate volume and filtrate flow rate as a function of time in the sequential filtration process for Seawater/KCL/Polymer mud and Freshwater/ Gypsum/Lignosulphonate mud respectively. The tests were performed at a low shear rate of 71 1/s for first 4 hours and then at a higher shear rate of 125 1/s for another 4 hours. Very little difference was found between the equilibrium filtrate flow rates in the first 4 hours and in the second one.

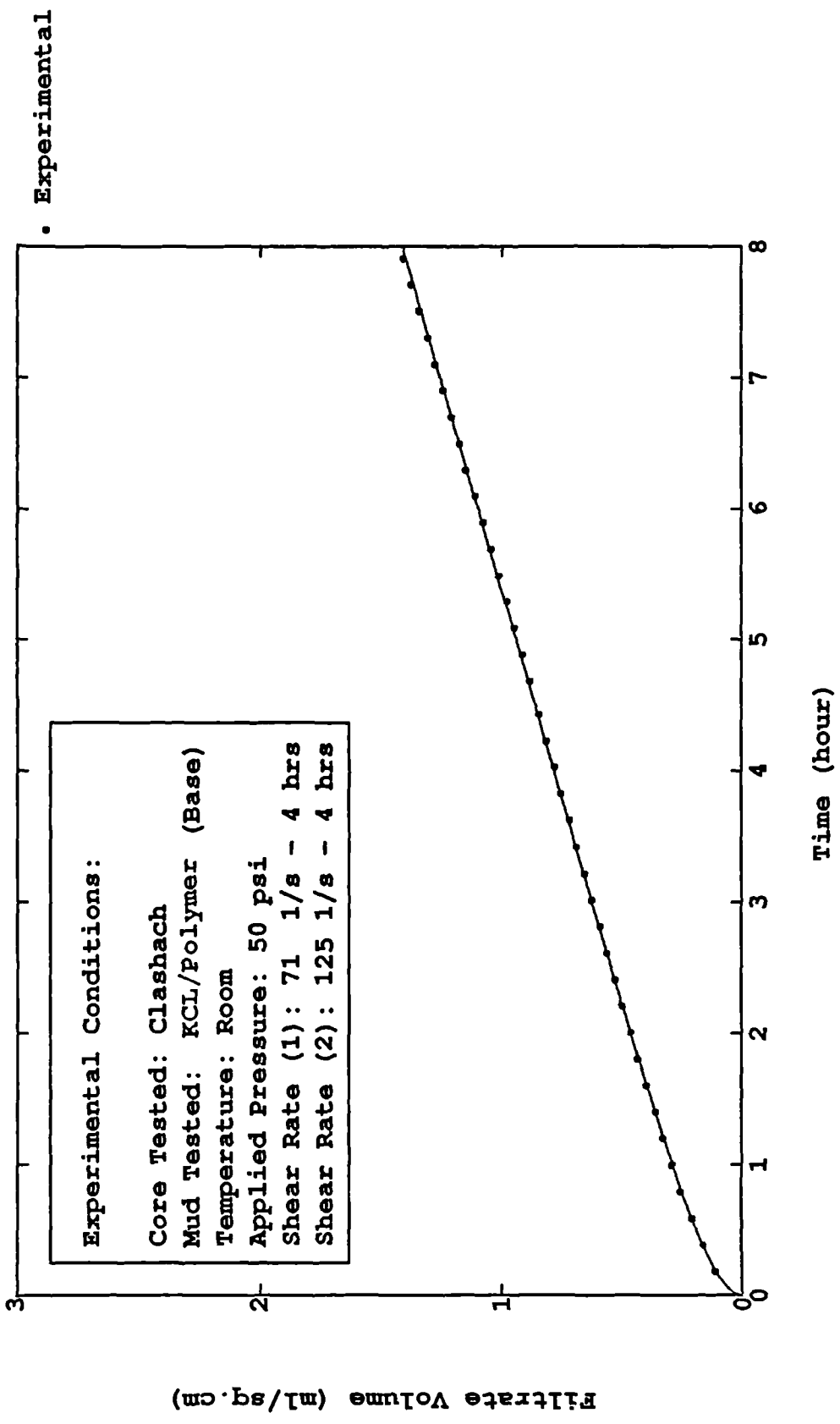


Figure (6-3.9) Cumulative Filtrate Volume per unit area as Function of Time in a Sequence of Dynamic-Dynamic Process

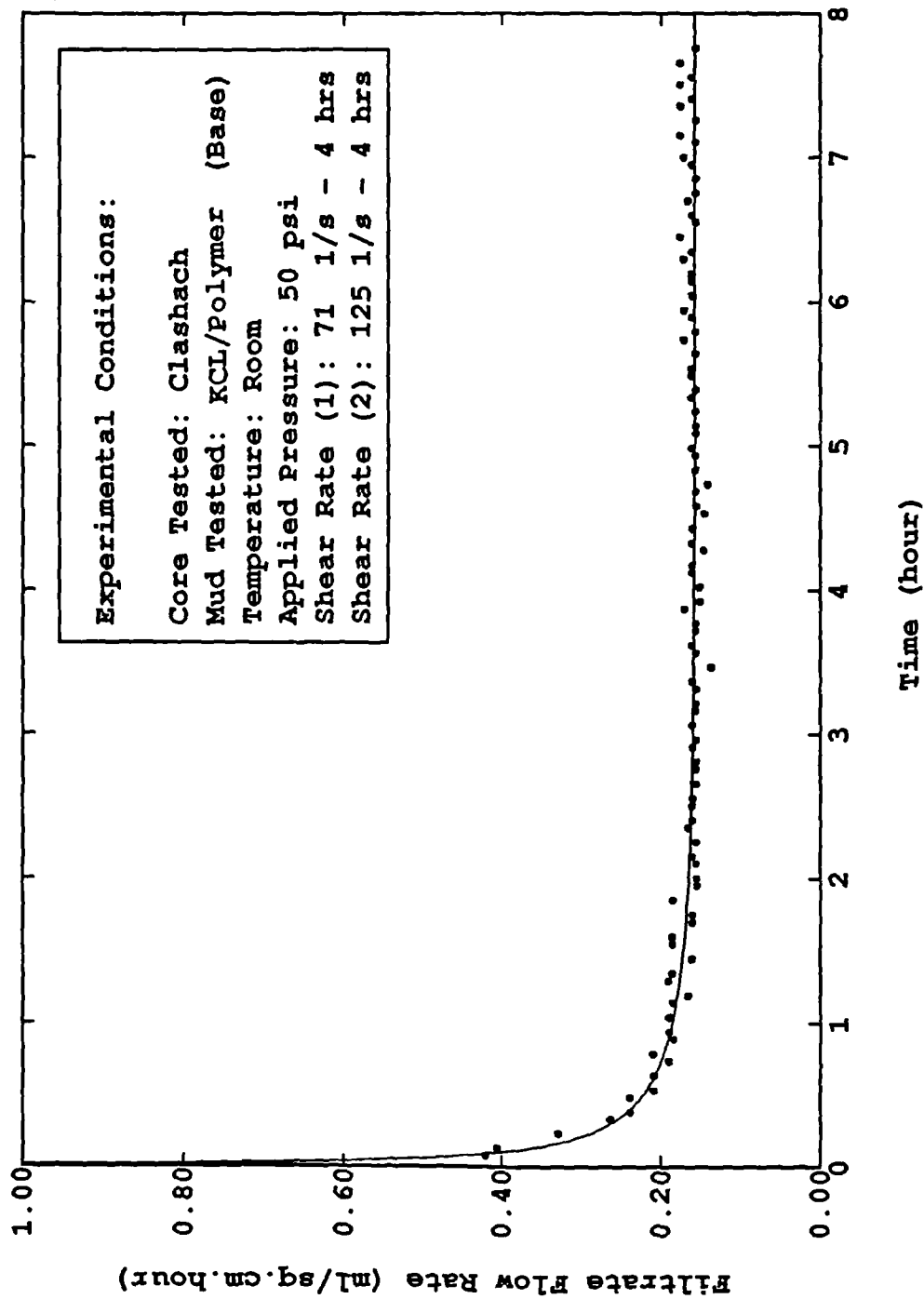


Figure (6-3.10) Filtrate Flow Rate as Function of Time in a Sequence of Dynamic-Dynamic Process

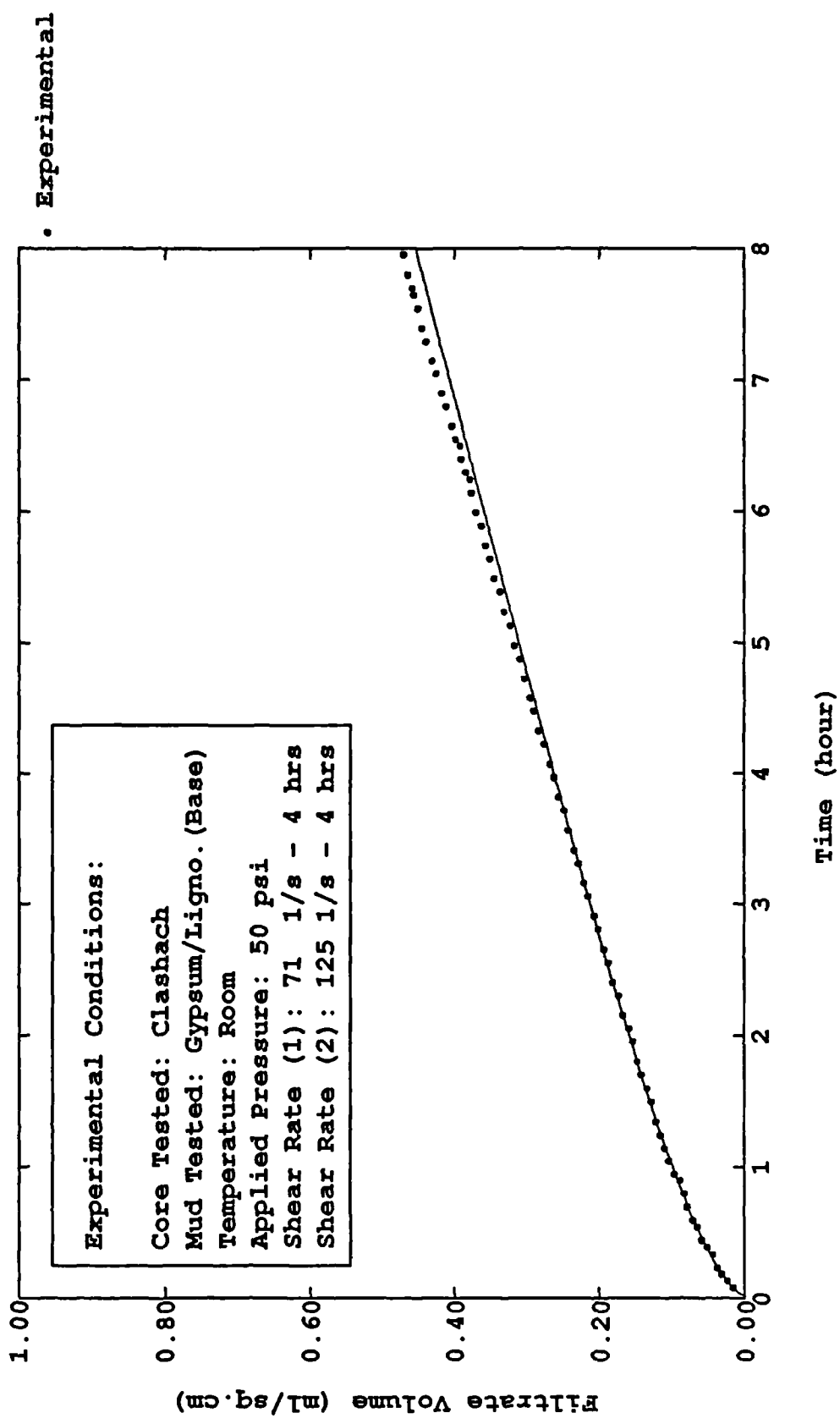
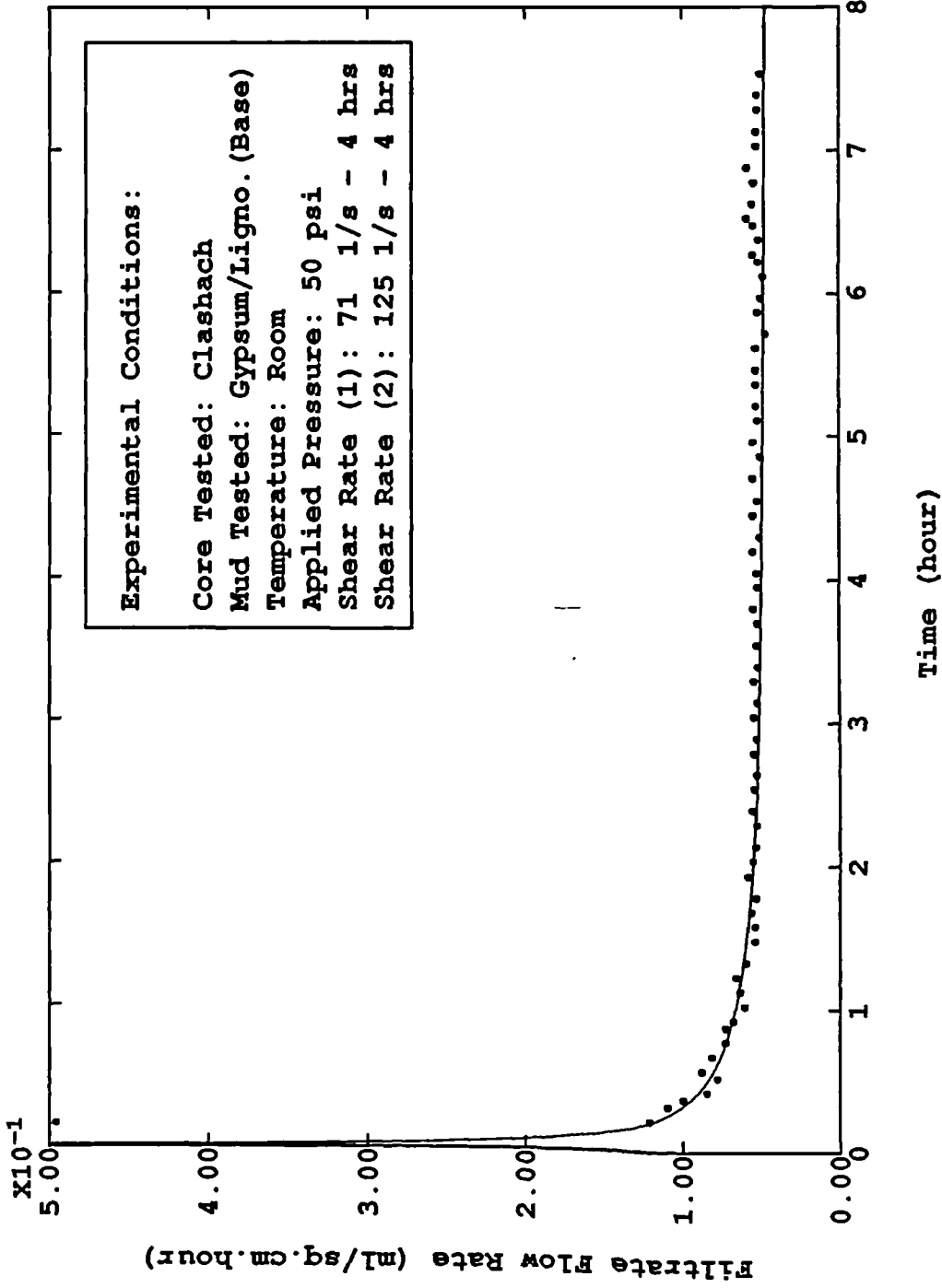


Figure (6-3.11) Cumulative Filtrate Volume per unit area as Function of Time in a Sequence of Dynamic-Dynamic Process



• Experimental

Figure (6-3.12) Filtrate Flow Rate as Function of Time in a Sequence of Dynamic-Dynamic Process

Chapter Seven

DISCUSSION OF EXPERIMENTAL RESULTS

In chapters five and six, the results of the experimental investigation of static and dynamic filtration were presented. In this chapter, an extensive discussion (analysis) on these results are presented.

7.1 DEVIATIONS FROM THE MODIFIED EQUATION

7.1.1 Static Filtration Modelling

There are many methods proposed to plot filtration experimental data V vs. t . However, which of these is the best has been addressed by a number of investigators. Through the history of drilling fluid filtration, to date, Ruth's equation is still the basic law even though a lot of research has been conducted to modify it.

There are several ways to express the filtration data:

$$\frac{t}{V} = a_2 V + a_1 \quad (7-1.1)$$

$$\frac{t - t_{sp}}{V - V_{sp}} = a_2 (V - V_{sp}) + a_1 \quad (7-1.2)$$

$$\frac{t - t_{sp} - t_0}{V - V_{sp}} = a_2(V - V_{sp}) + a_1 \quad (7-1.3)$$

$$\frac{dt}{dV} = a_2V + a_1 \quad (7-1.4)$$

An extensive literature review in chapter three revealed that deviation from classical filtration theory is inevitable. The generally accept explanations are as follows:

- (i) The assumption of constant pressure filtration is not satisfied;
- (ii) The filter medium resistance is not negligible or the filter medium is more or less capable of bridging on surface, plugging in the pores and thus inevitably leads to an increase in filter medium resistance.
- (iii) Filter cakes are to a greater or lesser extent compressible, so that the permeability of cakes is not constant, replacing the local specific cake resistance by the average specific cake resistance is by itself questionable. Further more, assuming the average specific cake resistance to be constant through out the whole filtration process in spite of the degree of compressibility of the filter cake which was initially observed and accepted by Ruth⁵⁹, has not been verified to date. The failure of CPC simulation which would had proved that the average specific cake resistance was variable, could no longer be used.

The general equation developed in this study is still not perfect but it is only considered to be better than other published so far. Three different types of filtration curves will be discussed below.

Figures(7-1.1) to (7-1.5) show an example in which filtration conducted was at a pressure of 500 psi for KCL/Polymer mud with the solids concentration of 140 lbs/bbl under static conditions. It is clearly demonstrated that the modified equation utilised in the study best fits the experimental data.

Figures(7-1.1) and (7-1.2) show the cumulative filtrate volume and filtrate flow rate as a function of time respectively. Unlike dynamic filtration, the filtrate flow rate under

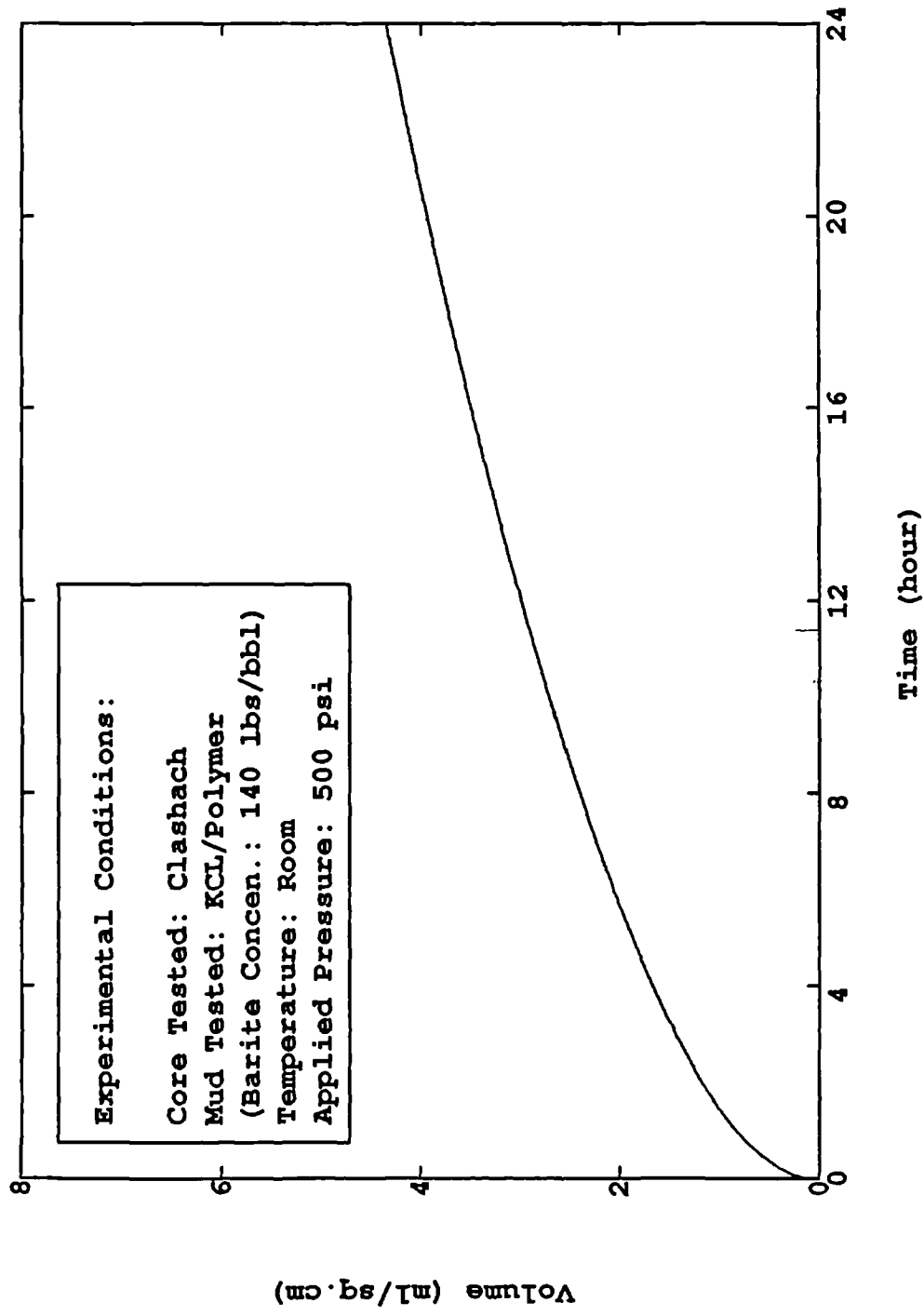


Figure (7-1.1) Cumulative Filtrate Volume per unit area as a Function of Time in Static Filtration.

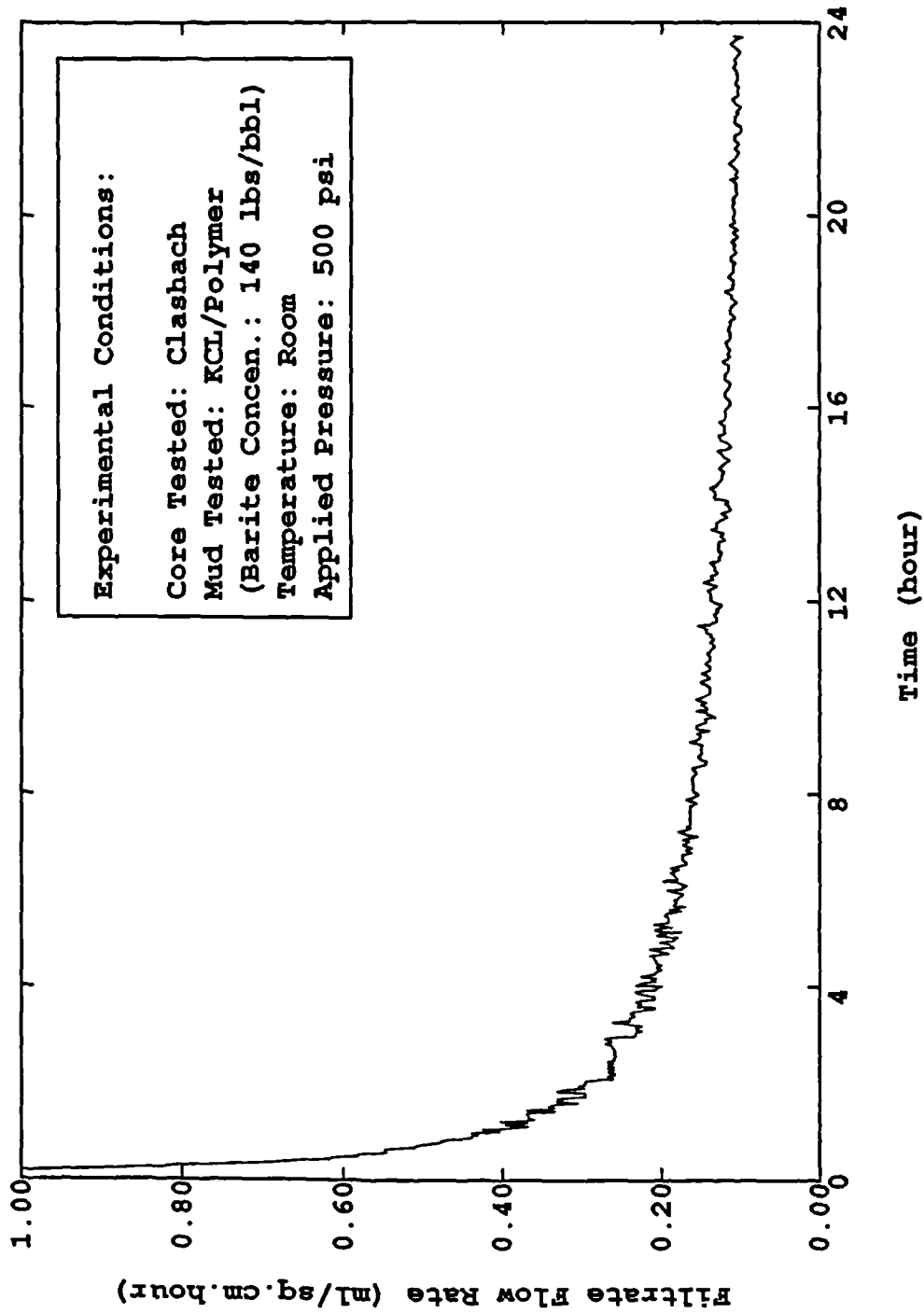


Figure (7-1.2) Filtrate Flow Rate as a Function of Time
 in Static Filtration Tests

static conditions still continues to decline after the filtration process has lasted for 23 hours.

For first type of filtration equation, Figure(7-1.3) shows the plot of time/volume versus volume. Unfortunately the negative filter medium resistance determined by interpolation of curve could not explained. Further, the resultant curve could not be expressed by a straight line as well.

For the second type of filtration equation, Figure(7-1.4) shows the plot of $(t - t_{sp}) / (V - V_{sp})$ versus $(V - V_{sp})$ in which the spurt loss and spurt time was subtracted from the cumulative volume and time respectively. This modification was first made by Bezemer and Havanaar²⁴ who considered that the spurt loss could be expressed as a part of filter medium resistance and it was verified that the filter medium resistance determined by interpolation of the above filtration curve is positive which avoided suggestion of the negative filter medium resistance as occurs in the first filtration model.

For third type of filtration equation, Figure(7-1.5) show the plot of $(t - t_{sp} - t_0) / (V - V_{sp})$ versus $(V - V_{sp})$ in which not only spurt loss and spurt time were subtracted from the cumulative volume and time respectively, but also a correction term was employed to represent the error caused by the variable pressure differential across the cake at the first stage of filtration process. This improvement was first used by Arthur⁹⁴. who combined the modifications produced by two former investigators.

Comparisons of the above three types of equations should verify that the third one provided the best fit for the experimental data.

It is therefore not necessary to show all the plots of experimental data to further confirm the conclusion postulated above.

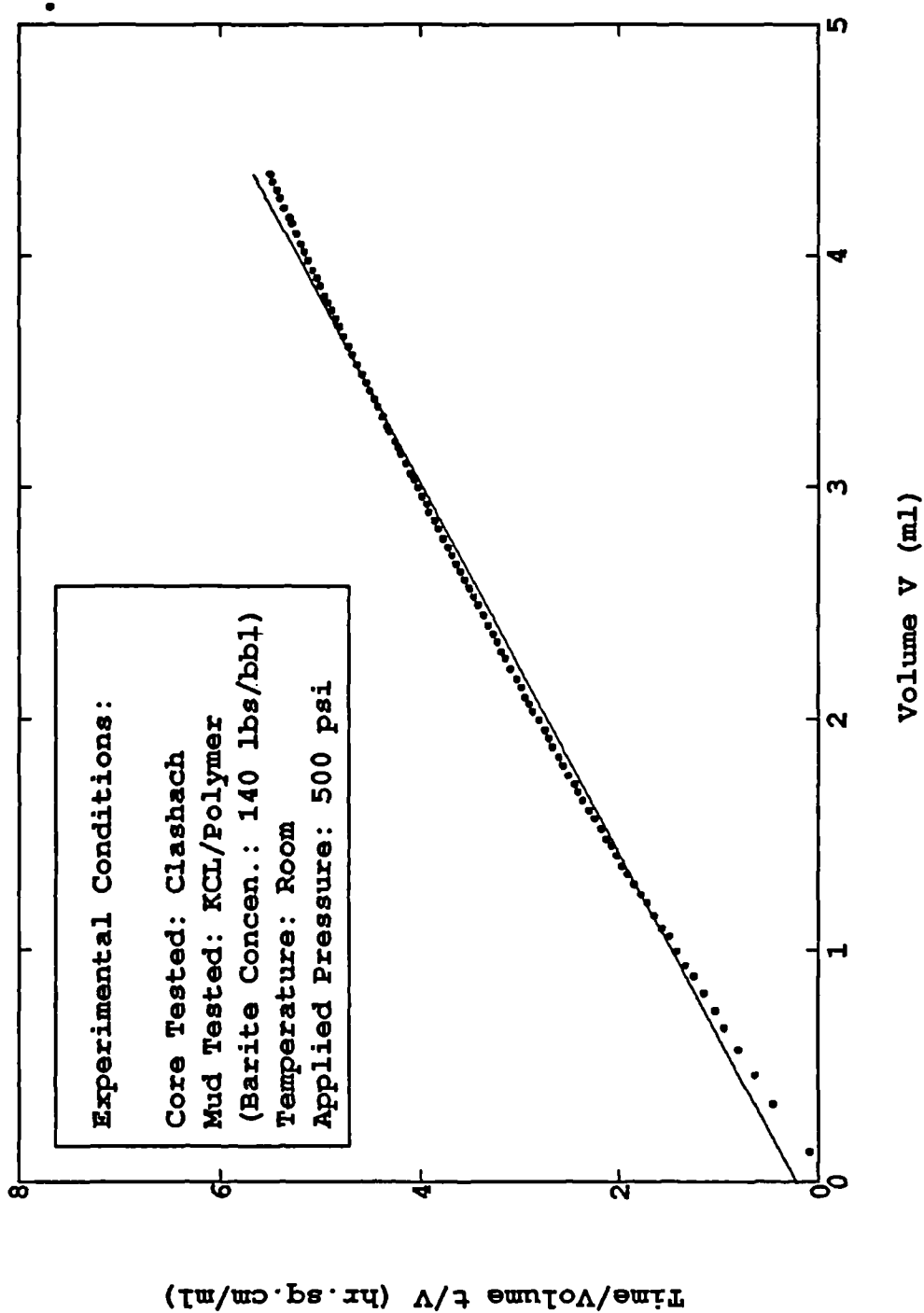


Figure (7-1.3) t/V vs. V Plotting in Static Filtration Tests

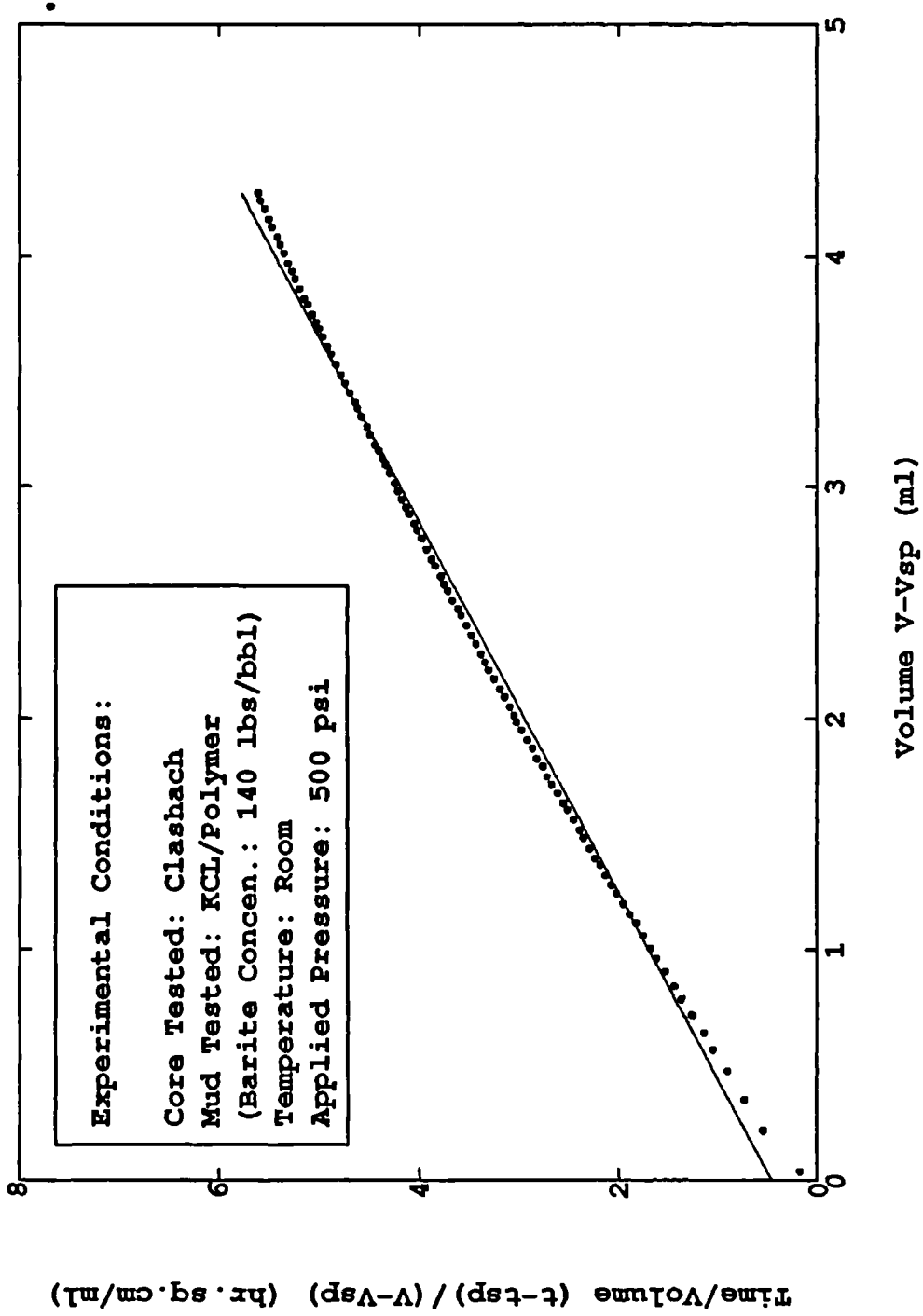


Figure (7-1.4) $(t-t_{sp}) / (V-V_{sp})$ vs. $V-V_{sp}$ Plotting in Static Filtration

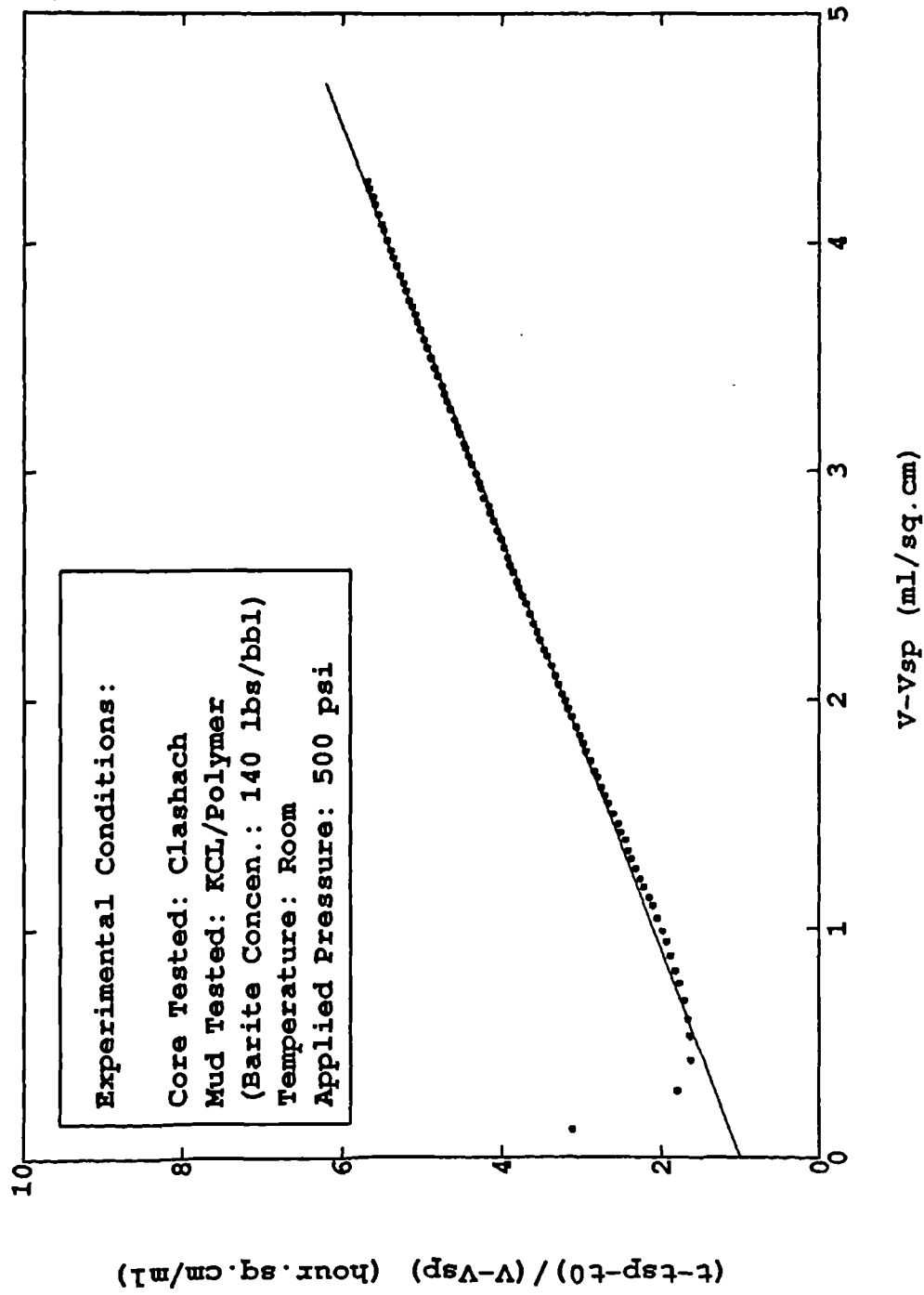


Figure (7-1.5) $(t-t_{sp}-t_0) / (V-V_{sp})$ vs. $V-v_{sp}$ Plotting in Static Filtration

7.1.2 Dynamic Filtration Modelling

From the survey of literature in chapter three, it is understood that only a few investigators^{6,21,24,49,45} have presented the dynamic filtration equations for drilling fluids. It is however necessary to conclude that all the equations are applicable for limited conditions and the irrelationship to classic static filtration equation has not been considered. During this investigation, a general equation which covers static and dynamic filtration conditions was produced and experimentally verified. In order to make it perfect, the parameters which possibly cause deviations and the conditions of the application of this equation are therefore needed to clarify.

All the variables which may cause deviations in static filtration as discussed above will produce the same effects in dynamic filtration. In addition, there is another assumption which may lead to deviation in dynamic filtration and that is the concept of the constant removal of a dynamically deposited cake.

Figure(7-1.6) shows theoretically the relationship of filter cake thickness between static and dynamic conditions as a function of time. The curves are produced using the general filtration equation developed in chapter three in this study based on the simulation of an experimental test. This test was conducted using clashach core for KCL/Polymer mud at pressure of 50 psi and shear rate of 71 1/s under room temperature. The curve marked by small triangles demonstrates the dynamic filter cake thickness as a function of time and the curve identified by dots demonstrates the total deposited filter cake thickness in dynamic filtration which includes the continuously removed filter cake thickness marked by small stars. The curve defined by inverted triangles was produced by assuming that the filter cake thickness is built-up according to the general equation under the same conditions as the above dynamic filtration processes except the shear rate on the cake is zero.

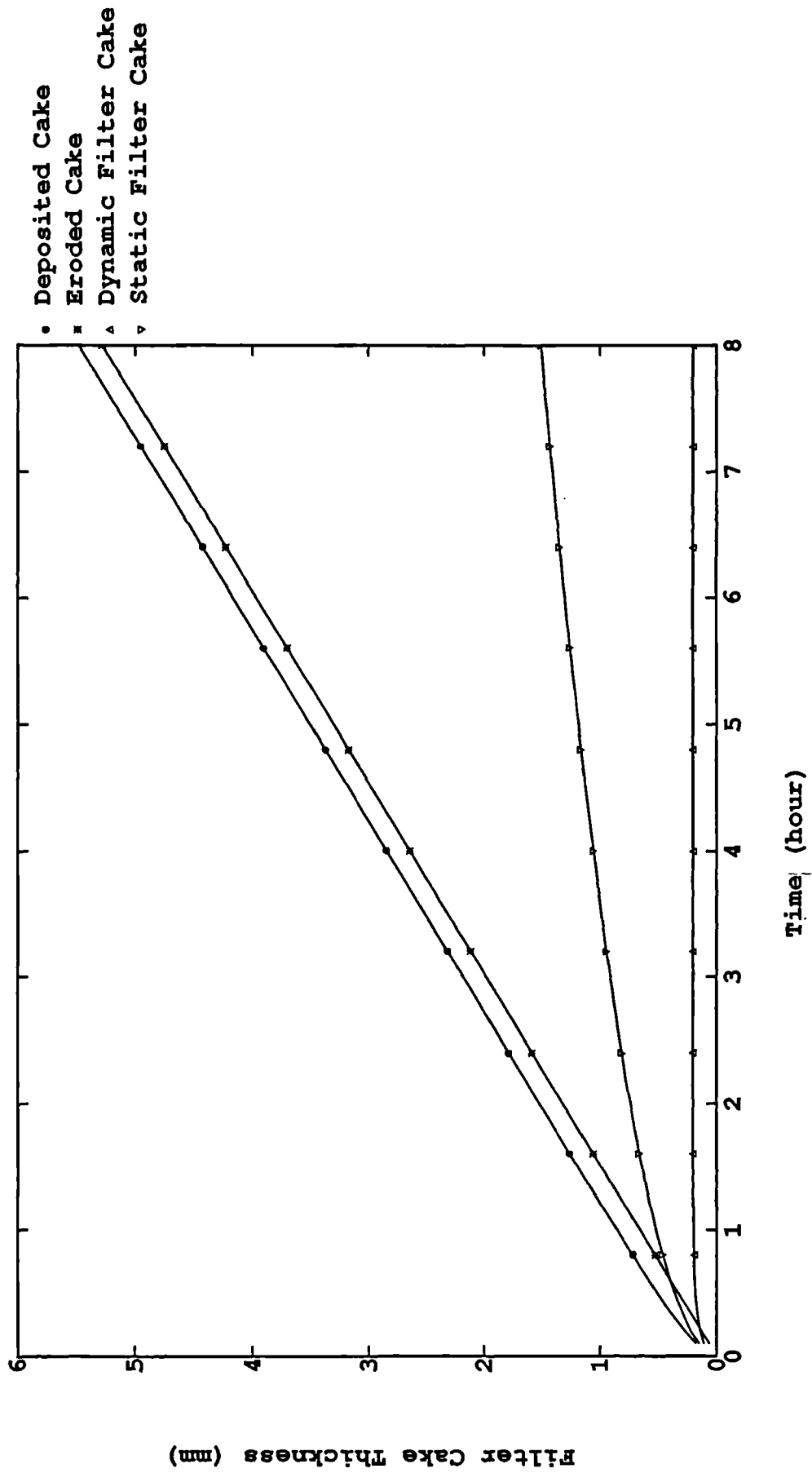


Figure (7-1.6) Theoretically Simulation of Filter Cake Building-Up as Function of Time for KCL/Polymer Mud

Figures(7-1.7) to (7-1.22) show the dynamic filtrate flow rate as a function of time for Seawater/KCL/Polymer mud and Freshwater/Gypsum/Lignosulphonate mud under different pressure and shear rate conditions. From all the plots, it is clear that under the same pressure and shear rate, the filtration rate for Seawater/KCL/Polymer mud is always greater than that for Freshwater/Gypsum/Lignosulphonate mud. This may be explained by the effect of bentonite in the Gypsum/Lignosulphonate mud.

7.2 PRESSURE DIFFERENTIAL ACROSS THE FILTER CAKE

According to constant pressure filtration theory, the pressure differential across the filter cake should be constant throughout the whole filtration process. However, this will never be reached in practice, because the filter medium resistance will never be zero whatever material. Of course, if size distribution and diameter of the filter medium and solids from slurry are suitable, the resistance of filter medium would be very small and could be neglected compared to the huge filter cake resistance. In fact, it is impossible to obtain the above conditions for drilling fluids. Therefore, the filter medium resistance is due not to the filter medium, but more important, the plugging and bridging of the pores on its surface will cause an effect of the same order of magnitude as the filter cake resistance. From the following pressure differential comparison between across the filter cake and across the filter medium, it will clarify the above analytical conclusion.

7.2.1 Pressure Differential Across Static Filtration Cake

According to Darcy's law, the pressure differential across a filter is expressed as:

$$\Delta P = \mu q R \quad (7-2.1)$$

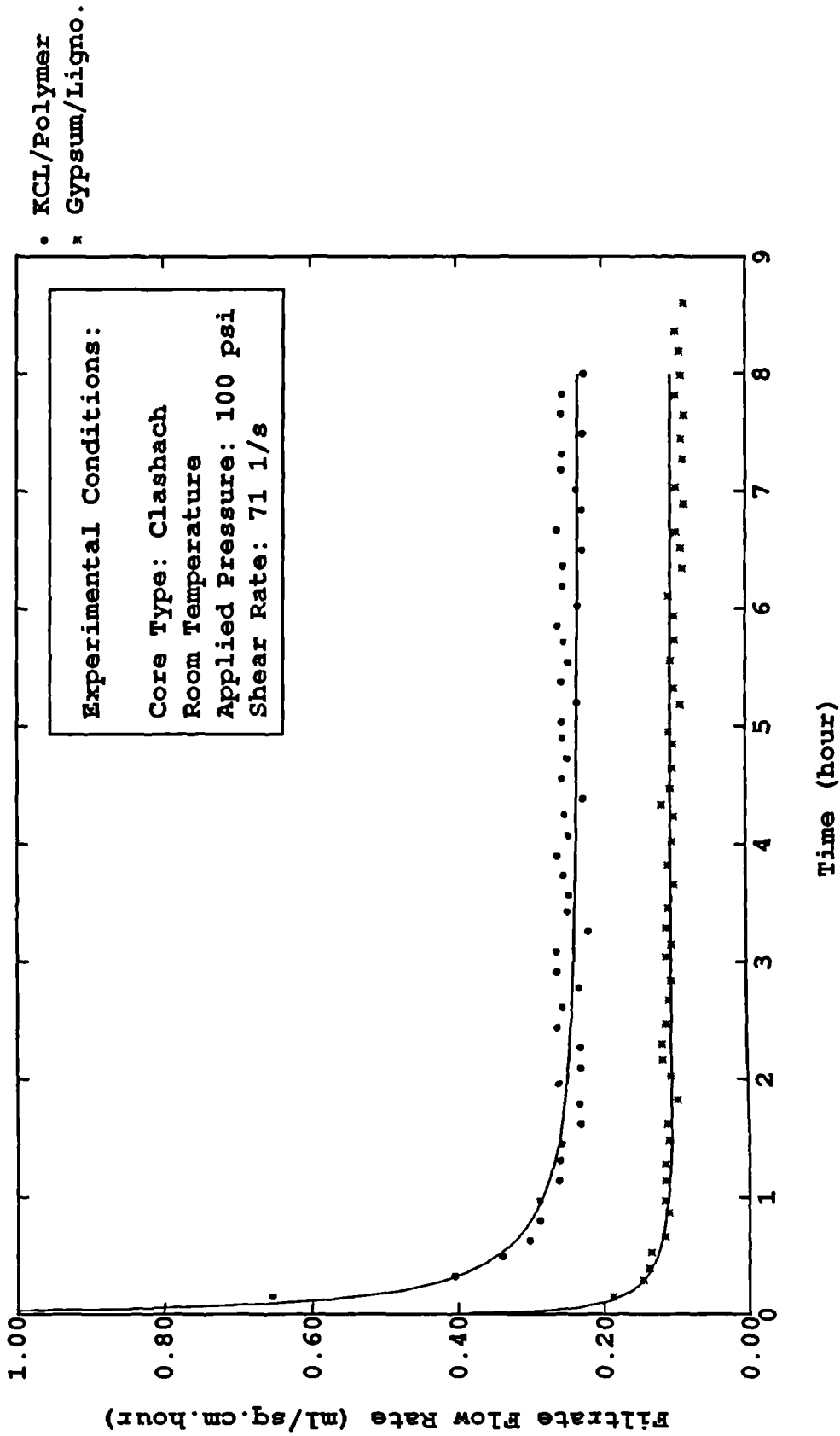


Figure (7-1.7) Comparison of Filtrate Flow Rates Calculated from Dynamic Filtration Equation (Correlated Results) and Experimental Data as Function of Time and Mud Types

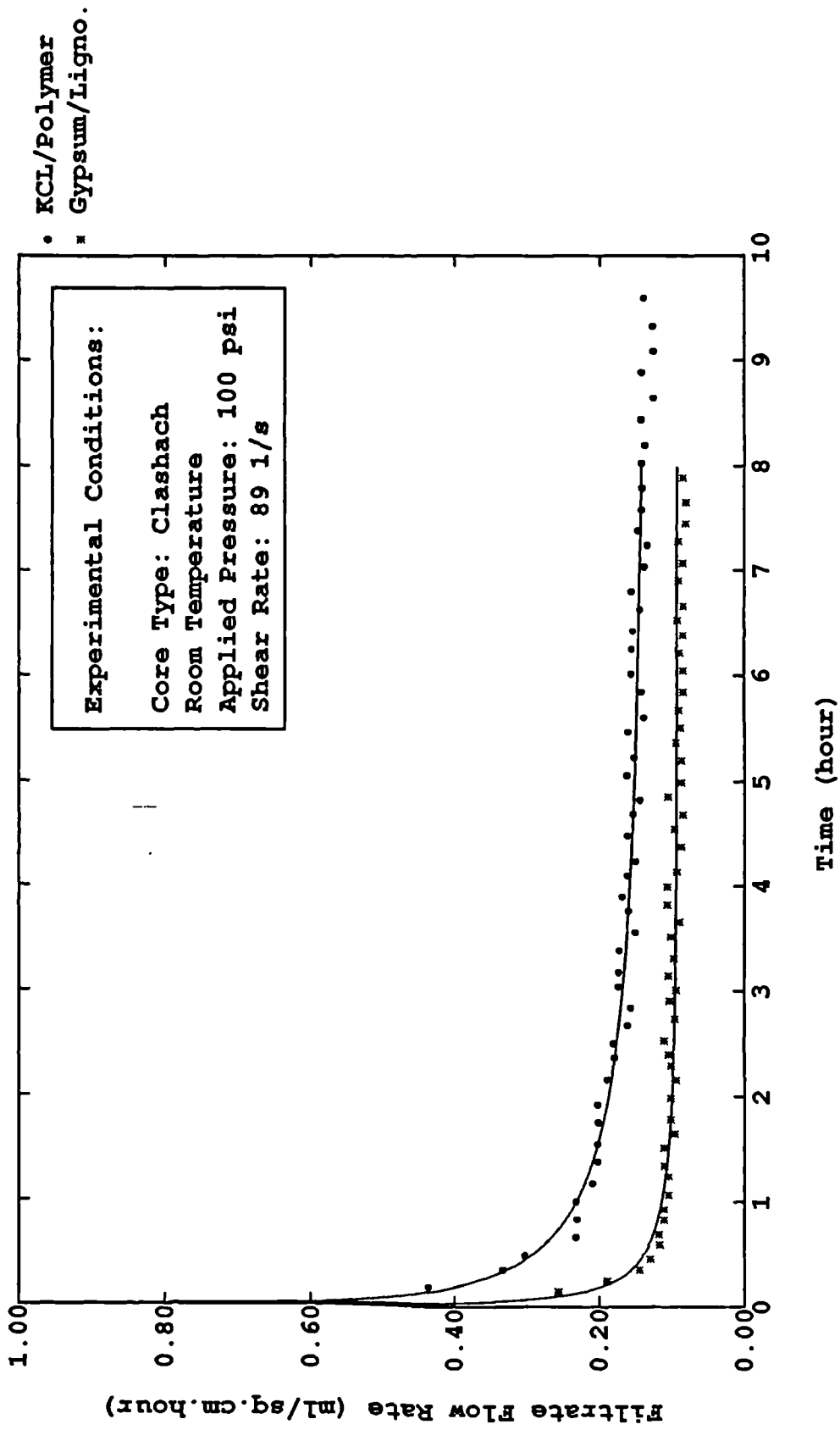


Figure (7-1.8) Comparison of Filtrate Flow Rates Calculated from Dynamic Filtration Equation (Correlated Results) and Experimental Data as Function of Time and Mud Types

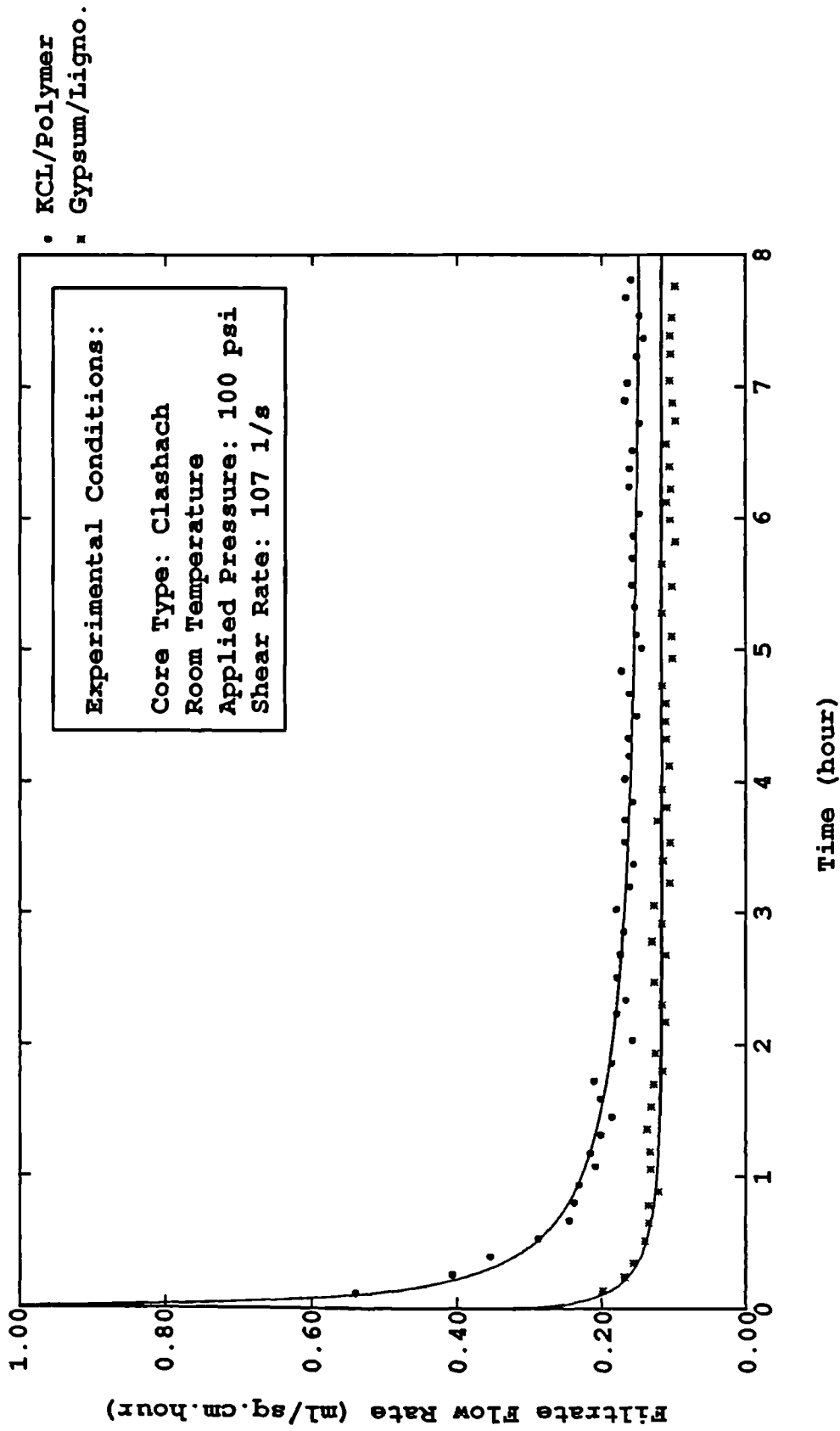


Figure (7-1.9) Comparison of Filtrate Flow Rates Calculated from Dynamic Filtration Equation (Correlated Results) and Experimental Data as Function of Time and Mud Types

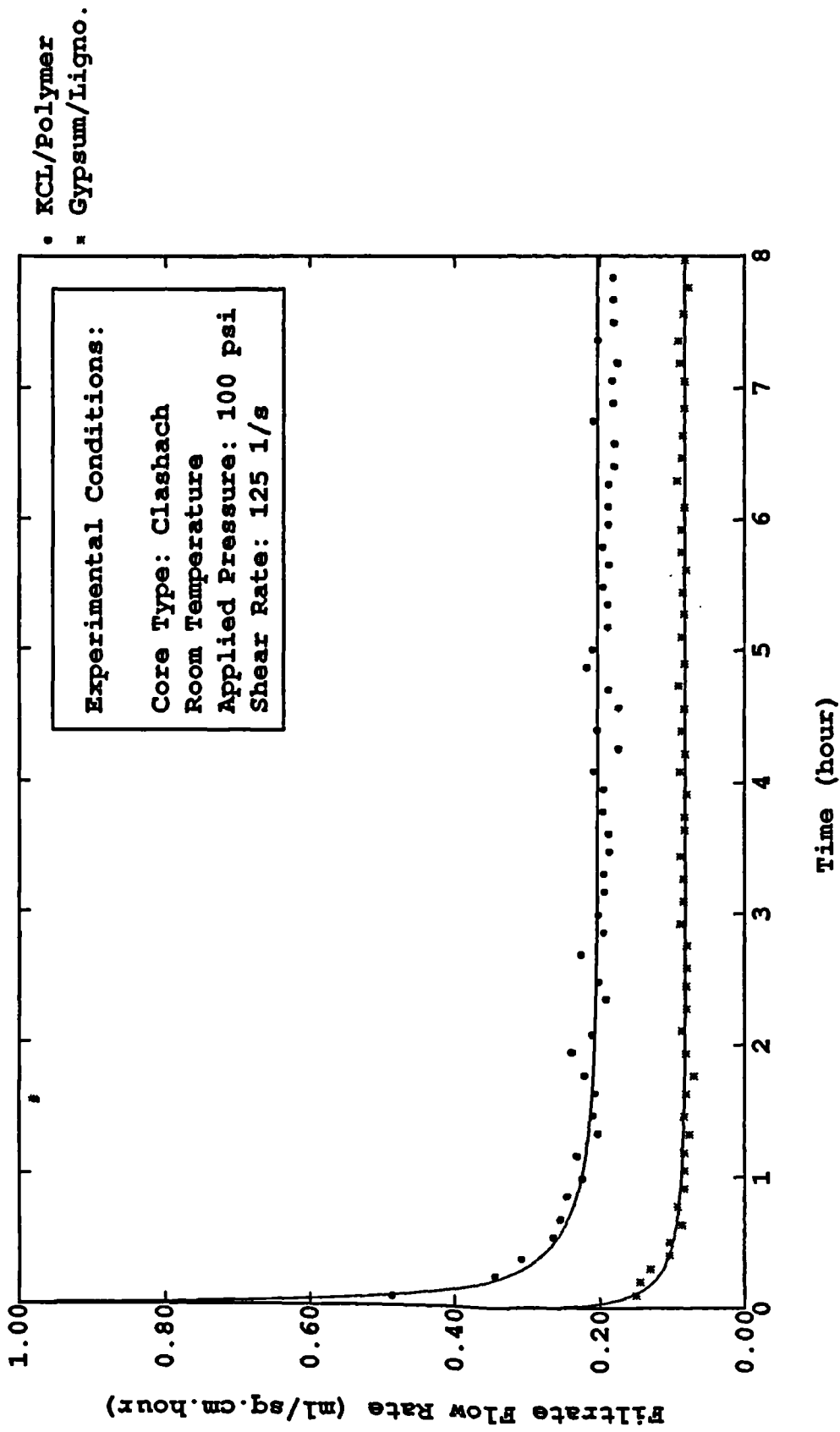


Figure (7-1.10) Comparison of Filtrate Flow Rates Calculated from
 Dynamic Filtration Equation (Correlated Results) and
 Experimental Data as Function of Time and Mud Types

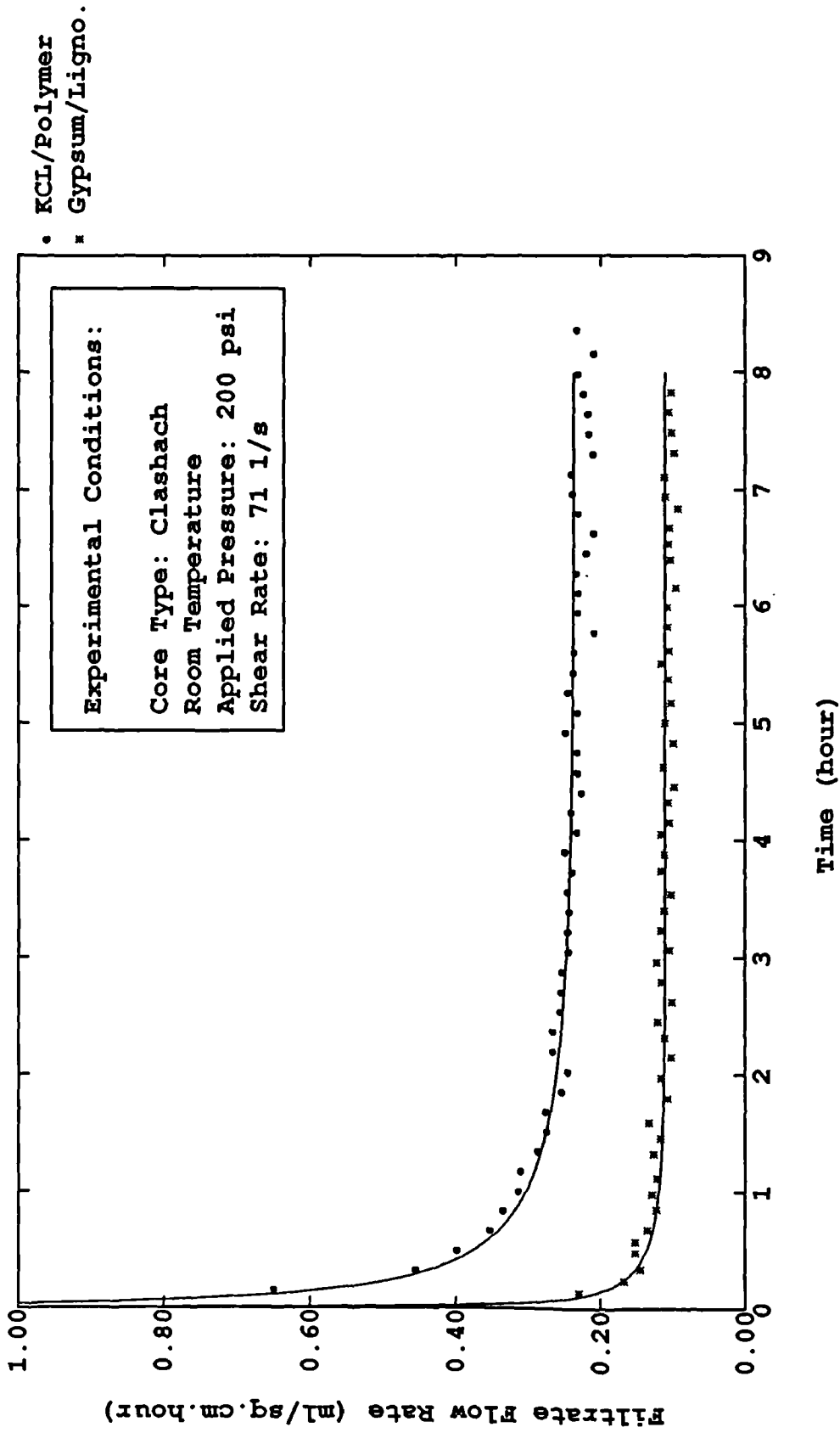


Figure (7-1.11) Comparison of Filtrate Flow Rates Calculated from Dynamic Filtration Equation (Correlated Results) and Experimental Data as Function of Time and Mud Types

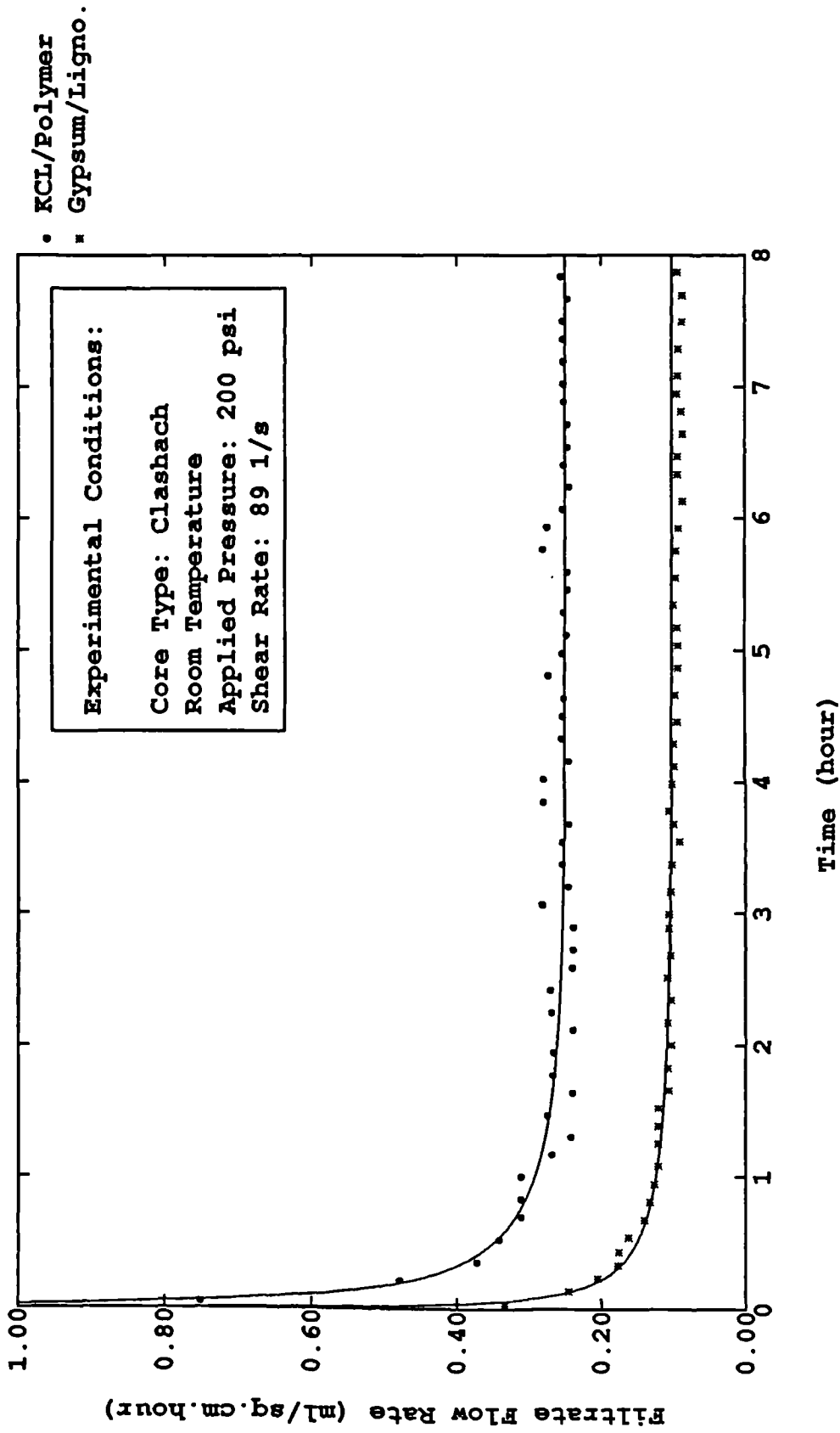


Figure (7-1.12) Comparison of Filtrate Flow Rates Calculated from Dynamic Filtration Equation (Correlated Results) and Experimental Data as Function of Time and Mud Types

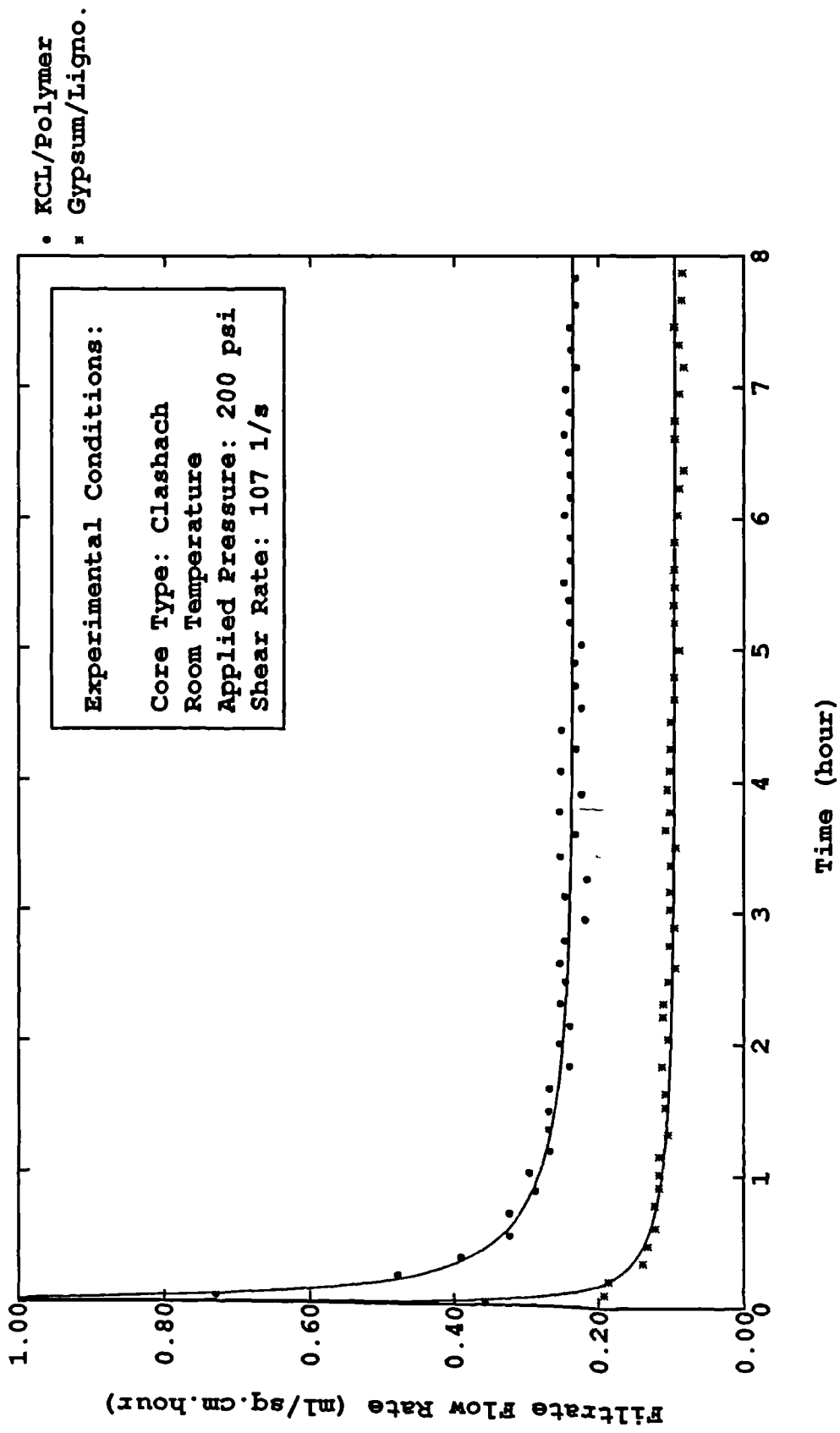


Figure (7-1.13) Comparison of Filtrate Flow Rates Calculated from Dynamic Filtration Equation (Correlated Results) and Experimental Data as Function of Time and Mud Types

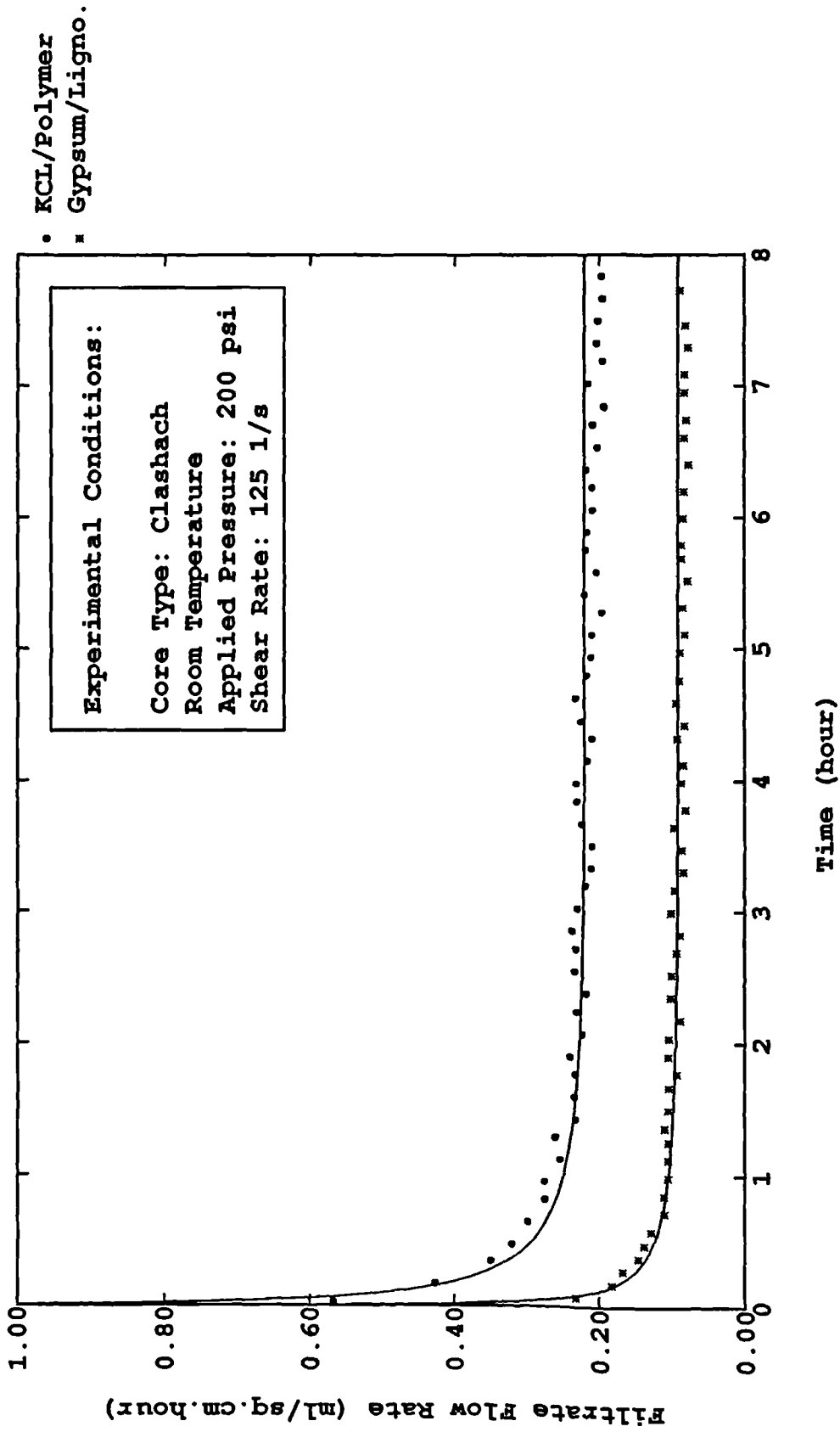


Figure (7-1.14) Comparison of Filtrate Flow Rates Calculated from Dynamic Filtration Equation (Correlated Results) and Experimental Data as Function of Time and Mud Types

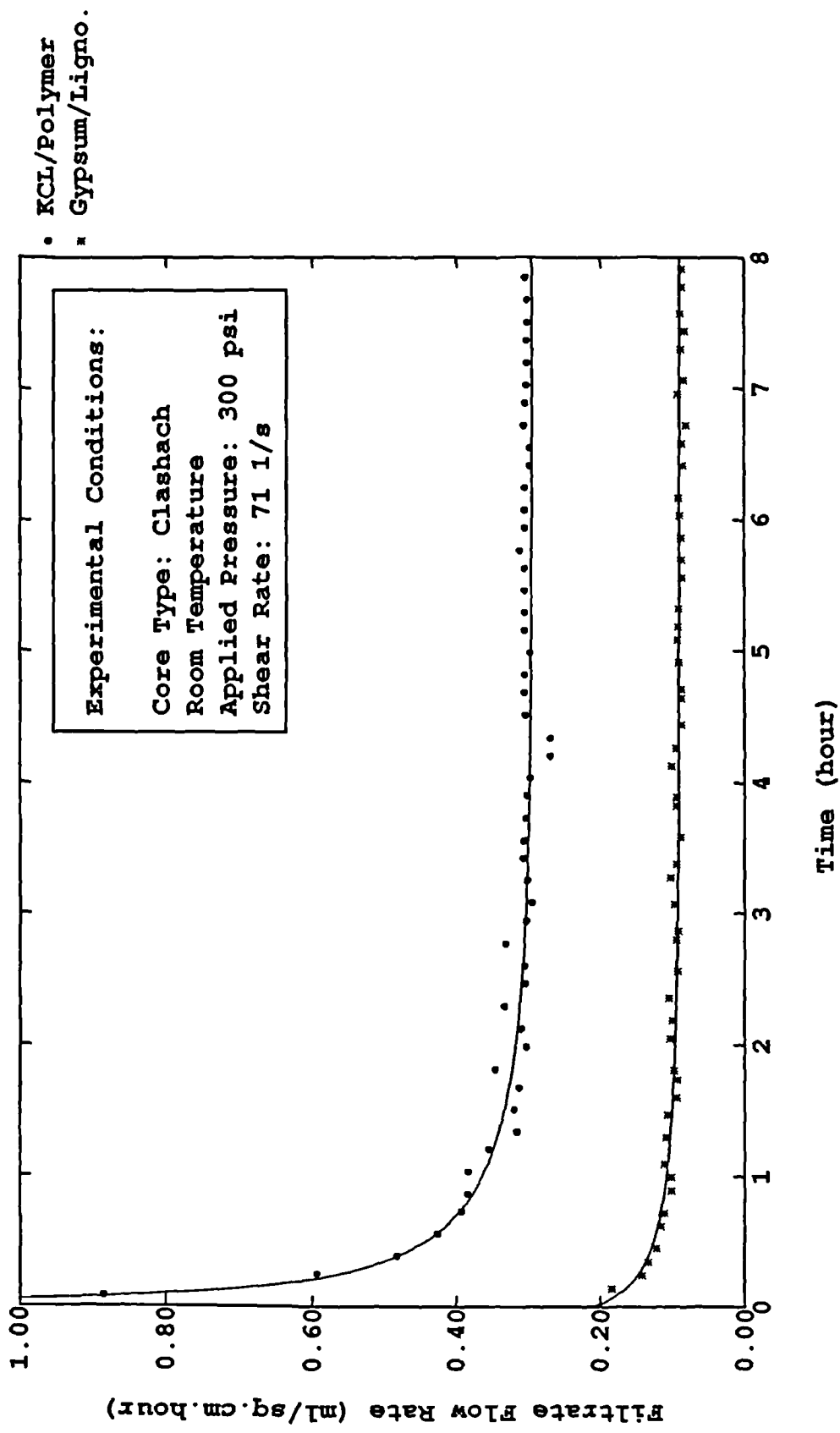


Figure (7-1.15) Comparison of Filtrate Flow Rates Calculated from Dynamic Filtration Equation (Correlated Results) and Experimental Data as Function of Time and Mud Types

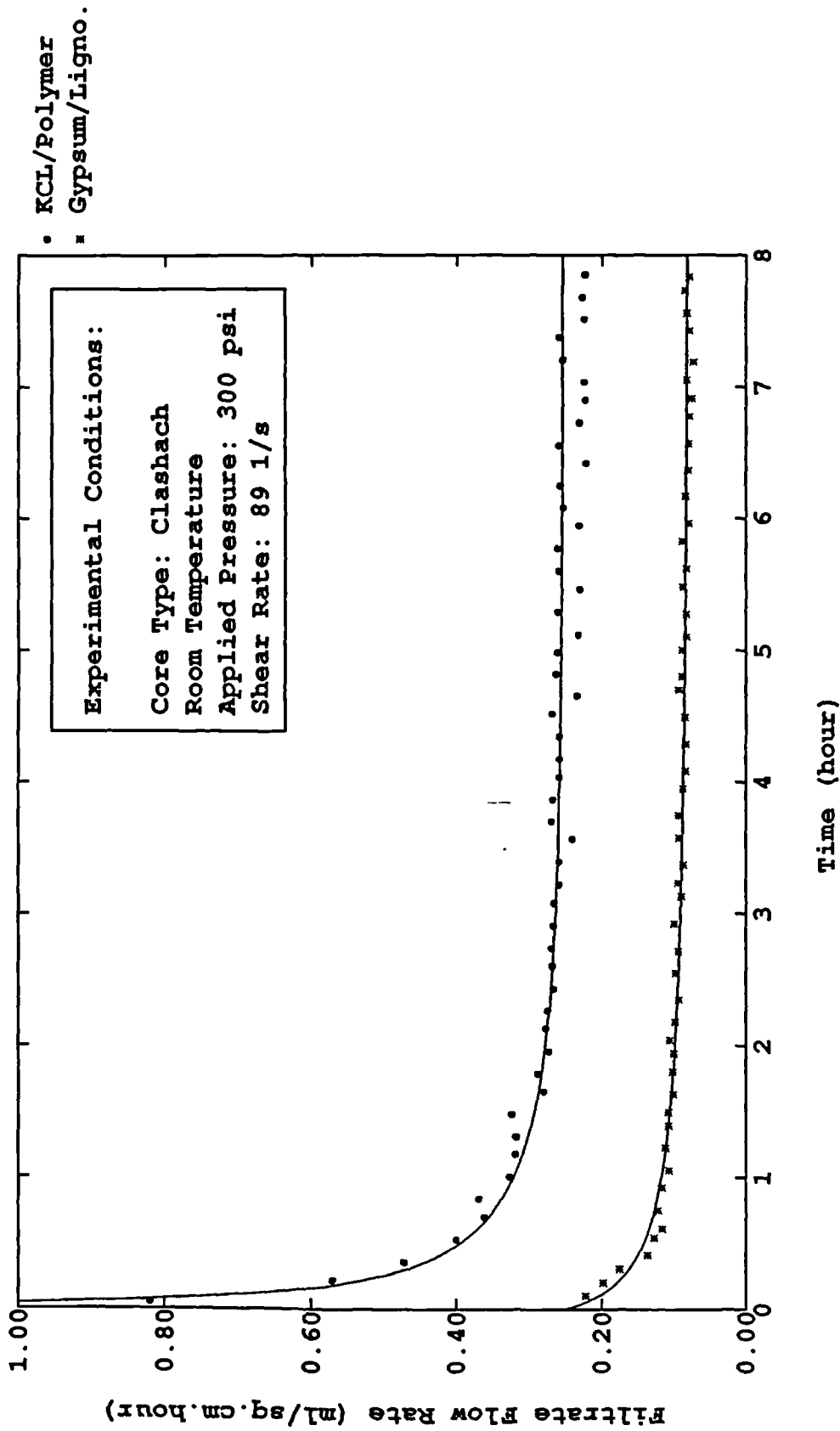


Figure (7-1.16) Comparison of Filtrate Flow Rates Calculated from Dynamic Filtration Equation (Correlated Results) and Experimental Data as Function of Time and Mud Types

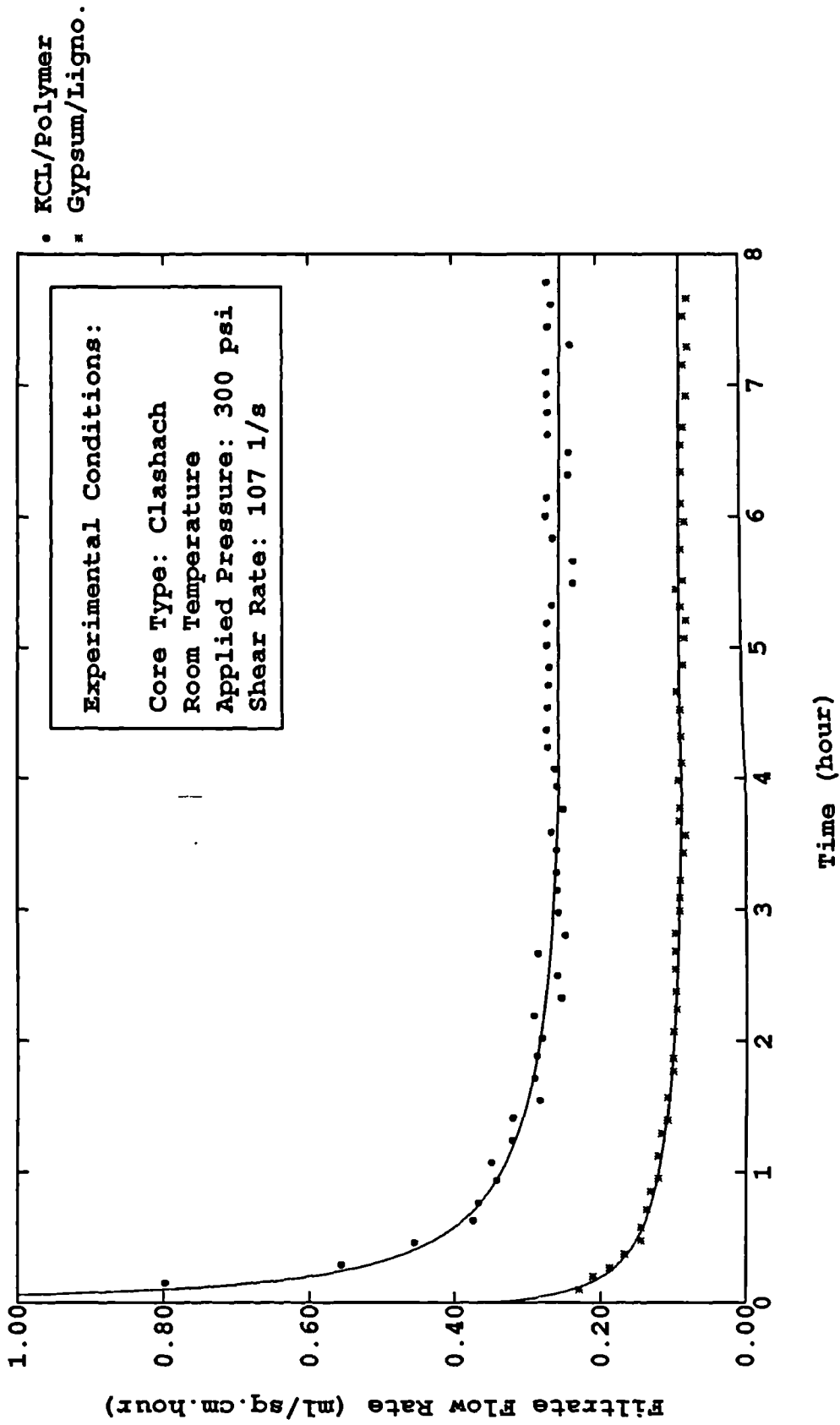


Figure (7-1.17) Comparison of Filtrate Flow Rates Calculated from Dynamic Filtration Equation (Correlated Results) and Experimental Data as Function of Time and Mud Types

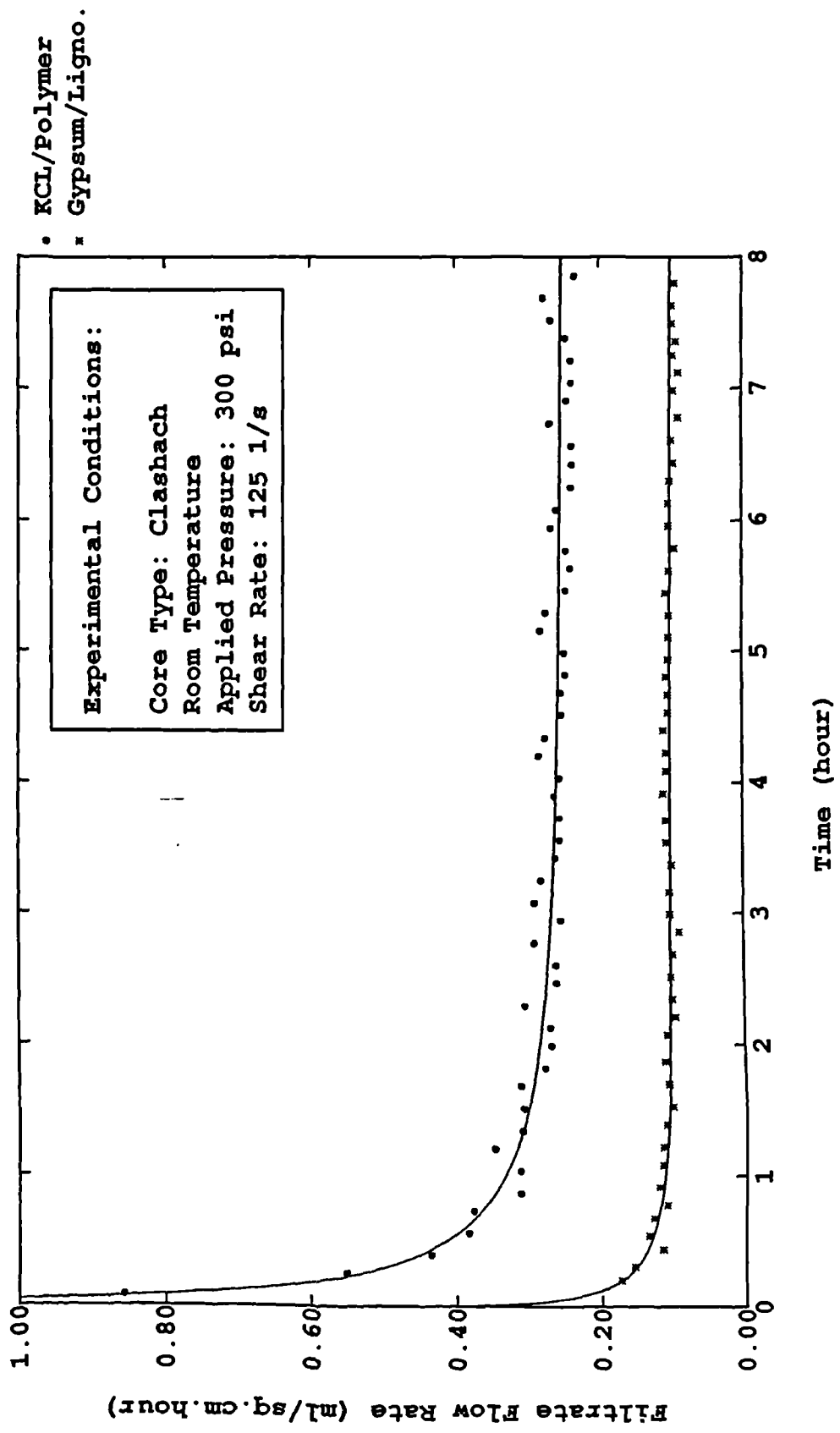


Figure (7-1.18) Comparison of Filtrate Flow Rates Calculated from Dynamic Filtration Equation (Correlated Results) and Experimental Data as Function of Time and Mud Types

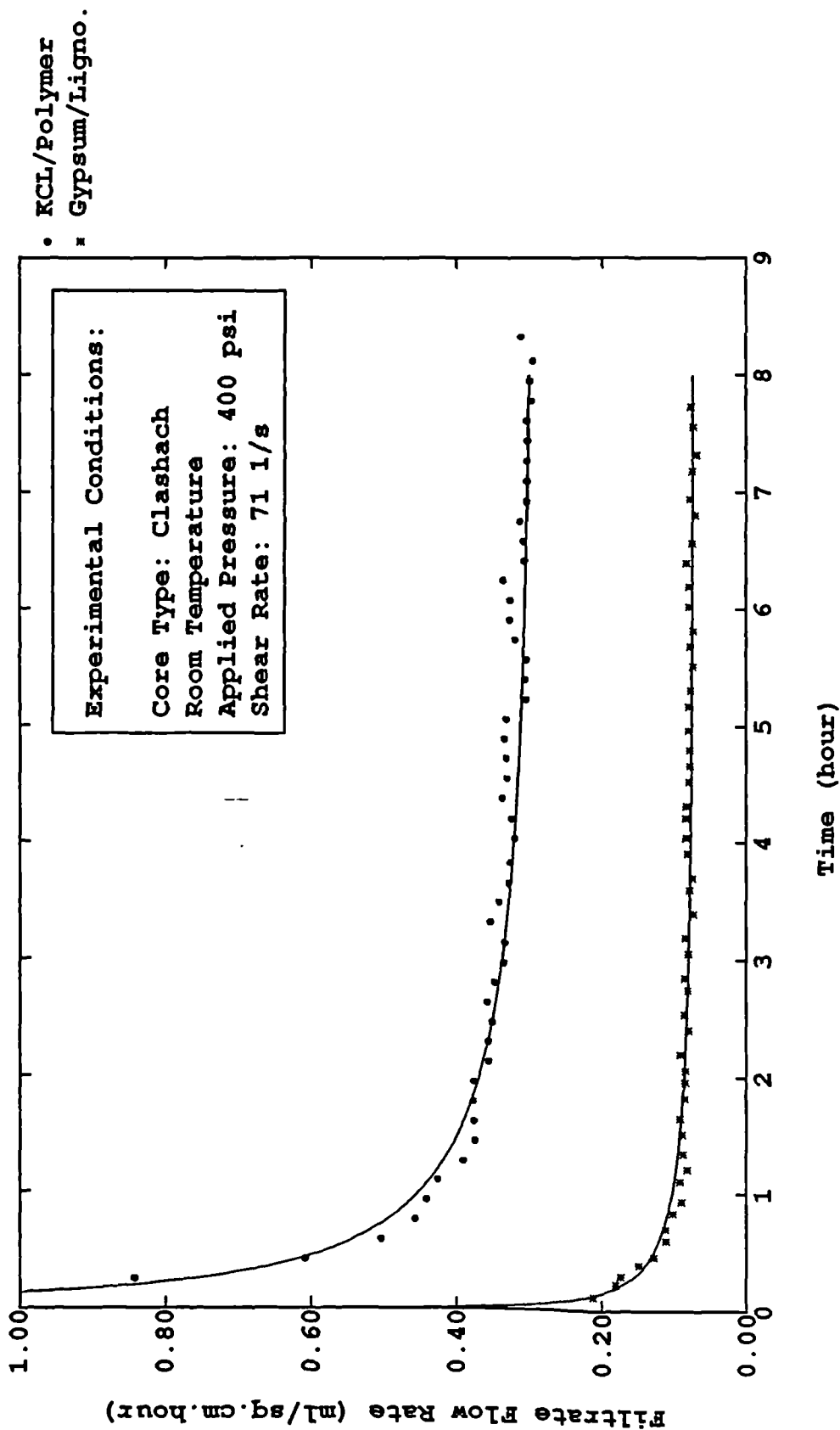


Figure (7-1.19) Comparison of Filtrate Flow Rates Calculated from Dynamic Filtration Equation (Correlated Results) and Experimental Data as Function of Time and Mud Types

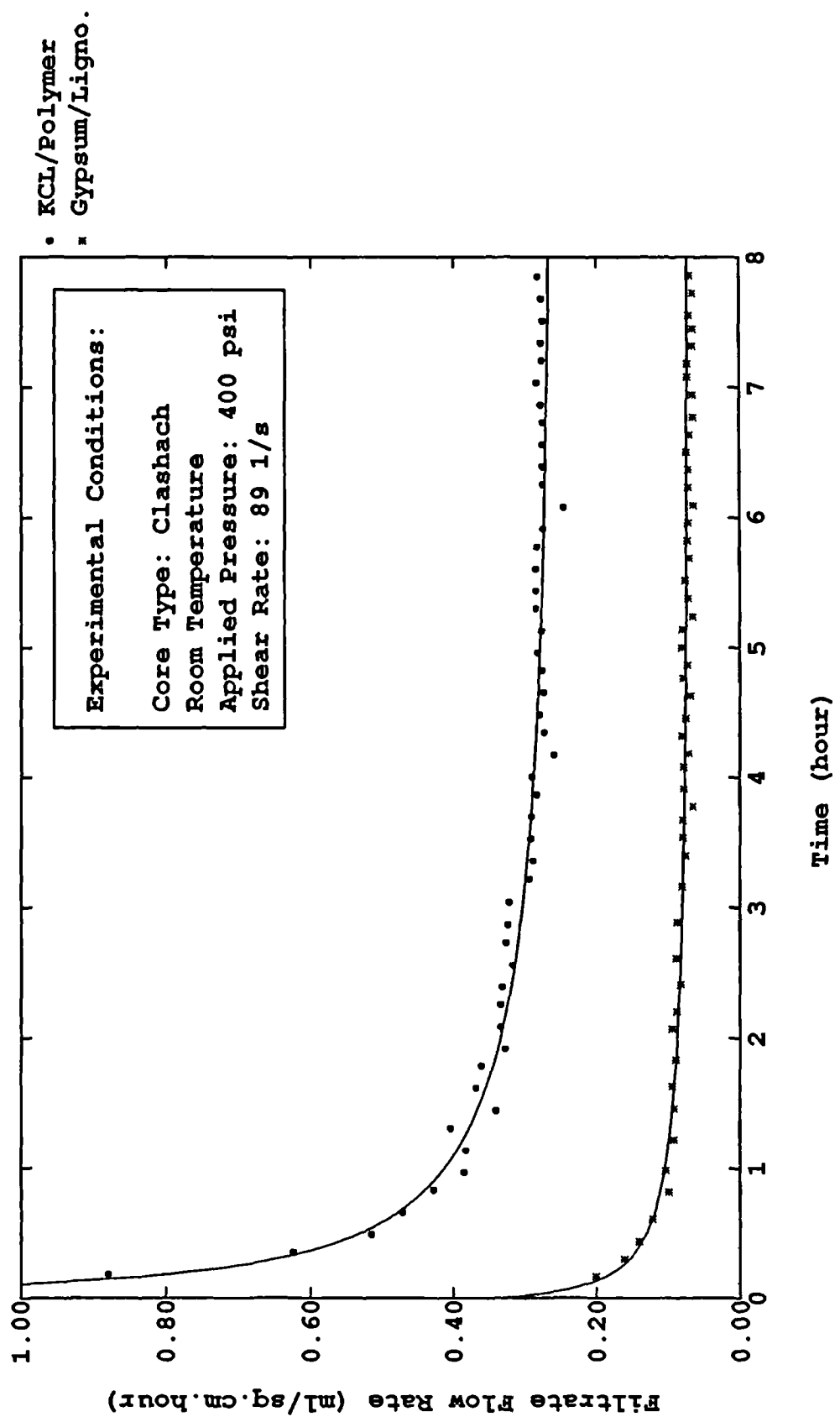


Figure (7-1.20) Comparison of Filtrate Flow Rates Calculated from Dynamic Filtration Equation (Correlated Results) and Experimental Data as Function of Time and Mud Types

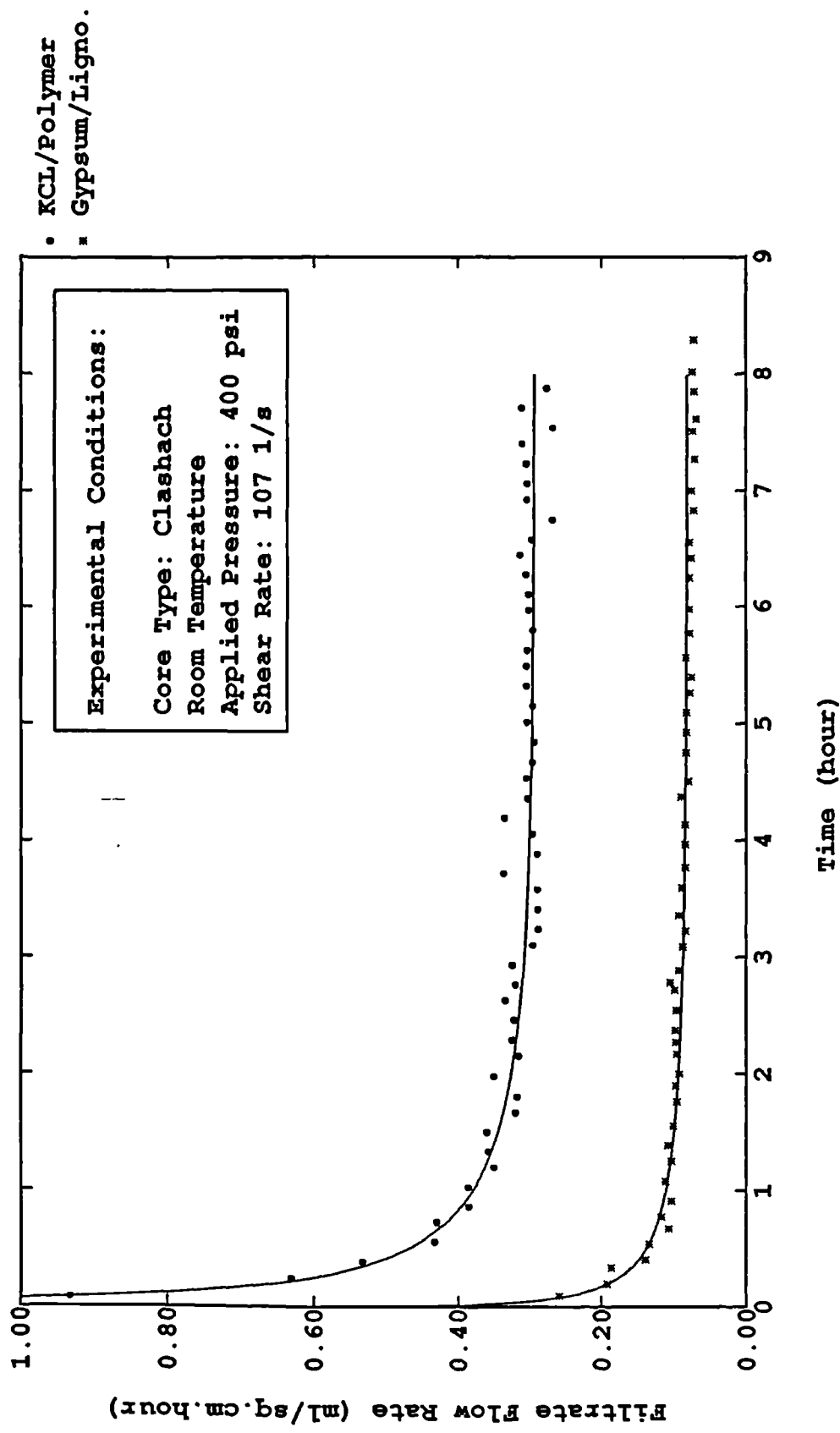


Figure (7-1.21) Comparison of Filtrate Flow Rates Calculated from Dynamic Filtration Equation (Correlated Results) and Experimental Data as Function of Time and Mud Types

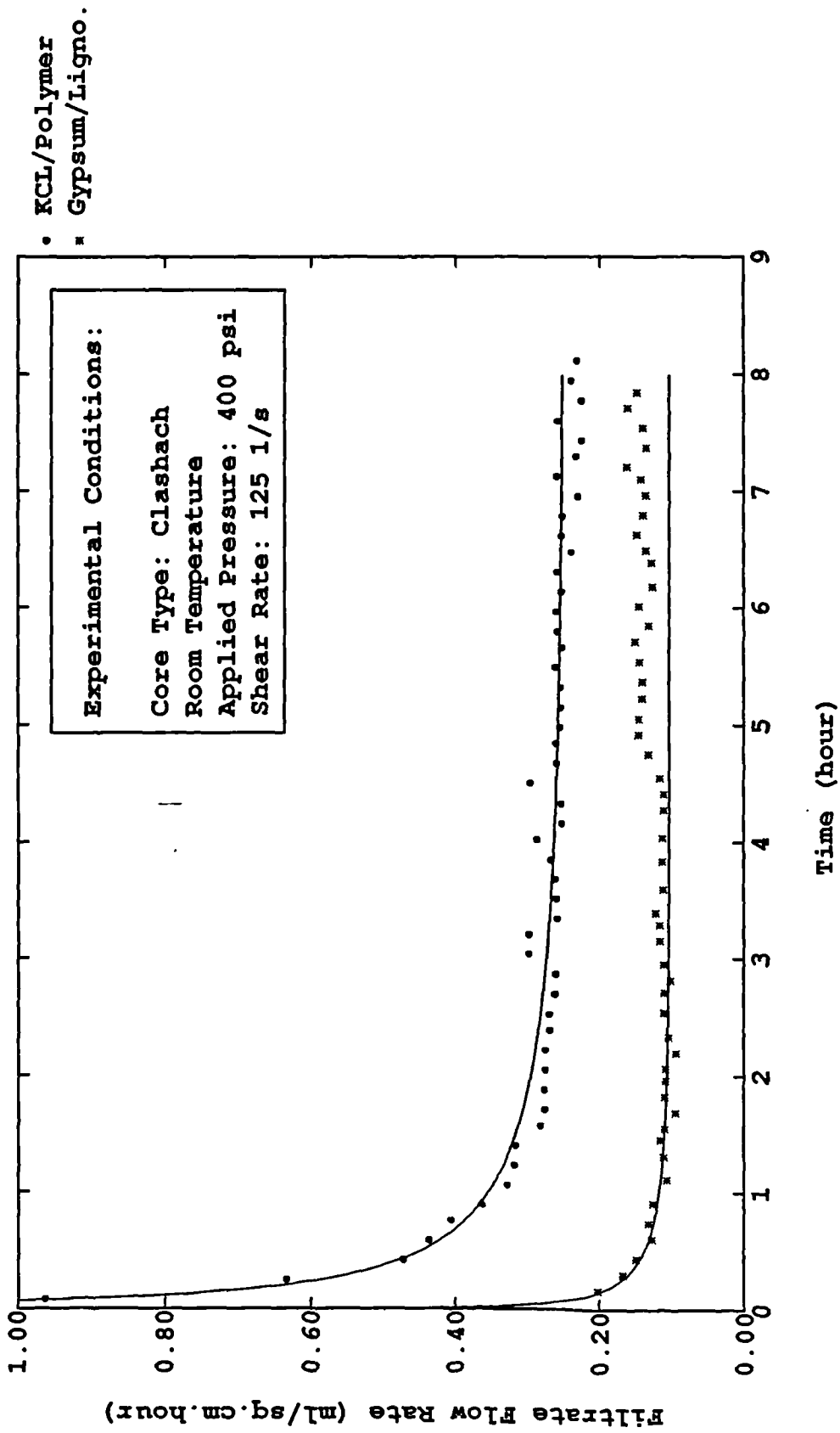


Figure (7-1.22) Comparison of Filtrate Flow Rates Calculated from Dynamic Filtration Equation (Correlated Results) and Experimental Data as Function of Time and Mud Types

where:

ΔP — pressure differential across a filter

μ — filtrate viscosity

q — filtrate flow rate through the filter

R — filter resistance

Now we can write the formula to calculate the pressure differential across filter cake and filter medium at any moment of filtration.

Differentiate both sides with respect to V' in equation(5-3.7) and rearrange, we obtain:

$$q' = \frac{1}{A} \frac{dV'}{dt'} = \frac{1}{A} \frac{1}{2a_2 V' + a_1} \quad (7-2.2)$$

From equation(7-2.1), we can calculate the actual pressure across filter medium as follows:

$$\Delta P_{\text{meff}} = \mu q' R_{\text{meff}} \quad (7-2.3)$$

Inserting q' from equation(7-2.2) and R_{meff} from equation(5-3.10) into equation(7-2.3) and arranging:

$$\Delta P_{\text{meff}} = \mu \cdot \frac{1}{A} \frac{1}{2a_2 V' + a_1} \cdot \frac{\Delta P A}{\mu} a_1 = \frac{a_1}{2a_2 V' + a_1} \Delta P \quad (7-2.4)$$

so that:

$$\Delta P_c = \Delta P - \Delta P_{\text{meff}} = \frac{2a_2 V'}{2a_2 V' + a_1} \Delta P \quad (7-2.5)$$

Combining equation(5-3.7) with equations(7-2.4) and (7-2.5), we can plot the differential pressure across either the cake or the filter medium as a function of time.

Figures(7-2.1) and (7-2.2) show the pressure across cake and core divided by the

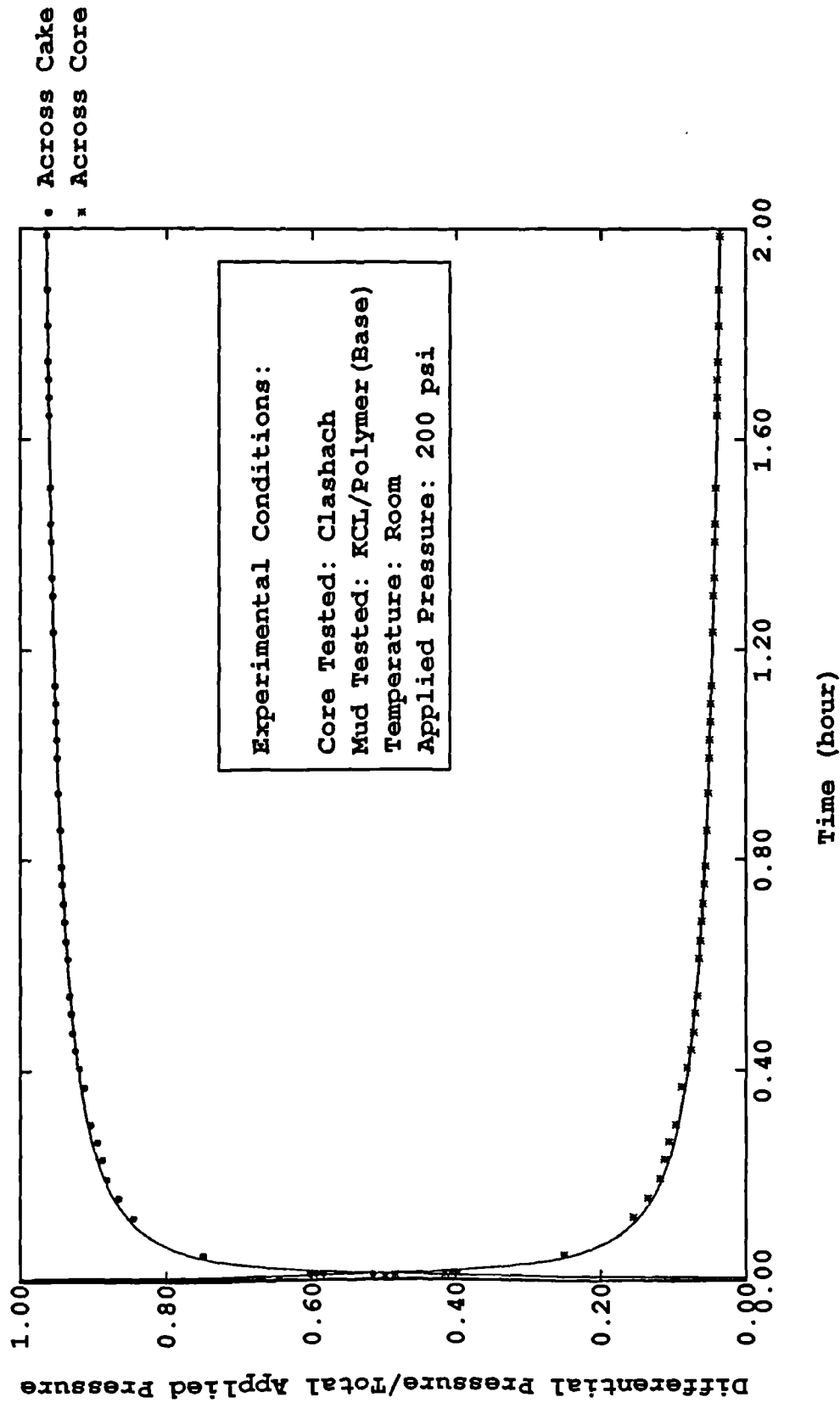


Figure (7-2.1) Pressure Differential Across Filter Cake and Filter Medium over the Total Applied Pressure as Function of Time for Static Filtration

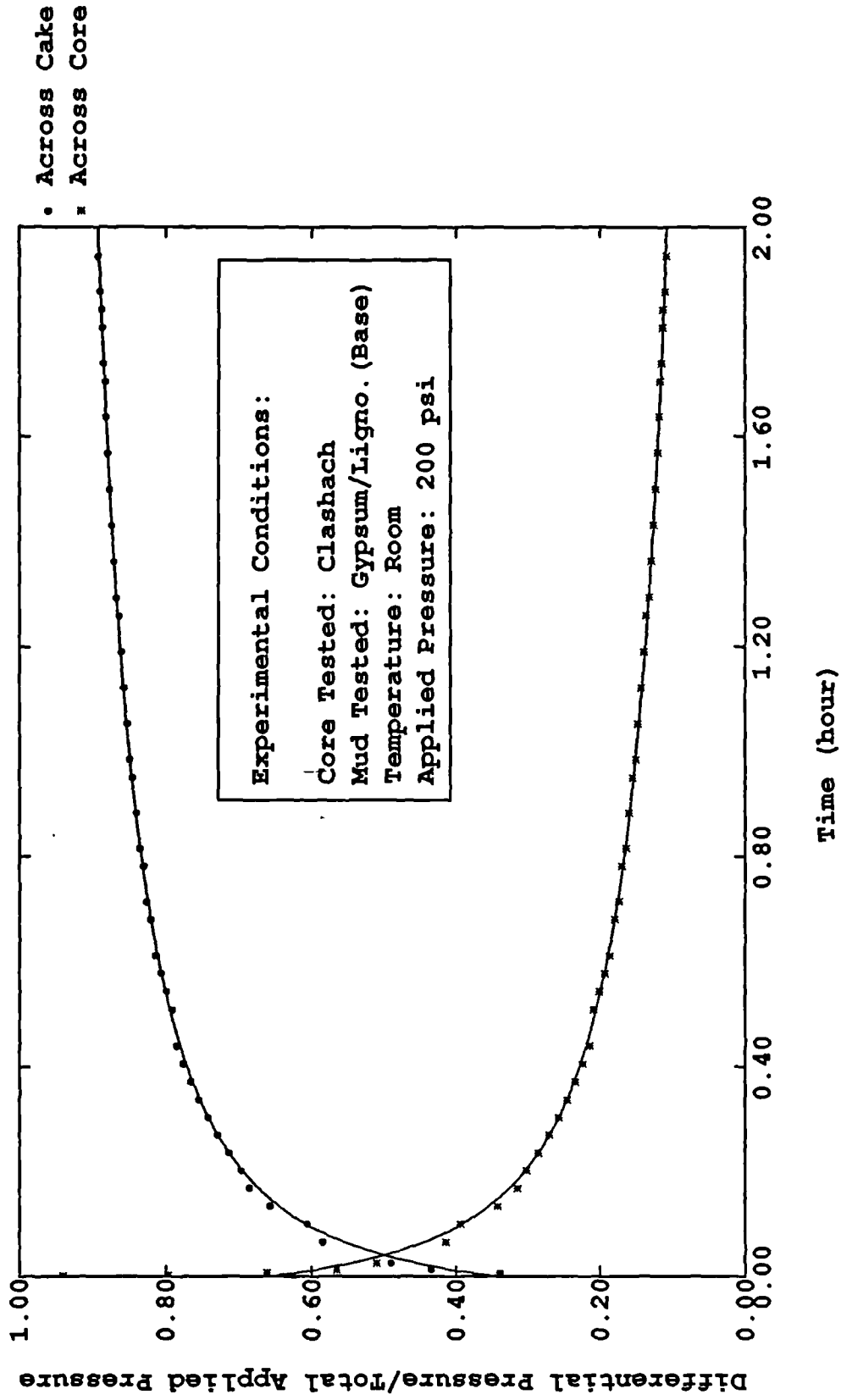


Figure (7-2.2) Pressure Differential Across Filter Cake and Filter Medium
 over the Total Applied Pressure as Function of Time for
 Static Filtration

total applied pressure of filtration as a function of time for Seawater/KCL/Polymer mud and Freshwater/Gypsum/Lignosulphonate mud at the pressure of 200 psi under static filtration conditions. The smooth lines are plotted using values of V' which are predicted by equation(5-3.7) and dotted points are plotted using values of V' from experimental data. It is not practical to include all the plots obtained in this thesis. However, from the plots postulated here, we can conclude:

- (1) For the Seawater/KCL/Polymer mud system, the percentage of pressure drop across the cake to the total applied pressure rapidly approaches a constant value after about half an hour. It is clear that the pressure drop across the cake continues to increase slightly with time. This is because the filtrate flow rate still decreases with time and leads to a decrease in pressure drop across the filter medium. The resistance caused by core and particle plugging and bridging (during spurt loss time) are large enough to be of the same order of magnitude as the cake resistance.
- (2) For Freshwater/Gypsum/Lignosulphonate mud system, the percentage of pressure drop across the cake over the total applied pressure approaches constant very slowly. The pressure drop across the filter cake are only about 90% of total applied pressure. This suggests that the resistance caused by core and particle plugging/bridging (during spurt loss time) are very large.

7.2.2 Pressure Differential Across Dynamic Filtration Cake

In a similar way, we can determine the pressure across the dynamic filter cake and core.

Differentiating both sides with respect to V' in equation(6-2.5) and rearranging, we get:

$$q' = \frac{1}{A} \frac{dV'}{dt'} = \frac{1}{A} \frac{1}{C_1 - C_2 C_3 e^{-C_3 V'}} \quad (7-2.6)$$

Inserting q' from equation(7-2.6) and R_{meff} from equation(6-2.11) into equation(7-2.3):

$$\Delta P_{meff} = \mu \cdot \frac{1}{A} \frac{1}{C_1 - C_2 C_3 e^{-C_3 V'}} \cdot \frac{\Delta P A}{\mu} (C_1 - C_2 C_3) = \frac{C_1 - C_2 C_3}{C_1 - C_2 C_3 e^{-C_3 V'}} \Delta P \quad (7-2.7)$$

Hence,

$$\Delta P_c = \Delta P - \Delta P_{meff} = \frac{C_2 C_3 (1 - e^{-C_3 V'})}{C_1 - C_2 C_3 e^{-C_3 V'}} \Delta P \quad (7-2.8)$$

With the help of equations(6-2.6), (7-2.7), (7-2.8), we can plot the pressure differential across either the cake or the filter medium as a function of time.

Figures(7-2.3) and (7-2.4) show the pressure drop across the cake and core divided by the total applied pressure of filtration as a function of time for Seawater/KCL/Polymer mud and Freshwater/Gypsum/Lignosulphonate mud at a pressure of 200 psi under dynamic conditions. The smooth lines were plotted using values of V' which are predicted by equation(6-2.6) and the dotted points are plotted using values of V' from the experimental data. Figures(7-2.5) and (7-2.6) are plotted for the first two hours in order to compare those plotted under static conditions.

Similar conclusions to those obtained for static filtration conditions can be drawn for dynamic filtration conditions. From the plots, however, they also clearly demonstrate the difference between the static and dynamic conditions namely that the pressure drop across the filter cake reaches a constant under dynamic conditions. This suggests that the filtrate flow rate reaches a constant after a period of time and thus leads to a constant pressure differential across the filter medium (core).

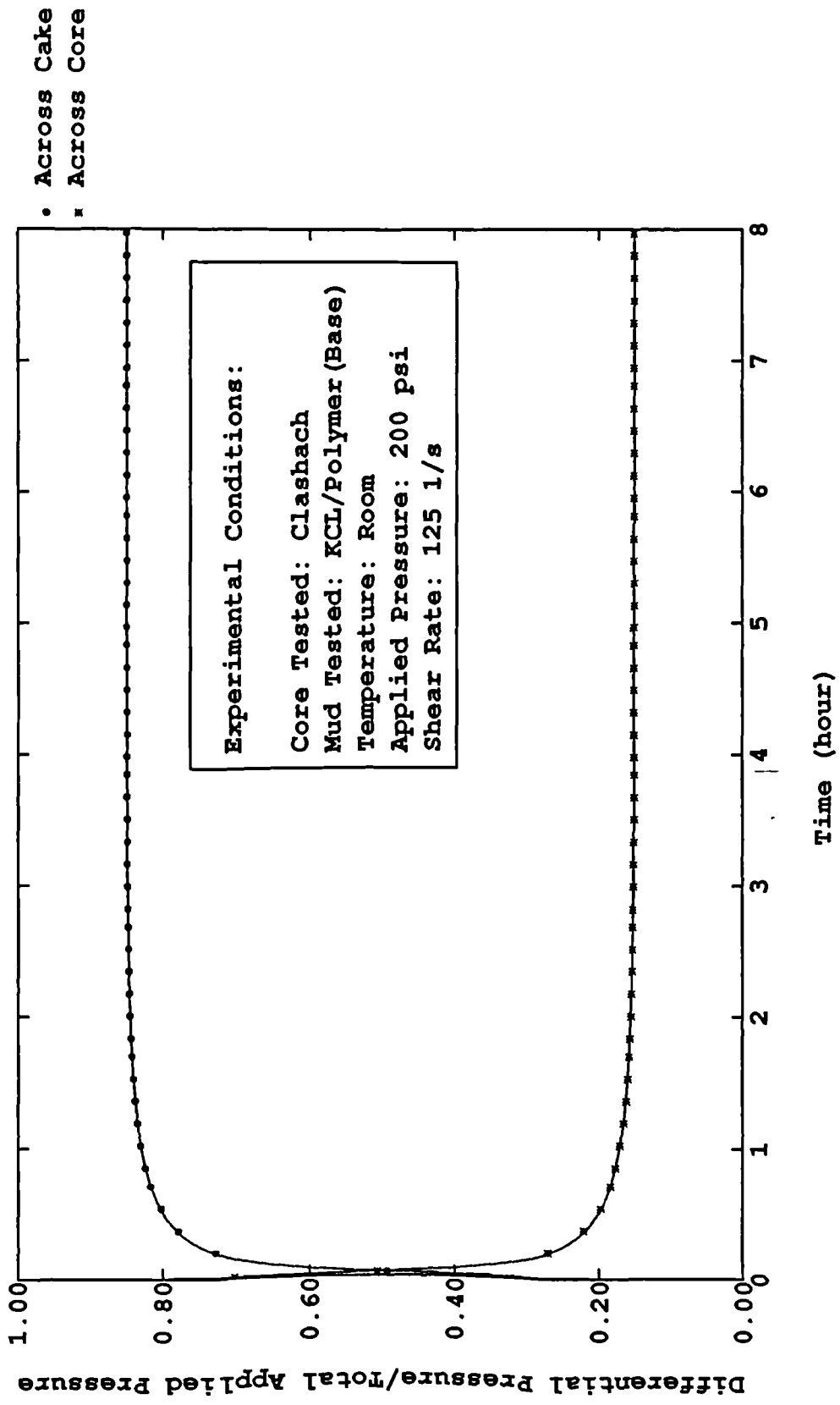


Figure (7-2.3) Pressure Differential Across Filter Cake and Filter Medium over the Total Applied Pressure as Function of Time for Dynamic Filtration

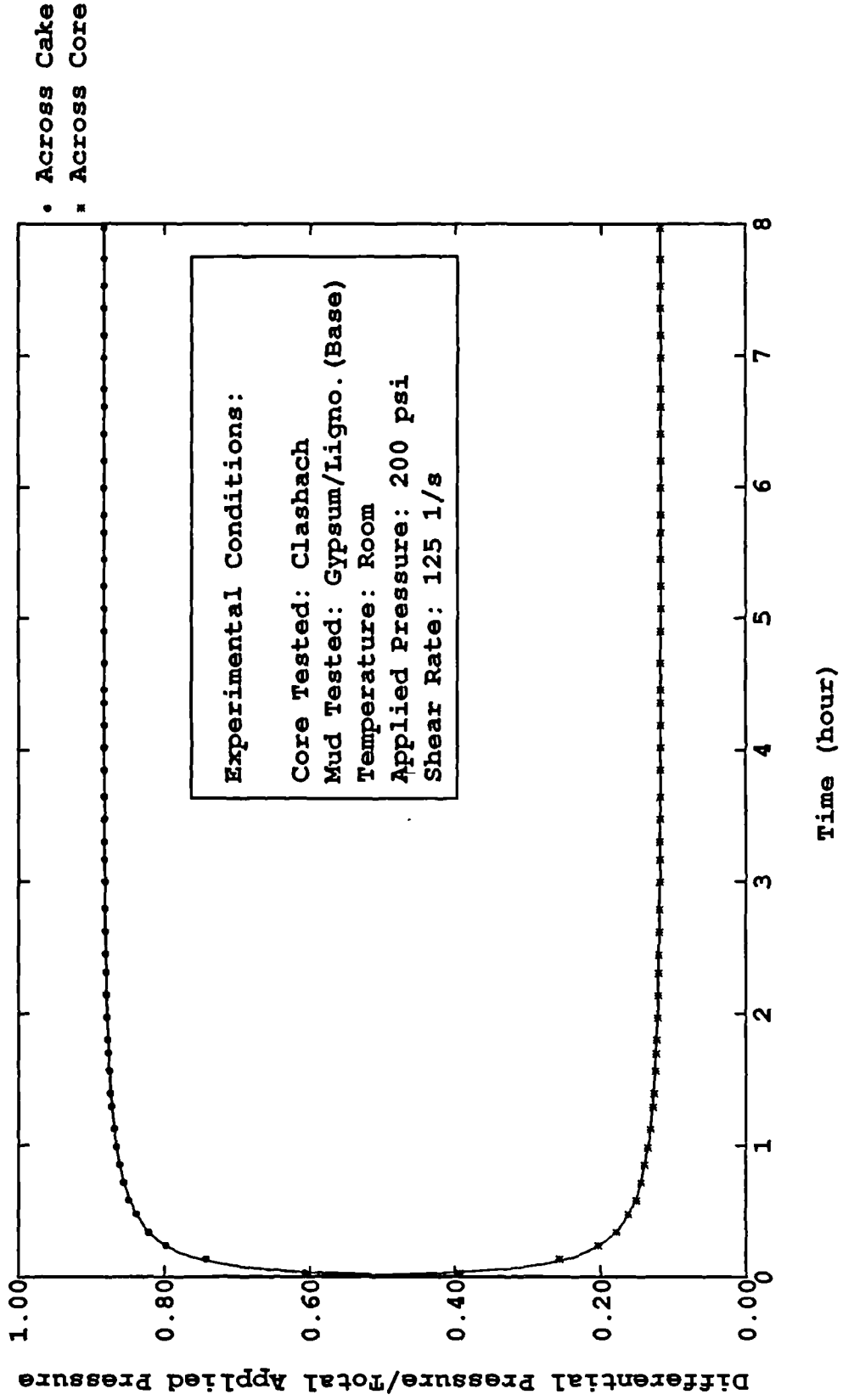


Figure (7-2.4) Pressure Differential Across Filter Cake and Filter Medium over the Total Applied Pressure as Function of Time for Dynamic Filtration

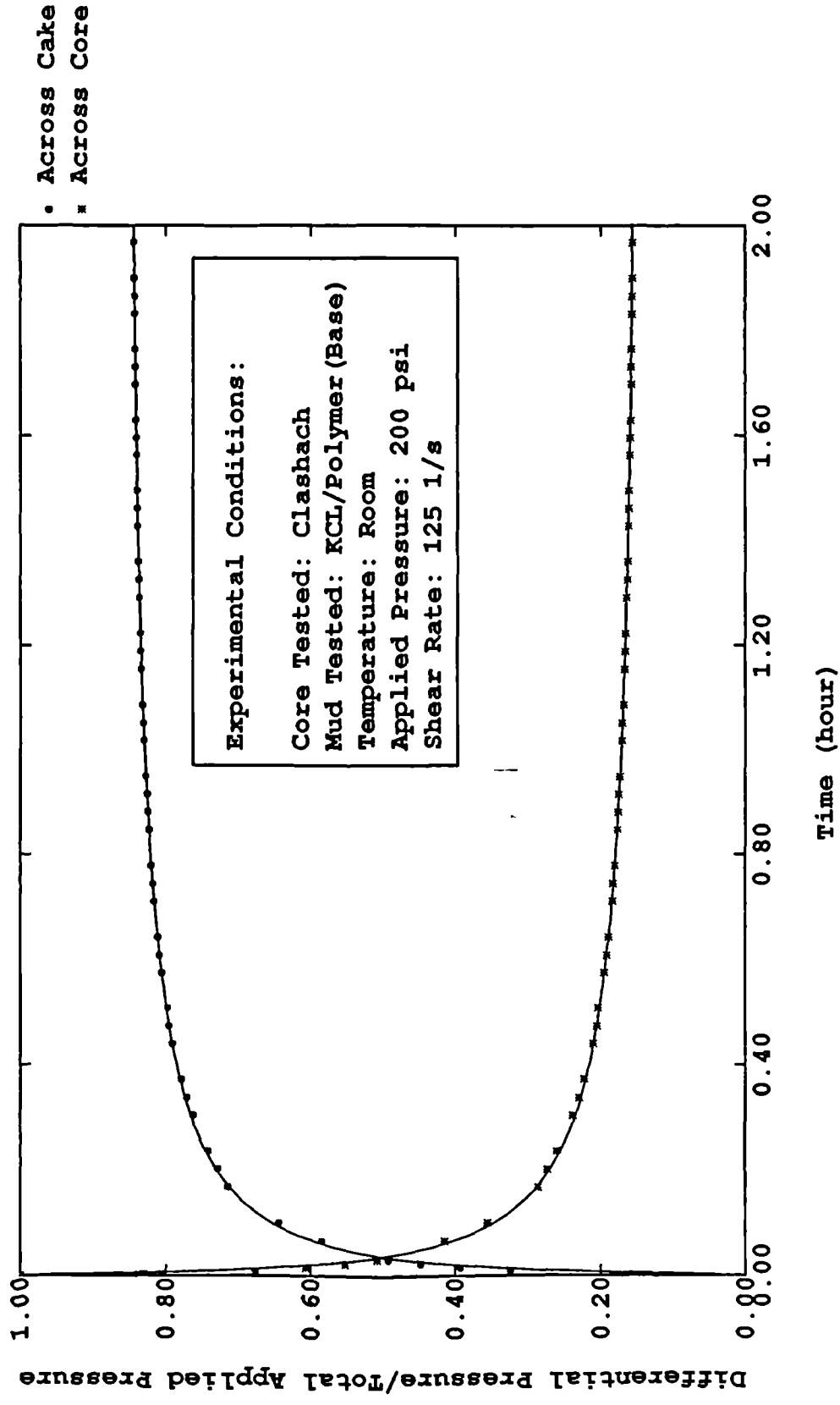


Figure (7-2.5) Pressure Differential Across Filter Cake and Filter Medium over the Total Applied Pressure as Function of Time for Dynamic Filtration

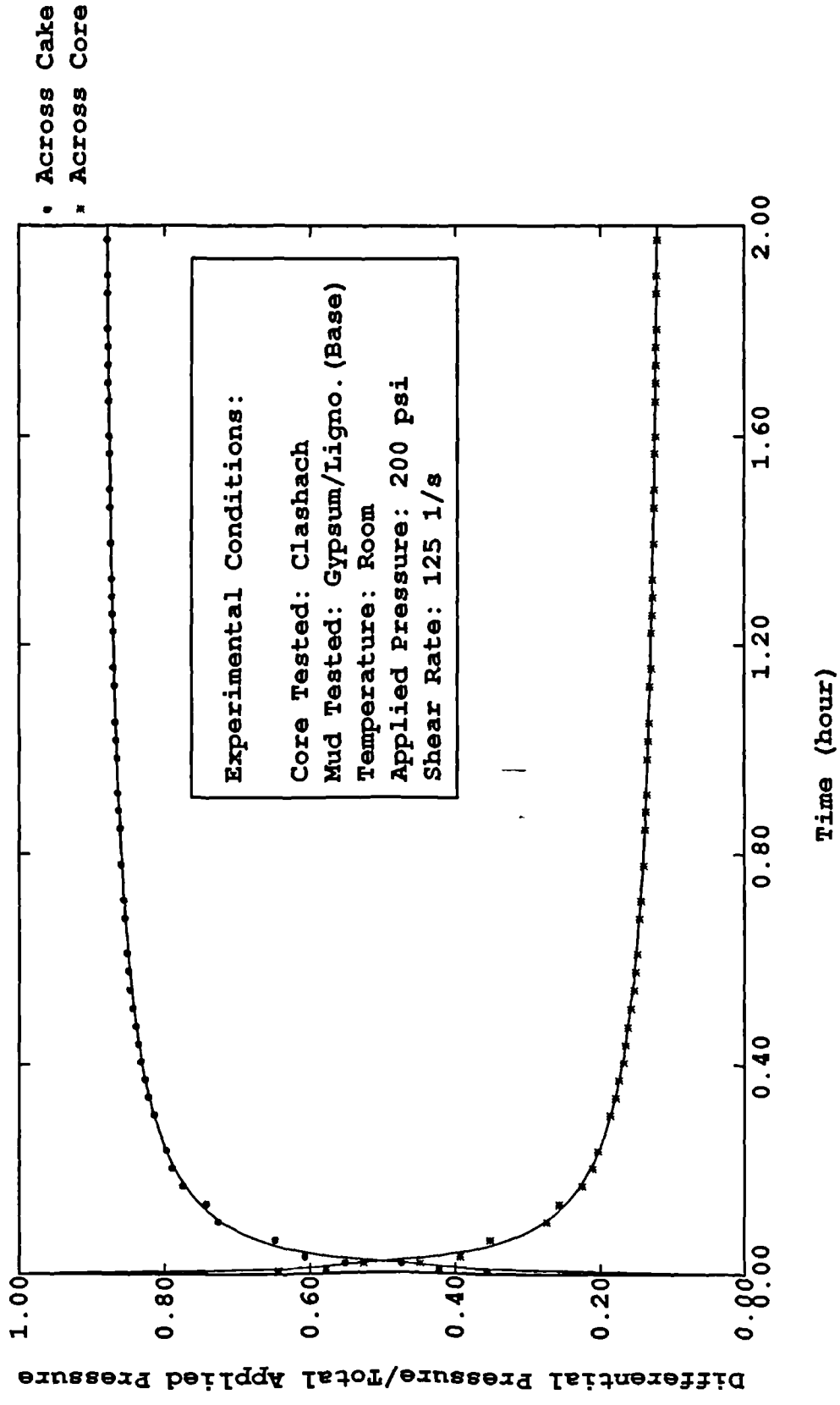


Figure (7-2.6) Pressure Differential Across Filter Cake and Filter Medium over the Total Applied Pressure as Function of Time for Dynamic Filtration

7.3 SUMMARY

7.3.1 Cake Erodability

Dynamic filter cakes differ from static cakes in that the soft surface layers of the static cake are not present in the dynamic cake⁹⁵. The surface can be eroded to an extent that depends on the shear stress exerted by the hydrodynamic force of the mud stream relative to the shear strength of the cake's upper layer. Obviously, the thickness of these soft surface layers (also called "transition region" which was originally defined by Ferguson and Klotz¹³ shown in Figure 2-1.1) would be the function of pressure, mud properties, temperature etc. When the shear stress produced by the mud stream attains a certain value which is big enough to erode all the soft surface layers, the mud stream would not wash away any solid filter cake and the erodability of the cake would be independent of the exerted shear stress.

Prokop¹⁰ made the direct measurement of the erodability of pre-formed filter cakes which were exposed to a circulation velocity of 300 ft/min (1.524 m/s). The circulating fluid was flowing in turbulent flow and was similar in composition to the filtrate from the muds which formed the cakes. A tenfold difference between the erosion rates was observed for the two muds tested. A caustic-quebracho-clay-barytes mud deposited a filter cake that would erode at 3×10^{-3} in/min (4.572 mm/hour), where as a clay-fresh-water mud deposited a filter cake that would erode at a rate of only 3×10^{-4} in/min (0.457 mm/hour).

In this study, the dynamic coefficients (B) obtained are from 0.859 Kg/m².s to 1.813 Kg/m².s for Seawater/KCL/Polymer mud, which correspond to erodabilities above from 0.072 mm/hr to 0.152 mm/hr. For Freshwater/Gypsum/Lignosulphonate mud, the

dynamic coefficients are from 0.860 Kg/m².s to 1.469 Kg/m².s, which correspond to erodabilities above from 0.080 mm/hr to 0.137 mm/hr. It should be noted that the erodability observed in this study is obtained when the cake is being formed.

7.3.2 Average Specific Cake Resistance

The experimental results presented in chapter five and six revealed that there is a big difference between the average specific resistance of static and dynamic cakes. It is clear that the average specific dynamic filter cake resistance is generally greater than the corresponding average specific static cake resistance. This may be caused by the plugging of the cake pore space because the small particles would be easier to invade the pore when they are moving cross the cake surface than when they are static.

Chapter Eight

COMPARISON OF PREDICTED AND EXPERIMENTALLY OBTAINED DATA

One of the purposes of this study was to predict filtration performance from laboratory tests data. This chapter presents the results produced by the models resulting from this work.

8.1 PREDICTIVE TECHNIQUE

If the general equation presented in chapter three is utilised to predict borehole filtration, the following important parameters must be determined:

- (i) The difference in properties of the filter cakes formed under static and dynamic conditions. i.e., average specific cake resistance, ratio of wet to dry cake mass;
- (ii) The effective filter medium resistance which is a function of applied pressure, shear rate, temperature, solids fraction in slurry and solids size distribution, the pore size and distribution in the core, etc.;
- (iii) The erodability of the dynamically deposited cake which would be a function of shear rate of mud, applied pressure, mud rheological properties, mud constituents, annular hydraulics, i.e., laminar or turbulent flow of muds, etc.

8.1.1 Estimation of Average Specific Cake Resistance

If the filter cake is incompressible and the particles from the slurry could not invade the filter cake, the average specific resistances of both static and dynamic filter cakes could be equal and in that case, the prediction of the dynamic filtration depends only upon the erodability of the dynamically deposited cake. In fact, the above case would never occur for drilling fluids. The results obtained in this study presented in chapter five and six clearly show a big difference between the dynamic filter cake specific resistances and static filter cake specific resistances. Therefore, extensive laboratory tests would be required if the accurate estimation of average specific cake resistance is necessary.

8.1.2 Prediction of Effective Filter Medium Resistance

If the filter medium material could not be invaded by the slurry particles and the first layer of the filter cake would form immediately after commencement of filtration, the spurt time should be very short and the effective filter medium resistance could be equal to the resistance caused by the filter medium itself. However, this is not the case in practice. So the effective filter medium resistance must be investigated before the filtration performance could be predicted. The prediction of the effective filter medium resistance should be efficient if the investigation was directed to determine the effects on the effective filter medium resistance of core material, original liquid permeability, pores sizes and their distribution, solids sizes and their distribution, pressure, temperature etc.

8.1.3 Determination of Erodability of Dynamically Deposited Cake

For static filtration prediction, this item could not be studied. However, the erodability of the dynamically deposited cake must be determined before the dynamic filtration equation could be used to predict the filtration performance. Generally, the erodability of dynamic filter cakes should be affected by variables such as, shear stress (or shear rate as favoured by some investigators), flow regime—turbulent or laminar flows, (if shear force is mechanical, this item is assumed to be laminar), pressure, temperature, mud properties which would control the strength of cake structure being eroded by either hydraulic or mechanical forces, etc.

8.1.4 Ratio of Wet to Dry Cake Mass or Cake Porosity

Many investigators have recognized that the classification of filter cakes as compressible and incompressible is unnecessary⁷⁶ and some have found that the average cake porosity is independent of time and filter cake geometry⁷⁹. Based on this result, the measured ratio of wet to dry cake mass would be valid and subsequently the cake porosity calculated directly from this ratio should be also valid. However, the effects of pressure and other parameters upon it should be determined by experimental tests. Whether the ratio of wet to dry cake mass varies between the static and dynamic cakes was not investigated during this study and simply the equivalence between them was assumed.

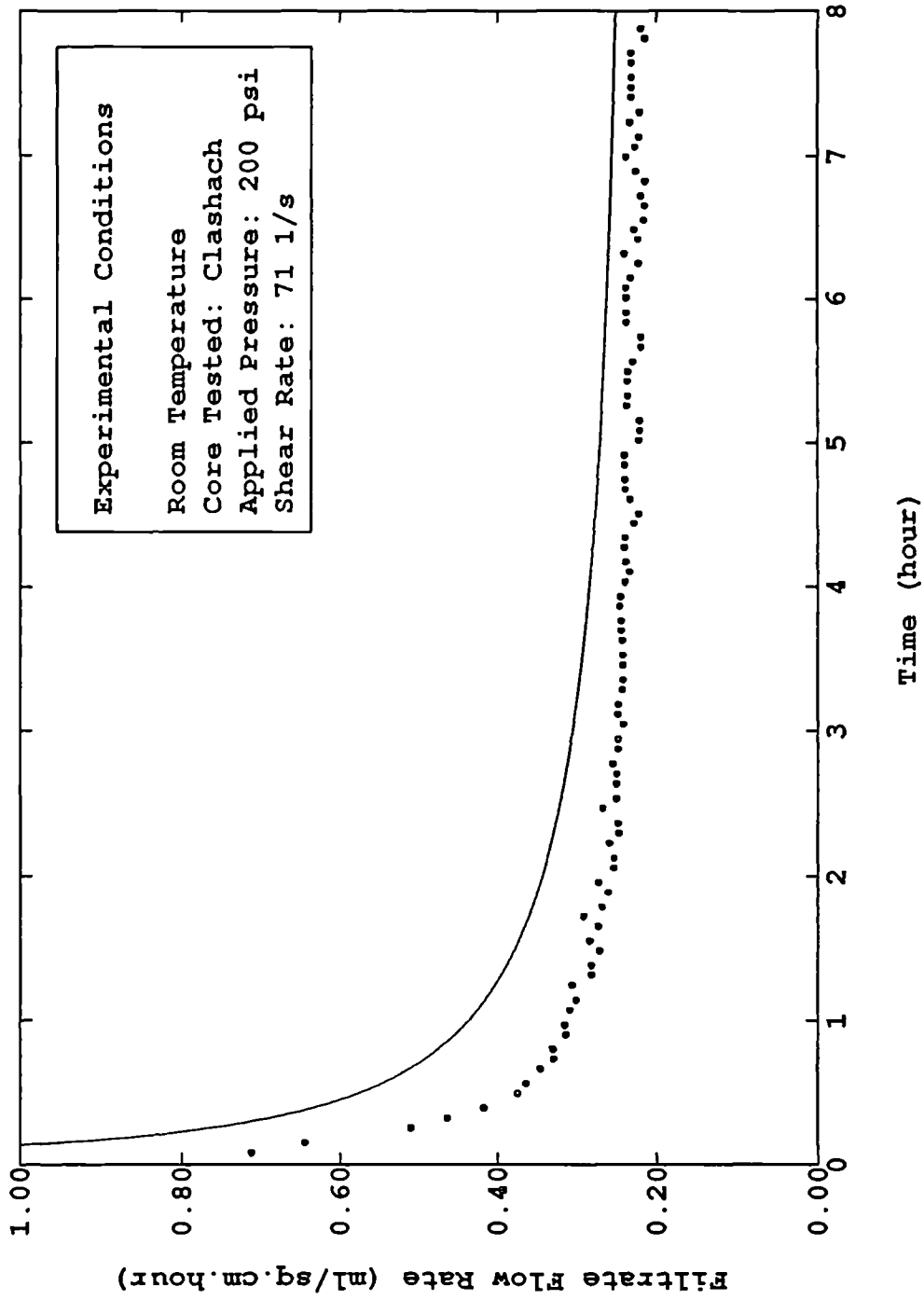
8.1.5 Assumptions on Spurt Time and Spurt Loss

The spurt loss might be obtained in laboratory tests and during the prediction, this value could be added directly to the cumulative filtrate volume.

8.2 PREDICTION OF DYNAMIC FILTRATION DATA FROM STATIC FILTRATION RESULTS

As pointed out earlier, it is possible to predict dynamic filtration data using the static filtration results such as, average specific cake resistance, effective filter medium resistance. An example for the prediction of dynamic filtration data using the statically obtained data is presented below:

The experiments were conducted on Seawater/KCL/Polymer mud system to compare the data predicted by dynamic equation and obtained experimentally. Figures(8-2.1) and (8-2.2) show the filtration flow rate and cumulative filtrate rate as a function of time respectively. The dots represent the measured experimental data and the smooth curves were plotted by the data predicted through dynamic filtration equation(6-2.5) in which m , α_{avg} , R_{meff} , t_{sp} , V_{sp} are correspondingly static experimental data and B is the dynamic experimental data obtained in chapter six. The predicted value are much higher than those obtained by experiment. However the two curves are rather similar in shape. It is understood that the difference between the test values and the theoretical values is caused by the difference between average specific resistance of dynamic cake and of static cake.



• Experimental
 Seawater/KCL/Polymer Mud

Figure (8 - 2.1) Comparison of Dynamic Filtration Predicted from Static Data and Experimental Results - Filtrate Flow Rate as a Function of Time

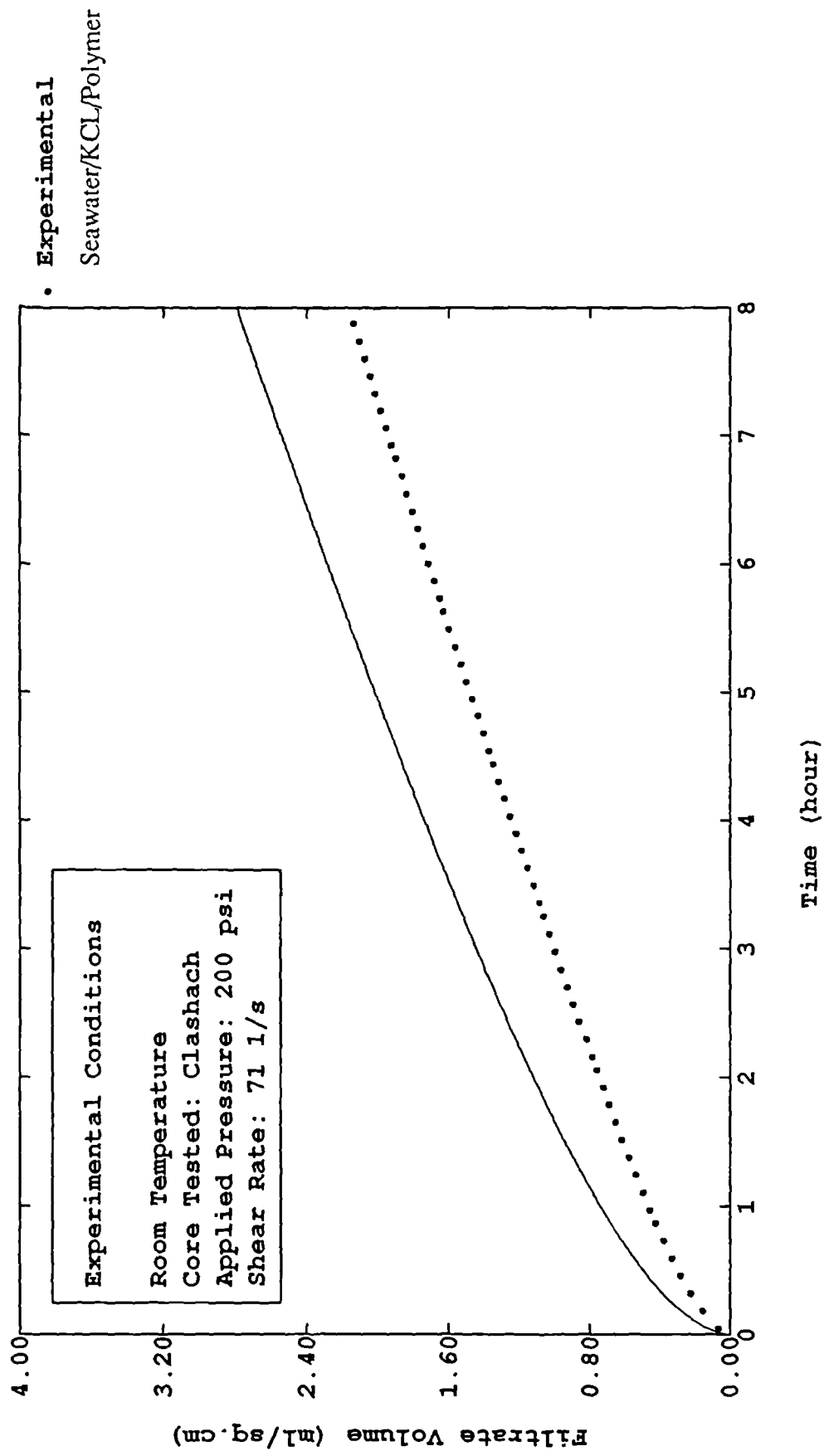


Figure (8 - 2.2) Comparison of Dynamic Filtration Predicted from Static Data and Experimental Results - Filtrate Volume as a Function of Time

8.3 PREDICTION OF FILTRATION DATA IN A SEQUENTIAL PROCESS

Static filtration of drilling fluids usually occurs after a dynamic cake has already been deposited upon the walls of the borehole. It is therefore necessary to predict the static fluid loss in which the filter cake forms upon a previously deposited dynamic filter cake and after that a dynamic filtration is usually resumed. In this case, a cyclical process occurs which can be by assuming three phases exist in a filtration process: dynamic-static-dynamic filtration. In the first phase, the prediction as discussed earlier in this chapter could be used. In the second phase, however, according to the static filtration equation(5-3.6), only the effective filter medium resistance is unknown because the other parameters can be obtained in a laboratory test. The effective filter medium resistance in this stage (second phase) would be the sum of the resistance caused by the dynamic filter cake that already deposited plus the effective filter medium resistance in the first phase. Based on this hypothesis, the static filtration upon a dynamic filter cake could be predictable. In the third phase, however, not only the effective filter medium resistance but also the cake erodability are unknowns according to equation(6-2.5). The effective filter medium resistance of third phase would be calculated by the effective filter medium resistance of second phase plus the filter cake resistance formed in the third phase. There is difficulty in determining the erodability of the filter cake in the third phase. The erodability would depend upon the thickness of the transition layer between mud cake and mud slurry which was defined by Ferguson and Klotz¹³. However, the transition region would become thinner after a static cake was deposited upon the dynamic cake because the pressure gradient decreased due to the huge static cake thickness. It is also necessary to note that the deposited static cake in second phase will not be removed unless the

pre-formed cake is to be removed by the resumption in mud flow. This has been addressed by a number of investigators, Some of which^{13,38} reported that the deposited cake could be wash away, but others¹⁰ presented the opposite conclusions. The experimental results conducted in this study show that a very little mud cake could be removed. This is evidenced by the operation that a very small increase in filtration rate occurs when the circulation (shear stress) is restarted. Therefore, in order to predict the data in the third phase, we assume that the filter cake deposited in the second phase could not be removed and the third phase would follow the normal dynamic filtration process.

Figure(8-3.1) and (8-3.2) are examples which show the filtrate flow rate and the cumulative filtrate volume as a function of time in a sequential filtration proceass at a pressure of 200 psi, respectively. The dots represent the experimental data points and the smooth curves represent the data generated by the general filtration equation in which the coefficients correspondent to the experimental conditions were obtained in chapter six.

Figure(8-3.3) through (8-3.6) are similar examples for two mud systems at a pressure of 50 psi.

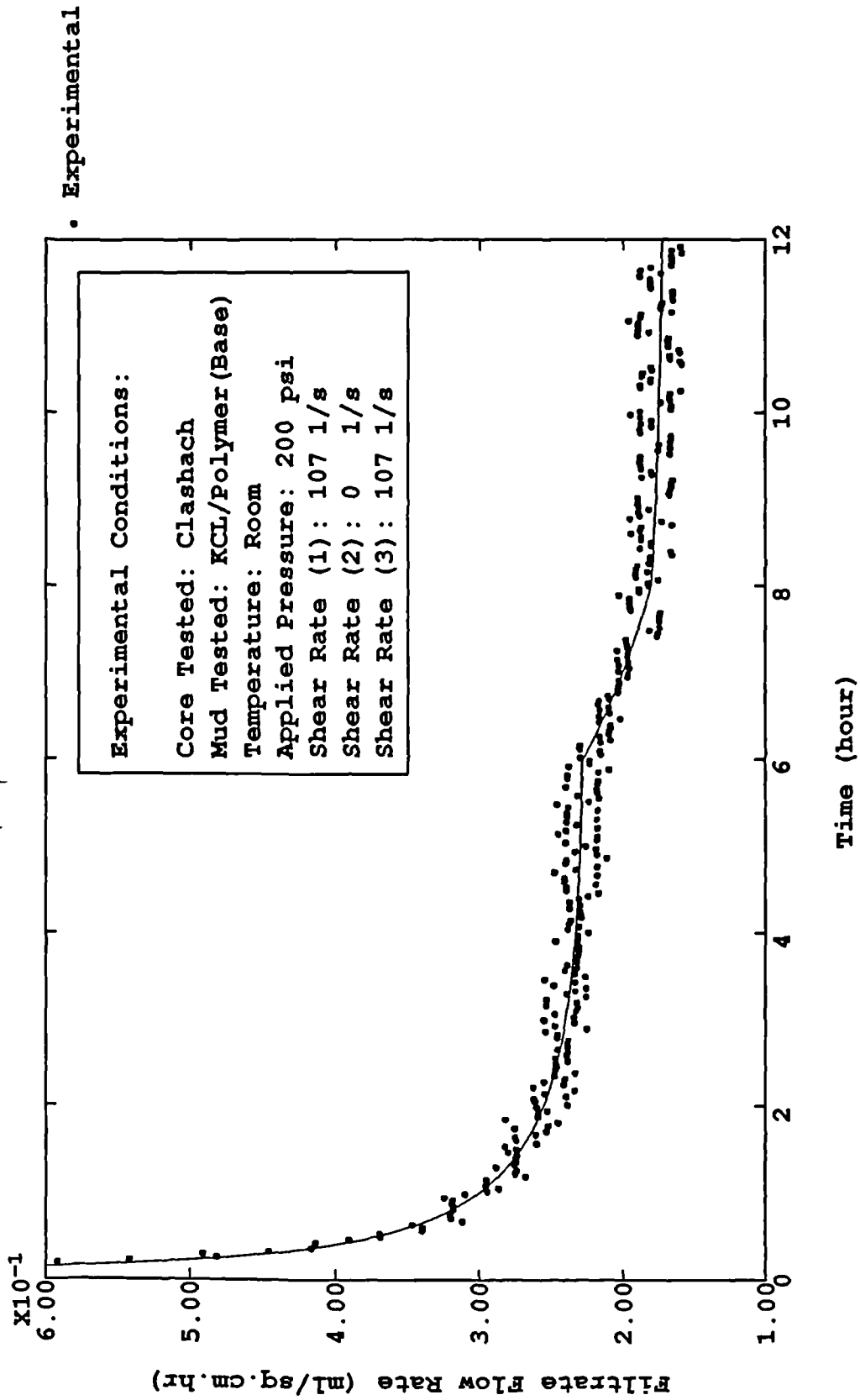


Figure (8-3.1) Filtrate Flow Rate as Function of Time for KCL/Polymer Mud in a Sequence of Dynamic-Static-Dynamic Process (Theoretically and Experimentally)

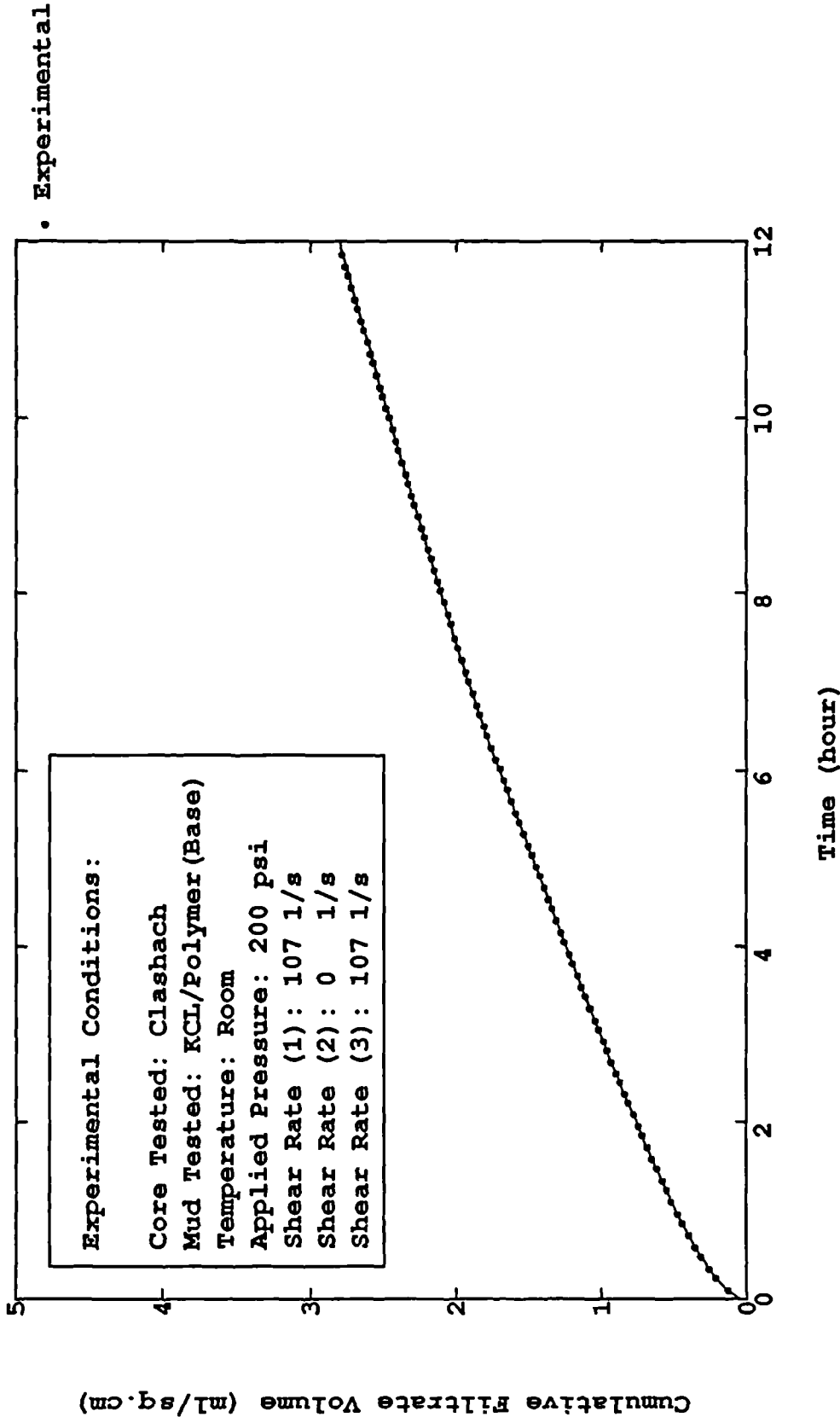


Figure (8-3.2) Cumulative Filtrate Volume as Function of Time for KCL/Polymer Mud in a Sequence of Dynamic-Static-Dynamic Process (Theoretically and Experimentally)

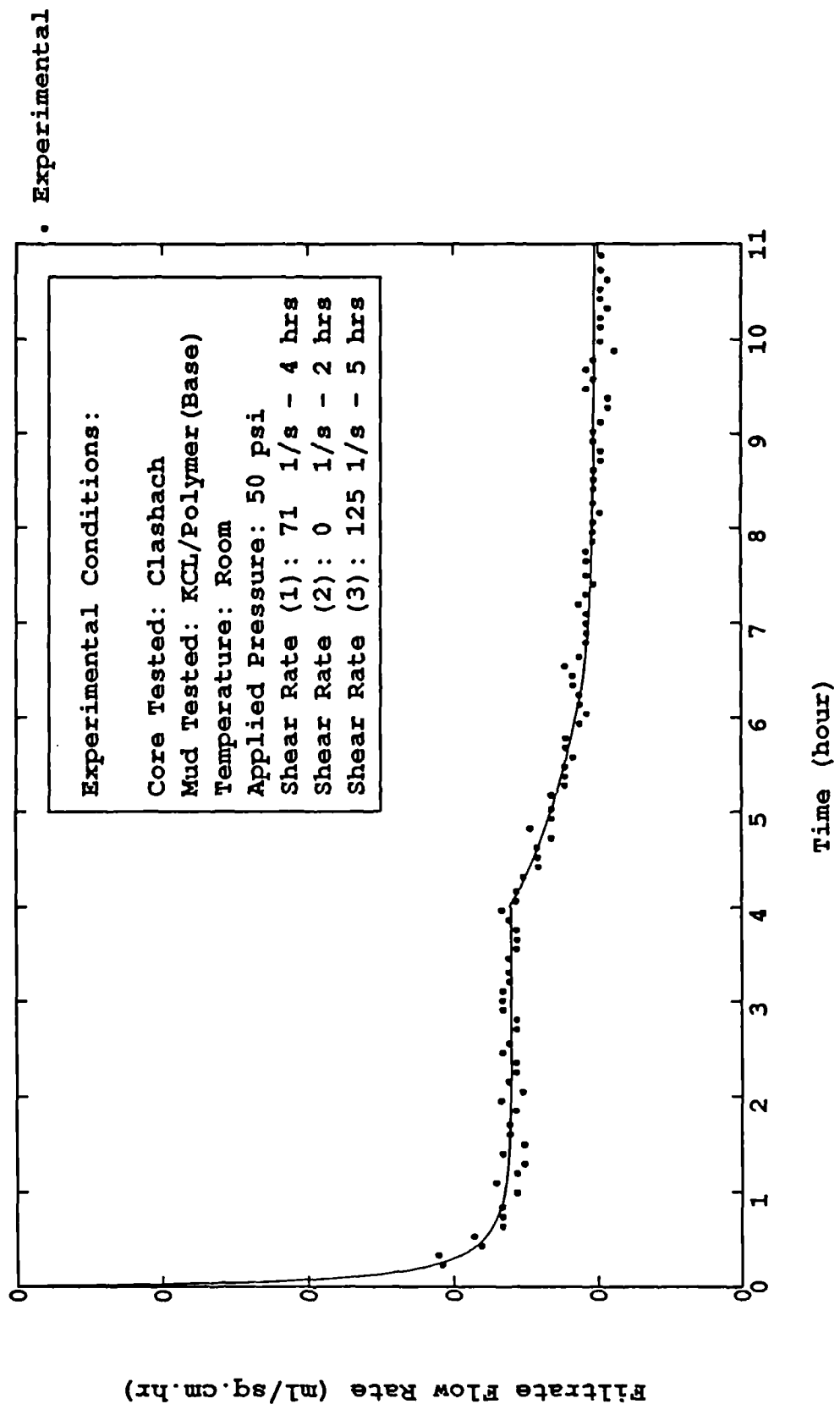


Figure (8-3.3) Filtrate Flow Rate as Function of Time for KCL/Polymer Mud in a Sequence of Dynamic-Static-Dynamic Process (Theoretically and Experimentally)

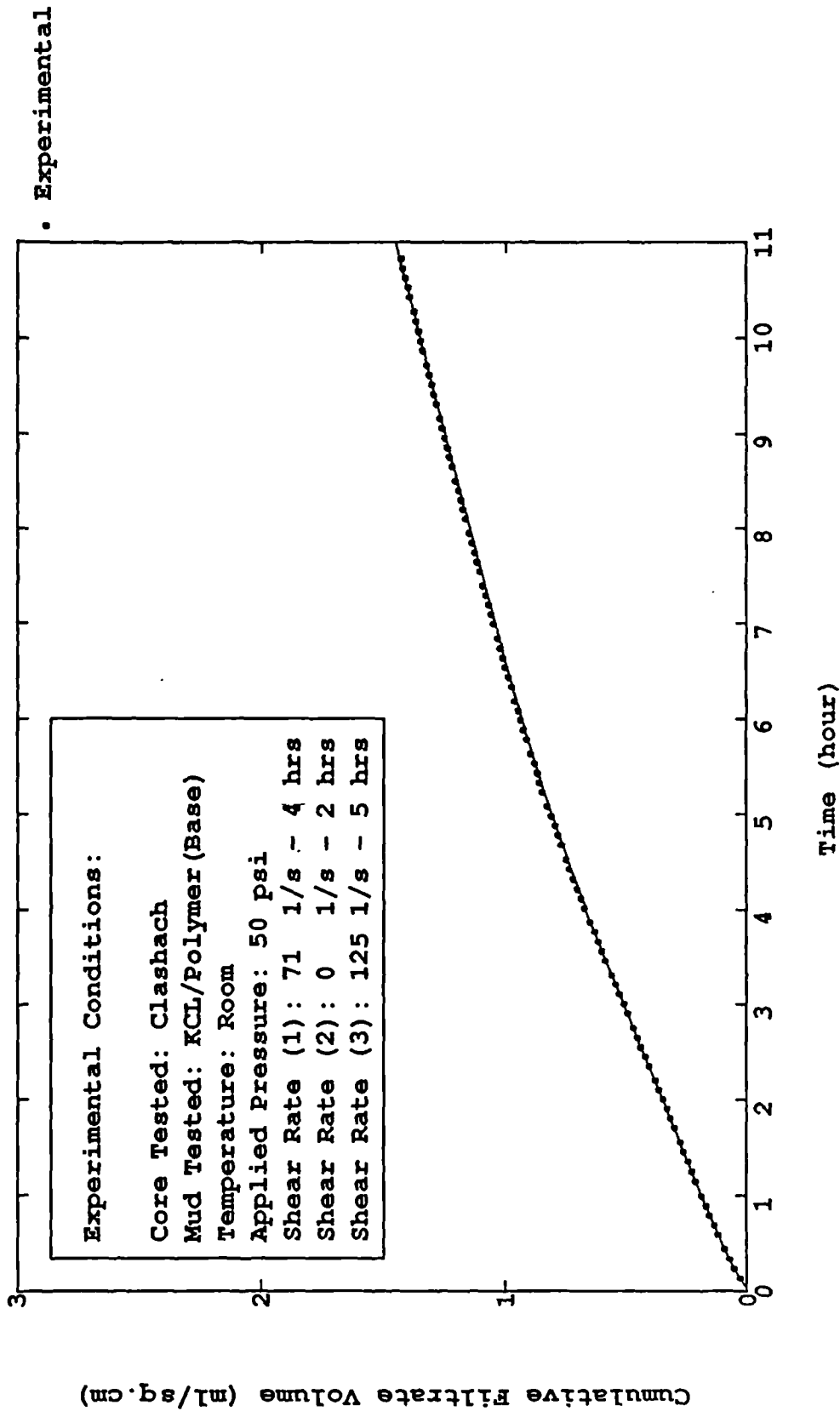
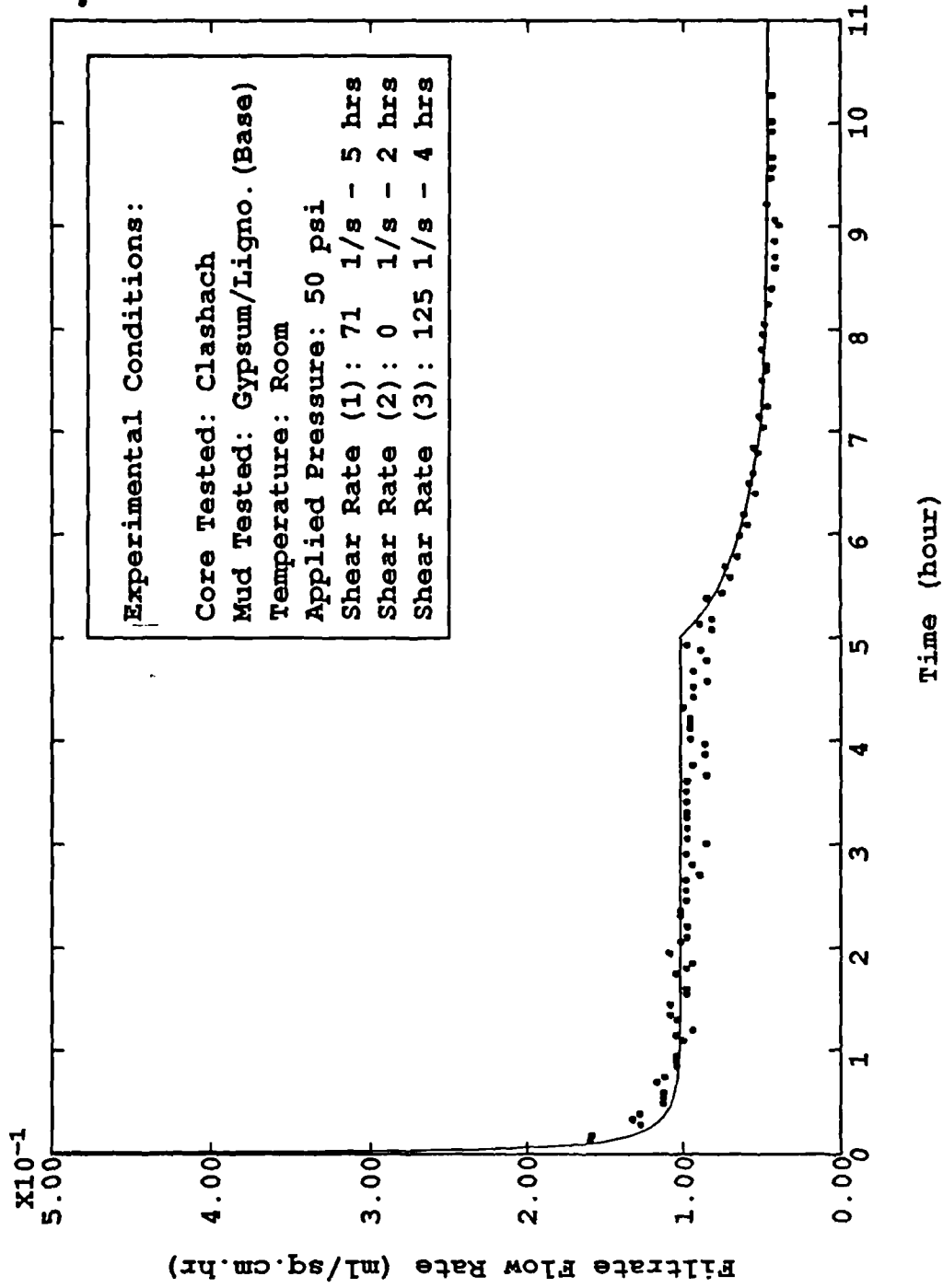


Figure (8-3.4) Cumulative Filtrate Volume as Function of Time for KCL/Polymer Mud in a Sequence of Dynamic-Static-Dynamic Process (Theoretically and Experimentally)



• Experimental

Figure (8-3.5) Filtrate Flow Rate as Function of Time for KCL/Polymer Mud in a Sequence of Dynamic-Static-Dynamic Process (Theoretically and Experimentally)

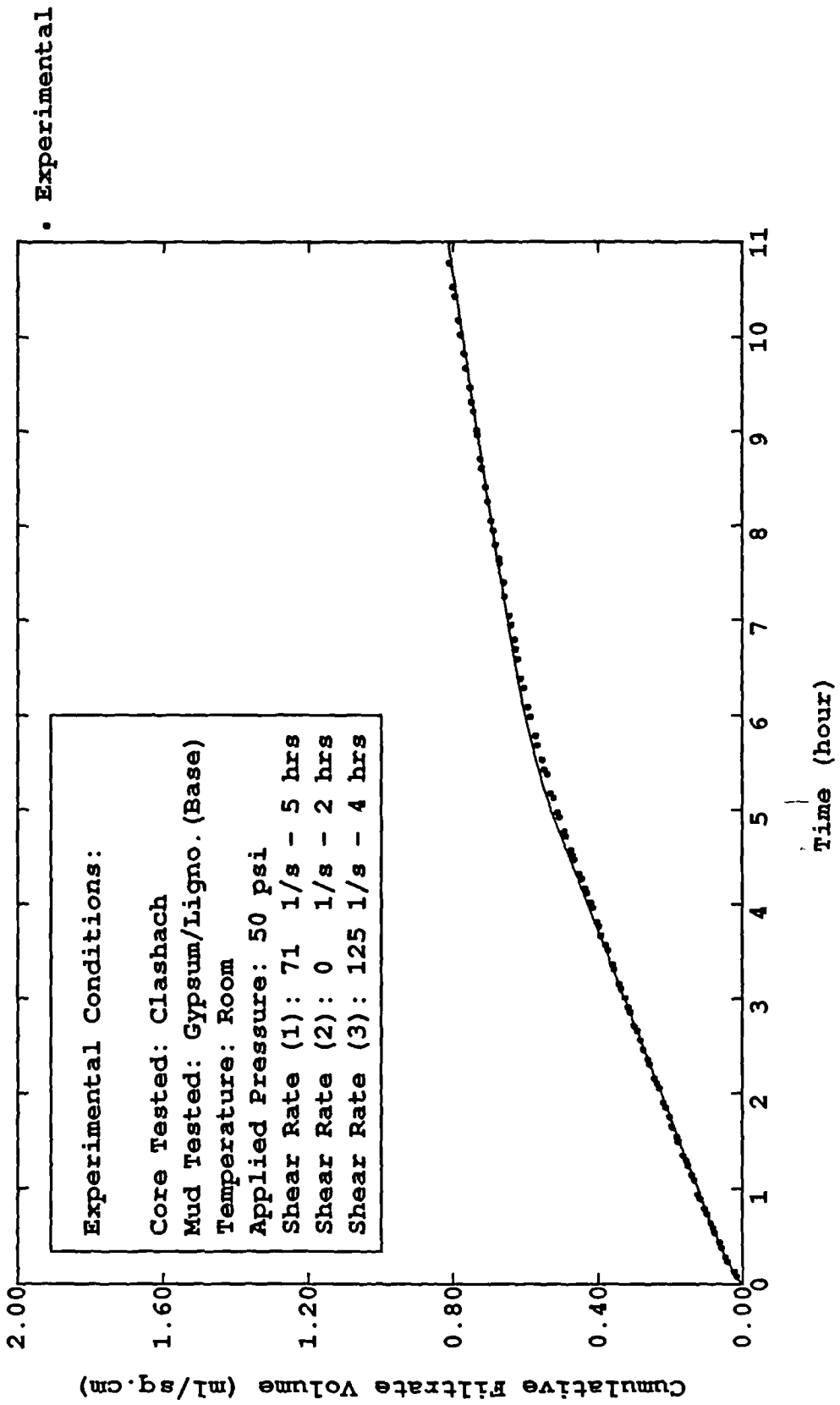


Figure (8-3.6) Cumulative Filtrate Volume as Function of Time for KCL/Polymer Mud in a Sequence of Dynamic-Static-Dynamic Process (Theoretically and Experimentally)

Chapter Nine

CONCLUSIONS

Previous chapters presented the results secured in this study both theoretically and experimentally. This chapter presents the conclusions which are drawn from this study in two separately sections.

9.1 EXPERIMENTAL CONCLUSIONS

9.1.1 Conclusions for Static Filtration Tests

1. The static filter cake thickness generally increased with increasing pressure for all muds tested. However, the increase in thickness would be faster when the barite concentration in slurry was at 140, 210 lbs/bbl. This supports the results that the filter cakes under these conditions would be less compressible.

2. The ratio of wet to dry cake mass decreased with increasing pressure for all muds tested. This decline was more substantial when barite concentration in slurry is at 50, 70 lbs/bbl. This supports the view that the filter cakes formed at these conditions would be more compressible.

3. Average specific cake resistance declined when the barite concentration increased and it would increase when the pressure increased. The effects of pressure on the average

specific cake resistance would be more significant when barite concentration in the slurry remained at a low level because the filter cake is more compressible at this condition. Thus effects would become weaker when the barite concentration was changed to a very high value. Also, the effect of pressure upon the average specific cake resistance would not be expressed by a “power law” relationship, which does not agree with Arthur⁹⁴. However, Tosun and Tiller⁷⁵ investigated the validity of the “power law” approximation and proposed that the “power law” approximate equations should not be used.

4. Static cake permeability for Seawater/KCL/Polymer mud tested in this study was observed between 0.3×10^{-6} and 5.2×10^{-6} darcy.

9.1.2 Conclusions for Dynamic Filtration Tests

1. The dynamic equilibrium filtration flow rate was attained at 2-4 hours for all muds tested. Specifically, the time to reach equilibrium for Freshwater/Gypsum/Ligno-sulphonate mud was less than that for Seawater/KCL/Polymer mud under the same conditions.

2. The spurt loss was very important for dynamic filtration which led to an enormous effective filter medium resistance and filtration then reached equilibrium at the end of spurt time. Figure(9-1.1) and Figure(9-1.2) show an example which illustrates this conclusion. It is clear that the cumulative filtrate volume increased linearly with time after commencement of filtration and the filtrate flow rate remained at a constant value thereafter.

3. The effect of shear rate (shear stress or annular velocity) on filtrate loss volume were quite complicated for both muds tested. This is in accord with the results reported by Peden⁸² that a maximum filtrate rate will occur at an intermediate value for the annular velocity. He explained the above phenomenon by two effects caused by annular velocity

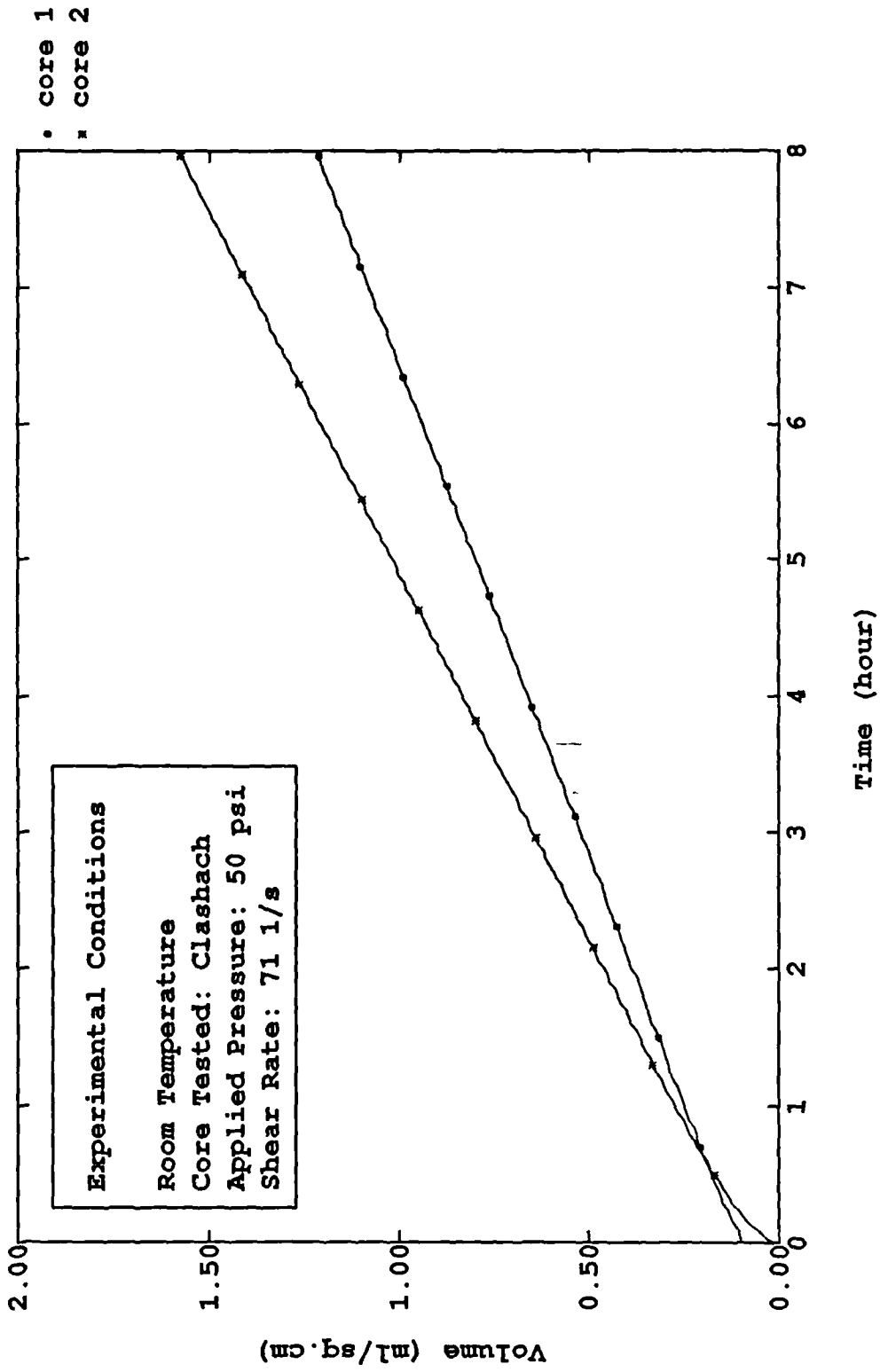


Figure (9 - 1.1) Examples illustrating the importance of the effective filter medium resistance relative to the cake resistance

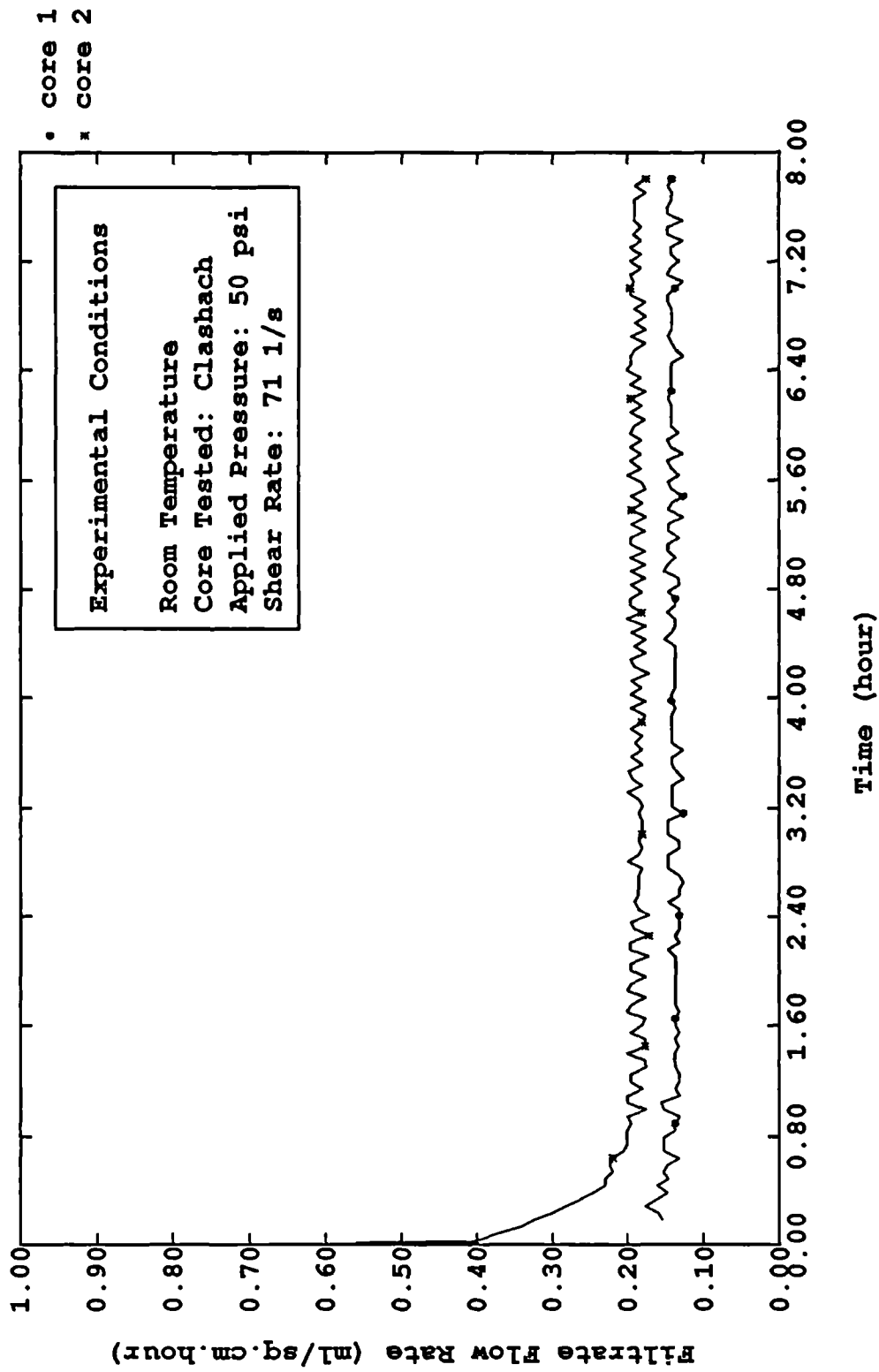


Figure (9 - 1.2) Examples illustrating the importance of the effective filter medium resistance relative to the cake resistance

upon the filtration systems: (a) to erode filter cakes; (b) to lower the permeability of the filter cake either by mechanical sorting or by changing the characteristics of the constituent molecules. He further concluded that at lower annular velocities the erosion mechanism predominates leading to increased fluid loss, at high rates, despite the increased mechanical erosive forces, the decline in cake permeability controls the fluid loss and hence a trend towards a reduction in fluid loss is observed.

3. The effect of pressure upon average specific cake resistance was demonstrated clearly for Freshwater/Gypsum/Lignosulphonate mud, which the average specific cake resistance increased with increasing in pressure. But it is rather complex for Seawater/KCL/Polymer mud. The “power law” relationship between average specific cake resistance and the differential pressure could not be applied as well.

4. The filter cakes formed under static and dynamic conditions could not be or at least were very hard to remove. The experimental results in this study suggested that only a little minimal increase in filtrate flow rate would occur. However, the removal of deposited cakes should depend upon a lot of factors such as pressure, temperature, the magnitude of shear rate on the cake surface, and whether or not the flow is turbulent or laminar, etc.

5. The erodability of dynamically deposited cake, K_{τ} , was found to be within the ranges of 0.761×10^{-5} - 1.778×10^{-5} Kg/N.s for Seawater/KCL/Polymer mud, and 0.354×10^{-5} - 0.572×10^{-5} Kg/N · s for Freshwater/Gypsum/Lignosulphonate mud.

9.2 GENERAL CONCLUSIONS

1. The modified classic static filtration equation which was initiated by Glenn *et al.*¹⁵ and Kozicki *et al.*⁹⁶ and was improved by Arthur⁹⁴ showed substantial advantages over the others when it is used to fit the static filtration data of drilling fluids.

2. The effective time of commencement of filtration, t_0 for a few of the static filtration tests exceeded the maximum range that observed by Arthur⁹⁴. Arthur⁹⁴ obtained a range of -28.79 to 29.33 seconds whereas the maximum of t_0 in this study reached to 3 minutes. This may be caused by the use of the heterogeneous Clashach cores.

3. The proposed dynamic filtration equation showed a very good agreement with the experimental data. Using cake characteristics observed in static filtration tests such as m , (ratio of wet to dry cake mass), the average specific dynamic cake resistance and cake erodability were calculated. It should be noted that in the above calculation, m was assumed to be equivalent for both static and dynamic cakes. Obviously, this would lead to errors. Unfortunately, the dynamic cake characteristics could not be measured owing to the extremely limited thickness of the cake deposited.

Chapter Ten

RECOMMENDATIONS FOR FUTURE WORK

The author would like to make following recommendations in three sections. Namely:

- (i) Filtration Modelling;
- (ii) Filtration Equipment;
- (iii) Theoretical Study of Filtration of Drilling Fluids.

10.1 FILTRATION MODELLING

10.1.1 Further Verification of Dynamic Filtration Equation Under Downhole Conditions

The fundamental basis of equipment utilized in this study is correct, but it might be questionable whether it can be used for routine tests, because the angle between the cone surface and the bottom plate surface is limited to 2 degrees and therefore, limited space exists for the filter cake to deposit on the core surface if the internal diameter of filtration cell is not big enough.

In this study, the dynamic filtration equation has already been shown to be in a substantial agreement with the experiment data under room temperature. However, further experimental data are required before it can be utilised to predict field filtration

data.

Firstly, the range of shear rates should be extended. Shear rates of 70-130 1/s have been used in the tests, however in actually drilling conditions, the shear rate range might be between 70-300 1/s (sometimes even higher). Also, whether the annular flow is turbulent or laminar would be a factor affecting dynamic filtration data or erodability.

Secondly, the high pressure/high temperature (HPHT) conditions should be investigated. Because temperatures in excess of 175 °F to 200 °F alter some commonly used drilling fluids additives, therefore the HPHT test should become the primary filtration control standard when the bottom hole temperature reaches this level. Usually the conditions for running HPHT filtration tests are at 300 °F temperature and 500-psi differential pressure. But the current procedure calls for a 500-psi pressure differential and the test temperature should approximate wellbore temperature. The effect of temperature was not studied and the pressure differential did not exceed 500-psi in this research programme due to equipment limitation.

Thirdly, the effects of mud compositions should be extensively tested. The dynamic coefficients would be influenced by those parameters which change the characteristics of the mud.

Fourthly, the filtration tests of oil base muds should be conducted.

10.1.2 Determination of Dynamic Filter Cakes Characteristics

So far, from the drilling fluids filtration history, very little has been published on dynamic filter cake characteristics. The thickness, ratio of wet to dry cake mass and the relevant average porosity of the dynamic filtration cakes, such data would be very useful to the modelling and prediction of dynamic filtration.

10.1.3 The Study of the Effect of Effective Filter Medium Resistance

The effective filter medium resistance would be a function of following parameters:

- (i) pressure,
- (ii) temperature,
- (iii) shear rate,
- (iv) solids fraction in slurry,
- (v) solid particle size distribution,
- (vi) filter medium liquid permeability,
- (vii) the surface pore size distribution of the filter medium.

The author considers that the particle and pore size distribution could be the decisive factors in defining effective filter medium resistance and suggest that an extensive study on this subject should cover both static and dynamic filtration tests. An understanding of pore plugging and the sizing of particulates for bridging in real (or closely simulated) formations may lead to some real progress in drilling fluids management and to lower drilling costs. The significance of the subject could be more if the people consider the filtration beneath-the-bit because in this case, the external filter cake deposited is instantly scraped and the internal cake formation is dependent upon the solid particle and pore size distribution, therefore the effective filter medium resistance is the filtration resistance.

10.1.4 Fluid Loss Study and Associated Formation Damage

One of the main objectives of any future filtration study could be to investigate the formation damage caused by the fluid loss. Therefore, it is believed that it would be the

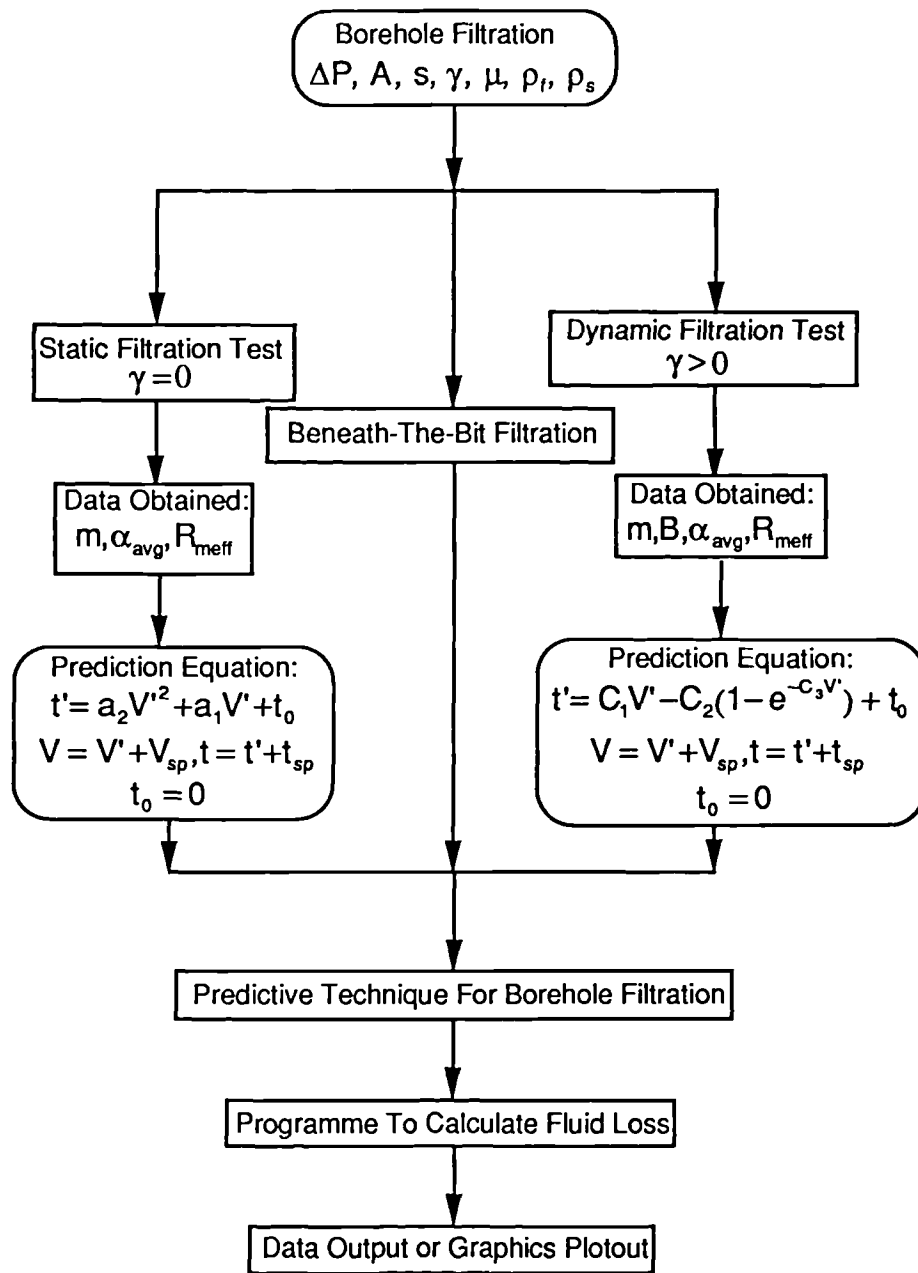
best way to conduct formation damage investigation while the filtration study is processing. Figure(10-1.1) showed the relationship between fluid loss and associated wellbore parameters and Figure(10-1.2) listed the borehole filtration prediction program.

10.2 FILTRATION EQUIPMENT

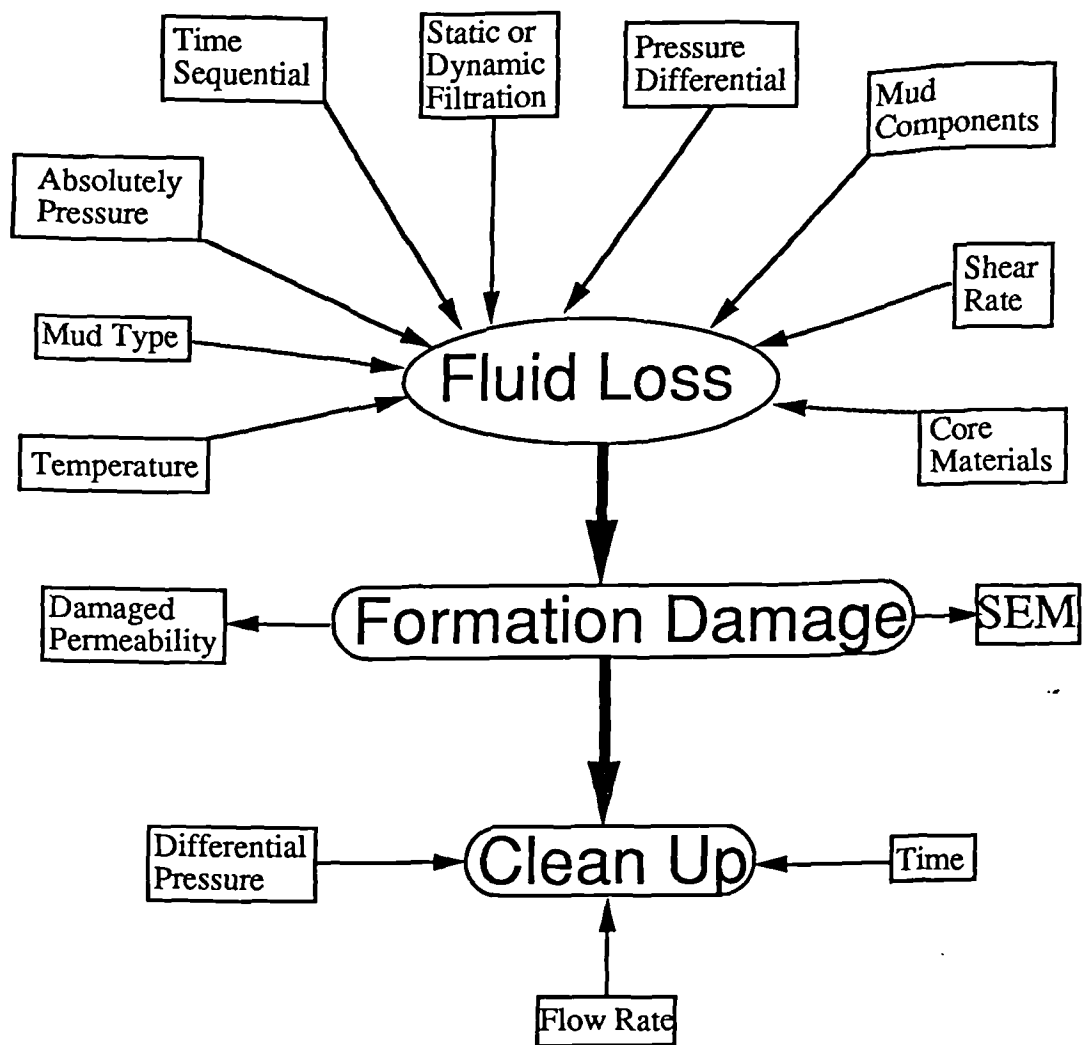
In order to simulate filtration in the drilled well more closely, it is necessary to limit the growth of the filter cake by either liquid or mechanical erosion. Over the years, a number of investigators have studied dynamic filtration in specially designed apparatus^{6,10,13,16,24}. The most meaningful results were obtained in systems that either closely simulated conditions in a drilling well, or which permitted the rate of shear at the surface of the cake—which is the critical factor limiting ^{cake} growth—to be calculated.

Ferguson and Klotz¹³ came close to simulating well conditions by measuring filtration rates through permeable lumnite cement and sand cylinders in a model well using full-size drilling tools. Horner *et al.*¹⁶ used a microbit drilling machine and rock cores. Novak and Krueger⁹ observed filtration rates through cores exposed on the side of an annulus through which mud was being circulated. A mechanical scraper enabled filtration conditions under the bit to be simulated when desired.

The rate of shear at the cake surface can be calculated in systems, such as that of Prokop¹⁰, in which mud is circulated under pressure through a permeable cylinder. The internal diameter of the cylinder should be large relative to the thickness of the filter cake so that the growth of the cake does not change the internal diameter significantly, and thereby change the rate of shear. Bezemer and Havenaar²⁴ developed a compact and very convenient dynamic filtration apparatus as shown in Figure(10-2.1), in which mud was filtered into a central core or sleeve of paper, while being sheared by an outer concentric cylinder rotating at constant speed. The equilibrium filtration rate and cake thickness were related to the rate of shear prevailing at the conclusion of the test.



Figure(10-1.1) A Schematic of the Computer Programme To Predict Wellbore Fluid Loss of Drilling Muds



Figure(10-1.2) A Schematic of Study on Relationship Between Fluid Loss and Wellbore Parameters and Associated Formation Damage

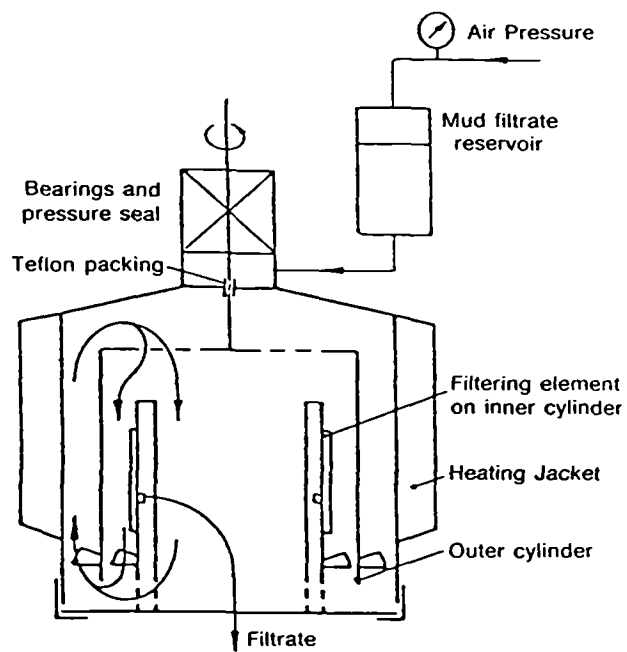


Figure (10 - 2.1) Schematic diagram of concentric cylinder dynamic filter tester

In order to simulate the bottom hole conditions, an ideal experimental filtration system might be a multifunctional circulating system in which mud is circulated around a closed circuit while being maintained at a designed temperature by heating coils, after equilibrium temperature and shear conditions have been obtained, various mud properties can be either intermittently or continuously measured by switching the flow through branch loops containing the appropriate apparatus. For instance, viscosity can be measured by passing the flow through a straight section of pipe of accurately-known internal diameter and measuring the differential pressure between two pressure taps thereon. The dynamic filtration rate can be measured by flowing the mud through permeable cylinders.

Wyant's³³ circuit as shown in Figure(10-2.2) includes high shear valves, which rapidly break down clay aggregates and rigid gel structures and a filtration cell and a corrosion unit. A more elaborate system by Lautrec³² enables rheological properties, and static and dynamic filtration, to be measured at flow rates upto 4 m/s, temperature upto 250 °C, and pressure upto 7250 psi.

10.3 THEORETICAL STUDY OF DYNAMIC FILTRATION —MULTIPHASE THEORY OF CAKE FILTRATION

Survey of the classic filtration theory(empirical analysis) in chemical engineering suggest that without the application of the multiphase cake filtration theory, the progress in cake filtration which has been essentially stagnant for more than three decades, would not occur^{65,99}.

The major disadvantages of empirical models are that they are usually limited in application to specific multiphase systems, have a narrow range of validity, must be independently verified for each substance and, hence, required a considerable amount of

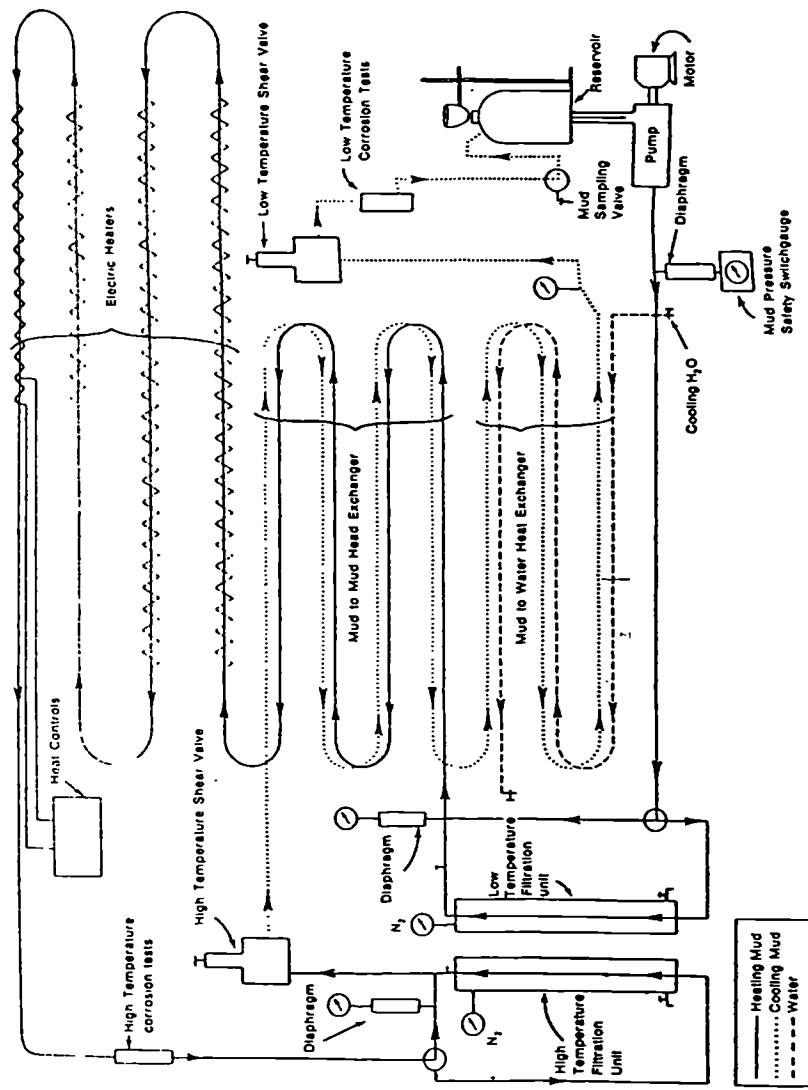


Figure (10 - 2.2) Multifunctional circulating system.

experimental principles to all substances that meet the assumptions used to develop the theory.

The development of multiphase equations of change using volume averaging technique and their application to the filtration process have been given by Tosun¹⁰¹ and Willis and Tosun⁷³.

The following summary of the advantages of multiphase theory over the empirical analysis were given by Willis *et al.*¹⁰³.

1. The procedure is systematic and requires specific assumptions to eliminate terms from the general equations.
2. The gross dimensions of the porous media can be of arbitrary geometry.
3. The interstitial boundary conditions appear as surface integrals in the multiphase equations which eliminates the need to specify any restrictive pore geometry (i.e., a bundle of parallel capillary tubes).
4. There is a continuity and motion equation for each phase, a total of eight scalar equations, rather than the rate expression and mass balance of the empirical approach.
5. The equations are applicable to liquid phases that are Newtonian or non-Newtonian and particulate phases which can be mobile, rigid or elastic, or soluble.

One of most important advantages is that this approach provides a rigorous framework for further study¹⁰².

If the filtration process is isothermal and composed of a solid particulate phase and continuous liquid phase, then there are two continuity conditions and two motion equations. The motion equations contain terms that represent the inertial, viscous, pressure, interfacial drag and the gravity forces.

Darcy's law can be obtained from the liquid phase equation of motion if the inertial force and viscous force are neglected. The remaining two terms represent the pressure

and drag forces and constitute Darcy's law. Such a simplification of the general liquid phase equation of motion has the following implications. Removing the inertial force means that the equation of motion is not explicitly dependent on time and hence Darcy's law holds at each instant throughout filtration. The absence of the viscous force implies that for a cylindrical filtration, the velocity profiles have no radial dependence and are flat. Willis and Tosun⁷³ showed by order of magnitude analysis that the drag and the pressure forces are greater than the inertial and viscous forces by about 6 orders of magnitude.

The solid particulate equation of motion is satisfied identically if the particulates do not deform under the stress that exist in a filter cake. This assumption does not , however, restrict the motion of these non-deformable particulates.

REFERENCES

1. Jones, P.H. and Babson, E.C. : "*Evaluation of Rotary Drilling Muds*". API **Drilling and Production Practice**, 1935, pp. 22-33
2. Jones, P.H. : "*Field Control of Drilling Mud*". API **Drilling and Production Practice**, 1937, pp. 24-29
3. Williams, M. and Canon, G.E. : "*Evaluation of Filtration Properties of Drilling Muds*". **The Oil Weekly**, June 20, 1938, pp. 25-32
4. Larsen, H.D. : "*Determination the Filtration Characteristics of Drilling Muds-Part I and Part II*". **The Petroleum Engineer**, Sept./Nov. 1938, pp. 42-48, 50-59
5. Byck, H.T. : "*Effect of Temperature on Plastering Properties and Viscosity of Rotary Drilling Muds*". **Pet.Trans. of AIME**. Vol. 136, 1940, pp. 165-173
6. Williams, M. : "*Radial Filtration of Drilling Muds*". **Pet.Trans. of AIME**. Vol. 136, 1940, pp. 57-69
7. Byck, H.T. : "*The Effect of Formation Permeability on the Plastering Behavior of Mud Fluids*". API **Drilling and Production Practice**, 1940. Also in **Oil and Gas Journal**, Vol. 39, No. 3, May 30, 1940, pp. 50-51
8. Gates, G.L. and Bowie, C.P. : "*Correlation of Certain Properties of Oil Well Drilling Fluids with Particle Size Distribution*". **Unite States Bureau of Mines**, R.I. 3645, 1942, pp. 1-22
9. Nowak, T.J. and Krueger, R.F., : "*The Effect of Mud Filtrates and Mud Particles upon the Permeabilities of Cores*". API **Drilling and Production Practice**, 1951, pp. 164-181
10. Prokop, C.L. : "*Radial Filtration of Drilling Muds*". **Pet.Trans. of AIME**. Vol. 195, 1952, pp. 5-10
11. Schremp, F.W. and Johnson, V.L. : "*Drilling Fluid Filter Loss at High Temperature and High Pressures*". **Pet.Trans. of AIME**. Vol. 195, 1952, pp. 157-162
12. Beeson, C.M. and Wright, C.C., : "*Loss of Mud Solids to Formation Pores*", **The Petroleum Engineer**, Aug. 1952, pp. B40-B52.
13. Ferguson, C.K. and Klotz, J.A. : "*Filtration From Mud During Drilling*". **JPT**, Feb., **Pet.Trans. of AIME**. Vol. 201, 1954, pp. 29-42
14. Havenaar, I. : "*Mud Filtration at the Bottom of the Borehole*". **Pet. Trans. of AIME**. Tech. Note 337, 1956, p. 312
15. Glenn, E.E., Slusser, M.L. and Huitt, J.L. : "*Factors Affecting Well Productivity-I. Drilling Fluid Filtration*". **Pet.Trans. of AIME**. Vol. 210, 1957, pp. 63-68

16. Horner, V., White, M.M., Cochran, C.D. and Deily, F.H. : "*Microbit Dynamic Filtration Studies*". *Pet.Trans. of AIME*. Vol. 210, 1957, pp. 183-189
17. Cunningham, R.A. and Eenick, J.G. : "*Laboratory Study of Effect of Overburden, Formation and Mud Column Pressures on Drilling Rate of Permeable Formations*". *Pet. Trans. of AIME*, Vol. 216, 1959, pp. 9-17
18. Milligan, D.I. and Weintritt, D.J. : "*Filtration of Drilling Fluids at Temperature of 300 °F and Above*". *API Drilling and Production Practice*, 1961, pp. 42-48
19. Gatlin, C. and Nemir, C.E. : "*Some Effects of Size Distribution on Particle Bridging in Lost Circulation and Filtration Tests*". *JPT*, June 1961, pp. 575-578
20. Krueger, R.F. : "*Evaluation of Drilling Fluid Filter Loss Additives Under Dynamic Conditions*". *JPT* Jan. 1963, pp. 90-98
21. Outmans, H.D. : "*Mechanics of Static and Dynamic Filtration in the Borehole*". *SPEJ*, Sept. 1963, pp. 236-244
22. Darley, H.C.H. : "*Designing Fast Drilling Fluids*". *JPT*, April 1965, pp. 465-470
23. Bo, M.K., Freshwater, D.C. and Scarlett, B. : "*The Effect of Particle Size Distribution on the Permeability of the Filter Cakes*". *Trans.Instr.Chem. Engrs.*, Vol. 43, 1965, pp. T228-T232
24. Bezemer, C. and Havenaar, I. : "*Filtration Behaviour of Circulating Drilling Fluids*". *SPEJ* Dec.1966, pp. 292-298
25. Young, F.S. and Gray, K.E. : "*Dynamic Filtration During Microbit Drilling*". *JPT*, Sept. 1967, pp. 1209-1224
26. Lawhon, C.P., Evans, W.M. and Simpsons, J.P. : "*Laboratory Drilling Rate and Filtration Studies of Emulsion Drilling Fluids*". *JPT* July 1967, pp. 943-948
27. Lawhon, C.P., Evans, W.M. and Simpson, J.P. : "*Laboratory Drilling Rate and Filtration Studies of Clay and Polymer Drilling Fluids*". *JPT* May 1967, pp. 688-694
28. Barkman, J.H. and Davidson, D.H. : "*Measuring Water Quality and Predicting Well Impairment*". *JPT*, July, 1972. pp. 865-873
29. Chelton, H.M. : "*Darcy's Law Applied to Drilling Fluid Filtration*". *SPE* 1649, 1967
30. Barrington, K.A. and Smith, G.H. : "*Apparatus for Determining Dynamic Fluid Loss*". *American Patent No.* 1,363,793.
31. Simpson, J.P. : "*Drilling fluid filtration under simulated downhole conditions*". *SPE* 4779, First SPE formation damage control symposium, New Orleans, L.A., Feb., 1974
32. Lautrec, J.D. : "*Behaviour of Mud Under Borehole Conditions*". *SPE* 4851, 1974
33. Wyant, R. : "*A Unique System for Preparation and Evaluation of High Temperature Drilling Fluids*". *SPE* 5515, 1975

34. Bannister, C.E. : "*Evaluations of Cement Fluid Loss Behaviour Under Dynamic Conditions*". SPE 7592, 1978
35. Simpson, J.P. : "*A New Approach to Oil Base Muds for Lower-Cost Drilling*". JPT, May, 1979. pp. 643-650
36. Sharma, S.M., Lall, R.C., Mathur, R.M. and Chilingarian G.V. : "*Effect of Various Drilling Fluid Additives on Water Loss and Permeability of Filter Cakes*". Energy Sources, 1980, Vol. 5, Ed. 2, pp. 171-181
37. Peden, J.M., Avalos M.R. and Arthur, K.G. : "*The Analysis of the Dynamic Filtration and Permeability Impairment Characteristics of Inhibited Water Based Muds*". SPE 10655 presented at the SPE Formation Control Symposium, held in Lafayette, LA, March 24-25, 1982
38. Peden, J.M., Arthur, K.G. and Avalos, M.R. : "*The Analysis of Filtration Under Dynamic and Static Conditions*". SPE 12503 presented at the Formation Control Symposium held in Bakersfield, CA, February 13-14, 1984
39. Wyant, R.E., Reed, R.L. Sifferman, T.R. and Wooten, S.O.: "*Dynamic Fluid-Loss Measurement of Oil Mud Additives*". SPE14246 presented at the 60th Annual Technical Conference and Exhibition of the Society of Petroleum Engineers held in Las Vegas, NV September 22-25, 1985
40. Vaussard, A., Martin, M., and Patroni, J.M. : "*An Experimental Study of Drilling Fluids Dynamic Filtration*". SPE 15412 presented at the 61st Annual Technical Conference and Exhibition of the Society of Petroleum Engineers held in New Orleans. LA Oct. 5-6, 1986
41. Bizanti, M. : "*Mud Filtration While Drilling*". Okla. Univ. *et al.* **Drilling Muds Nat. Conf., Proc.**, Norman, Okla, May, 1986, pp. 44-62
42. Hartmann, A., Ozerler, M., Marx, C. and Neumann, H.J. : "*Analysis of Mudcake Structures Formed Under Simulated Borehole Conditions*". SPE 15413 presented at 61st Annual Technical Conference and Exhibition of the Society of Petroleum Engineers held in New Orleans. LA Oct. 5-6, 1986. Also on SPE Drilling Engineering, Dec. 1988. pp. 395-402
43. Jamison, D.E. and Fisk, J.V.: "*Apparatus for Dynamically Measuring Fluid Loss Characteristics*". 1988 US Patent No. 4,748,849
44. Zamora, M. Lai, D.T. and Dzialowski, A.K. : "*Innovative Devices for Testing Drilling Muds*". IADC/SPE 17240 presented at the 1988 IADC/SPE Drilling Conference held in Dallas, Texas, Feb 28-Mar 2, 1988. pp. 511-518. Also on SPE Drilling Engineering, Mar. 1990. pp. 11-16 .
45. Fordham E.J., Ladva, H.K.J., Hall, C., Baret, J-F. and Sherwood, J.D. : "*Dynamic Filtration of Bentonite Muds Under Different Flow Conditions*". SPE 18038 presented at the 63rd Annual Technical Conference and Exhibition of the Society of Petroleum Engineers held in Houston, TX, October 2-5, 1988
46. Fisk, J.V and Jamison, D.E. : "*Physical Properties of Drilling Fluids at High Temperatures and Pressures*". IADC/SPE 17200 presented at the 1988 IADC/SPE Drilling Conference held in Dallas, Texas, Feb. 28-Mar. 2, 1988. Also on SPE Drilling Engineering, Dec. 1989. pp. 341-346
47. Arthur, K.G. and Peden, J.M. : "*The Evaluation of Drilling Fluid Filter Cake Properties and Their Influence on Fluid Loss*". SPE 17617 presented at the SPE international meeting on Petroleum Engineering, held in Tianjin, China,

November 1-4, 1988

48. Plank, J.P. and Gossen, F.A. : "*Visualization of Fluid-Loss Polymer in Drilling Mud Filter Cakes*". SPE 19534 presented at the 64th Annual Technical Conference and Exhibition of the society of Petroleum Engineers held in San Antonio, TX, Oct 8-11, 1989
49. Hassen, B.R., : "*New Technique Estimates Drilling Filtrate Invasion*". SPE 8971, 4th SPE Symposium on Formation Damage Control, Bakersfield, C.A., 28-29, Jan, 1980
- (50) Poiseuille, J.L. : *Compt. Rend.*, Vol. 15, 1842. p. 1167
51. Darcy, H.P.G. : "*Les Fontaines Publique de la Ville de Dijon*". Vactor Delmont, Paris, 1856.
52. Almy, C. and Lewis, W.K. : "*Factors Determining the Capacity of a Filter Press*". *J Ind.Eng.Chem.*, Vol. 4, July, 1912, pp. 528-532
53. Sperry, D.R. : "*The Principles of Filtration*". *Met.Chem.Eng.*, Vol. 15, No. 4, 1916, pp. 198-203
54. Baker, F.P. : "*A study of the Fundamental Laws of Filtration Using Plant-Scale Equipment*". *J Ind.Eng.Chem.* Vol. 13, 1921, pp. 610-612
55. Sperry, D.R. : "*Letter to the Editor*". *J Ind.Eng.Chem.*, Vol. 13, 1921, pp. 1163-1164
56. Baker, F.P. : "*Letter to the Editor*". *J Ind.Eng.Chem.*, Vol. 13, 1921, pp. 1164-1165
57. Weber, H.C. and Hershey, R.L. : "*Some Practical Applications of the Lewis Filtration Equation*". *Ind.Eng.Chem.*, Vol. 18, April, 1926, pp. 341-344
58. Ruth, B.F., Montillon, G.H. and Montonna, R.E. : "*Studies in Filtration-I and II*". *Ind.Eng.Chem.*, Vol. 25, 1933, pp. 76-82; 153-161
59. Ruth, B.F. : "*Studies in Filtration-III. Derivation of General Filtration Equations*". *Ind.Eng.Chem.*, Vol. 27, 1935, pp. 708-723
60. Carman, P.C. : "*Fundamental Principles of Industrial Filtration*". *Trans.Inst. Chem.Engrs.(London)*, Vol. 16, 1938, pp. 168-188
61. Rietema, K. : "*Stabilized Effects in Compressible Filter Cakes*". *Chem.Eng.Sci.*, Vol. 2, 1953, pp. 88-94
62. Wronski, S.K., Bin, A.K. and Laskowski, L.K. : "*Anomalous Behaviour During the Initial Stage of Constant Pressure Filtration*". *Chem.Eng. J*, Vol. 12, 1976, pp. 143-147
63. Baird, R.L. and Perry, M.G. : "*The Distribution of Porosity in Filter Cakes*", *Filtration & Separation*, Vol. 4, 1967, pp. 471-474
64. Shirato, M., Sambuichi, M., Kato, H. and Aragaki, T. : "*Internal Flow Mechanism in Filter Cakes*". *AIChE Journal*, Vol. 13, 1969, pp. 405- 409
65. Tosun, I. and Willis, M.S. : "*Making the Case for the Multiphase Filtration Theory*". *Filtration & Separation*, July/August, 1989. pp. 295-299
66. Willis, M.S., Shen, M. and Gray, K.J.,: "*Investigation of the Fundamental*

- Assumptions Relating Compression-Permeability Data With Filtration*".
Can.J.Chem.Eng., Vol. 52, 1974, pp. 331-337
67. Ruth, B.F. : "*Correlating Filtration Theory with Industry Practice*".
Ind.Eng.Chem., Vol. 38, 1946, pp. 564-571
68. Grace, H.P. : "*Resistance and Compressibility of Filter Cakes I and II*".
Chem.Eng.Prog., Vol. 49, 1953, pp. 303-318; 367-377
69. Tiller, F.M. : "*The Role of Porosity in Filtration-Part I, Numerical Methods for Constant Rate and Constant Pressure Filtration Based on Kozeny's Law*".
Chem.Eng.Prog., Vol. 49, 1953, pp. 467-479
70. Tiller, F.M. : "*The Role of Porosity in Filtration-Part II, Analytical Equation for Constant Rate Filtration*". **Chem.Eng.Prog.** Vol. 51, 1955, pp. 282-290
71. Kottwitz, F.A. and Boylan, D.R. : "*Prediction of Resistance of cake in Constant Pressure Cake Filtration*". **AIChE Journal**, Vol. 4, 1958, pp. 175-180
72. Tiller, F.M. and Huang, C.J. : "*Theory*", **Ind.Eng.Chem.**, Vol. 53, 1961, pp. 529-537
73. Willis, M.S. and Tosun, I. : "*A Rigorous Cake Filtration Theory*".
Chem.Eng.Sci., Vol. 35, 1980. pp. 2427-2438
74. Shirato, M., Aragaki, T., Mori, R. and Sawamoto, K. : "*Prediction of Constant Pressure and Constant Rate Filtrations Based on the Appropriate Correction for SideWall Friction in Compression Permeability Cell Data*". **J Chem.Eng.** (Japan), Vol. 4, 1968, pp. 172-177
75. Tosun, I. and Willis, M.S. : "*On the Validity of the Power Law Approximation in Filtration Theory*". **Chem.Eng.Sci.**, Vol. 37, 1982. pp. 1421-1422
76. Tosun, I. and Willis, M.S. : "*Energy Efficiency in Cake Filtration*". **Filtrtion & Separation**, Vol. 22 (2), 1985. pp. 126-127
77. Tiller, F.M., Haynes, S. and Lu, W. : "*The Role of Porosity in Filtration VII-Effect of Side Wall Friction in Compression Permeability Cells*". **AIChE Journal**, 18, 1972. pp.13-20
78. Tiller, F.M. and Green, T.C. : "*The Role of Porosity in Filtration IX-Skin Effect with Highly Compressible Materials*". **AIChE Journal**, Vol. 19, 1973, pp. 1266-1269
79. Tosun, I. and Willis, M.S. : "*The Effect of the Filter Cake Geometry on Average Porosity*". **Chem.Eng. J** Vol. 35, 1987, pp.99-106
80. Tiller, F.M. and Cooper, H.R. : "*The Role of Porosity in Filtration IV-Constant Pressure Filtration*". **AIChE Journal** Vol. 6, 1960, pp. 595-601
81. Bierck, B.R., Wells, S.A. and Dick, R.I. : "*Compressible Cake Filtration: Cake Formation and Shrinkage Using Synchrotron X-Rays*". **J Water Pollut. Control Fed.** Vol. 60, 1988, pp. 645-650
82. Peden, J. : "*The Filtration and Associated Permeability Impairment Characteristics of Drilling and Completion Fluids*". **Ph.D Thesis**, 1983, Heriot-Watt University.
83. Mahajan, N.C. and Barron, B.M. : "*Bridging Particle Size : A Key Factor in the Design of Non-Damaging Completion Fluids*", **SPE 8792**, 4th SPE Symposium

on Formation Damage Control, Bakersfield, C.A., 28-29, Jan, 1980

84. Ershagi, I. and Azari, M. : "*Modelling of Filter Cake Build-Up Under Dynamic Static Conditions*". SPE 8902, 50th Annual California Regional Meeting of SPE, 9-11, April, 1980
85. Krueger, R.F. and Vogel, L.C. : "*Damage to Sandstone Cores by Particles from Drilling Fluid*". API Drilling and Production Practice, 1954, pp.158-171
86. Beck, R.W., Nuss, W.F. and Dunn, T.H. : "*Flow Properties of Drilling Muds*". API Drilling and Production Practice, 1947, pp. 9-22
87. Sawdon, W.A. : "*Control of Colloidal Properties is Vital in Mud Conditioning*". The Petroleum Engineer, Vol. 62, 1935, pp. 50-56
88. Krumbein, W.C. and Monk, G.D. : "*Permeability as a Function of the Size Parameters of an Unconsolidated Sand*". Pet.Trans.AIME, Vol. 151, 1943, pp.153-163
89. Abrams, A. : "*Mud Design to Minimize Rock Impairment due to Particle Invasion*". JPT, May 1977, pp. 586-592
90. McCuire, P.L. and McFall, A.L. : "*An Investigation of Low Invasion Fluids for Pressure Coring*". 5th Annual U. S. D.O.E. Symposium on E.O.R., Tulsa, 1979
91. Porter, K.E. : "*A Basic Scanning Electron Microscope Study of Drilling Fluids*". SPE 8790, 4th SPE Symposium on Formation Damage Control, Bakersfield, C.A., 28-29, Jan, 1980
92. Dickey, G.D. and Bryden, C.L. : "*Theory and Practice of Filtration*". Reinhold Publishing Corp., New York, 1946
93. Ghofrani, R. : "*Dynamic Filtration of Bentonite Drilling Fluids and Filter Cake Removal*". Erdoel Ergas Zeitschrift, 93(4), 177, pp. 137-151
94. Arthur, K.G. : "*An Experimental and Theoretical Study of the Filtration Characteristics of Water-Based Drilling Muds*". Ph.D thesis, Heriot-Watt University, 1986
95. Darley, H.C.H. and Gray, G.R. : "*Composition and Properties of Drilling and Completion Fluids*". Fifth Edition, Gulf Publishing Company, 1988.
96. Kozicki, F.M., Rao, A.R.K. and Tiu, C. : "*On the parabolic Representation of Constant Pressure Filtration*". Canad.J.Chem.Eng., Vol. 48, 1970, p. 463
97. von Engelhardt, W. and Schindewolf, E. : "*The Filtration of Clay Suspensions*". Kolloidz, Vol. 127, 1952, pp. 150-164.
98. Streeter, V.L. and Wylie, E.B., 1985, : "*Fluid Mechanics*". Part 4 — Dimensional Analysis and Dynamic Simulatude. 1985
99. Willis, M.S. : "*A Multiphase Theory of Filtration*". Prog in Filtration & Separation, Vol. 3, 1983
100. Cheremisinoff, N.P. and Azbel, D.S. : "*Liquid Filtration*". ISBN 0-250-40600-4, Ann Arbor Science Publishers.
101. Tosun, I. : "*Application of Multiphase Theory to Filtration*". Ph.D Thesis, 1977, University of Akron, Akron, Ohio.

102. Tosun, I. and Willis, M.S. : "*Cake Filtration Theory: An Overview*". **The Fourth World Filtration Conference Proceeding**. April, 1986.
103. Willis, M.S., Bridges, W.G. and Collins, R.M. : "*The Initial Stages of Filtration and Deviations From Parabolic Behaviour*". **Filtech Conference**, 1981.
104. Peden, J.M. : "*Reducing Formation Damage by Better Filtration Control*". **OFFSHORE SERVICES AND TECHNOLOGY**, Jan, 1982. pp. 26-28
105. Krueger, R.F. : "*An Overview of Formation Damage and Well Productivity in Oilfield Operations*". **JPT**, Feb, 1986. pp.131-152
106. Porter, K.E. : "*An Overview of Formation Damage*". **JPT**, Aug, 1989, pp.780-786
107. Tiller, F.M., Crump, J.R. and Ville, F., **Fine Particles Processing**, Vol. 2, p. 1549. (1980)
108. Davidson, D.H., **SPE 8210**, 1979.
109. Donaldson, E.C. and Baker, B.A. **SPE 6905**, 1977.
110. Champlin, J.B.F. **SPEJ**, December 1971, pp. 367-373

APPENDIX I

Program to Calculate the Coefficients of Dynamic Filtration Equations.

```

***** ***** Program DyFit *****
C
C   Programme DyFit is designed to correlated the
C   experimental data with the developed dynamic filtration model.
C   The output will give the regressed coefficients by the
C   least square method and correlation deviations, CC(I,J),Fsumsq(I)
C
C   Program DyFit
C   =====
C
1   REAL X(9,1000),Y(9,1000),Xa(1000),Ya(1000),Xsp(9),Ysp(9),DELT,
2   Xx(9,1000),Yy(9,1000),C(4),CC(9,4),DELTA(9,5),FSUMSQ(9),
   Xt(1000),Yvol(1000),t0
   INTEGER NUMDAT,NPTS(9),llab,llable,I,J,K,YN,VALUE,Icheck,Imode
   CHARACTER*80 YORN*10
   COMMON Xt,Yvol,Ipts
C
C   Reading the original data from the "[.TEMP]TEMP.DAT"
C   =====
9999 OPEN(3,STATUS = 'OLD',FILE = '[.TEMP]TEMP')
   READ(3,9999) NUMDAT
   FORMAT(1X,I4)
   DO I = 1,NUMDAT
       READ(3,9999) NPTS(I)
       DO J = 1,NPTS(I)
           READ(3,9998) X(I,J),Y(I,J)
9998   FORMAT(1X,2E12.5)
       END DO
   END DO
   CLOSE(3)
C   Calculating from here
C   =====
10  DO 150 I = 1,NUMDAT
     DO 20 J = 1,NPTS(I)
         Xa(J) = X(I,J)
         Ya(J) = Y(I,J)
20  CONTINUE
     t0 = 4.0
C   Determining Spurt Loss & Spurt Time
C   =====
     CALL SPURT(t0,Xa,Ya,NPTS(I),Xsp(I),Ysp(I))
     DO 40 J = 1,NPTS(I)
         Xa(J) = X(I,J)-Xsp(I)
         Ya(J) = Y(I,J)-Ysp(I)
40  CONTINUE
     DO 80 J = 1,NPTS(I)
         Xx(I,J) = Xa(J)
         Yy(I,J) = Ya(J)

```

```

      Xt(J) = Xa(J)
      Yvol(J) = Ya(J)
80    CONTINUE
      Ipts = NPTS(I)
C     Sorting data points to appreciable distribution density
C     =====
90    WRITE(6,*) '  The Correlation Technique:'
      WRITE(6,*) '  ====='
      WRITE(6,100)
      WRITE(6,110)
      WRITE(6,120)
      WRITE(6,130)
100   FORMAT($,10X,'1.  No derivatives are required;')
110   FORMAT($,10X,'2.  First derivatives are required;')
120   FORMAT($,10X,'3.  First & second derivatives are required;')
130   FORMAT($,5X,'Which Way Will You Choose_[RETURN for "3"]:' )
      READ(5,'(A)') YORN
      IF (YORN.EQ.' ')YORN='3'
      Imode = VALUE(YORN)
      IF (Imode.LT.-3.OR.Imode.GT.3)GOTO 90
      WRITE(6,140)
140   FORMAT($,5X,'Do Checking Derivatives?(y/n)_[RETURN for "n"]:' )
      READ(5,'(A)') YORN
      Icheck = 0
      IF (YORN.EQ.'Y'.OR.YORN.EQ.'y')Icheck = 1
      CALL DFLnag(Imode,Icheck,C,SUM)
C     =====
      DO 150 K = 1,4
          CC(I,K) = C(K)
          FSUMSQ(I) = SUM
150   CONTINUE
200   STOP
      END
C
***** ***** END OF PROGRAM *****
*
***** ***** SUBROUTINE DFLnag *****
C
C     The subroutine is designed to obtain the coefficients by
C     correlating the dynamic filtration model with the experimental
C     obtained data by calling NAG library routine E04HEE
C     E04HEE is a comprehensive modified Gauss-Newton algorithm for
C     finding an unconstrained minimum of a sum of squares of M
C     non-linear functions in N variables (M>=N). First and Second
C     derivatives are required.
C
      SUBROUTINE DFLnag(Imode,Icheck,C,SUM)
C     =====
C
C     Imode, on entry, gives message to select one model.
C     Icheck, on entry, gives message to/not to check first and second
C     derivatives.
C     C(N), on exit, gives the coefficients of the model which are
C     determined by correlating experimental data.
C     SUM, on exit, gives the total sum of the squares
C     which minimized
C
      REAL Xt(1000),Yvol(1000),FVEC(1000),FJAC(1000,4),X(4),C(4),
1     S(4),V(4,4),B(10),W(10000),ETA,XTOL,STEPMX,FSUMSQ,SUM
      INTEGER M,N,LJ,LV,IW(100),LIW,LW,IFAIL,Ipts,Imode,Icheck,

```

```

&          I,IPRINT,MAXCAL,NF,NITER
EXTERNAL LSQFUN10,LSQFUN11,LSQFUN20,LSQFUN21,
&          LSQHES30,LSQHES31,LSQMON
COMMON Xt,Yvol,Ipts
M   = Ipts
LJ  = M
N   = 4
LV  = 4
LIW = 100
LW  = 10000
LB  = 10
IF (Icheck.EQ.0)GOTO 40
C =====
10  CALL INITIAL(0,X)
    IFAIL = -1
C   Check the first derivatives
C   =====
    IF (Imode.EQ.2.OR.Imode.EQ.3) THEN
        CALL
E04YAE(M,N,LSQFUN21,X,FVEC,FJAC,LJ,IW,LIW,W,LW,IFAIL)
    ELSE IF (Imode.EQ.-2.OR.Imode.EQ.-3) THEN
        CALL
E04YAE(M,N,LSQFUN20,X,FVEC,FJAC,LJ,IW,LIW,W,LW,IFAIL)
    ELSE ! IF (Imode.EQ.1.OR.Imode.EQ.-1) THEN
        GOTO 40
    END IF
    WRITE(6,20) IFAIL
20  FORMAT($,1X,'IFAIL = "',I2,'" ',2X,'First derivatives were calculated
&   correctly!')
    IFAIL = 0
C   Check the evaluation of B
C   =====
    IF (Imode.EQ.3) THEN
        CALL E04YBE(M,N,LSQFUN21,LSQHES31,X,FVEC,FJAC,LJ,B,LB,
&   IW,LIW,W,LW,IFAIL)
    ELSE IF (Imode.EQ.-3) THEN
        CALL E04YBE(M,N,LSQFUN20,LSQHES30,X,FVEC,FJAC,LJ,B,LB,
&   IW,LIW,W,LW,IFAIL)
    ELSE ! IF (Imode.EQ.2.OR.Imode.EQ.-2) THEN
        GOTO 40
    END IF
    WRITE(6,30) IFAIL
30  FORMAT($,1X,'IFAIL = "',I2,'" ',2X,'Second derivatives were
&   calculated correctly!')
C   Continue setting parameters for E04HEE
C   =====
40  IPRINT = 0
    MAXCAL = 50*N
    IF (Imode.EQ.1.OR.Imode.EQ.-1)MAXCAL = 500*N
    ETA   = 0.9
    XTOL  = 10.0*SQRT(X02AAE(XTOL))
    STEPMX = 500.0
    I     = 1
    CALL INITIAL(I,X)
    IFAIL = 1
C   =====
50  IF (Imode.EQ.1) THEN
    CALL E04FCE(M,N,LSQFUN11,LSQMON,IPRINT,MAXCAL,ETA,XTOL,
1     STEPMX,X,FSUMSQ,FVEC,FJAC,LJ,S,V,LV,NITER,NF,IW,
2     LIW,W,LW,IFAIL)

```

```

ELSE IF (Imode.EQ.-1) THEN
CALL E04FCE(M,N,LSQFUN10,LSQMON,IPRINT,MAXCAL,ETA,XTOL,
1   STEPMX,X,FSUMSQ,FVEC,FJAC,LJ,S,V,LV,NITER,NF,IW,
2   LIW,W,LW,IFAIL)
C   No derivatives are required when above routines are excuting
ELSE IF (Imode.EQ.2) THEN
CALL E04GDE(M,N,LSQFUN21,LSQMON,IPRINT,MAXCAL,ETA,XTOL,
1   STEPMX,X,FSUMSQ,FVEC,FJAC,LJ,S,V,LV,NITER,NF,IW,
2   LIW,W,LW,IFAIL)
ELSE IF (Imode.EQ.-2) THEN
CALL E04GDE(M,N,LSQFUN20,LSQMON,IPRINT,MAXCAL,ETA,XTOL,
1   STEPMX,X,FSUMSQ,FVEC,FJAC,LJ,S,V,LV,NITER,NF,IW,
2   LIW,W,LW,IFAIL)
C   The first derivatives are required when above routines are excuting
ELSE IF (Imode.EQ.3) THEN
CALL E04HEE(M,N,LSQFUN21,LSQHES31,LSQMON,IPRINT,
1   MAXCAL,ETA,XTOL,STEBMX,X,FSUMSQ,FVEC,FJAC,LJ,S,V,LV,
2   NITER,NF,IW,LIW,W,LW,IFAIL)
ELSE IF (Imode.EQ.-3) THEN
CALL E04HEE(M,N,LSQFUN20,LSQHES30,LSQMON,IPRINT,
1   MAXCAL,ETA,XTOL,STEBMX,X,FSUMSQ,FVEC,FJAC,
2   LJ,S,V,LV,NITER,NF,IW,LIW,W,LW,IFAIL)
C   The first & second derivatives are required when above routines
C   are excuting
ELSE
WRITE(6,*)'ABNORMAL EXIT'
CALL EXIT
END IF

C   =====
C   since IFAIL was set to 1 before entering E04HEE, it is essential
C   to test whether IFAIL is non-zero on exit.
WRITE(*,60) IFAIL
60  FORMAT(/,$,1X,'Current Failure No. is "',I2,'" . Please pay
&  attention!',/)
IF (IFAIL.EQ.-1) THEN
I=I+1
CALL INITIAL(I,X)
IFAIL = 1
GOTO 50
ELSE IF (IFAIL.EQ.0) THEN
GOTO 100
ELSE IF (IFAIL.EQ.2) THEN
IFAIL = 1
GOTO 50
ELSE IF (IFAIL.EQ.3) THEN
I=I+20
CALL INITIAL(I,X)
IFAIL = 1
GOTO 50
ELSE IF (IFAIL.EQ.4) THEN
I=I+1
CALL INITIAL(I,X)
IFAIL = 1
GOTO 50
ELSE
WRITE(6,70) IFAIL
70  FORMAT($,1X,'IFAIL = ',I2)
CALL EXIT
END IF
100 DO 150 I = 1,N

```



```

      C(I) = X(I)
150  CONTINUE
      SUM = FSUMSQ
200  RETURN
      END
C    ===
      SUBROUTINE LSQFUN10(IFLAG,M,N,XC,FVECC,IW,LIW,W,LW)
C    ++++++
C    LSQFUN must calculate the vector of values fi(x) at any point X.
C
      INTEGER IFLAG,M,N,IW(LIW),LIW,LW,I,Ipts
      REAL XC(4),FVECC(M),W(10000),Xt(1000),Yvol(1000)
      REAL DEMO,EDEMO
      COMMON Xt,Yvol,Ipts
      DO 100 I = 1,M
          DEMO = -Yvol(I)*XC(3)
          IF (DEMO.GT.80.0.OR.Xt(I).EQ.0.0) THEN
              IFLAG=-1
              GOTO 200
          END IF
          EDEMO = EXP(DEMO)
          FVECC(I) = (Yvol(I)*XC(1)-XC(2)*(1.0-EDEMO)+XC(4))-Xt(I)
100  CONTINUE
200  RETURN
      END
C    ===
      SUBROUTINE LSQFUN11(IFLAG,M,N,XC,FVECC,IW,LIW,W,LW)
C    ++++++
C    LSQFUN must calculate the vector of values fi(x) at any point X.
C
      INTEGER IFLAG,M,N,IW(LIW),LIW,LW,I,Ipts
      REAL XC(4),FVECC(M),W(10000),Xt(1000),Yvol(1000)
      REAL DEMO,EDEMO
      COMMON Xt,Yvol,Ipts
      DO 100 I = 1,M
          DEMO = -Yvol(I)*XC(3)
          IF (DEMO.GT.80.0.OR.Xt(I).EQ.0.0) THEN
              IFLAG=-1
              GOTO 200
          END IF
          EDEMO = EXP(DEMO)
          FVECC(I) = (Yvol(I)*XC(1)-XC(2)*(1.0-EDEMO)+XC(4))/Xt(I)-1.0
100  CONTINUE
200  RETURN
      END
C    ===
      SUBROUTINE LSQFUN20(IFLAG,M,N,XC,FVECC,FJACC,LJC,IW,
&      LIW,W,LW)
C    ++++++
C    LSQFUN must calculate the vector of values fi(x) and Jacobian
C    matrix of first derivatives delt_fi/delt_Xj at any point X.
C
      INTEGER IFLAG,M,N,LJC,IW(LIW),LIW,LW,I,Ipts
      REAL XC(4),FVECC(M),FJACC(LJC,4),W(10000),Xt(1000),Yvol(1000)
      REAL DEMO,EDEMO
      COMMON Xt,Yvol,Ipts
      DO 100 I = 1,M
          DEMO = -Yvol(I)*XC(3)
          IF (DEMO.GT.80.0) THEN
              IFLAG=-1

```

```

          GOTO 200
        END IF
        EDEMO = EXP(DEMO)
        FVECC(I) = Yvol(I)*XC(1)-XC(2)*(1.0-EDEMO)+XC(4)-Xt(I)
        FJACC(I,1) = Yvol(I)
        FJACC(I,2) = EDEMO-1.0
        FJACC(I,3) = -1.0*XC(2)*Yvol(I)*EDEMO
        FJACC(I,4) = 1.0
100    CONTINUE
200    RETURN
      END
C      ===
      SUBROUTINE LSQFUN21(IFLAG,M,N,XC,FVECC,FJACC,LJC,
&      IW,LIW,W,LW)
C      ++++++
C      LSQFUN must calculate the vector of values fi(x) and Jacobian
C      matrix of first derivatives delt_fi/delt_Xj at any point X.
C
      INTEGER IFLAG,M,N,LJC,IW(LIW),LIW,LW,I,Ipts
      REAL XC(4),FVECC(M),FJACC(LJC,4),W(10000),Xt(1000),Yvol(1000)
      REAL DEMO,EDEMO
      COMMON Xt,Yvol,Ipts
      DO 100 I = 1,M
        DEMO = -Yvol(I)*XC(3)
        IF (DEMO.GT.80.0.OR.Xt(I).EQ.0.0) THEN
          IFLAG=-1
          GOTO 200
        END IF
        EDEMO = EXP(DEMO)
        FVECC(I) = (Yvol(I)*XC(1)-XC(2)*(1.0-EDEMO)+XC(4))/Xt(I)-1.0
        FJACC(I,1) = Yvol(I)/Xt(I)
        FJACC(I,2) = (EDEMO-1.0)/Xt(I)
        FJACC(I,3) = -1.0*XC(2)*Yvol(I)*EDEMO/Xt(I)
        FJACC(I,4) = 1.0/Xt(I)
100    CONTINUE
200    RETURN
      END
C      ===
      SUBROUTINE LSQHES30(IFLAG,M,N,FVECC,XC,B,LB,IW,LIW,W,LW)
C      ++++++
C      Routine to calculate the elements of the symmetric matrix
C      B(X)=EPSTAFi(X)Gi(X)
C      at any point X, where Gi(X) is the Hessian matrix of fi(X)
C
      INTEGER IFLAG,M,N,LB,IW(LIW),LIW
      REAL FVECC(M),XC(4),B(LB),W(10000)
      REAL Xt(1000),Yvol(1000),DEMO,EDEMO,SUM32,SUM33
      INTEGER I
      COMMON Xt,Yvol,Ipts
      DO 50 I=1,LB
        B(I)=0.0
50    CONTINUE
        SUM32 = 0.0
        SUM33 = 0.0
        DO 100 I = 1,M
          DEMO = -Yvol(I)*XC(3)
          EDEMO = EXP(DEMO)
          SUM32 = SUM32 + FVECC(I)*(-1.0)*Yvol(I)*EDEMO
          SUM33 = SUM33 + FVECC(I)*XC(2)*Yvol(I)*Yvol(I)*EDEMO
100    CONTINUE

```

```

        B(5) = SUM32
        B(6) = SUM33
200  RETURN
      END
C     ===
      SUBROUTINE LSQHES31(IFLAG,M,N,FVECC,XC,B,LB,IW,LIW,W,LW)
C     ++++++
C     Routine to calculate the elements of the symmetric matrix
C     B(X)=EPSTAFi(X)Gi(X)
C     at any point X, where Gi(X) is the Hessian matrix of fi(X)
C
      INTEGER IFLAG,M,N,LB,IW(LIW),LIW,LW
      REAL FVECC(M),XC(4),B(LB),W(10000)
      REAL Xt(1000),Yvol(1000),DEMO,EDEMO,SUM32,SUM33
      INTEGER I
      COMMON Xt,Yvol,Ipts
      DO 50 I=1,LB
        B(I)=0.0
50    CONTINUE
        SUM32 = 0.0
        SUM33 = 0.0
        DO 100 I = 1,M
          DEMO = -Yvol(I)*XC(3)
          EDEMO = EXP(DEMO)
          SUM32 = SUM32 + FVECC(I)*(-1.0)*Yvol(I)*EDEMO/Xt(I)
          SUM33 = SUM33 + FVECC(I)*XC(2)*Yvol(I)*Yvol(I)*EDEMO/Xt(I)
100   CONTINUE
        B(5) = SUM32
        B(6) = SUM33
200  RETURN
      END
C     ===
      SUBROUTINE LSQMON(M,N,XC,FVECC,FJACC,LJC,S,IGRADE,
1      NITER,NF,IW,LIW,W,LW)
C     Monitoring routine
C     ++++++
C     If Iprint >= 0, this subroutine is suitable for monitoring
C     the minimization process.
      INTEGER M,N,LJC,IGRADE,NITER,NF,IW(LIW),LIW,LW,I,Ipts
      REAL XC(N),FVECC(M),FJACC(LJC,N),S(N),W(LW),Xt(1000),
&      Yvol(1000),DEMO,EDEMO
      COMMON Xt,Yvol,Ipts
      WRITE(6,20) ((I,XC(I)),I=1,N)
20    FORMAT($,1X,4('XC(',I1,') = ',F9.3,1X))
200  RETURN
      END
C     ===
      SUBROUTINE INITIAL(N,X)
C     ++++++
C     Routine to produce a set of initial values of X array
      REAL X(4),Y(10000,4)
      INTEGER I,J,K,L,M,N,Iseed
      Iseed = 999
      IF (N.EQ.0)GOTO 150
      M = 0
      DO 50 L = 1,20
        DO 50 K = 1,20
          DO 50 J = 1,5
            DO 50 I = 1,5
              M = M+1

```

```

        Y(M,1) = I*25.0
        Y(M,2) = J*40.0
        Y(M,3) = K*0.1
        Y(M,4) = -L*0.01
50  CONTINUE
    DO 100 I = 1,4
        X(I) = Y(N,I)
100  CONTINUE
    GOTO 200
150  X(1) = 100.0*RAN(Iseed)
    X(2) = 100.0*RAN(Iseed)
    X(3) = 10.0*RAN(Iseed)
    X(4) = 1.0*RAN(Iseed)
200  RETURN
    END
C    ===
C    SUBROUTINE SPURT(t0,t,V,N,tsp,Vsp)
C    =====
    REAL t0,t(1000),V(1000),tsp,Vsp,tran,tspurt,t1,t2,V1,V2
    INTEGER N,K
    tspurt = t0
    IF (tspurt.LT.0.0)tspurt=0.0
    DO 100 K=1,N
        tran=t(K)*60.0
        IF (tran.EQ.tspurt) THEN
            Vsp=V(K)
            GOTO 200
        ELSE IF (tran.GT.tspurt.AND.tran.LT.(tspurt+3.0)) THEN
            t1=t(K-1)
            V1=V(K-1)
            t2=t(K)
            V2=V(K)
            Vsp=V1+(tspurt/60.0-t1)*(V2-V1)/(t2-t1)
            GOTO 200
        ELSE IF (tran.GE.(tspurt+3.0)) THEN
            Vsp=V(K-1)
            GOTO 200
        ELSE
            GOTO 100
        END IF
100  CONTINUE
200  tsp=tspurt/60.0
    RETURN
    END
C    ===
C    FUNCTION VALUE(STRING)
C    =====
    CHARACTER*(*) STRING
    CHARACTERC1 CHAR,DIGITS(10)
    INTEGER I,CHLOOK,SWITCH,NONEXT,VALUE
    DATA DIGITS/'0','1','2','3','4','5','6','7','8','9'/
C
C    Written by S J PENG, 15/12/89
C    This function finds the value of a string of digits.
C    The parameter:
C        STRING --- Input, Character*(*) --- a valid string of
C                    digits, left justified, terminated by a blank.
C
    I=1
    VALUE = 0

```

```

NONEXT = 0
SWITCH = 1
C
C   For each new digit, adjust the answer based on that digit's value
C
10  IF (STRING(I).EQ.' ')GOTO 100
    CHAR = STRING(I:I)
    I = I + 1
    IF (CHLOOK(CHAR,DIGITS,10,10).EQ.0) THEN
        IF (NONEXT.EQ.1)GOTO 100
        GOTO 10
    ELSE
        NONEXT = 1
        IF (STRING(I-2:I-2).EQ.'-')SWITCH = -1
        VALUE = 10*VALUE + CHLOOK(CHAR,DIGITS,10,10) - 1
        GOTO 10
    ENDIF
100  VALUE = VALUE*SWITCH
200  RETURN
    END
C
C   ===
C   INTEGER FUNCTION CHLOOK(KEY,ARRAY,ASIZE,N)
C   =====
C   INTEGER ASIZE,N,I
C   CHARACTER*(*) KEY,ARRAY(ASIZE)
C
C   This integer function looks up a string of any length in an array
C   of strings. It returns the position of the first occurrence (or 0
C   if no occurrence).
C
C   These parameters are used:
C   KEY --- input, character --- string we are looking for.
C   ARRAY --- input, character array of length asize --- array
C           in which to search for string.
C   ASIZE --- input, integer --- length of the array.
C   N --- input, integer --- position of array in use.
C
    CHLOOK = 0
    DO 50 I = 1,N
        IF (KEY.EQ.ARRAY(I)) THEN
            CHLOOK = I
            GOTO 200
        ENDIF
50  CONTINUE
200  RETURN
    END
C
C   ===
***** ***** END OF SUBROUTINE *****

```